SYNCHROTRON RADIATION AS THE SOURCE OF THE POLARIZED DECIMETER RADIATION FROM JUPITER

Thesis by

David B. J. Chang

In Partial Fulfillment of the Requirements

for the Degree of

Doctor of Philosophy

California Institute of Technology

Pasadena, California

1962

ACKNOWLEDGMENTS

I am indebted to Professor Leverett Davis, Jr., both for suggesting the thesis problem and for guiding this work to its completion. The generous giving of his time, help and encouragement are sincerely appreciated. I also appreciate his permission to base Sections I and IIIB closely on two joint papers.

Special thanks are also due Dr. James E. Drummond, head of the Plasma Physics Laboratory of the Boeing Scientific Research Laboratories, for the opportunity of using the Boeing technical support facilities. I am grateful to the Boeing Scientific Research Laboratories for the use of their computer to carry out the numerical computations presented in Appendix D and for employment during summers that enabled me to work on some aspects of these problems. The numerical results of Appendix D were obtained through the enthusiastic programming efforts of George Pettigrew and James May of the Applied Mathematics Section of the Boeing Airplane Company. Some of the preliminary numerical calculations were performed by Oliver Weaver and Terry Mast of the 1960 Freshman class of the California Institute of Technology, and I am grateful for their help.

I also wish to express my gratitude for the graduate fellowships received from the National Science Foundation and the Danforth Foundation, and for a tuition grant from the California Institute of Technology.

ABSTRACT

A Stokes parameter description is developed for synchrotron radiation from a group of ultrarelativistic electrons with any specified distribution of positions, energies and directions of motion. This description is used to study the radiation from a shell of ultrarelativistic electrons trapped in a dipole field. It is found that the polarization observed for the 31 cm radiation from Jupiter could be obtained from such shells provided a large number of the electrons have relatively flat helices.

The problem of obtaining high energy, flat-helix electrons in a planetary magnetic field is considered. In particular, the effects of large scale magnetic disturbances on trapped particles are studied by following the particle guiding center motions through a disturbance. The guiding center motions of relativistic particles are determined by using relativistically correct drift velocity expressions obtained by application of an asymptotic approximation method of Bogolyubov and Zubarev. It has been found that these magnetic disturbances might lead to a high density of high energy, flat helix electrons; however, many disturbances are required for appreciable diffusion to occur. Magnetic activity at Jupiter must be very great if this type of mechanism is to provide the relatively flat helix electrons required for the decimeter radiation from Jupiter to be synchrotron radiation.

TABLE OF CONTENTS

PART	TITLE	PAGE
I	INTRODUCTION	1
II	SYNCHROTRON RADIATION FROM ULTRARELATIVISTIC ELECTRONS IN A DIPOLE FIELD . . .	16
	IIA Geometry	20
	IIB Distribution of Electrons Along a Tube of Flux	26
	IIC Radiation from a Thin Shell of Electrons . .	29
III	SOURCE OF HIGH ENERGY ELECTRONS FOR JUPITER	41
	IIIA General Considerations	41
	1. Energy Loss	41
	2. Scattering	43
	3. Electrons from Neutron Albedo . . .	52
	IIIB Effect of Large-scale Magnetic Fluctuations on Trapped Electrons	57
	1. Particle Motion	59
	2. Particle Diffusion	79
	3. Steady State Solutions	80
	4. Transient Solution	86
IV	SUMMARY	98
	APPENDICES	100
	A. Summary of the Published Observations of Jupiter's Decimeter Radiation	100
	B. Properties of Synchrotron Radiation . . .	108
	1. Synchrotron Radiation from a Single Electron	111
	(a) Radiation from an electron in a circular orbit	111
	(b) Radiation from an electron in a helical orbit	125
	2. Radiation from a Group of Electrons . .	134
	(a) Derivation of the power spectrum . .	136
	(b) Stokes parameters for synchrotron radiation from electrons with an arbitrary angular distribution	138

TABLE OF CONTENTS (cont.)

PART	TITLE	PAGE
	(c) An example: power law distribution function	149
C.	A Derivation of Relativistic Drift Velocities by the Asymptotic Approximation Method of Bogolyubov and Zubarev	157
D.	Numerical Results for Synchrotron Radiation from Ultrarelativistic Electrons in a Dipole Field	167
	REFERENCES	178

I. INTRODUCTION

The synchrotron radiation mechanism has been mentioned several times since 1958 in connection with decimeter radiation from the planet Jupiter. In this thesis, we shall consider in more detail the possibility that this mechanism is responsible for Jupiter's decimeter radiation.

The published data on intensities are summarized in tabular form in Appendix A. The equivalent blackbody temperatures at 3 cm range from 140°K to about 200°K and are not too different from the 130°K infrared (radiometric) value given by Menzel, Coblentz, and Lampland (1926). At the longer wavelengths, however, the equivalent blackbody temperatures are seen to be much higher. Thus, at 10 cm, published temperatures range from around 300°K to over 800°K; at 21 cm, from 2000°K to around 3500°K; at 31 cm, around 5500°K; and at 68 cm, from 10,000°K to 70,000°K. The indication is that the flux density is roughly constant with wavelength in the decimeter range of wavelengths. In Figure 1, the flux density corrected for a thermal radiation of 130°K is plotted as a function of wavelength.

It is rather difficult at this stage of the observations to reach very definite conclusions about time variations in the intensities. Apparently, much of the scatter in values may be attributed to noise problems inherent in the observations. On the other hand, it appears that there might be some time variations in the intensities arising from

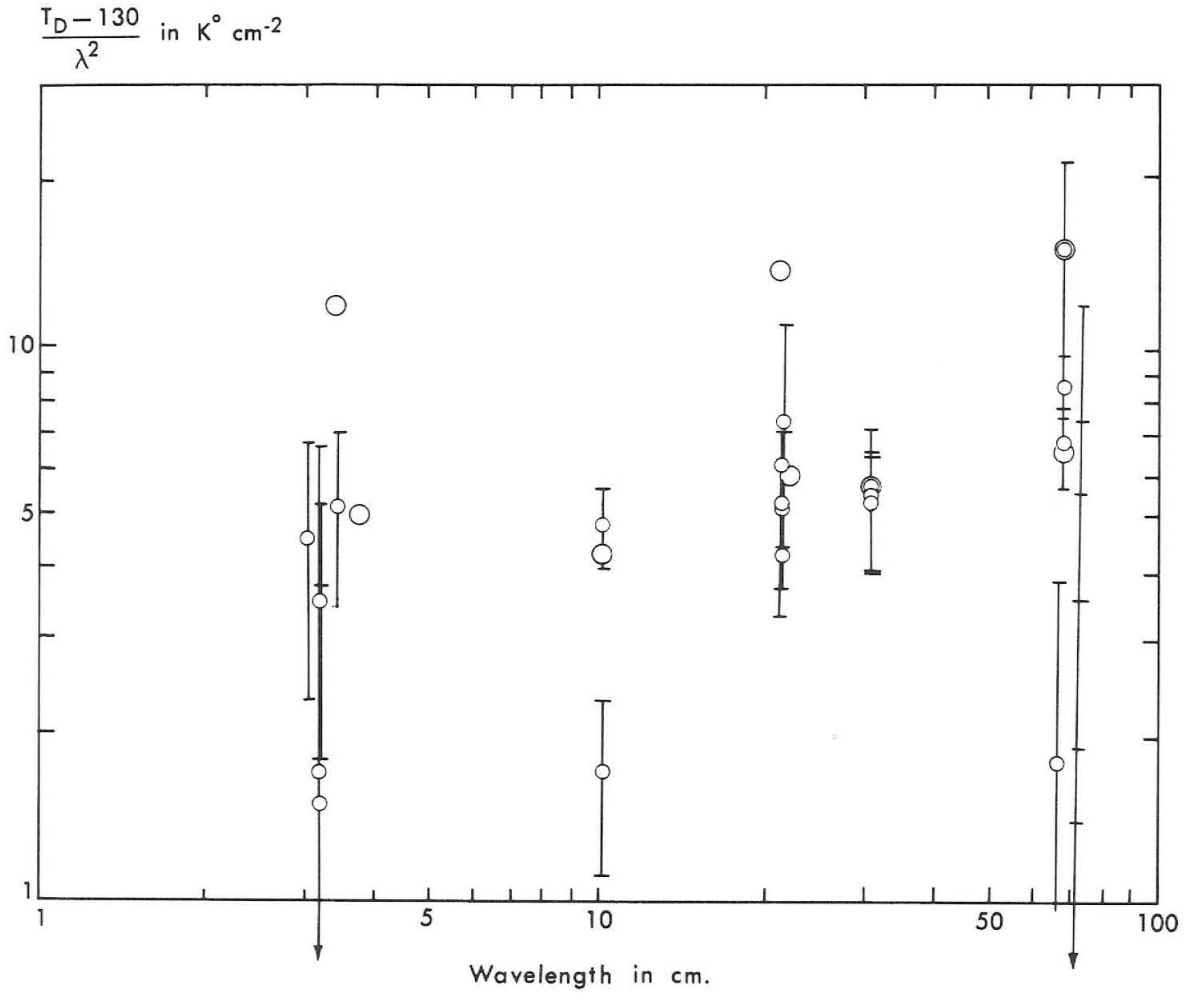

Figure 1. Observed radiation flux from Jupiter, corrected for a thermal emission of 130°K. (See Table III of Appendix A.) (The large circles correspond to the entries in Table III for which the error is not indicated.)

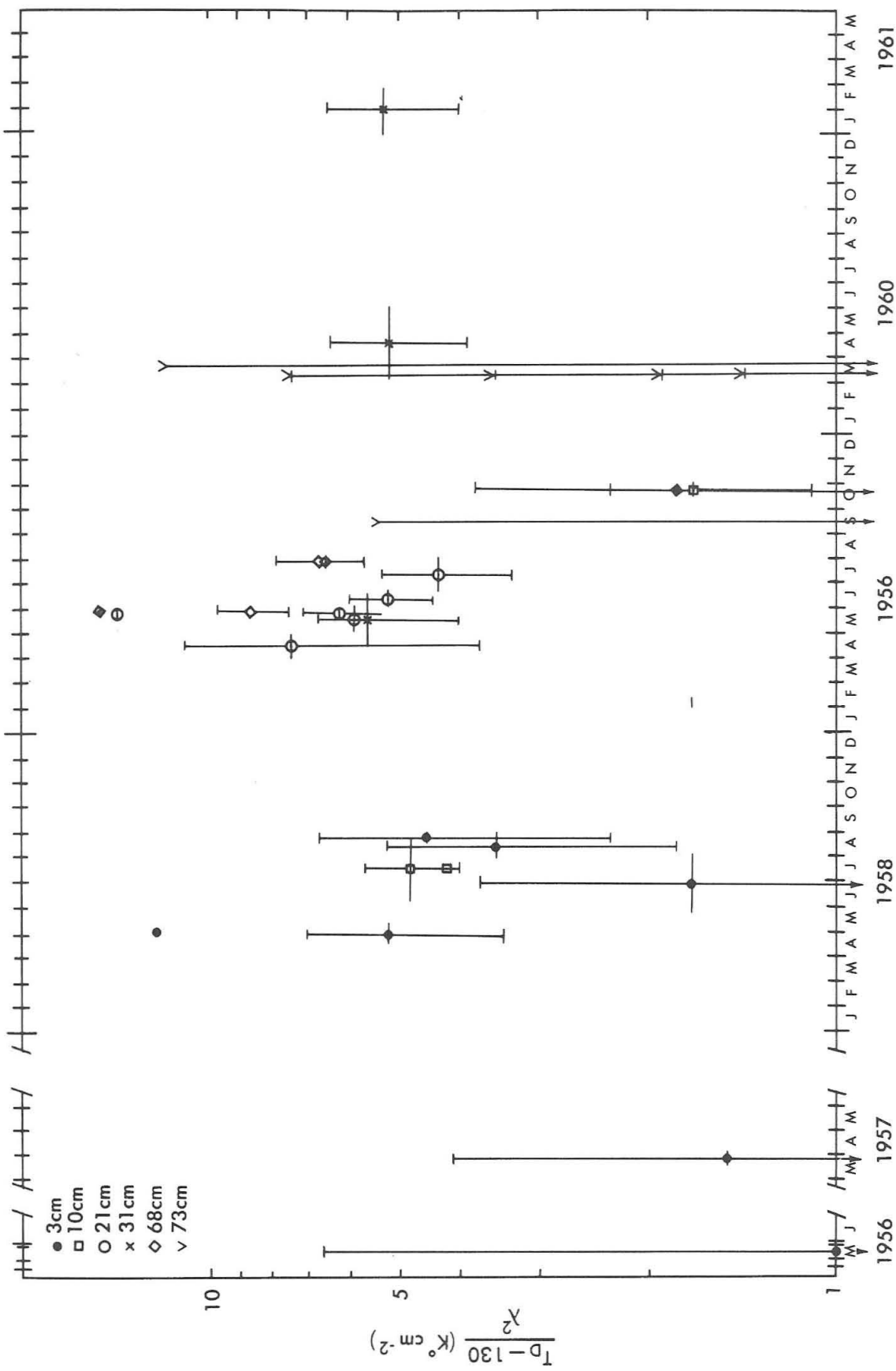

Figure 2. Observed radiation flux from Jupiter (corrected for a thermal emission of 130°K) vs. time of observation. (See Table III of Appendix A.)

other causes. Most noticeable in Figure 1 are the variations at 10 cm and 68 cm. More revealing in this connection is the graph of Figure 2 (patterned after a similar plot appearing in Field (1961)) in which the flux densities corrected for a thermal radiation of 130°K are plotted as a function of the time of observation. The low intensities measured at 10 cm and 68 cm correspond to observations made in October, 1959, and might suggest that the general level of the intensity changed in a time of the order of a few months. The three series of observations at 31 cm made in the middle of 1959, the middle of 1960 and the beginning of 1961 --- none were made in October, 1959 --- do not show any evidence of a long term variation. Some success seems to have been achieved in correlating short term variations (of the order of hours) with rotation of the planet, although these results are not conclusive. A complete picture of the variations must await the results of further observations.

In addition to the flux measurements, the polarization and the E-W angular extent of the radiation at 31 cm have been measured with a variable spacing interferometer by Radhakrishnan and Roberts (1960). The radiation was found to be strongly linearly polarized, the radiation with the electric vector parallel to the equatorial plane of the planet being approximately 1.7 times as intense as in the orthogonal polarization (giving a percentage polarization of $100 \left[\frac{1.7-1}{1.7+1} \right] \approx 26\%$). The

observations (which were made in April, 1960) were insufficient to determine a detailed distribution of intensity, but are consistent with an equatorial ring of mean diameter about three times the diameter of Jupiter. The polarization of these observations are represented schematically in Figure 3 (which has been copied from Davis and Chang (1961a)). In this figure the lengths of the double-ended arrows are proportional to the intensities observed for the radiation with electric vectors in the indicated directions.

To explain the relatively flat decimeter spectrum, theoretical investigations have been made of four possible sources: (1) thermal emission from a deep atmosphere with a thermal gradient [Field (1959); Giordmaine (1960)], (2) free-free transitions in an ionized atmosphere [Field (1959); Roberts and Stanley (1959)], (3) cyclotron radiation from nonrelativistic electrons in a Jovian Van Allen belt [Field (1959, 1960, 1961)], and (4) synchrotron radiation from relativistic electrons in a Jovian Van Allen belt [Drake and Hvatum (1959); Field (1959, 1960, 1961); Roberts and Stanley (1959); Davis and Chang (1961a); Kellogg, (1961)].

In investigating the thermal emission possibility, both Field (1959) and Giordmaine (1960) assumed the favorable case of an atmosphere with a steep adiabatic temperature gradient in which the only absorption is due to ammonia. Both concluded that, although thermal emission could account for a sizeable portion of the 3 cm radiation ---

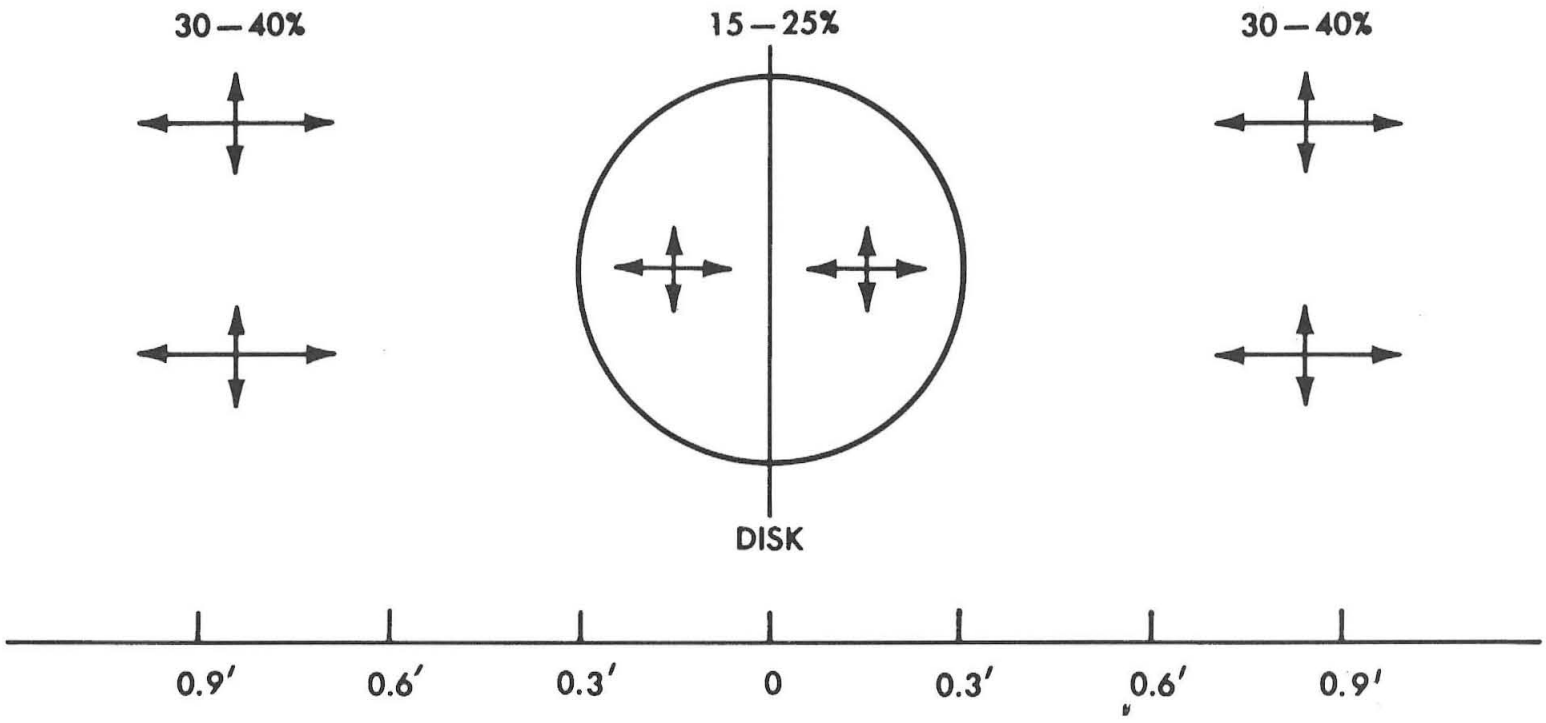

Figure 3. Schematic distribution of polarized 31cm radiation from Jupiter.

in fact, Giordmaine concluded that all of the 3 cm radiation could be explained in terms of thermal radiation, it could not explain the very high equivalent disk temperatures at the long wavelengths.

In investigating the free-free transition possibility, both Field (1959) and Roberts and Stanley (1959) found that if the radio emission were to originate from an area equal to that of the optical disk, quite a high value would be required for the integral of the square of the electron density over the thickness of the radiating region:

$$\int n_e^2 \, ds \gtrsim 10^{25} \text{ cm}^{-5} .$$

Roberts and Stanley explored the possibility that Jupiter could collect the required atmosphere from hot interplanetary material. They found that gravitational forces alone are insufficient, but remarked that a magnetic field might prove adequate.

Field discounted an ionospheric free-free transition source by combining the 10^{25} cm^{-5} figure with the results of observations made of radiation from Jupiter at wavelengths of around 20 meters. To date, apparently three types of radio emission have been recorded from Jupiter. Thermal emission and the relatively-flat-spectrum decimeter radiation comprise two, while the third type consists of bursts of radiation which last seconds or minutes and which occur only in a narrow band of frequencies between about 15 and 25 Mc/sec. Right-hand circular polarization has been reported for a number of bursts [Franklin

and Burke (1958)]. The bursts seem to originate in a small area, and the determination over a five year interval of the Jovian period of rotation from the bursts has indicated a quite constant period [Carr, Smith, Pepple, and Barrow (1958)]. This constancy has led to the suggestion that the source is rather close to the planet, possibly in the ionosphere --- and that the circular polarization is due to the propagation of only a single magneto-ionic mode through the ionosphere. According to Carr (1959), this polarization implies a magnetic field of about 7 gauss. Field concludes that for a magnetic field of this magnitude, the ionosphere required by the 10^{25} cm^{-5} figure is too dense to allow transmission of the 18 Mc/sec bursts. Field notes that high magnetic fields (600 gauss or more) would transmit the 18 Mc/sec bursts, but that then the particle flux necessary to maintain the ionosphere would not be able to penetrate the fields to do so. (Field estimates that the radiation flux from the sun is too small by a factor of 3000 to maintain an ionosphere of such high density at Jupiter.) A conclusive objection to both the thermal radiation and free-free transition sources is provided by the observations of polarization which were made after these sources were first proposed.

On the basis of the large amount of energy available in non-relativistic electrons from the sun, Field, until recently [Field (1961)], has favored an explanation of the radiation in terms of cyclotron radiation

from nonrelativistic electrons [Field (1959, 1960)]. However, this explanation requires an exceedingly high magnetic field: a polar field of 18,500 gauss, in order to have the 31 cm radiation originate at three Jovian radii. An even higher polar field on the order of 1.6×10^5 gauss is required if in addition a relatively flat frequency spectrum of $\lambda^{1/3}$ is desired [Field (1961)]. Such high fields imply a stiff field pattern with few fluctuations or irregularities that could produce diffusion or acceleration of the electrons; on the one hand, this suggests a very long time constant for variations in the radiation, and on the other hand, it is difficult to see how the solar wind could penetrate into such high field regions either to supply nonrelativistic electrons or to replenish the energy radiated by the trapped electrons. In his latest article, Field (1961) has ruled out his cyclotron model on the basis of the time variation at 10 and 68 cm. The cyclotron model predicts that for a variable flux, the spectrum is not flat but quite steep (varying as λ^p with $p \approx 4\ 1/3$).

The synchrotron radiation mechanism was first proposed by Drake. He suggested that the emission might emanate from relativistic particles trapped in the Jovian equivalent of the terrestrial Van Allen belts. It was estimated that a magnetic field in the radiating region of 5 gauss and a total number of particles 10^6 times greater than in the terrestrial system would suffice to explain the observations, this estimate being based on the assumption that the particle energy spectrum

was similar to the rather steep spectrum observed in the terrestrial Van Allen belts [Drake and Hvatum (1959), Drake (1961)]. Roberts and Stanley (1959) observed that if the energy distribution were the same at all points of the field, a distribution as steep as that ($\sim E^{-6}dE$) observed by Vernov et al. (1959) in the earth's Van Allen belt would lead to a very steep radio spectrum ($\sim \lambda^{5/2}$) instead of the relatively flat spectrum observed. They remarked that if the Jupiter radiation is synchrotron emission, either the energy distribution of the relativistic electrons is quite different from that in the earth's Van Allen belt, or the more energetic electrons are trapped in the stronger parts of the field. Assuming electrons present in a field of 7 gauss with the steep E^{-6} dE energy spectrum, they estimated the density of relativistic electrons required in a radiating region which subtended the same solid angle as Jupiter's disk and which had a thickness 1.4 times Jupiter's radius. A density of 10^{-2} electrons per cm^3 with energies greater than 1 Mev was obtained, a density which they estimated to exceed that in the earth's Van Allen belt by a factor $\sim 3 \times 10^4$.

Field (1959) discussed the number of relativistic electrons which could be expected from various sources. He estimated that the total observed radio emission is 5×10^{16} ergs sec^{-1}. Taking the source to be the size of Jupiter, this would correspond to an outward flux through a spherical surface of radius $R_J = 7.18 \times 10^9$ cm of $\sim 8 \times 10^{-5}$ ergs cm^{-2} sec^{-1}. Field estimated that at the earth, the upper limit on the

energy flux of electrons in the primary cosmic radiation is only 5 per cent of this figure; that the energy flux of secondary electrons leaving the top of the earth's atmosphere is only 4 per cent of this figure; and that the rate at which relativistic electrons from the sun are supplied to Jupiter's disk is 10^5 erg sec^{-1}, only 1/50 of the radio emission rate. Field concluded that these relativistic electron sources were not adequate. He decided, however, that the energy flux of nonrelativistic particles from the sun was adequate to account for the emission, but that a rather high efficiency would have to be postulated for any local acceleration process which would convert part of this flux to relativistic energies.

These considerations were made before the large angular extent of the radiating region was known. With a larger radiating region, the energy requirements are not as severe. The discovery of Radhakrishnan and Roberts that the 31 cm radiation from Jupiter is polarized and that the source is likely to be several times the diameter of the planet, led Davis to re-examine the synchrotron radiation possibility [Davis and Chang (1961a)]. Energy considerations were supplemented by considerations bearing on the containment, time scale and geometric aspects of the problem. Table I, taken from Davis and Chang (1961a), lists some relevant quantities calculated for uniform fields of 0.1, 1 and 10 gauss. The entries giving the electron density and the electron energy density are based on (1) an energy spectrum $n(E)dE = kE^{-1}dE$ between the

Table I. Quantities to be considered in connection with the energetics, containment and time variation aspects of the synchrotron radiation explanation. $E_c(\lambda)$, the critical energy for the wavelength λ, is the energy for which Schwinger's critical frequency is equal to c/λ.

Magnetic field B =		0.1 gauss	1 gauss	10 gauss
Critical energy E_c for radiation at wavelengths of: (in Mev)	3 cm	75	25	7.5
	30 cm	25	8	2.5
	300 cm	8	2.5	0.8
Time for energy to go from E_c(30 cm) to $\frac{1}{2}E_c$(30 cm) (in years)		30	1	1/30
Gyroradius for E_c(30 cm) (in km)		10	1/3	10^{-2}
No. of electrons per cm^3 if total volume is $10\,V_J$		2×10^{-2}	2×10^{-3}	2×10^{-4}
Electron energy per unit volume (erg cm^{-3})		8×10^{-7}	2.5×10^{-8}	8×10^{-10}
$\frac{B^2}{8\pi}$ (erg cm^{-3})		4×10^{-4}	0.04	4.0

critical energies* for wavelengths of 3 cm and 300 cm with sharp cut-offs beyond, (2) a source volume ten times that of Jupiter, $10 V_J$, and (3) a figure of 2.8×10^{16} erg/sec for the total synchrotron radiation power emitted by Jupiter at wavelengths greater than 3 cm. Magnetic fields on the order of 1 gauss look attractive: the relativistic electron energies required are not excessive; the time scales compare favorably with those of the observed variations, and it is not difficult to find reasonable combinations of wave velocities and interaction lengths which give characteristic Fermi acceleration times of this magnitude [Davis (1958)]; and finally, the fields are not so large that the solar wind cannot transfer energy to the fields for acceleration processes, but are large enough to contain the required densities of electrons.

While discussions based on uniform magnetic fields are sufficient to establish certain orders of magnitude, an investigation of the polarization and angular extent of the radiation requires some discussion of the actual field configuration and the distribution of electrons in this field. Davis has suggested that if Jupiter's field resembles that of a dipole, a large fraction of the radiating electrons might have to be in flat helices near the equatorial plane in order to give the observed polarization. The general idea is that electrons with steep helices would radiate most efficiently from regions of the field which are too close to

---

*See page 135.

the planet to give an extended source or for which the inclination of the magnetic field leads to the wrong polarization. Davis suggests that the observational result that the outer regions of the source are more strongly polarized than the central region might be explained if the equivalent of two shells of electrons are present, the outer shell comprising electrons with very flat helices and the inner shell having a somewhat larger proportion of its electrons in steeper helices. A more reasonable distribution is a thick shell with the proportion of steep helices rising as one goes inward.

The difficulties encountered by the thermal radiation, free-free transition, and cyclotron explanations, and the more favorable circumstances provided for the synchrotron source explanation by the recent observation of a large source region, have made it worthwhile to study in more detail the dipole model and the related problem of obtaining relativistic electrons in the desired spatial and energy distributions. This thesis presents the results of this study.*

Section II discusses the radiation from a shell of relativistic electrons trapped in a dipole field. Numerical calculations for this radiation are summarized in Appendix D. If it is assumed that Jupiter has a magnetic field resembling that of a dipole with axis near the axis of rotation, the results of section II and Appendix D show that a large

---

*Some of these results appear elsewhere: Chang (1960), Davis and Chang (1961a), Davis and Chang (1961b).

portion of the electrons must be confined near the equatorial plane in order for the synchrotron radiation to give the observed polarization. In section III the problem of obtaining relativistic electrons in this type of spatial distribution is discussed. Investigation of a model describing the effects of large scale magnetic fluctuations on trapped electrons yields some encouraging results. A summary of the results is presented in section IV.

The results of a more general nature are presented in Appendices B and C. In Appendix B, the properties of synchrotron radiation are discussed: A Stokes parameter description is developed for the radiation from a group of ultrarelativistic particles with arbitrary energy and angular distributions. This treatment provides the basis for the discussion of the dipole field model in section II. In Appendix C, the asymptotic approximation method of Bogolyubov and Zubarev is used to obtain a systematic derivation of relativistic drift velocities. These drift velocities play an important role in the diffusion model investigated in section III.

II. SYNCHROTRON RADIATION FROM ULTRARELATIVISTIC ELECTRONS IN A DIPOLE FIELD

The Stokes parameter description of synchrotron radiation developed in Appendix B is applied here to describe the radiation from ultrarelativistic electrons trapped in a dipole field.* A complete definition of the Stokes parameters is given on page 138 of Appendix B. Briefly, I measures the total intensity, V' the amount of elliptical polarization, and Q and U the amount and orientation of the plane polarized component. Q and U are defined in terms of the intensity, $\mathcal{I}(\eta)$, passed by a receiver that measures only the plane polarized component whose electric vector makes a specified angle η with an appropriately selected reference direction. Then $Q = \mathcal{I}(0°) - \mathcal{I}(90°)$ and $U = \mathcal{I}(45°) - \mathcal{I}(135°)$. If the source has a known plane of symmetry and this is used as the zero for η, then U should be zero and the classical degree of polarization is $p = |Q/I|$, the plane of polarization being $\eta = 0°$ if $Q > 0$ and $\eta = 90°$ if $Q < 0$.

In the frequency range df at f, the Stokes parameters of the synchrotron radiation from ultrarelativistic electrons in the differential volume dV are:

---

*The results of Appendix B are summarized in Table IV on page 145 and in Table V on pages 154-156.

$$I(f)dVdf = \frac{CBdVdf}{R^2} \int \rho(E,\alpha^*)F\left(\frac{f}{f_c^*}\right)\,dE \qquad (1)$$

$$Q(f)dVdf = -\frac{CB\cos 2\chi dVdf}{R^2} \int \rho(E,\alpha^*)F_p\left(\frac{f}{f_c^*}\right)\,dE \qquad (2)$$

$$U(f)dVdf = -\frac{CB\sin 2\chi\, dVdf}{R^2} \int \rho(E,\alpha^*)F_p\left(\frac{f}{f_c^*}\right)\,dE \qquad (3)$$

$$V'(f)dVdf = 0 \quad . \qquad (4)$$

The meanings of the various symbols are given below. R is the distance from the differential source volume dV to the observer; B is the magnetic field intensity at the source; $\rho(E,\alpha)dVdEd\alpha$ is the number of electrons in the volume dV with energies in the range dE at E and helix angles in the range $d\alpha$ at α (where an electron's helix angle α is the angle between the magnetic field $\vec{B}$ and the electron's velocity); α^* is the angle between the magnetic field and a (unit) vector $\vec{i}$ directed toward the observer. The angle χ is the angle measured clockwise by the observer from the (arbitrary) coplanar vector $\vec{i}_\ell$ involved in the definition of the Stokes parameters to the projection of the magnetic field onto a plane at right angles to the line of sight --- i.e., QdV is the part of the intensity IdV with electric vector along the direction $\vec{i}_\ell$ minus the part of IdV with electric vector along the direction $\vec{i}_r = \vec{i}_\ell \times \vec{i}$.

The functions F and F_p are given by

$$F\left(\frac{f}{f_c^*}\right) = \frac{f}{f_c^*} \int_{\frac{f}{f_c^*}}^{\infty} K_{\frac{5}{3}}(\eta)\, d\eta \qquad (5)$$

and

$$F_p\left(\frac{f}{f_c^*}\right) = \frac{f}{f_c^*}\, K_{\frac{2}{3}}\left(\frac{f}{f_c^*}\right) \quad , \qquad (6)$$

in which $K_{\frac{2}{3}}$ and $K_{\frac{5}{3}}$ are modified Bessel functions of the second kind, and

$$f_c^* = LB \sin \alpha^* E^2 \quad . \qquad (7)$$

The constants C and L have the values:

$$C = 3.73 \times 10^{-23} \text{ erg sec}^{-1} \text{gauss}^{-1}$$

$$L = 1.608 \times 10^{13} \text{ sec}^{-1} \text{gauss}^{-1} \text{Bev}^{-2} \quad .$$

The foregoing equations indicate that the parameters of the radiation from a differential volume dV in the dipole field may be evaluated providing that 1° the magnetic field B, 2° the angle α^*, 3° the angle χ, and 4° the distribution function $\rho(E, \alpha^*)$ are known. The first three quantities are simply matters of geometry, while the fourth depends on the way in which the electrons are injected into the field and on their subsequent motion in the field. The differential volume dV may be selected arbitrarily, but a proper choice simplifies

the integration over the volume to give the total intensity; the behavior of an electron in a magnetic field provides a guide in this choice.

IIA. Geometry

Consider first the geometry. The coordinate system adopted is shown in figure 4. The dipole is taken to lie normal to the line of sight. The unit vector $\vec{i}_r$ has been taken along the dipole. The unit vector $\vec{i}$ is directed toward the observer, and $\vec{i}_\ell = \vec{i} \times \vec{i}_r$ is in the equatorial plane. Polar coordinates (r, θ, ϕ) are employed; the length ℓ shown is the projection of r onto the $\vec{i}_\ell$ direction. A "planet" of radius R_J is shown centered at the origin.

The magnetic field line which runs through the point (r, θ, ϕ) intersects the equatorial plane $(\theta = \frac{\pi}{2})$ at the radius r_E, where

$$r_E = \frac{r}{\sin^2\theta} \quad . \tag{8}$$

The line intersects the planet at the colatitude θ_J, where

$$\theta_J = \sin^{-1}\left(\left(\frac{R_J}{r_E}\right)^{\frac{1}{2}}\right) \quad . \tag{9}$$

In terms of $B(r_E, \frac{\pi}{2})$, the field at the radius r_E in the equatorial plane, the field at (r, θ, ϕ) is

$$B(r,\theta) = B(r_E, \tfrac{\pi}{2}) \quad \frac{(1 + 3\cos^2\theta)^{1/2}}{\sin^6\theta} \quad , \tag{10}$$

ϕ having been dropped in the argument because of the symmetry.

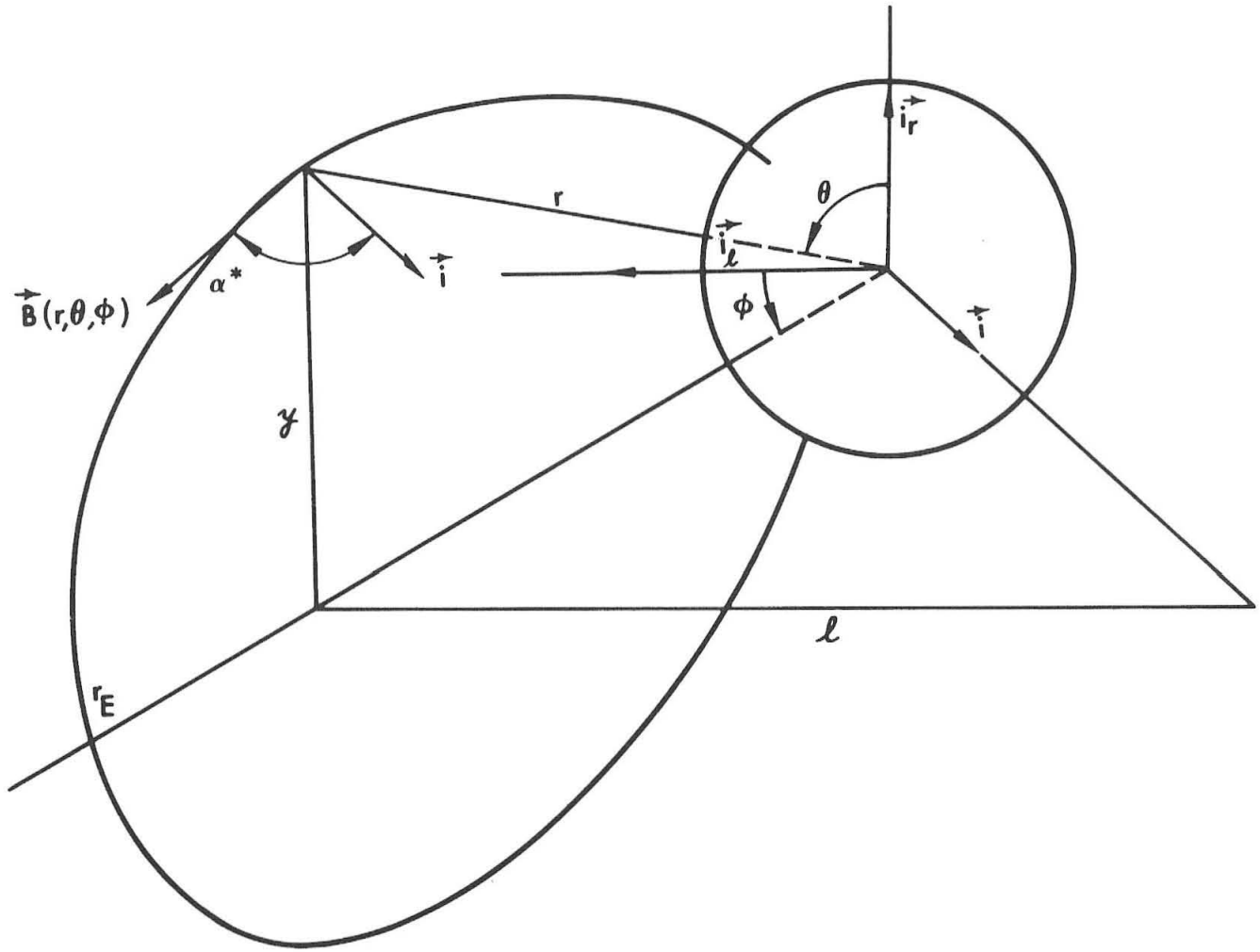

Figure 4. Coordinate system for describing synchrotron radiation from electrons in a dipole field. The unit vector $\vec{i}$ is directed towards the observer; $\vec{i}_r$ is directed along the dipole, and $\vec{i}_\ell = \vec{i} \times \vec{i}_r$. A spherical planet is shown centered at the dipole.

$B(r_E, \frac{\pi}{2})$ is related to $B(R_J, \frac{\pi}{2})$, the field at the equator of the planet, by the equation

$$B(r_E, \tfrac{\pi}{2}) = B(R_J, \tfrac{\pi}{2}) \left(\frac{R_J}{r_E}\right)^3 \quad . \tag{11}$$

The angle α^* is $\frac{\pi}{2}$ all along the field lines which lie in the plane at right angles to the line of sight ($\phi = 0$, $\phi = \pi$), and is $\frac{\pi}{2}$ for all field lines where they cross the equatorial plane ($\theta = \frac{\pi}{2}$). At a general θ and ϕ, it is given by:

$$\cos \alpha^* = \frac{\vec{i} \cdot \vec{B}}{B} = \frac{3 \sin\theta \cos\theta \sin\phi}{(1 + 3\cos^2\theta)^{1/2}} \tag{12}$$

and

$$\sin \alpha^* = \frac{(1 + 3\cos^2\theta - 9 \sin^2\theta \cos^2\theta \sin^2\phi)^{1/2}}{(1 + 3\cos^2\theta)^{1/2}} \quad . \tag{13}$$

The quantities $\cos 2\chi$ and $\sin 2\chi$ entering into the second and third Stokes parameters may be found from the relations:

$$\cos 2\chi = 2\left[\frac{\vec{i}_\ell \cdot (\vec{i} \times \vec{B}) \times \vec{i}}{B \sin \alpha^*}\right]^2 - 1 = \frac{1}{B^2 \sin^2 \alpha^*}[(\vec{i}_\ell \cdot \vec{B})^2 - (\vec{i}_r \cdot \vec{B})^2] \tag{14}$$

and

$$\sin 2\chi = 2\left[\frac{\pm[\vec{i}_r \cdot (\vec{i} \times \vec{B}) \times \vec{i}]}{B \sin a^*}\right]\left[\frac{\pm[\vec{i}_\ell \cdot (\vec{i} \times \vec{B}) \times \vec{i}]}{B \sin a^*}\right] \tag{15}$$

$$= \frac{2}{B^2 \sin^2 a^*} (\vec{i}_r \cdot \vec{B})(\vec{i}_\ell \cdot \vec{B}) \quad .$$

For the dipole field,

$$\frac{\vec{i}_\ell \cdot \vec{B}}{B} = \frac{3 \sin\theta \cos\theta \cos\phi}{(1 + 3\cos^2\theta)^{1/2}} \tag{16}$$

and

$$\frac{\vec{i}_r \cdot \vec{B}}{B} = \frac{3\cos^2\theta - 1}{(1 + 3\cos^2\theta)^{1/2}} \quad ; \tag{17}$$

so that

$$\cos 2\chi = \frac{1}{\sin^2 a^*}\left[\frac{9 \sin^2\theta \cos^2\theta (1 + \cos^2\phi) - (1 + 3\cos^2\theta)}{(1 + 3\cos^2\theta)}\right]$$

$$= \frac{-9 \sin^2\theta\cos^2\theta(1 + \cos^2\phi) + (1 + 3\cos^2\theta)}{9 \sin^2\theta \cos^2\theta \sin^2\phi \quad - (1 + 3\cos^2\theta)} \tag{18}$$

and

$$\sin 2\chi = \frac{1}{\sin^2 a^*}\left[6 \sin\theta \cos\theta \cos\phi \, \frac{(3\cos^2\theta - 1)}{(3\cos^2\theta + 1)}\right]$$

$$= \frac{6 \sin\theta \cos\theta \cos\phi (3\cos^2\theta - 1)}{1 + 3\cos^2\theta - 9 \sin^2\theta \cos^2\theta \sin^2\phi} \quad . \tag{19}$$

It is convenient to take the differential volume dV to be that along a tube of flux, since the trajectory of an electron traversing a region of the magnetic field with a small gradient encloses a constant flux. If at (r, θ, ϕ) the cross section of a tube of flux is $dA(r, \theta)$ and the differential distance along the tube is $ds(r, \theta)$, then

$$dV(r,\theta) = dA(r,\theta)\, ds(r,\theta) \quad . \tag{20}$$

The cross sectional areas at any two points along the tube of flux are related by the condition that $B(r,\theta)dA(r,\theta)$ is a constant along the tube. Thus, $dA(r,\theta)$ can be expressed in terms of $dA(r_E, \frac{\pi}{2})$, the cross sectional area in the equatorial plane. Expressing the latter as

$$dA\left(r_E, \frac{\pi}{2}\right) = r_E\, dr_E\, d\phi \quad , \tag{21}$$

we have,

$$dA(r,\theta) = \frac{B\left(r_E, \frac{\pi}{2}\right) r_E\, dr_E\, d\phi}{B(r,\theta)}$$

$$= \frac{\sin^6\theta\, r_E\, dr_E\, d\phi}{(1+3\cos^2\theta)^{1/2}} \quad . \tag{22}$$

Since the differential arc length ds is

$$ds(r,\theta) = r_E \sin\theta(1+3\cos^2\theta)^{1/2}\, d\theta \quad , \tag{23}$$

this gives

$$dV(r,\theta) = r_E^2 \sin^7\theta d\theta d\phi dr_E \quad . \tag{24}$$

The volume decreases considerably as the polar regions are approached.

An additional geometrical factor which may be taken into account is the obscuration of the radiating region by the planet. The planet lies between the observer and the radiating region when both of the following hold:

$$\sin^2\theta(1 - \sin^2\theta \sin^2\phi)^{1/2} < \frac{R_J}{r_E}$$

$$\pi < \phi < 2\pi \quad . \tag{25}$$

IIB. Distribution of Electrons Along a Tube of Flux

Neglecting scattering, Liouville's theorem may be applied to express the distribution density of electrons at any point along a line of force in terms of the distribution density at the point where the line of force intersects the equatorial plane. Since we have $\rho(\vec{r}, E, \alpha)d\alpha dE dV$ particles in the range indicated and since their directions of motion occupy a solid angle $2\pi \sin\alpha \, d\alpha$, then if the distribution has cylindrical symmetry about a line of force, the associated flux density per unit solid angle is $\rho/2\pi v \sin\alpha$, where v is the velocity. Assuming that there is no change in energy, v is constant. Appealing to the well-known theorem (a consequence of Liouville's theorem) that the flux per unit solid angle in any beam of noninteracting charged particles in a static magnetic field remains constant, we have

$$\frac{D}{Dt}\left[\frac{\rho}{\sin\alpha}\right] = 0 \quad , \tag{26}$$

where $\frac{D}{Dt}$ denotes the total time derivative. In other words, a particle sees the same value of $\rho(\vec{r}, E, \alpha)/\sin\alpha$ in all regions accessible to it. The adiabatic invariant

$$\frac{\sin^2\alpha}{B} = \text{const.} \tag{27}$$

defines these accessible regions. Thus, if the distribution density at the equator is $\rho\left((r_E, \frac{\pi}{2}) E, \alpha_E\right)$ --- it will be assumed that particle

drifts result in azimuthal symmetry so that ϕ need not be specified --- then, with $r_E = r \sin^{-2}\theta$,

$$\rho\left((r,\theta),E,\alpha\right) = \frac{\rho\left((r_E,\frac{\pi}{2}),E,\alpha_E = \sin^{-1}\left(\sqrt{\frac{B(r_E,\frac{\pi}{2})}{B(r,\theta)}}\sin\alpha\right)\right)}{\sqrt{\frac{B(r_E,\frac{\pi}{2})}{B(r,\theta)}}}$$

$$\cdot \frac{(1+3\cos^2\theta)^{1/4}}{\sin^3\theta}\ \rho\left(\left(\frac{r}{\sin^2\theta},\frac{\pi}{2}\right),E,\alpha_E = \sin^{-1}\left(\frac{\sin^3\theta\sin\alpha}{(1+3\cos^2\theta)}^{1/4}\right)\right) . \tag{28}$$

As an example, suppose that

$$\rho\left(r_E,\frac{\pi}{2}\right),E,\alpha_E = \begin{cases} N(r_E,E)\sin^p\alpha_E & \text{if } \alpha_L \le \alpha_E \le \pi - \alpha_L \\ 0 & \text{otherwise ,} \end{cases} \tag{29}$$

(where, for instance, α_L might be determined by the condition that particles with $\sin\alpha < \sin\alpha_L$ would collide with the planet and be absorbed, i.e.,

$$\sin^2\alpha_L = \frac{B(r_E,\frac{\pi}{2})}{B(R_J,\theta_J)} \cdot \frac{\sin^6\theta_J}{1+3\cos^2\theta_J)^{1/2}} = \frac{R_J{}^3/r^3{}_E}{(4-3R_J/r_E)^{1/2}} . \tag{30}$$

Then

$$\rho\left((r,\theta),E,\alpha\right) = \begin{cases} 0 & \text{if } \sin^2\alpha < \dfrac{B(r,\theta)}{B(r_E,\frac{\pi}{2})}\sin^2\alpha_L \\ N(r_E,E)\left[\dfrac{B(r_E,\frac{\pi}{2})}{B(r,\theta)}\right]^{\frac{p-1}{2}}\sin^p\alpha & \text{otherwise} \end{cases} \tag{31}$$

i.e.,

$$\rho\left((r,\theta),E,\alpha\right) = \begin{cases} 0 & \text{if } \sin^2\alpha < \dfrac{(1+3\cos^2\theta)^{1/2}}{\sin^6\theta}\sin^2\alpha_L \\ N\left(\dfrac{r}{\sin^2\theta},E\right)\dfrac{\sin^{3(p-1)}\theta\,\sin^p\alpha}{(1+3\cos^2\theta)^{\frac{p-1}{4}}} & \text{otherwise} \end{cases} \tag{32}$$

The angular and energy distributions are the same all along the line of force, except for the cutoffs for the former. The spatial density is not necessarily constant; in fact, only when $p = 1$ and $\alpha_L = 0$, i.e., when the velocity distribution is isotropic, is the spatial density constant along a line of force. If $p = 1$, but $\alpha_L > 0$, the density decreases as the polar regions are approached. Also, if steeper helices are favored ($p > 1$), the density decreases towards the poles.

IIC. Radiation from a Thin Shell of Electrons

The only quantity which remains to be specified before the radiation is determined is the distribution density function at the equator, $\rho((r_E, \frac{\pi}{2}), E, a_E)$. This will depend on the particular source assumed for the radiating electrons, and we shall have to discuss the injection and acceleration details of the source. Before doing this, however, we consider in this section the properties of the radiation originating from a thin shell of electrons. More specifically, we take

$$\rho((r_E, \tfrac{\pi}{2}), E, a_E) = \begin{cases} \dfrac{\eta(E)\sin a_E}{R_E \delta R_E} & R_E < r_E < R_E + \delta R_E \\ & \text{and} \\ & \sin a_E > \sin a_L \\ 0 & \text{otherwise} \end{cases} , \qquad (33)$$

where $\dfrac{\delta R_E}{R_E} \ll 1$. This is a distribution which at the colatitude θ is isotropic for helix angles a between the cut offs $a_1(\theta)$ and $\pi - a_1(\theta)$, where

$$\sin a_1(\theta) = \frac{(1 + 3\cos^2\theta)^{1/4}}{\sin^3\theta} \sin a_L \qquad (34)$$

Some relatively easily calculable functions are obtained by taking three special cases* of $\eta(E)$:

(i) $$\eta(E) = C_1 \delta(E - E_0) \qquad (35)$$

(ii) $$\eta(E) = C_1 E^{-(\gamma+1)} \qquad (36)$$

---

*See page 151 of Appendix B.

$$\text{(iii)} \qquad \eta(E) = \begin{cases} C_1 E^{-\frac{5}{3}} & E_{min} < E < E_{max} \\ 0 & \text{otherwise} \end{cases} . \qquad (37)$$

The first case gives rise to expressions containing trigonometric functions and the tabulated functions $F(x) = x \int_x^\infty K_{\frac{5}{3}}(x)dx$ and $F_p(x) = xK_{\frac{2}{3}}(x)$. The second case is expressible entirely in terms of trigonometric functions. The third case gives rise to expressions containing trigonometric functions and the tabulated functions $G^W(x) = \frac{3}{2}x^{\frac{1}{3}}K_{\frac{1}{3}}(x) - \frac{3}{4}x^{\frac{1}{3}}[F(x)-F_p(x)]$ and $G_p^W(x) = x^{\frac{1}{3}}K_{\frac{1}{3}}(x)$. Case (i) enables one to determine, by superposition, the radiation produced by any specified energy distribution; cases (ii) and (iii) are chosen to resemble distributions associated with galactic and solar cosmic rays and the relativistic electrons responsible for radio noise in other sources.

The calculation of the Stokes parameters for these distributions is straightforward. It is apparent that in addition to the fourth Stokes parameter $V'(f)dV$ being zero (eq. 4), the parameter obtained by integrating $U(f)dV$ over any region symmetric about $\phi = \frac{\pi}{2}$ is also zero. This is due to the combined effect of the symmetry of the field and the presence of the factor $\sin 2\chi$ in the expression for $U(f)dV$. Consequently, we calculate only the first and second Stokes parameters. Also, because of the symmetry, it is necessary to integrate only over one octant of the shell if the effect of shielding is taken care of properly.

The expressions for the first two Stokes parameters of the radiation originating from the region of the field contained between the planes ℓ_1, and $\ell_2 > \ell_1$ and between the planes $-\ell_1$ and $-\ell_2$ (where $\ell = r \sin\theta \cos\phi = r_E \sin^3\theta \cos\phi$) are summarized in Table II for cases (i) - (iii).* In each of the three cases, the expressions are in the form of a double integral over θ and ϕ of integrands which are zero when either condition I or condition II holds. Condition I expresses the fact that only the radiation originating from the region between the planes ℓ_1 and $\ell_2 > \ell_1$, and between $-\ell_1$ and $-\ell_2$ is being described. Condition II accounts for the variation of the cut-off helix angle $\alpha_1(\theta)$ with θ, the ϕ dependence arising from the fact that only those electrons with helix angles very close to α^* radiate. Provision for the obscuration of the radiating region by the planet is obtained by the factor $\frac{1}{2}$ in the integrand whenever $\sin^4\theta(1 - \sin^2\theta \sin^2\phi) \leq \left(\frac{R_J}{r_E}\right)^2$. It is assumed in the expressions that α_L has been selected so that no electrons collide with the planet. The integrands also depend on θ and ϕ through the variation with position of the density distribution function $\rho(E, \alpha^*)$, the volume element dV, the orientation of the field --- as described by the angles χ and α^*, the field intensity B, and the dependence of the radiation efficiency on the latter two.

---

*The brightness pattern in the $y = r\cos\theta = r_E \sin^2\theta\cos\theta$ (polar) direction can be obtained from the table simply by replacing condition I there by "$r_E \sin^2\theta\cos\theta < y_1$ or $r_E \sin^2\theta\cos\theta > y_2$," and replacing the remaining ℓ's by y's.

TABLE II. FIRST AND SECOND STOKES PARAMETERS FOR SYNCHROTRON RADIATION FROM A DIPOLE FIELD.

The table lists expressions for the contributions of electrons in the strips.*

$$\ell_1 \leq \left| r_E \sin^3\theta \cos\phi \right| \leq \ell_2 .$$

(See Fig. 4) for an equatorial distribution function

$$\rho((r_E, \tfrac{\pi}{2}), E, \alpha_E) = \begin{cases} \dfrac{\eta(E)\sin\alpha_E}{2\cos\alpha_L R_E \delta R_E} & \text{if } R_E < r_E < R_E + \delta R_E \text{ and } \sin\alpha_E > \sin\alpha_L , \\ 0 & \text{otherwise} \end{cases}$$

where $\dfrac{\delta R_E}{R_E} \ll 1$.

The expressions contain the functions $\xi(\theta,\phi)$ and $u(\theta,\phi)$:

$$\xi(\theta,\phi) = G \sin^6\theta \left[1 + 3\cos^2\theta - 9\sin^2\theta\cos^2\theta\sin^2\phi\right]^{-\frac{1}{2}}$$

$$u(\theta,\phi) = \begin{cases} 0 & \text{when either condition I or condition II holds} \\ \dfrac{1}{2} & \text{when neither condition I nor condition II holds and } \sin^4\theta(1-\sin^2\theta\sin^2\phi) \leq \left(\dfrac{R_J}{r_E}\right)^2 \\ 1 & \text{when neither condition I nor condition II holds and } \sin^4\theta(1-\sin^2\theta\sin^2\phi) > \left(\dfrac{R_J}{r_E}\right)^2 \end{cases}$$

where

condition I: $r_E \sin^3\theta\cos\phi < \ell_1$ or $r_E \sin^3\theta\cos\phi > \ell_2$

*See the footnote on page 31.

condition II: $$\frac{\sin^3\theta[1 + 3\cos^2\theta - 9\sin^2\cos^2\theta\sin^2\phi]^{\frac{1}{2}}}{(1 + 3\cos^2\theta)^{3/4}} < \sin\alpha_L$$

The constants G, A_I, A_{II} and A_{III} are defined:

$$G = \frac{fR_E^3}{LE^2B(R_J, \frac{\pi}{2})R_J^3} \; ; \quad A_I = \frac{2CC_1B(R_J, \frac{\pi}{2})R_J^3}{\pi R^2 R_E^2}$$

$$A_{II} = \frac{2}{\pi}^{\frac{\gamma-8}{2}} \frac{(\gamma+\frac{10}{3})}{(\gamma+2)} \Gamma(\tfrac{3\gamma+2}{12}) \Gamma(\tfrac{3\gamma+10}{12}) \frac{CC_1L^{\frac{\gamma}{2}}}{f^{\frac{\gamma}{2}}}$$

$$\frac{[B(R_J, \frac{\pi}{2})]^{\frac{\gamma+2}{2}} R_J^{\frac{3}{2}(\gamma+2)}}{\cos\alpha_L R^2 R_E^{\frac{3\gamma+4}{2}}}$$

$$A_{III} = \frac{CC_1L^{1/3}[B(R_J, \frac{\pi}{2})]^{\frac{4}{3}} R_J^4}{8\pi f^{1/3}\cos\alpha_L R^2 R_E^2}$$

CASE (i) $\eta(E) = C_1\delta(E-E_o)$

$$I(\ell_1\ell_2) = A_I \int_o^{\frac{\pi}{2}}\int_o^{\frac{\pi}{2}} u(\theta,\phi)(1+3\cos^2\theta-9\sin^2\theta\cos^2\theta\sin^2\phi)^{1/2}\sin\phi \; F(\xi(\theta,\phi))d\theta d\phi$$

$$Q(\ell_1,\ell_2) = A_I \int_o^{\frac{\pi}{2}}\int_o^{\frac{\pi}{2}} u(\theta,\phi)\frac{[1+3\cos^2\theta-9\sin^2\theta\cos^2\theta(1+\cos^2\phi)]\sin\theta}{[1+3\cos^2\theta-9\sin^2\theta\cos^2\theta\sin^2\phi]^{1/2}} \; F_p(\xi(\theta,\phi)d\theta d\phi$$

where

$$F(\xi) = \xi \int_{\xi}^{\infty} K_{\frac{5}{3}}(x)dx \; ; \qquad F_p(\xi) = \xi K_{\frac{2}{3}}(\xi)$$

CASE (ii) $\eta(E) = C_1 E^{-(\gamma-1)}$

$$I(\ell_1,\ell_2) = A_{II} \int_0^{\frac{\pi}{2}} \int_0^{\frac{\pi}{2}} u(\theta,\phi) \frac{[1+3\cos^2\theta-9\sin^2\theta\cos^2\theta\sin^2\phi]^{\frac{\gamma+2}{4}}}{(\sin\theta)^{3\gamma-1}} d\theta d\phi$$

$$Q(\ell_1,\ell_2) = \frac{\gamma+2}{\gamma+\frac{10}{3}} A_{II} \int_0^{\frac{\pi}{2}} \int_0^{\frac{\pi}{2}} u(\theta,\phi) \frac{[1+3\cos^2\theta-9\sin^2\theta\cos^2\theta(1+\cos^2\phi)]}{[1+3\cos^2\theta-9\sin^2\theta\cos^2\theta\sin^2\phi]^{\frac{2-\gamma}{4}}(\sin\theta)^{3\gamma-1}}$$

$$d\theta d\phi$$

CASE (iii) $\eta(E) = \begin{cases} C_1 E^{-5/3} & E_{min} < E < E_{max} \\ 0 & \text{otherwise} \end{cases}$

$$I(\ell_1,\ell_2) = A_{III} \int_0^{\frac{\pi}{2}} \int_0^{\frac{\pi}{2}} u(\theta,\phi) \frac{[1+3\cos^2\theta-9\sin^2\theta\cos^2\theta\sin^2\phi]^{2/3}}{\sin\theta}$$

$$\left[G^W(\xi_{min}(\theta,\phi)) - G^W(\xi_{max}(\theta,\phi))\right] d\theta d\phi$$

$$Q(\ell_1,\ell_2) = A_{III} \int_0^{\frac{\pi}{2}} \int_0^{\frac{\pi}{2}} u(\theta,\phi) \frac{[1+3\cos^2\theta-9\sin^2\theta\cos^2\theta(1+\cos^2\phi)]}{[1+3\cos^2\theta-9\sin^2\theta\cos^2\theta\sin^2\phi]^{1/3}\sin\theta}$$

$$\left[G_p^W(\xi_{min}(\theta,\phi)) - G_p^W(\xi_{max}(\theta,\phi))\right] d\theta d\phi$$

where

$$G_p^W(\xi) = \xi^{1/3} K_{\frac{1}{3}}(\xi)$$

$$G^W(\xi) = \frac{3}{2}\xi^{1/3} K_{\frac{1}{3}}(\xi) - \frac{3}{4}\xi^{4/3}\left[\int_{\xi}^{\infty} K_{\frac{5}{3}}(x)dx - K_{\frac{2}{3}}(\xi)\right]$$

($\xi_{min}(\theta,\phi)$ and $\xi_{max}(\theta,\phi)$ are $\xi(\theta,\phi)$ evaluated for $E = E_{max}$ and $E = E_{min}$, respectively)

The Fourier cosine transform of a Stokes parameter is more closely related to radio interferometric measurements than the parameter itself [Brown and Lovell (1957)]. The cosine transform with respect to the (equatorial) variable $\ell = r \sin\theta \cos\phi$ of the parameters listed in Table II are obtained simply by multiplying the integrands by

$$\cos k\ell = \cos [k r_E \sin^3\theta \cos\phi] \tag{38}$$

and setting $\ell_1 = 0$, $\ell_2 = r_E$. Similarly, the cosine transforms with respect to the polar dimension $y = r \cos\theta$ are obtained by multiplying the integrands by

$$\cos ky = \cos [k r_E \sin^2\theta \cos\theta] \tag{39}$$

and setting $\ell_1 = 0$, $\ell_2 = r_E$.

The integrals of Table II have been evaluated on a Boeing IBM 7090 computer for the ten strips $\frac{\ell_1}{r_E} = \frac{\ell_2}{r_E} - \frac{1}{10} = \frac{j}{10}$ $(j = 0,1,\ldots,9)$, and for $\sin\alpha_L = 0.15$, 0.4, 0.7. In the calculations, the equatorial radius of the shell has been set equal to three times the radius of the planet, $r_E = 3R_J$. The limiting mirror points for $\sin\alpha_L = 0.15$, 0.4 and 0.7 are shown in Figure 5, in which are plotted some lines of force in the dipole shell $r_E = 3 R_J$ as seen from a direction perpendicular to the dipole. In case (i), the parameter G entering into the argument $\xi(\theta,\phi)$ of the radiation efficiency functions $F(\xi)$ and $F_p(\xi)$ has been set equal to 0.01, 0.1, 1.0 and 10. The parameter G is the value of ξ for

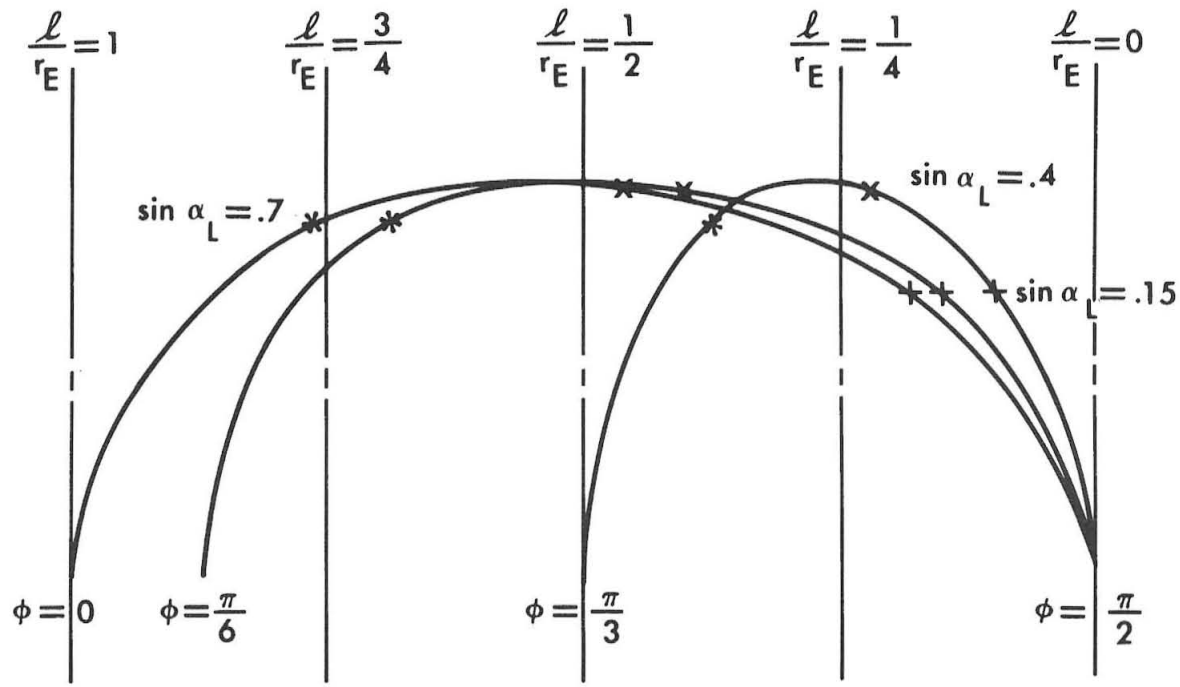

Figure 5. Some lines of force in a dipole shell as seen from a direction perpendicular to the dipole. The limiting mirror points for $\sin \alpha_L = .15$, .4 and .7 are indicated.

electrons in the equatorial plane; the parameter G depends on the observed frequency f, the magnetic field where the shell crosses the equatorial plane and the energy E_o of the source electrons. In case (ii), the parameter γ defining the steepness of the electron energy spectrum has been set equal to 0, 2 and 4; and in case (iii), the pair (ξ_{min}, ξ_{max}) which defines the upper and lower cutoffs of the energy spectrum, has been determined by setting the corresponding pair (G_{min}, G_{max}) equal to the ten ordered pairs which can be formed from the numbers 0.01, 0.1, 1.0 and 1000. In addition to the first and second Stokes parameters, the Fourier cosine transforms corresponding to equations 38 and 39 have also been evaluated for these examples, with the transform variable k equal to 0, 1/3, 2/3, 1, 3/2 and 2.

The computer results are displayed in graphical form in Figures 12 through 20 in Appendix D. Figures 12-14 apply to case (i). Figure 12 displays the first and second Stokes parameters and the percentage polarization; more specifically, the figure consists of histograms of I/A_I, Q/A_I and $p = \frac{Q}{I}$ vs. $\frac{\ell}{r_E} = \sin^3\theta \cos\phi$ (where the symbols have the meanings assigned in TableII). In Figure 13 are plotted the normalized cosine transforms $\mathcal{I}_\ell = \int_0^\infty \frac{I}{A_I} \cos k\ell \, d\ell$ and $\mathcal{Q}_\ell = \int_0^\infty \frac{Q}{A_I} \cos k\ell \, d\ell$, and the degree of polarization based on the transforms $p_\ell = \frac{\mathcal{Q}_\ell}{\mathcal{I}_\ell}$.

Figure 14 presents the transform results with respect to the polar direction; i.e., in this figure are plotted the cosine transforms $\mathcal{I}_y = \int_0^\infty \frac{I}{A_I} \cos kydy$ and $Q_y = \int_0^\infty \frac{Q}{A_I} \cos kydy$ and the degree of polarization $p_y = Q_y/\mathcal{I}_y$, where $y = r \cos\theta = r_E \sin^2\theta\cos\theta$. Figures 15-17 and Figures 18-20 are the analogous plots for cases (ii) and (iii), respectively.

For the details of the way in which the intensity and polarization behave as a result of the variation over the source region of the field intensity and direction and the electron angular and spatial distribution, reference may be made to the graphical results. The results seem to confirm Davis' suggestion that the proper polarization is achieved only when a large fraction of the electrons have relatively flat helices. It seems necessary to hypothesize a second, inner group of electrons with relatively steep helices in order to explain the decrease in the degree of polarization with increasing interferometer spacing.* The graphs show that with a single shell of relatively flat helix electrons, the degree of polarization based on the cosine transforms increases with increasing transform variable k over an appreciable range of k, as the transform "selects" those portions of the radiating shell where field alignment, radiation efficiency, electron density and radiating angle combine to give higher degrees of polarization.

---

*See Figure 3.

The polarization results, although depending strongly on the helix angle distribution of the electrons are seen not to depend very much on the frequency observed or on the energy of the electrons, as long as the electron energies are not so low as to give radiation at the observing frequency from inefficient radiating conditions corresponding, for instance, to G = 10. Thus, the polarization does not depend very strongly on the value of the spectral index or on the value of the energy cutoffs, as long as the radiation at the frequency of interest originates from particles some of which radiate relatively efficiently at that frequency. It seems possible to achieve the observed polarization and intensity behavior by means of synchrotron radiation from ultrarelativistic electrons in a dipole field provided that there are present enough electrons with relatively flat helices.

III. SOURCE OF HIGH ENERGY ELECTRONS FOR JUPITER

In this section, some of the problems involved in obtaining high energy, relatively flat-helix electrons in a region three Jovian radii from the center of Jupiter are discussed. The discussion concerns mainly the diffusion and acceleration of trapped electrons due to large-scale magnetic fluctuations: this is the subject of section IIIB. By way of introduction, section IIIA briefly mentions in connection with Jupiter some results that investigators of cosmic rays and of the earth's Van Allen belt have obtained on energy loss, scattering and neutron albedo.

IIIA. General Considerations

1. Energy loss

To estimate the electron energy loss in the region, reference is made to the work of Ginzburg (1959) on the origin of cosmic radiation. Ginzburg gives expressions for the energy loss of relativistic electrons due to ionization, bremsstrahlung, Compton processes and synchrotron radiation. The ionization loss of a relativistic electron of energy E in atomic hydrogen is

$$\frac{dE}{dt} = -7.62 \times 10^{-9}\, n \left(20.1 + 3\, \ell n \frac{E}{m_o c^2}\right) \text{ ev sec}^{-1}, \qquad (40)$$

where n is the number density of hydrogen in cm^{-3}, m_o is the electron rest mass and c is the speed of light; in ionized hydrogen, the

ionization loss is

$$\frac{dE}{dt} = -7.62 \times 10^{-9} n \left(\ell n \frac{E}{m_o c^2} - \ell n\, n + 74.6 \right) \text{ ev sec}^{-1} . \qquad (41)$$

An approximate result for the energy loss due to bremsstrahlung in hydrogen is given by

$$\frac{dE}{dt} = -8 \times 10^{-16} nE \text{ ev sec}^{-1} , \qquad (42)$$

where E is in ev; and the loss due to the inverse Compton effect is

$$\frac{dE}{dt} = -1.9 \times 10^{-14} \rho \left(\frac{E}{m_o c^2} \right)^2 \text{ ev sec}^{-1} , \qquad (43)$$

where ρ is the average density of radiation energy in ev cm^{-3}. Finally, the energy loss due to synchrotron radiation is

$$\frac{dE}{dt} = 0.98 \times 10^{-3} B_\perp^2 \left(\frac{E}{m_o c^2} \right)^2 \text{ ev sec}^{-1} , \qquad (44)$$

where $B_\perp$, measured in gauss, is the component of the magnetic field perpendicular to the direction of motion.

To obtain an order of magnitude estimate of the energy loss in the Jovian Van Allen belt, assume the region at three Jovian radii to contain a hydrogen plasma with density equal to the 1 cm^{-3} of the interstellar medium in the galactic disk*; take $\rho = 10^6$ ev cm^{-3}, corresponding

*The assumption of 1 proton cm^{-3} may be bad. However, the study of the background plasma to be expected will have to be deferred until another time.[5] In passing, we remark that even an increase in density by a factor of 10^5 gives a lifetime longer than that due to synchrotron radiation.

to $\sim 7.5 \times 10^{17}$ watts of solar radiation falling on Jupiter's disk; and set $B_\perp$ equal to 1 gauss. An electron with $E = 10\, m_o c^2 = 5.1 \times 10^7$ ev then loses 4×10^{-9} ev sec^{-1} due to bremsstrahlung, 5.86×10^{-7} ev sec^{-1} due to ionization, 1.9×10^{-6} ev sec^{-1} due to the inverse Compton effect and 10^{-1} ev sec^{-1} due to synchrotron radiation. The loss due to synchrotron radiation dominates the other three by several orders of magnitude, and this is true also at higher energies. Synchrotron radiation causes an electron with $E = 10\, m_o c^2$ in a one gauss field to lose half of its energy in a time of the order of a year.

2. Scattering

Several authors have pointed out in connection with the earth's Van Allen belt that particle lifetime in a dipole field is determined both by the energy loss in the trapping region itself and by the scattering of the particles into trajectories which carry them down into the denser atmosphere. Thus, Christophilos (1959), Welch and Whitaker (1959), Wentworth, MacDonald and Singer (1959), and Kellogg (1960) have estimated the lifetime determined by coulomb scattering. From Wentworth et al., we obtain an approximate expression for this lifetime for relativistic electrons:

$$\tau = 2.245 \times 10^{13} \frac{\frac{E}{m_o c^2}\left(2 + \frac{E}{m_o c^2}\right)^{3/2}}{n_E\left(1 + \frac{E}{m_o c^2}\right)\ell n\, D}\left(1 - 10^{-\frac{3}{2k'}}\right) \text{ sec}, \qquad (45)$$

where n_E is the background electron density, and k' is a constant which depends on the line of force and is of the order of 100 for a line of force which intersects the equatorial plane at $r_E = 3R_J$. The quantity ℓnD is the slowly varying function of the energy, temperature and density which enters into the coulomb scattering formulas* and will be taken to be of the order of 30. For $n_E = 1\ \text{cm}^{-3}$ and $E/m_o c^2 = 10$, equation 45 gives $\tau \approx 10^{12}$ sec.

To estimate the scattering due to the inverse Compton effect, we refer to Heitler (1954) and Feenberg and Primakoff (1948). In a collision, a high energy electron is scattered through an average angle of the order $\left(\frac{m_o c^2}{E}\right)^{1/2}$ (with the photon's energy not changing appreciably). The cross-section for Compton scattering (in the rest frame of the electron) is given by the Klein-Nishina formula, which for low and high energies is approximately

$$\sigma_L = \frac{8}{3}\pi r_o^2 \qquad h\nu' \ll m_o c^2 \qquad (46)$$

and

---

*See, for instance, Spitzer (1956).

$$\sigma_H = \pi r_o^2 \frac{m_o c^2}{h\nu'} \left[\ell n \frac{2h\nu'}{m_o c^2} + \frac{1}{2} \right] \qquad h\nu' >> m_o c^2 \qquad (47)$$

respectively, where $r_o = \frac{e^2}{m_o c^2} = 2.8 \times 10^{-13}$ cm is the classical radius of the electron and $h\nu'$ is the energy of the photon in the rest frame of the electron. The energy $h\nu$ of a photon in a system in which the electron has a speed v and in which the electron and photon are moving at an angle θ with respect to one another, is related to the energy $h\nu'$ by

$$h\nu \frac{(1 - \frac{v}{c} \cos\theta)}{(1 - \frac{v^2}{c^2})^{1/2}} = h\nu' . \qquad (48)$$

The energy density of sunlight at Jupiter is of the order of 10^6 ev cm^{-3} i.e., 8×10^5 1.35 ev photons cm^{-3}. Thus, in the rest frame of a high energy electron moving with speed v in the vicinity of Jupiter, there exists a practically unidirectional stream of photons with a density of $8 \times 10^5 (1 - \frac{v^2}{c^2})^{-1/2}$ cm^{-3} and with energies on the order of $1.35 (1 - \frac{v^2}{c^2})^{-1/2}$ ev. Consider an electron for which $(1 - \frac{v^2}{c^2})^{-1/2} = 10$. In the electron rest frame, the electron encounters on the order of $8 \times 10^5 (1 - \frac{v^2}{c^2})^{-1/2} c\sigma_L = 10^{-7}$ photons per unit time. In Jupiter's frame of reference, the electron therefore encounters on the order of $8 \times 10^5 c\sigma_L = 10^{-8}$ photons per second, and thus in one second is scattered through a mean square angle of the order of

$(8 \times 10^5 \, c\sigma_L) \frac{mc^2}{E} = 10^{-9}$. Appreciable scattering due to the inverse Compton effect thus requires on the order of 10^9 seconds.

To estimate the scattering due to bremsstrahlung, we refer again to Heitler (1953). A high energy electron is scattered through an average angle of the order of $\frac{mc^2}{E}$. In a hydrogen plasma of density n, the electron is therefore scattered through a mean square angle of order $nc\sigma_B(\frac{m_o c^2}{E})^2$ in unit time, where σ_B is an effective scattering cross section for bremsstrahlung.* We shall determine σ_B by setting it equal to πb_c^2, where b_c is the impact parameter for which Coulomb scattering gives a deflection of $\frac{m_o c^2}{E}$, i.e.,

$$\frac{m_o c^2}{E} = \frac{2e^2}{b_c E} \; ; \quad b_c = \frac{2e^2}{m_o c^2} = 5.6 \times 10^{-13} \text{ cm} \tag{49}$$

and

$$\sigma_B = \pi b_c^2 = 4\pi r_o^2 = 9.85 \times 10^{-25} \text{ cm}^2 . \tag{50}$$

Then, taking $n = 1$ and $\frac{E}{m_o c^2} = 10$, we find that an electron is scattered in one second through a mean square angle of the order of $(1)(3 \times 10^{10})(10^{-2})(9.85 \times 10^{-25}) \approx 10^{-18}$. Appreciable scattering

*The total cross section for bremsstrahlung diverges for photons with low wave number, but just as it is possible to define an effective cross section for energy loss due to bremsstrahlung, since a low wave number photon contributes little energy, we employ the same reason to define a finite effective cross section for scattering.

due to bresmstrahlung thus requires on the order of 10^{18} seconds.

The change in the electron's helix angle due to synchrotron radiation is easy to estimate by noting that the velocity component along the magnetic field is unchanged due to the radiation. Thus, from equa-44 for the rate of energy loss, we obtain

$$\frac{\cos a_2}{\cos a_1} = \frac{E_2}{E_1}\left[\frac{E_1^2 - m_o c^2}{E_2^2 - m_o c^2}\right]^{\frac{1}{2}} \tag{51}$$

where a_1 and a_2 are the helix angles when the energies are E_1 and E_2, respectively. For $\frac{E_1}{m_o c^2} = 10$, and $\frac{E_2}{m_o c^2} = 5$, we have

$\frac{\cos a_2}{\cos a_1} = \frac{5}{10}\left[\frac{100-1}{25-1}\right]^{1/2} = 1.015$. Not much change in the helix angle occurs in the time required for an electron with $E = 10\ m_o c^2$ to lose half of its energy (which in a 1 gauss field is of the order 10^7 sec.). This is understandable since at these high energies the energy radiated causes mainly a change in the relativistic mass rather than a change in the velocity. It appears, then, that the change in the helix angle due to ionization, the inverse Compton effect, bremsstrahlung, and synchrotron radiation is not appreciable in the time required for the energy to change by an appreciable amount due to synchrotron radiation.

In addition to the change in the helix angle due to the foregoing processes, the helix angle can also change due to interactions with electromagnetic waves. It is convenient in studying these

interactions to discuss individually waves with time scales shorter than or on the order of the Larmor period of the electron, waves with time scales long compared to the Larmor period but shorter than or on the order of the mirror period --- where the mirror period is the time that it takes an electron to drift back and forth between its mirror points, and finally waves with time scales long compared to the mirror period but shorter than or on the order of the azimuthal drift period --- where the azimuthal drift period is the time that it takes an electron to drift once around the planet. In the absence of all three types of waves, the actions associated with the Larmor, mirror and azimuthal drift periods are all adiabatic invariants (Northrup and Teller (1959)). In the presence of waves of the first type, none of the actions are invariant; for waves of the second type, only the action associated with the Larmor period (i.e., the magnetic moment) is an adiabatic invariant; and for waves of the third type, both the Larmor and mirror actions are adiabatically invariant.

To get some idea of the time scales involved, the Larmor period T_L, mirror period T_m and azimuthal drift period T_a are given by the expressions [Hamlin, Karplus, Vik and Watson (1961)]:

$$T_L = \frac{2\pi E}{eBc} \quad , \tag{52}$$

$$T_m = \frac{4r_e}{v} \int_{\theta_t(a_E)}^{\pi/2} \frac{\sin\theta(1+3\cos^2\theta)^{1/2}\, d\theta}{\left[1-\sin^2 a_E \frac{(1+3\cos^2\theta)^{1/2}}{\sin^6\theta}\right]^{1/2}} \tag{53}$$

and

$$T_a = \frac{eB(r_E, \frac{\pi}{2}) r_E^2 c}{(3/2\pi)Ev^2} \frac{\displaystyle\int_{\theta_t(a_E)}^{\pi/2} \frac{\sin\theta(1+3\cos^2\theta)^{1/2}\, d\theta}{\left[1-\sin^2 a_E \frac{(1+3\cos^2\theta)^{1/2}}{\sin^6\theta}\right]^{1/2}}}{\displaystyle\int_{\theta_t(a_E)}^{\pi/2} \frac{\sin^3\theta(1+\cos^2\theta)\left[1-\frac{1}{2}\sin^2 a_E \frac{(1+3\cos^2\theta)^{1/2}}{\sin^6\theta}\right] d\theta}{(1+3\cos^2\theta)^{3/2}\left[1-\sin^2 a_E \frac{(1+3\cos^2\theta)^{1/2}}{\sin^6\theta}\right]^{1/2}}}, \tag{54}$$

where

$$\frac{\sin^6\theta_t}{1+3\cos^2\theta_t} = \sin^2 a_E \ , \tag{55}$$

v is the speed of the particle, and the other symbols have the same meaning as in the discussion of the geometry of the dipole field in Section II. Hamlin, Karplus, Vik and Watson (1961) show by numerical integration of equations 53 and 54 that good approximations to T_m and T_a are

$$T_m = \frac{r_E}{v} \left[5.20 - 2.24 \sin a_E\right] \tag{56}$$

$$T_a = \frac{eB(r_E, \frac{\pi}{2})\, r_E^2 c}{(3/2\pi)Ev^2} \left[\frac{1}{0.35 + 0.15 \sin a_E}\right]. \tag{57}$$

For $E = 10\, m_o c^2$, $r_E = 3R_J$ and $B(r_E, \frac{\pi}{2}) = 1$ gauss, these equations give $T_L \approx 10^{-6}$, $T_m \approx 1$ sec and $T_a \approx 5 \times 10^4$ sec.

Wentzel (1961a, 1961b) and Dragt (1961) have discussed, in connection with the earth, the effect on trapped particles of hydromagnetic waves with time scales on the order of the Larmor periods. Both find that appreciable scattering of a particle occurs only for the resonance condition when the particle sees a hydromagnetic wave with frequency equal to its Larmor frequency. This does not require that the frequency of the hydromagnetic wave be equal to the Larmor frequency, but rather that the "Doppler shifted" wave frequency be the same as the Larmor frequency. Dragt gives for the lifetime:

$$T = \frac{2}{\pi^2} \frac{1}{\eta^2} \frac{B_o^2}{B_{hm}^2} T_b \tag{58}$$

where B_o is the original (average) magnetic field, B_{hm} is the amplitude of the hydromagnetic wave, and η is the number of half wave lengths satisfying the resonance condition which an electron sees in one mirror period. From Wentzel we obtain a lifetime:

$$T \approx \frac{1}{2\eta} \frac{B_o^2}{B_{hm}^2} T_b \,. \tag{59}$$

Dragt remarks that the spectrum of the hydromagnetic waves is likely to contain a cutoff at the ion cyclotron frequency due to the inability of

hydromagnetic waves to propagate across magnetic field lines if the hydromagnetic wave frequencies exceed the ion cyclotron frequency. Thus, for an electron to see a wave with frequency equal to its Larmor frequency, it must either be in a rather steep helix or be quite relativistic ($E/m_o c^2 \approx \mathcal{O}(1840)$). Unless either of these two conditions is satisfied, waves of this type will not cause appreciable scattering of electrons.*

Parker (1961) has investigated the effect of waves with time scales long compared to the Larmor period but on the order of the mirror period. He finds for a lifetime:

$$T \geq 12\left(\frac{B_o}{B_{hm}}\right)^2 T_b \,, \tag{60}$$

where $\frac{B_{hm}}{B_o}$ is the relative amplitude of hydromagnetic disturbances with time scales close to the mirror period. For a rough estimate of $\frac{B_{hm}}{B_o}$, assume first that the solar wind stops where the pressure of the magnetic field balances the pressure of the wind. For a wind at Jupiter consisting of $\frac{10}{25}$ atoms cm^{-2} travelling at a speed of 500 km sec^{-1}, this occurs for a magnetic field B such that

$$\frac{B^2}{8\pi} \approx \left(\frac{10}{25}\right)(2 \times 10^{-24})(5 \times 10^7)^2 \tag{61}$$

*Dessler (1961) has suggested that the resonance condition can be achieved for electrons at Jupiter by interaction with whistlers (Helliwell & Bell (1960)). The details of this interaction have not yet been investigated.

i.e., for $B = 2 \times 10^{-4}$ gauss. (This would mean that the wind stops at fifty Jovian radii from Jupiter if the field is that of a dipole and $B \approx 1$ gauss at three radii.) Next assume that in the region where the wind is stopped, $\frac{B_{hm}}{B_o} = 1$ (Parker (1958)). Then, requiring that the energy transported inward toward the planet by hydromagnetic waves be constant, we have that

$$\frac{B_o^2}{B_{hm}^2} \propto r_E^2 B_o^3 \propto B_o^{7/3} \quad . \tag{62}$$

Thus, when $B_o = 1$ gauss, $\left(\frac{B_o}{B_{hm}}\right)^2 = \mathcal{O}(10^{\frac{28}{3}})$. For $T_m = 1$ sec, this type of scattering leads to lifetimes on the order of 10^{10} sec.

Finally, Parker (1960) has suggested that hydromagnetic disturbances with time scales longer than the mirror period but shorter than the azimuthal drift period are effective both in determining the radial distribution of particles and also in obtaining particles with relatively flat helices. Because of this last feature, we have investigated this type of disturbance in some detail, and this is the subject of Section IIIB. The results we obtain differ from the results obtained by Parker.

3. Electrons from Neutron Albedo

It might be thought that since Jupiter has such a large surface area the production of neutrons by the stoppage of cosmic rays in the

atmosphere would lead to an ample number of electrons through the decay

$$n \rightarrow p + e^{-} + \bar{\nu} ,$$

a process which yields electrons with an energy distribution peaked around 300 kev and with maximum energies of 780 kev. On the other hand, since the decay has a half-life of only 12 minutes and upward moving neutrons are mostly slow, we are concerned essentially only with those neutrons that decay near where the line of force that reaches the equator at $3R_J$ enters the top of the atmosphere, i.e., 55° latitude unless Jupiter has a very high atmosphere. The decay electrons would then be in steep helices at the equator. Moreover, the fact that light elements (H,He) form the bulk of Jupiter's atmosphere is unfavorable for the albedo source explanation: the neutrons due to spallation from excited heavy nuclei are lacking here, while for light nuclei, the reaction products could be strongly peaked in the direction of travel of the incoming high energy particles and would be directed mainly toward the planet rather than out toward the radiation belt.

Another factor which acts against the albedo source explanation is that the large dipole moment which Jupiter must have to give the magnetic fields appropriate for the radiation, serves to keep cosmic rays from penetrating to the atmosphere. In fact, it seems that this one fact is enough to nullify the advantage of the large surface area.

Thus, in the Stormer cone approximation, at the latitude λ on the surface of Jupiter, cosmic rays with momentum of magnitude p can arrive only from directions lying within a cone whose axis lies in the east-west direction and whose half angle π-X may be found from the equation

$$p = \frac{eM_J}{cR_J^2} \left[\frac{\cos^4\lambda}{[[1 - \cos X \cos^3\lambda]^{1/2} + 1]} \right]^2 , \tag{63}$$

where M_J is Jupiter's dipole moment [Hooper and Scharff(1958)]. The number of cosmic rays incident per unit time on the surface between latitudes λ and $\lambda + d\lambda$ is

$$F_\lambda d\lambda = 2\pi R_J^2 \cos\lambda \, d\lambda \int_{p_{min}}^{p_{max}} \int_0^{\pi - X(p)} 2\pi \cos x \, dx \, I(p) dp , \tag{64}$$

assuming an isotropic distribution of cosmic rays at infinity with an intensity of $I(p)dp$ particles with p in the range $(p, p+dp)$ per steradian per unit time. Taking

$$I(p) = \begin{cases} C_1 p^{-(\gamma+1)} & \text{if } p > p_{min} \\ 0 & \text{if } p < p_{min} \end{cases} \tag{65}$$

and

$$p_{min} < p_c$$

(where p_c is the value of p for which equation 64 gives $X = \pi$), we have

$$F_\lambda d\lambda = \frac{R_J^{2\gamma+2}}{M_J^{\gamma}} \quad S(\lambda)\ d\lambda \tag{66}$$

with

$$S(\lambda) = 2\pi C_1' \cos\lambda \int_{\frac{cR_J^2 p_c}{eM_J}}^{\infty} x^{-(\gamma+1)} \left[1 - \frac{1}{\cos^6\lambda} \left[1 - \left(1 - \frac{\cos^2\lambda}{x^{1/2}} \right)^2 \right]^2 \right]^{1/2} dx. \tag{67}$$

From the definition of p_c, it is seen that $S(\lambda)$ does not depend on R_J or M_J.

For orders of magnitude, compare $F_\lambda d\lambda$ for Jupiter to $F_\lambda d\lambda$ for earth, taking the field three Jovian radii from the center of Jupiter to be the same as that at the surface of the earth:

$$\frac{(F_\lambda d\lambda)_{\text{Jupiter}}}{(F_\lambda d\lambda)_{\text{Earth}}} \approx \frac{1}{200} \tag{68}$$

(for λ at which $p_{min} < p_c$).

Equation 68 shows that when the magnetic cutoff energy is greater than the minimum cosmic ray energy, the number of cosmic rays arriving in a given belt of latitudes is greater by a factor of 200 on the earth

than on Jupiter. Taking the minimum cosmic ray kinetic energy to be $\frac{1}{2}$ Bev, equation 63 shows that $p_{min} < p_c$ at latitude 55° on both earth and Jupiter so that equation 68 applies. Field (1959) estimated that if the particle energy flux of secondary electrons leaving the top of Jupiter's atmosphere were the same as that leaving the top of the earth's atmosphere, this would equal only four percent of Jupiter's decimeter radiation flux.* Combining this estimate with the 1/200 factor strongly suggests that neutron albedo is an inadequate source of electrons.

---

*See page 11.

IIIB. Effect of Large-Scale Magnetic Fluctuations on Trapped Electrons*

A variety of mechanisms have been explored recently in efforts to explain the origin and loss of the electrons in the earth's Van Allen zone. Presumably the same type of mechanisms might operate in a magnetic field about Jupiter. Parker (1960) has pointed out one mechanism that is likely to operate. Any moderately rapid deviation from cylindrical symmetry in the magnetic field perturbation will lead to a violation of the third adiabatic invariant and radial diffusion of the charged particles that are normally confined to a particular shell in the magnetic field. If the features of the magnetic perturbation are such that the first and second adiabatic invariants are not violated, those particles which diffuse inward both gain energy and attain flatter helices. The last two features have led us to a closer study of this mechanism. It appears that although the basic plan of Parker's analysis is correct his diffusion equation is not adequate and his expression for the average radial motion of a particle in a single magnetic storm is not carried to high enough order to give the coefficients in the Fokker-Planck equation that must be used. This section is an attempt to remedy these deficiencies. The new diffusion equation is

*This section is based closely on Davis and Chang (1961b).

then solved and it is found that while many of the characteristics of Parker's solution are preserved, the number of particles to be expected at small radii is relatively very much greater.

The model used for a magnetic storm, both by Parker and here, is the original model of Chapman and Ferraro (1931) for the initial phase. In this, the solar plasma is represented by a plane, perfectly conducting front pressing into the magnetic field. Even if a different model of a storm were used, essentially the same results should be obtained provided the perturbation were not axially symmetric. In both analyses the particles are assumed to have mirror points near the magnetic equatorial plane. Presumably the effects for particles in steep helices will have the same general character, but a reasonably complete analysis of this case would be much more difficult. If r denotes the distance from the center of the planet of a particle and L that of the plane plasma front, both analyses assume that r/L is small and they will break down near the outer boundary of the magnetic field. However, in this region diffusion to the outer boundary and loss of particles is very rapid and for our purposes an accurate treatment in this region should not be necessary. The particle energies are assumed to be low enough so that the radii of curvature in the magnetic field are small compared to r and the motion is treated by following the guiding center. The energies must be high enough so that the particles will

drift a substantial fraction of the distance around the planet while the initial phase of a magnetic storm is dying out.*

1. Particle Motion

In terms of the guiding center motion, a storm causes a particle to change its radial coordinate because the drifts resulting from the induced electric fields and the geometry of the distorted magnetic field are not in the same direction as the steady state drifts. The essential features of the diffusion mechanism may be understood from a treatment of the motion of those particles that remain in the planet's magnetic equatorial plane where the field is $B(r)\vec{i}_z$. Thus, we have a two-dimensional diffusion problem in which the only drift velocities present are normal to this field and are due to gradients in the magnetic field and the presence of electric fields. A particle of mass m, charge e and speed w will experience a drift velocity **

$$\vec{v}_B = \frac{mcw^2}{2eB^2} (\vec{i}_z \times \nabla B) \tag{69}$$

(where c is the velocity of light) due to the presence of a gradient in the magnetic field intensity, and will have a drift velocity

$$\vec{v}_E = c \frac{\vec{E} \times \vec{i}_z}{B} \tag{70}$$

---

*See page 49.

**See Appendix C.

whenever an electric field $\vec{E}$ is present. Corresponding to the geomagnetic situation in which the earth's magnetic field experiences only an occasional large scale disturbance, let us consider an equilibrium field configuration $\vec{B}_o = B_o(r)\,\vec{i}_z$ which is subject to an occasional distortion. In the equilibrium configuration and during any later static periods, the particles drift along countours of constant magnetic field intensity. Thus, the coordinate that describes the shell on which the particle is drifting is the magnetic field strength at the guiding center, and this becomes the most useful coordinate with which to describe the location of the particle. During the disturbance of the magnetic field, which is assumed not to change the symmetry about the equatorial plane, the drift is compounded of a motion along the distorted contour of constant B passing through the particle and a drift due to the induced electric fields. The latter carries the guiding center to a new shell where B has a different value. Corresponding to the geomagnetic case in which a magnetic storm consists of a sudden commencement phase followed by a gradual return to normal, let us consider disturbances to consist of two phases. The initial phase, although long compared to the gyroperiod, is of such short time scale that the particle drift velocities are essentially all due to the induced electric fields, i.e., we have only an essentially instantaneous displacement of the plasma and the trapped particle guiding centers. In the second phase, the magnetic field returns to the equilibrium configuration so gradually that

$|\vec{v}_B| >> |\vec{v}_E|$. We must now find the change in B experienced by a guiding center during these processes.

The change in magnetic field ΔB when the guiding center undergoes a small displacement $\vec{\rho}_D = (\vec{v}_B + \vec{v}_E)\,\delta t$ in the time interval δt, is given by

$$B = \delta B + \vec{\rho}_D \cdot \nabla B = \delta B + \vec{\rho}_E \cdot \nabla B \tag{71}$$

where δB denotes the change in B at a fixed point, $\vec{\rho}_E = \vec{v}_E \delta t$, and $\vec{v}_B \delta t \cdot \nabla B = 0$ since $\vec{v}_B$ is perpendicular to ∇B. From the Maxwell equation $\nabla \times \vec{E} = -\frac{\vec{i}_z}{c} \frac{\partial B}{\partial t}$ and the hydromagnetic condition for a perfect conductor, $\vec{E} + \vec{v}_E \times \vec{B}/c = 0$, it follows that

$$\delta B = \frac{\partial B}{\partial t}\,\delta t = -\nabla \cdot (B\vec{\rho}_E) . \tag{72}$$

Equations 71 and 72 may be combined to give

$$\frac{dB}{dt} = -B(\nabla \cdot \vec{v}_E) \tag{73}$$

or

$$\Delta_1 B \cong -B(\nabla \cdot \vec{\rho}_{E1}) . \tag{74}$$

In equation 74, and in the following, the approximation sign indicates that the displacement $\vec{\rho}$ is so small that the variation of $\vec{v}$ and B during the displacement is being neglected. The suffix 1 in equation 74 indicates that this equation gives the change in magnetic field experienced by a

particle during the initial phase of the disturbance, $\vec{\rho}_{E1}$ being the displacement of the plasma in the first phase at the position of the particle. After this sudden change is over, each particle then drifts without changing its own B as long as the field is static, but different particles drift on different contours.

The duration, T, of the second phase of the storm is such that $|\vec{v}_B| >> |\vec{v}_E|$. This means that a particle mainly drifts around a moving contour of constant magnetic field during the second phase, but it also has a slower drift, governed at each instant by equation 73, to new contours. Since this drift varies with position around the contour, a suitably weighted average must be used. Assume an adiabatic change; i.e., one in which there is no correlation between the location on the contour of the guiding center and the rate of distortion. The amount of time dt spent traveling a differential arc ds along a distorted contour is

$$dt = \frac{ds}{v_B} = \frac{2eB^2 ds}{mcw^2 |\nabla B|} \quad . \tag{75}$$

The time to make one revolution is $\oint ds/v_B$, and the fraction of the time, either in one revolution or the entire interval T, spent in a particular ds is

$$\frac{dt}{T} = \frac{ds/v_B}{\oint ds/v_B} \quad . \tag{76}$$

For small distortions of the equilibrium configuration, $\vec{\rho}_{E2}(s) = \vec{v}_E T$ evaluated at any position given by s, the distance along the contour, would be the displacement experienced in the second phase by a particle that remained at s during the entire interval T and did not move along the contour. Thus, taking the fraction 76 of the change in B, $-B\nabla\cdot\vec{\rho}_{E2}(s)$, associated with $\vec{\rho}_{E2}$ by 74, and integrating over the contour, the change in B at the guiding center during the second phase is found to be

$$\Delta_2 B \cong -\frac{\oint v_B^{-1} B \nabla\cdot\vec{\rho}_{E2}\, ds}{\oint v_B^{-1}\, ds} \cong -B\frac{\oint |\nabla B|^{-1}\, \nabla\cdot\vec{\rho}_{E2}\, ds}{\oint |\nabla B|^{-1} ds} \qquad (77)$$

This is valid for adiabatic changes and has been checked in a simple example by comparison with the result obtained from the third adiabatic invariant. The total net change in B experienced by a particle during a storm is

$$\Delta B = \Delta_1 B + \Delta_2 B \quad ; \qquad (78)$$

thus, a particle that initially drifted around an equilibrium contour B_o will, after the storm, drift around a contour $B_o + \Delta B$.

The total change in B is seen to depend only on B_o and the position on the B_o contour of the particle during the first, non-adiabatic phase. This position may be indicated by an arc length s along the contour. Then if $P(B_o;s)\, ds$ is the probability that a particle drifting around

a contour is in ds at s and if $\Delta B(s)$ is the ensuing change given by 78, the average ΔB taken over all particles on one contour is

$$\langle \Delta B \rangle = \oint \Delta B(s) P(B_o;s)\, ds \tag{80}$$

for one storm. Similarly, the average per storm of $(\Delta B)^2$ is

$$\langle (\Delta B)^2 \rangle = \oint [\Delta B(s)]^2 P(B_o;s)\, ds\ . \tag{81}$$

If before the storm the density does not vary with time, $P(B_o;s)\, ds$ must be proportional to the amount of time spent by a particle drifting with velocity V_B through the arc length ds at s; that is, by equation 76. (Actually, the result is the same if the density does vary since the onset of a storm is uncorrelated with the electron positions.) This then gives:

$$\langle \Delta B \rangle = \frac{\oint \Delta B \frac{ds}{V_B}}{\oint \frac{ds}{V_B}} \tag{82}$$

and

$$\langle (\Delta B)^2 \rangle = \frac{\oint (\Delta B)^2 \frac{ds}{V_B}}{\oint \frac{ds}{V_B}} \tag{83}$$

The effect of many storms may be described by forming a Fokker-Planck equation with the coefficients in this equation being determined by equations 82 and 83 [Chandrasekhar (1943)]. If the

expressions of equations 82 and 83 depend on a parameter ξ (which describes the details of the storm, generalization to the case where a set of parameters is needed being obvious), then, letting n indicate the number of storms and $\chi(B,n)dB$ the number of particles in the magnetic field range dB at B after n storms, the Fokker-Planck equation is

$$\frac{\partial \chi}{\partial n} = - \frac{\partial}{\partial B} \left[D_B \chi \right] + \frac{1}{2} \frac{\partial^2}{\partial B^2} \left[D_{BB} \chi \right] \tag{84}$$

where

$$D_B = \left\langle \Delta B \right\rangle_{av} = \int \rho(\xi) \left\langle \Delta B \right\rangle_{\xi} d\xi \tag{85}$$

$$D_{BB} = \left\langle (\Delta B)^2 \right\rangle_{av} = \int \rho(\xi) \left\langle (\Delta B)^2 \right\rangle_{\xi} d\xi \tag{86}$$

and where $\rho(\xi)d\xi$ is the probability of finding the parameter ξ in the range $d\xi$ at ξ. The subscript ξ on the brackets denotes that the averages are evaluated for a particular ξ.

The foregoing will now be applied to particle diffusion in the particular model of the solar wind-perturbed geomagnetic field adopted by Parker. Thus, let us consider the magnetic field configuration that should be produced by a magnetic dipole $\vec{M}$ in the presence of a perfectly conducting infinite plane, which simulates the front of the solar wind. Introducing a polar coordinate system with the dipole directed in the $\theta = 0$ direction at the origin, and with the conducting plane at a

distance L away in the direction $\theta = \frac{\pi}{2}$ and $\phi = \frac{3\pi}{2}$, the field at a point (r, θ, ϕ) on the dipole side of the conducting plane is given by

$$B_r = \frac{2M}{r^3}\cos\theta + \frac{M}{8L^3}\left[-\cos\theta + \frac{3r}{2L}\sin 2\theta \sin\phi + O\left(\frac{r^2}{L^2}\right)\right] \quad (87a)$$

$$B_\theta = \frac{M \sin\theta}{r^3} + \frac{M}{8L^3}\left[\sin\theta + \frac{3r}{2L}\cos 2\theta \sin\phi + O\left(\frac{r^2}{L^2}\right)\right] \quad (87b)$$

$$B_\phi = \frac{3Mr}{16L^4}\cos\theta\cos\phi\left[1 + O\left(\frac{r}{L}\right)\right] . \quad (87c)$$

The expression B_ϕ differs from that of Parker's equation 13 in which $B_\phi = \frac{M}{8L^3} O\left(\frac{r^2}{L^2}\right)$. The equilibrium configuration is to be given by equations 87 with $L = \infty$; the initial phase occurs when the conducting plane is suddenly brought up to $(L, \frac{\pi}{2}, \frac{3\pi}{2})$ and the second phase when the plane is slowly withdrawn to infinity.

The displacement $\vec{\rho}_E$ is easily calculated by using the fact that in a perfectly conducting plasma the particles move with the lines of force during a disturbance. Consequently, $\vec{\rho}_E$ may be determined from the equations for the lines of force in both the undistorted and distorted configurations providing one can identify which line of force in the distorted state corresponds to a line in the undistorted state. For the case of the dipole and its image, the identification is easily made since sufficiently close to the dipole the field is essentially undisturbed by the presence of the image. The equations of a line of force are:

$$\frac{dr}{B_r} = \frac{r d\theta}{B_\theta} = r \sin\theta \frac{d\phi}{B_\phi} \quad . \tag{88}$$

or, from equation 87,

$$\frac{1}{r}\frac{dr}{d\theta} = \frac{B_r}{B_\theta} = \frac{2\cos\theta}{\sin\theta} - \frac{3r^3\cos\theta}{8L^3\sin\theta}\left[1 + \frac{r\sin\phi}{L\sin\theta}(1-3\sin^2\theta)+O(\frac{r^2}{L^2})\right] \tag{89}$$

$$\frac{d\phi}{d\theta} = \frac{B_\phi}{\sin\theta\, B_\theta} = \frac{3r^4\cos\theta\cos\phi}{16\,L^4\sin\theta}\left[1 + O(\frac{r}{L})\right] \tag{90}$$

These can now be integrated by successive approximations. If all terms of order $(r/L)^3$ or higher are neglected, integration gives

$$r = R\sin^2\theta, \quad \phi = \phi_o \quad . \tag{91}$$

where R and ϕ_o are constants of integration. If equations 91 are substituted into the higher order terms, they become functions of θ only. Integration and simplification then give

$$r = R\sin^2\theta\left[1 - \frac{R^3\sin^6\theta}{16L^3}\left[1 - \frac{2R\sin\theta\sin\phi_o}{L}(\sin^2\theta - \frac{3}{7}) + O(\frac{R^2}{L^2})\right]\right] \tag{92}$$

$$\phi = \phi_o + \frac{3R^4\sin^7\theta\cos\phi_o}{7{\cdot}16\,L^4}\left[1 + O(\frac{R}{L})\right] \tag{93}$$

We must now show that 92 and 93, with R and ϕ_o fixed, always describe the same line of force and that it is not necessary to replace R and ϕ_o by functions of two other constants and of L. The electric field that

moves the plasma with the lines of force should be finite everywhere and hence the displacement is expected to be proportional to B^{-1}; i.e., to $r^3/L^3 = (R/L)^3 \sin^6\theta$. Inspection of 92 and 93 shows that they do have the required character and that it would not be possible to replace R and ϕ_o by functions of L.

When $L \to \infty$, R and ϕ_o are just the coordinates where the line of force intersects the equatorial plane $\theta = \pi/2$. After the disturbance the corresponding coordinates are

$$r_1 = R\left[1 - \frac{R^3}{16L^3} + \frac{R^4 \sin\phi_o}{14L^4} + O\left(\frac{R^5}{L^5}\right)\right] \tag{94}$$

$$\phi = \phi_o + \frac{3R^4 \cos\phi_o}{112L^4} + O\left(\frac{R^5}{L^5}\right)$$

The field in the equatorial plane is, by equation 87b,

$$B = \frac{M}{r^3}\left[1 + \frac{r^3}{8L^3}\left[1 - \frac{3r}{2L}\sin\phi + O\left(\frac{r^2}{L^2}\right)\right]\right] \tag{95}$$

Before the disturbance the particle is at R, ϕ_o where the field is $B_o = M/R^3$. Afterward, the field is found by substituting equations 94 in equation 95 and the change is

$$\Delta_1 B = \frac{5}{16}\frac{B r^3}{L^3} - \frac{45}{112} B\left(\frac{r}{L}\right)^4 \sin\phi + B\,O\left(\frac{r^5}{L^5}\right) \tag{96}$$

Likewise, by equation 77,

$$\Delta_2 B = - \langle \Delta_1 B \rangle \quad [1 + O(\frac{r^3}{L^3})] \quad . \tag{97}$$

where the higher order terms arise from the use of the undisturbed contour in the integration. This then gives for ΔB,

$$\Delta B = - \frac{45}{112} \quad B(\frac{r}{L})^4 \sin\phi + B\, O(\frac{r^5}{L^5}) \tag{98}$$

so that

$$\langle \Delta B \rangle = O + B\, O(\frac{r^5}{L^5}) \tag{99}$$

and

$$\langle (\Delta B)^2 \rangle = (\frac{45}{112})^2 \quad \frac{M^2}{2r^6} \quad [(\frac{r}{L})^8 + O(\frac{r^9}{L^9})] \quad . \tag{100}$$

since in the final state $B = M/r^3$.

The foregoing simple calculation only shows $\langle \Delta B \rangle$ to be zero up to terms of order $(R/L)^5$; however, it may be shown that $\langle \Delta B \rangle$ is zero up to terms of order $(R/L)^8$. This follows when somewhat more care is taken in exhibiting the cancellation effect that the second phase has on the change in field experienced during the initial phase. In an infinitesimal perturbation of the field configuration away from its undistorted state, the change in field experienced if the perturbation is applied adiabatically is only very slightly different from the average of the changes experienced if the perturbation is applied suddenly. This suggests that if in a larger perturbation the particle motion were to be expressed in terms of quantities evaluated on the initial undistorted

contour - by a series expansion, say, in variables describing the extent to which the particles are displaced from the undistorted contour - then the expression for the change in field experienced during the adiabatic perturbation might contain some terms identical to some of those contained in an expression for the average of changes in a sudden perturbation. Such a procedure would then be useful in exhibiting the cancellation effect occurring in an adiabatic release of a suddenly applied perturbation. The uncancelled terms would be associated with the difference in the motion of a particle away from its undistorted contour in an adiabatic perturbation from that in a sudden perturbation. That is, when the cancellation effect has been exhibited, the evaluation of the remaining terms involves consideration of the effect of distorted contours which was neglected in obtaining equation 99. The series expansion suggested above, coupled with an iteration procedure, has proved useful in treating this problem.

More explicitly, define ℓ to be the distance the front of the solar wind is from the dipole and define quantities β and β_L by

$$\beta = M/8\ell^3, \quad \beta_L = M/8L^3 . \tag{101}$$

Next let $\Theta(\beta, B, \phi)$ be the total rate (with respect to β) at which the magnetic field is changing for a line of force at the point defined by B and ϕ when the field configuration is given by β. In terms of β_L and $\Theta(\beta, B, \phi)$, the change in magnetic field experienced by a particle during

the sudden initial phase of a storm is

$$\Delta_1 B = \int_0^{\beta_L} \Theta(\beta, B, \phi)\, d\beta \,, \tag{102}$$

where B and ϕ are evaluated along a trajectory appropriate to the starting position of the particle, i.e., B and ϕ are given by equations 92, 93 and 87b. In terms of $\Theta(\beta, B, \phi)$, the change in magnetic field experienced during the adiabatic return to the undistorted field is

$$\Delta_2 B = \int_{\beta_L}^{0} \left[\int_0^{2\pi} \Theta(\beta, B, \phi) \frac{r d\phi}{\left|\frac{dB}{dr}\right|} \Big/ \int_0^{2\pi} \frac{r d\phi}{\left|\frac{dB}{dr}\right|} \right] d\beta \,, \tag{103}$$

in which the B in the integrands is to be taken along trajectories appropriate to the adiabatic phase. We shall later determine the functional form of this B by iteration.

The form of $\Theta(\beta, B, \phi)$ may be determined from equations 87b and 94 . Thus, substitution of equations 94 and 101 in equation 87b yields

$$B(\beta, B_o, \phi_o) = B_o\left[1 + \frac{5}{2}\frac{\mathbf{B}}{B_o} - \frac{45}{7}\left(\frac{\beta}{B_o}\right)^{\frac{4}{3}} \sin\phi_o + O(\beta^{\frac{5}{3}}/B_o^{\frac{5}{3}})\right] \,, \tag{104}$$

where we have set

$$B_o = M/R^3 \tag{105}$$

(ϕ_o and B_o now identifying the position of the line of force when $\ell \to \infty$). Differentiating equation 104 with respect to β gives

$$\frac{dB}{d\beta} = \frac{5}{2} - \frac{60}{7}\left(\frac{\beta}{B_o}\right)^{\frac{1}{3}} \sin \phi_o + O(\beta^{2/3}/B_o^{2/3}) . \qquad (106)$$

Replacing ϕ_o in this equation by the expression for ϕ_o obtained by inverting equation 94 , and replacing B_o by the expression for B_o obtained by inverting equation 104 , gives the desired result:

$$\Theta(\beta, B, \phi) = \frac{5}{2} - \frac{60}{7}\left(\frac{\beta}{B}\right)^{1/3} \sin \phi + f_1(\phi, \frac{\beta}{B}) , \qquad (107)$$

where $f_1(\phi, \frac{\beta}{B})$ is an expression of $O(\beta^{2/3}/B^{2/3})$. Similarly, if $\dot{\phi}(\beta, B, \phi)$ is the rate (with respect to β) at which ϕ is changing for a line of force at the point defined by B and ϕ when the field configuration is given by β, we find

$$\dot{\phi}(\beta, B, \phi) = \frac{1}{B}\left[\frac{4}{7}\left(\frac{\beta}{B}\right)^{1/3} \cos \phi + h_1(\phi, \frac{\beta}{B})\right] \qquad (108)$$

where $h_1(\phi, \frac{\beta}{B})$ is an expression of $O(\beta^{2/3}/B^{2/3})$.

We may now calculate $\Delta_1 B$ according to equation 102. As described earlier, $\Theta(\beta, B, \phi)$ in the integrand will be written as a series expression. Then,

$$\Delta_1 B = \int_0^{\beta_L} [\Theta(\beta, B, \phi_o) + \frac{\partial \Theta}{\partial B}(B - B_o) + \frac{\partial \Theta}{\partial \phi}(\phi - \phi_o) + \cdots] \, d\beta , \qquad (109)$$

where the partial derivatives are evaluated at (B_o, ϕ_o), i.e.,

$$\frac{\partial \Theta}{\partial B} = \frac{1}{B_o} \frac{20}{7} \left(\frac{\beta}{B_o}\right)^{1/3} \sin \phi_o + \frac{\partial f_1}{\partial B} \tag{110}$$

$$\frac{\partial \Theta}{\partial \phi} = -\frac{60}{7} \left(\frac{\beta}{B_o}\right)^{1/3} \cos \phi_o + \frac{\partial f_1}{\partial \phi} \quad . \tag{111}$$

In equation 109, $B - B_o$ and $\phi - \phi_o$ may be determined by iteration:

$$B_n - B_o = \int_o^\beta \Theta(\beta, B_{n-1}, \phi_{n-1}) d\beta \quad , \quad B_{-1} = B_o \tag{112}$$

$$\phi_n - \phi_o = \int_o^\beta \Phi(\beta, B_{n-1}, \phi_{n-1}) d\beta \quad , \quad \phi_{-1} = \phi_o \quad . \tag{113}$$

To obtain an expression for $\Delta_1 B$ accurate through terms of $O(\beta^{8/3}/B_o^{8/3})$ - and as we shall see, this order is sufficient - it is only necessary to express $B - B_o$ through terms of $B_o O(\beta^{4/3}/B_o^{4/3})$ and $\phi - \phi_o$ through terms of $O(\beta^{4/3}/B_o^{4/3})$. This is obtained by setting $n = 1$ in equations 112 and 113:

$$B_1 - B_o = B_o \left[\frac{5}{2} \frac{\beta}{B_o} - \frac{45}{7} \left(\frac{\beta}{B_o}\right)^{4/3} \sin \phi_o + O(\beta^{5/3}/B_o^{5/3}) \right], \tag{114}$$

$$\phi - \phi_o = \frac{3}{7} \left(\frac{\beta}{B_o}\right)^{4/3} \cos \phi_o + O(\beta^{5/3}/B_o^{5/3}) \, . \tag{115}$$

Combining equations 109 and 115, we obtain directly

$$\Delta_1 B = \int_0^{\beta_L} \Theta(\beta, B_o, \phi_o) d\beta + \frac{150}{49} B_o \left(\frac{\beta}{B_o}\right)^{7/3} \sin\phi_o - \frac{3\cdot 900}{8\cdot 49} B_o \left(\frac{\beta}{B_o}\right)^{8/3} \sin^2\phi_o -$$

$$- \frac{3\cdot 180}{8\cdot 49} \left(\frac{\beta}{B_o}\right)^{8/3} \cos^2\phi_o + \frac{5}{2} \int_0^{\beta_L} \beta \frac{\partial f_1}{\partial B} d\beta + B_o O(\beta^3/B_o^3) \qquad (116)$$

in which the integral of $\beta \frac{\partial f_1}{\partial B}$ is of $O(\beta^{8/3}/B_o^{8/3})$. The average of the $\Delta_1 B$ is

$$\langle \Delta_1 B \rangle = \frac{1}{2\pi} \int_0^{2\pi} \int_0^{\beta_L} \Theta(\beta, B_o \phi_o) d\beta d\phi_o + \frac{5}{4\pi} \int_0^{2\pi} \int_0^{\beta_L} \beta \frac{\partial f_1}{\partial B} d\beta -$$

$$- \frac{3\cdot 540}{8\cdot 49} B_o \left(\frac{\beta}{B_o}\right)^{8/3} + B_o O(\beta^3/B_o^3) \qquad (117)$$

Now calculate $\Delta_2 B$ according to equation 103. From equations 87b and 94, we find

$$r/\left|\frac{\partial B}{dr}\right| = \frac{(2\ell)^2}{3B_o} \left(\frac{\beta}{B_o}\right)^{2/3} \left[1 - \frac{5}{2} \frac{\beta}{B_o} + \frac{33}{7} \left(\frac{\beta}{B_o}\right)^{4/3} \sin\phi_o \right. \qquad (118)$$

$$\left. + O(\beta^{5/3}/B_o^{5/3}) \right]$$

Factoring out $(1 - \frac{5}{3}\frac{\beta}{B})$ after expressing B_o and ϕ_o in terms of B, ϕ and β, gives

$$r/\left|\frac{\partial B}{dr}\right| \propto 1 - 6\left(\frac{\beta}{B}\right)^{4/3} \sin\phi + O(\beta^{5/3}/B^{5/3}) . \tag{119}$$

Thus,

$$\Delta_2 B = \frac{1}{2\pi}\int_{\beta_L}^{o}\left[\int_{o}^{2\pi}\Theta(\beta,B,\phi)\left[1-6\left(\frac{\beta}{B}\right)^{4/3}\sin\phi + j(\phi,\frac{\beta}{B})\right] d\phi\right]\left[1-\left\langle j(\phi,\frac{\beta}{B})\right\rangle\right] d\beta \tag{120}$$

where $j(\phi,\beta/B)$ is of $O(\beta^{5/3}/B^{5/3})$ and

$$\langle j(\phi,\beta/B)\rangle = \frac{1}{2\pi}\int_{o}^{2\pi} j(\phi,\beta/B)\, d\phi . \tag{121}$$

Again expanding $\Theta(\beta,B,\phi)$ in series,

$$\Delta_2 B = \frac{1}{2\pi}\int_{\beta_L}^{o}\left[\int_{o}^{2\pi}\left[\Theta(\beta,B_o\phi) + \frac{\partial\Theta}{\partial B}(B-B_o)+\cdots\right]\left[1-6\left(\frac{\beta}{B}\right)^{4/3}\sin\phi + j(\phi,\frac{\beta}{B})\right] d\phi\right]\left[1-\left\langle j(\phi,\frac{\beta}{B})\right\rangle\right] d\beta . \tag{122}$$

In the integrand, $B-B_o$ may be determined by an iteration procedure analogous to that of equation 112. The first approximation is given by

$$B_1 - B_o = \Delta_1 B + \frac{1}{2\pi} \int_{\beta_L}^{\beta} \left[\int_o^{2\pi} \Theta(\beta, B_o + \Delta_1 B, \phi) \left[1 - 6\left(\frac{\beta}{B_o}\right)^{4/3} \sin\phi + \right. \right.$$

$$\left. \left. + j\left(\phi, \frac{\beta}{B_o}\right) \right] d\phi \right] \left[1 + \left\langle j\left(\phi, \frac{\beta}{B_o}\right) \right\rangle \right] d\beta \,. \qquad (123)$$

Noting that an expression for $\Delta_2 B$ accurate through terms of $B_o \mathcal{O}(\beta^{8/3}/B_o^{8/3})$ requires $B - B_o$ in equation 122 to be expressed only through terms of $B_o \mathcal{O}(\beta^{4/3}/B_o^{4/3})$, we see that the first approximation of equation 123 is adequate, giving

$$B - B_o = \frac{5}{2}\beta - \frac{45}{7}\left(\frac{\beta_L}{B_o}\right)^{4/3} B_o \sin\phi_o + B_o \mathcal{O}(\beta^{5/3}/B_o^{5/3}) \,. \qquad (124)$$

Evaluation of equation 122 then gives

$$\langle \Delta_2 B \rangle = \frac{1}{2\pi} \int_{\beta_L}^{o} \int_o^{2\pi} \Theta(\beta, B_o, \phi) d\phi d\beta + \frac{5}{4\pi} \int_{\beta_L}^{o} \int_o^{2\pi} \beta \frac{\partial f_1}{\partial B} d\phi d\beta -$$

$$- \frac{3:360}{8:14}\left(\frac{\beta_L}{B_o}\right)^{8/3} B_o + B_o \mathcal{O}(\beta_L{}^3/B_o{}^3) \,. \qquad (125)$$

From equations 117 and 125, we find

$$\langle \Delta B \rangle = \langle \Delta_1 B \rangle + \langle \Delta_2 B \rangle = -\frac{3 \cdot 1800}{8 \cdot 49} \left(\frac{\beta}{B_o}\right)^{8/3} B_o + B_o O(\beta_L{}^3/B_o{}^3)$$

$$= -3 \left(\frac{15}{112}\right)^2 \left(\frac{r}{L}\right)^8 B_o + B_o O\left(\frac{r^9}{L^9}\right) . \qquad (126)$$

Since in the initial and final states r depends only on B, we may then, to the order indicated, calculate the corresponding averages of the change in the radial coordinate r from equations 100 and 126 by the approximate relations

$$\langle \Delta B \rangle = \frac{\partial}{\partial r}\left[\frac{M}{r^3}\right] \langle \Delta r \rangle + \frac{1}{2} \frac{\partial^2}{\partial r^2} \left[\frac{M}{r^3}\right] \langle (\Delta r)^2 \rangle \qquad (127)$$

$$\langle (\Delta B)^2 \rangle = \left[\frac{\partial}{\partial r}\left[\frac{M}{r^3}\right]\right]^2 \langle (\Delta r)^2 \rangle \quad . \qquad (128)$$

This gives finally

$$\langle \Delta r \rangle = gkL \left(\frac{r}{L}\right)^a \left[1 + O\left(\frac{r}{L}\right)\right] \qquad (129)$$

$$\langle (\Delta r)^2 \rangle = 2kL^2 \left(\frac{r}{L}\right)^{a+1} \left[1+O\left(\frac{r}{L}\right)\right] \qquad (130)$$

with

$$a = 9, \; k = \frac{1}{4}\left(\frac{15}{112}\right)^2, \; g = 8 . \qquad (131)$$

These results are different from those obtained by Parker. His analysis gives 129 and 130 but with

$$a = 9,\ k = \frac{1}{2}\left(\frac{15}{112}\right)^2,\ g = 0\ . \tag{132}$$

Moreover, the actual differential equation that he solves is not the Fokker-Planck equation based on his analysis but is a heuristically derived diffusion equation. However, his equation is obtained if one takes

$$a = 9,\ k = \left(\frac{15}{112}\right)^2,\ g = a + b + 1 = 49/4\ . \tag{133}$$

Hence Parker's treatment may be regarded as a discussion of case 133. Note that the three cases have the same values of a and nearly the same values of k. Differences in k are trivial, affecting only the time scale, and the value will depend on the precise model used for the magnetic disturbance. The essential difference between the treatments arises from the difference in the values of g. In order to treat all these cases, and perhaps others that may arise from different models of magnetic disturbances, the equations will be solved with general values of a, k, and g insofar as this is practical.

2. Particle Diffusion

Denoting by $\phi^*(r,n)\,dr$ the number of particles in dr at r following n storms, the diffusion is governed by the Fokker-Planck equation.

$$\frac{\partial \phi^*}{\partial n} = -\frac{\partial}{\partial r}\left[\langle \Delta r \rangle\ \phi^*\right] + \frac{1}{2}\ \frac{\partial^2}{\partial r^2}\left[\ \langle (\Delta r)^2 \rangle\ \phi^*\right] \tag{134}$$

Following Parker's notation, one may let $\psi = \phi^*/2\pi r$ be the density per unit area in the equatorial plane and $\Psi = \psi/2z\,(r)$ be the density per unit volume, where z(r) is the small distance above and below the equatorial plane within which the particles are confined. From Parker we get $z(r) = z(R)R^{-5/4}r^{5/4}$ or, more generally,

$$r\,z(r) = \kappa L^2 (r/L)^b/4\pi\,, \tag{135}$$

with $b = 9/4$ for the actual model. Thus,

$$\phi^* = 2\pi r\psi = L^2 \kappa\,(r/L)^b\,\Psi \tag{136}$$

This can be substituted in equation 134 to get differential equations in Ψ instead of ϕ^*, but it seems easier to solve equations in ϕ^* and to use equation 136 to express the boundary conditions in terms of ϕ^*. In terms of the new variables

$$\tau = kn, \quad x = r/L \tag{137}$$

and on substitution from equations 129 and 130, equation 134 reduces to:

$$\frac{\partial \phi^*}{\partial \tau} = - g \frac{\partial (x^a \phi^*)}{\partial x} + \frac{\partial^2 (x^{a+1} \phi^*)}{\partial x^2} \qquad (138)$$

In the above derivation it has been assumed that L is the same for all storms. If L is replaced by a suitable average value and the connection between n and τ is suitably smoothed, equation 138 remains valid even if there are variations from storm to storm.

3. Steady State Solutions

The difference between solutions with different values of g may be illustrated by a simple example which may have some relevance in ths discussion of trapped particles, although we do not urge here that it be regarded as particularly realistic. Consider the steady state situation where the left-hand side of equation 138 is zero. Suppose the electron density in the interplanetary plasma is Ψ_1 and suppose that these electrons diffuse into the planetary magnetic field, starting at $r = r_1$, where the magnetic field is assumed to terminate at the equator. Assume further that the particles are removed at $r = r_o < r_1$, which may be regarded as the position of either the surface of the planet or as the point where some unspecified process removes particles faster than they can diffuse in. Thus we have the boundary conditions

$$\phi^*(r_1) \equiv \phi_1^* = L^2 K (r_1/L)^b \Psi_1; \quad \phi^*(r_o) = 0 \qquad (139)$$

It is then easily found that the solution of equation 138 is

$$\phi^*(r) = \left[\left(\frac{r}{r_1}\right)^{-a}\right]\left[\frac{r^{g-1} - r_o^{g-1}}{r_1^{g-1} - r_o^{g-1}}\right] \phi_1^* \tag{140}$$

and that the particle density is

$$\Psi(r) = \left(\frac{r}{r_1}\right)^{-(a+b)} \frac{r^{g-1} - r_o^{g-1}}{r_1^{g-1} - r_o^{g-1}} \Psi_1 \quad . \tag{141}$$

Equation 141 is plotted in Figure 6 for the case* $r_1 = 10\ r_o$ with a = 9, b = 9/4, g = 8, 4, 0 and 49/4, which correspond, respectively, to our model, to a model in which $\langle \Delta B \rangle = O(R^9/L^9)$, to the model with Parker's $\langle \Delta r \rangle$ and $\langle (\Delta r)^2 \rangle$, and to Parker's diffusion equation. Note that the cases g = 8, 4 and 0 predict a high peak in the particle density whereas the case g = 49/4 has no peak.

Thus far we have lumped together all electrons regardless of energy. If we define $N(r,E)\,dE$ to be the density at r of particles with kinetic energies between E and E + dE; i.e., $\Psi(r) = \int N(r,E)dE$, we can determine N from the above discussion by including in it only particles of the appropriate energy. We have assumed throughout that the first adiabatic invariant

$$R_m^2 \sin^2\theta / B = I, \tag{142}$$

where R_m is the magnetic rigidity, is not violated and hence, as pointed out by Kellogg (1959), when a particle drifts in it is accelerated by the electric fields associated with the drift motion. For non-relativistic

---

*See page 52.

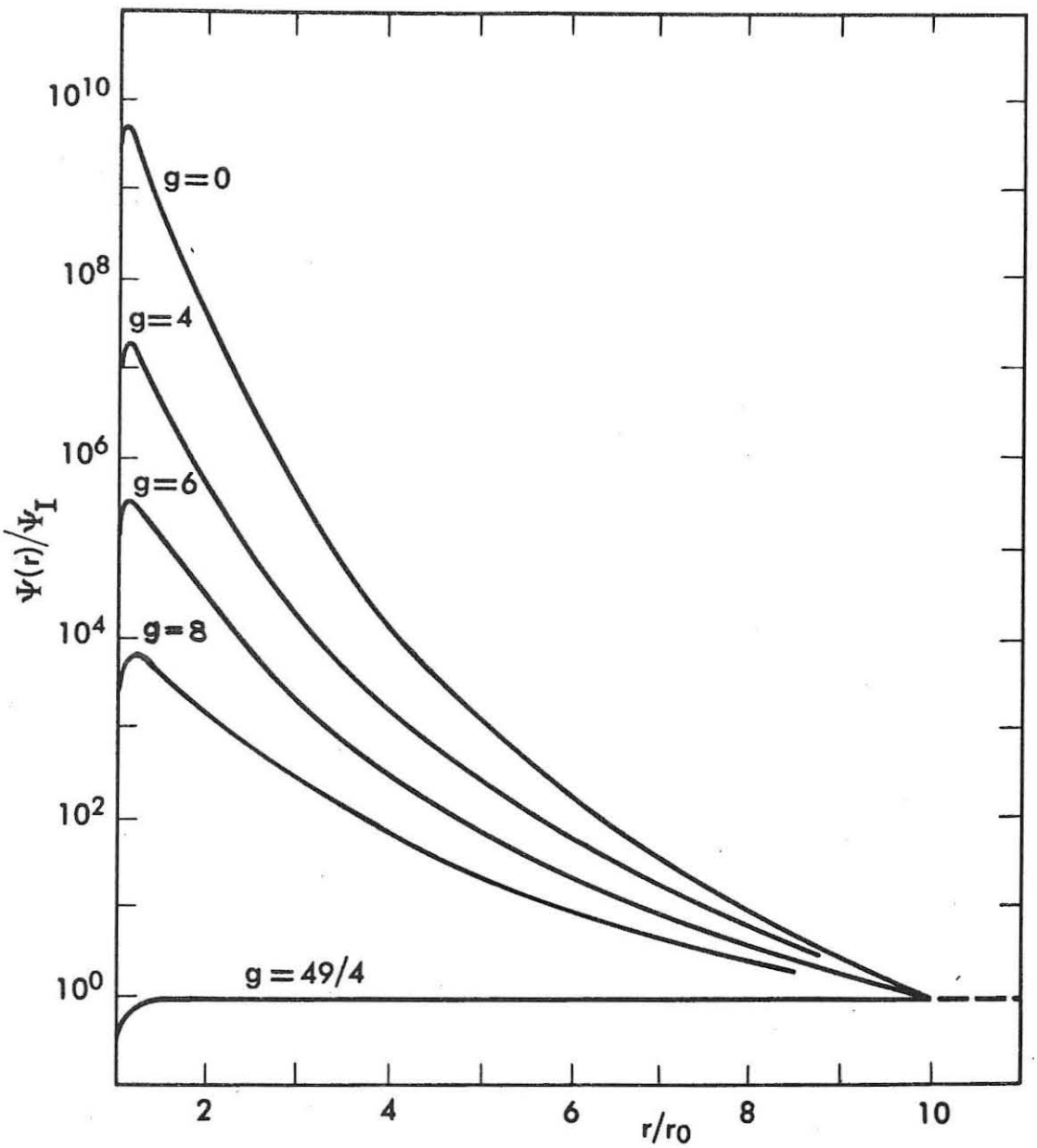

Figure 6. The ratios $\Psi(r)/\Psi_1$ of the particle density at r to the density at r_1, as given by eq. (141) for the case $r_1 = 10\,r_o$, $a = 9$ and $b = 9/4$.

particles, R_m is proportional to the velocity and R_m^2 to E. Since we are concerned with the case where $\theta \approx 90°$ and $B \propto r^{-3}$, equation 142 gives

$$E(r)r^3 = \text{const.} \tag{143}$$

and the particles which at r_2 are spread out over a range of energies dE_1 at E_1 will at r be found spread out over $dE = (r_1/r)^3 dE_1$ at an energy $E = (r_1/r)^3 E_1$. Thus we get

$$N(r,E) = \left(\frac{r}{r_1}\right)^{-(a+b-3)} \frac{r^{g-1} - r_o^{g-1}}{r_1^{g-1} - r_o^{g-1}} N_1\left(\frac{Er^3}{r_1^3}\right) \tag{144}$$

where $N(r_1, E) \equiv N(E)$ is the density in interplanetary space. If relativistic effects are significant, the equations are more complicated unless one goes to the highly relativistic limit, in which case equation 143 becomes

$$E(r)\, r^{3/2} = \text{const.} \tag{145}$$

with corresponding changes in equation 144.

The peak shown in Figure 6 becomes much more prominent if one considers a differential energy spectrum that has the usual dependence on energy. If the time average of the electron energy distribution at r_1 should be given by $\langle N_1(r_1, E)\rangle\, dE = C_o E^{-s-1} dE$, then the time average at other radii is given by

$$\langle N(r,E)\rangle\, dE = C(r)\, E^{-s-1}\, dE \tag{146}$$

where for most of the range $C(r) \approx (r_1/r)^{a+b+1-g+3s} C_o$ when $g > 1$ and $C(r) \approx (\frac{r_1}{r})^{a+b+3s}$ when $g < 1$. For the case of major interest where $a = 9$, $b = 9/4$, and $g = 6$, this gives $C(r) \approx (r_1/r)^{4+3s} C_o$.

In the above solution it has been assumed that the source of the electrons is the interplanetary plasma which reaches $r = r_1$. Actually, nothing would be changed if a steady source produced the density $N_1(E)$ well within the planetary field and the particles diffused both inward and outward to a termination of the planetary magnetic field farther out. The source could even fluctuate with time provided we let $N_1(E)$ denote the average density produced at r_1 and then regard the above solutions as giving the time energy densities as a function of τ. If the time constant of the fluctuations is less than that for diffusion to r_1 the actual density will be essentially constant in time and given by the expressions above. The solution in the region $r > r_1$ for this case is obtained from the above solutions by replacing r_o by r_2, the radius at which ϕ^* drops to zero at the outer boundary of the magnetic field, and by taking $r_1 < r < r_2$. If this is done for equation 144 and r_2 is then allowed to approach infinity, one finds that for the situation treated in equation 146, $C(r) \approx (r_1/r)^{a+b+3s} C_o$ for $g > 1$ and $C(r) \approx (\frac{r_1}{r})^{a+b+3s+1-g} C_o$ when $g < 1$; $C(r) \approx (r_1/r)^{11+3s} C_o$ in the case of interest, in the region outside the source.

The source strength required at r_1 is easily obtained from the net flux away on each side. Let the net flux outward at radius r per

unit magnetic storm be denoted by $J(r,n)$. Since the right hand side of equation 134 must give the negative of the divergence of this flux, one finds that

$$J(r,n) = \langle \Delta r \rangle \phi^* - \frac{1}{2} \frac{\partial}{\partial r} [\langle (\Delta r)^2 \rangle \phi^*]$$

$$= -kL x^g \frac{\partial (x^{a+1-g} \phi^*)}{\partial x} = -kL^2 \kappa x^g \frac{\partial (x^{a+b+1-g} \Psi)}{\partial x} \qquad (147)$$

The literature contains various suggestions that interplanetary electrons could diffuse into or be trapped by a planetary field or that low energy electrons from the magnetosphere could be accelerated by magnetic fluctuations or plasma oscillations to provide the source of high energy electrons. Davis has suggested the following variant of these proposals. The boundary between a planetary field and the interplanetary plasma is almost surely unstable because of the relative motion due to the earth's orbital motion and perhaps the solar wind. Particularly when interplanetary plasma presses with greater than usual force, the instabilities may well allow bubbles of plasma to penetrate into the planetary magnetic field. These diamagnetic bubbles will tend to be expelled again by magnetic pressure, but they will also tend first to break up by flute instabilities, to become very long and slender, and then by their finite conductivity to allow the planetary field to run uniformly through them. During this process, the particles in the plasma experience an increase in magnetic field strength and consequently should be accelerated in a direction normal to the magnetic field.

4. Transient Solution

The nature of the transient solution to equation 138 depends somewhat on the value of g. We shall conclude by presenting the time dependent solution of equation 138, subject to the condition that initially there is a ring of N particles at $r = r_1 = x_1 L$, i.e., that

$$\phi^*(x,o) = (N/L)\delta(x-x_1) . \tag{148}$$

The equation obtained by taking the Laplace transform of equation 138 is

$$s\bar{\Phi} - \phi^*(x,o) = -g\frac{\partial}{\partial x}(x^a\bar{\Phi}) + \frac{\partial^2}{\partial x^2}(x^{a+1}\bar{\Phi}) \tag{149}$$

where $\bar{\Phi}(x,s)$ is the Laplace transform of ϕ^*, $\bar{\Phi} = \int_o^\infty e^{-s\tau}\phi^* d\tau$. The last equation is thrown into a more familiar form by introducing the new variable $\theta = x^{a+1}\bar{\Phi}$:

$$\frac{\partial^2\theta}{\partial x^2} - \frac{g}{x}\frac{\partial\theta}{\partial x} + \left(\frac{g}{x^2} - \frac{s}{x^{a+1}}\right)\theta = -\phi^*(x,o) . \tag{150}$$

From Jahnke and Emde (1945), a solution to the corresponding homogeneous equation is:

$$\theta = x^{\frac{g+1}{2}}\left[C_1 I_p\left(\frac{2\sqrt{s}}{|a-1|}\frac{1}{x^{\frac{a-1}{2}}}\right) + C_2 K_p\left(\frac{2\sqrt{s}}{|a-1|}\frac{1}{x^{\frac{a-1}{2}}}\right)\right] \tag{151}$$

where

$$p = \left|\frac{g-1}{a-1}\right| \tag{152}$$

and where I_p and K_p are modified Bessel functions of order p. If the initial distribution consists of a ring of N particles at x_1, then equation 150 becomes

$$\frac{\partial^2\theta}{\partial x^2} - \frac{g}{x}\frac{\partial\theta}{\partial x} + \left(\frac{g}{x^2} - \frac{s}{x^{a+1}}\right)\theta = -\frac{N}{L}\delta(x-x_1) \tag{153}$$

Requiring ϕ^* to be finite at the origin $x = 0$, and placing an absorbing boundary at $x_2 \to \infty$, the solution to equation 153 has the form

$$\theta(x,s) = \begin{cases} A_+ x^{\frac{g+1}{2}} I_p\left(\frac{2\sqrt{s}}{a-1}\frac{1}{x^{\frac{a-1}{2}}}\right) & x \geq x_1 \\ A_- x^{\frac{g+1}{2}} K_p\left(\frac{2\sqrt{s}}{a-1}\frac{1}{x^{\frac{a-1}{2}}}\right) & 0 \leq x \leq x_1 \end{cases} \tag{154}$$

when $a > 1$, and

$$\theta(x,s) = \begin{cases} C_+ x^{\frac{g+1}{2}} K_p\left(\frac{2\sqrt{s}}{1-a}\frac{1}{x^{\frac{a-1}{2}}}\right) & x \geq x_1 \\ C_- x^{\frac{g+1}{2}} I_p\left(\frac{2\sqrt{s}}{1-a}\frac{1}{x^{\frac{a-1}{2}}}\right) & 0 \leq x \leq x_1 . \end{cases} \tag{155}$$

when $a < 1$. The constants are determined by requiring $\theta(x_1+) = \theta(x_1-)$ and $\left(\frac{\partial\theta}{\partial x}\right)_{x_1+} - \left(\frac{\partial\theta}{\partial x}\right)_{x_1-} = -\frac{N}{L}$, the latter condition being obtained upon integrating equation 153. For equation 154, this gives

$$\theta(x,s) = \begin{cases} \frac{N}{L}\frac{2}{a-1}\, x_1^{\frac{1-g}{2}}\, x^{\frac{1+g}{2}}\, K_p\left(\frac{2\sqrt{s}}{a+1}\,\frac{1}{x_1^{\frac{a-1}{2}}}\right) I_p\left(\frac{2\sqrt{s}}{a-1}\,\frac{1}{x^{\frac{a-1}{2}}}\right) & x \geq x_1 \\ \frac{N}{L}\frac{2}{a-1}\, x_1^{\frac{1-g}{2}}\, x^{\frac{1+g}{2}}\, I_p\left(\frac{2\sqrt{s}}{a-1}\,\frac{1}{x_1^{\frac{a-1}{2}}}\right) K_p\left(\frac{2\sqrt{s}}{a-1}\,\frac{1}{x^{\frac{a-1}{2}}}\right) & 0 \leq x \leq x_1 \end{cases} \tag{156}$$

when $a > 1$ and

$$\theta(x,s) = \begin{cases} \frac{N}{L}\frac{2}{1-a}\, x_1^{\frac{1-g}{2}}\, x^{\frac{1+g}{2}}\, I_p\left(\frac{2\sqrt{s}}{1-a}\, x_1^{\frac{1-g}{2}}\right) K_p\left(\frac{2\sqrt{s}}{1-a}\, x^{\frac{1-a}{2}}\right) & x \geq x_1 \\ \frac{N}{L}\frac{2}{1-a}\, x_1^{\frac{1-g}{2}}\, x^{\frac{1+g}{2}}\, K_p\left(\frac{2\sqrt{s}}{1-a}\, x_1^{\frac{1-a}{2}}\right) I_p\left(\frac{2\sqrt{s}}{1-a}\, x^{\frac{1-a}{2}}\right) & 0 \leq x \leq x_1 , \end{cases} \tag{157}$$

when $a < 1$. From Erdelyi, Magnus, Oberhettinger and Triconi (1954), we find as the inverse Laplace transform of the $\Phi = x^{-(a+1)}\theta$ corresponding to both equations 156 and 157:

$$\phi^*(x,\tau) = \frac{N}{L|a-1|}\,\frac{x_1^{\frac{1-g}{2}}\, x^{\frac{g-2a-1}{2}}}{\tau}\, \exp\left[-\frac{1}{\tau(a-1)^2}\left(\frac{1}{x_1^{a+1}}+\frac{1}{x^{a+1}}\right)\right] I_p\left(\frac{2}{\tau(a-1)^2}\,\frac{1}{x_1^{\frac{a-1}{2}}\, x^{\frac{a-1}{2}}}\right). \tag{158}$$

The result is in the standard form of solutions to diffusion problems.

The particle density per unit volume obtained from equation 158 is

$$\Psi(\xi,\tau) = \frac{N|a-1|}{2KL^3 x_1^{(b+1)}}\ \xi^{\frac{g-1-2a-2b}{2}}\ \nu^{-1}\exp\left[-\frac{1}{2\nu}\left(1+\frac{1}{\xi^{a-1}}\right)\right] I_p\left(\frac{1}{\nu\xi^{\frac{a-1}{2}}}\right) \tag{159}$$

where the new variables

$$\xi = \frac{x}{x_1} = \frac{r}{r_1} \quad \text{and} \quad \nu = \frac{(a-1)^2}{2}\ x_1^{a-1}\,\tau \tag{160}$$

have been introduced to simplify the expression. Equation 159 reduces to Parker's corresponding solution for the case $g = a+b+1$.

The nature of the solution may be seen by considering its various asymptotic forms. The following calculations parallel Parker's treatment of the case $g = a+b+1$. Equation 159 has the following asymptotic forms. For $\nu\xi^{\frac{a-1}{2}} \ll 1$, the asymptotic expression $I_p(y) = e^y (e\pi y)^{-1/2}\,[1+O(1/y)]$ is used to obtain

$$\Psi(\pi,\nu) = \frac{N|a-1|}{2^{3/2}\pi^{1/2}KL^3 x_1^{(b+1)}}\ \xi^{\frac{2g-3-3a-4b}{4}}\ \nu^{-1/2}$$

$$\exp\left[-\frac{1}{2\nu}\left(1-\frac{1}{\xi^{\frac{a-1}{2}}}\right)^2\right]\left[1+O\left(\nu\xi^{\frac{a-1}{2}}\right)\right]. \tag{161}$$

When ν becomes large compared to unity, a useful form of this expression obtains on separating out $\exp(-1/2\nu)$:

$$\Psi(\xi,\nu) = \frac{N|a-1|}{2^{3/2}\pi^{1/2}KL^3x_1^{b+1}}\,\xi^{\frac{2g-3-3a-4b}{4}}\,\nu^{-1/2}$$

$$\exp\left[-\frac{1}{2\nu\xi^{a-1}}+\frac{1}{\nu\xi^{\frac{a-1}{2}}}\right]\left[1+O\left(\nu\xi^{\frac{a-1}{2}};\frac{1}{\nu}\right)\right] \qquad (162)$$

At the other extreme, suppose $\nu\xi^{\frac{a-1}{2}} >> 1$. Then the expression $I_p(y) = [\Gamma(p+1)]^{-1}(y/2)^p[1+O(y^2)]$ is used to obtain

$$\Psi(\xi,\nu) = \frac{N|a-1|}{KL^3x_1^{b+1}\Gamma(p+1)2^{p+1}}\,\xi^{\frac{g-1-2(a+b)-p(a-1)}{2}}\,\nu^{-(p+1)}$$

$$\exp\left[-\frac{1}{2\nu}\left(1+\frac{1}{\xi^{a-1}}\right)\right]\left[1+O\left(\frac{1}{\nu^2\xi^{a-1}}\right)\right], \qquad (163)$$

or, on expanding the exponential,

$$\Psi(\xi_1\nu) = \frac{N|a-1|}{KL^3x_1^{b+1}\Gamma(p+1)2^{p+1}}\,\xi^{\frac{g-1-2(a+b)-p(a-1)}{2}}\,\nu^{-(p+1)}$$

$$\exp(-1/2\nu)\left[1+O\left(\frac{1}{\nu^2\xi^{a-1}};\frac{1}{\nu\xi^{a-1}}\right)\right]. \qquad (164)$$

When ν becomes very large,

$$\Psi(\xi,\nu) = \frac{N|a-1|}{\kappa L^3 x_1^{b+1}\Gamma(p+1)2^{p+1}}\,\xi^{\frac{g-1-2(a+b)-p(a-1)}{2}}\,\nu^{-(p+1)}$$

$$\left[1+O\left(\frac{1}{\nu^2\xi^{a-1}};\frac{1}{\nu\xi^{a-1}};\frac{1}{\nu}\right)\right]. \qquad (165)$$

The total particle flux (net number of particles flowing past ξ per magnetic storm) may be calculated from the expression

$$J(r,n) = -kLx^g\,\frac{\partial}{\partial x}\,(x^{a+1-g}\,\phi^*) = -k\kappa L^3 x_1^{a+b}\,\xi^g\,\frac{\partial}{\partial\xi}\,(\xi^{a+b+1-g}\,\Psi).$$

For the $\Psi(\xi,\nu)$ of equation 159,

$$J(r_1 n) = -\frac{N|a-1|kx_1^{a-1}}{2}\,\xi^{\frac{g-a}{2}}\,\nu^{-1}\exp\left[-\frac{1}{2\nu}\left(1+\frac{1}{\xi^{a-1}}\right)\right]\left[\left(\frac{1-g}{2}\,\xi^{\frac{a-1}{2}}+\frac{a-1}{2\nu}\,\frac{1}{\xi^{\frac{a-1}{2}}}\right)\right.$$

$$\left. I_p-\frac{a-1}{2\nu}\,I'_p\right] \qquad (166)$$

where the argument of the Bessel function and its derivative is $(\nu\xi^{\frac{a-1}{2}})^{-1}$. When $\nu\xi^{\frac{a-1}{2}} \gg 1$, the Bessel function and its derivative may be expanded to give

$$J(r,n) = \frac{-N|a-1|kx_1^{a-1}}{\Gamma(p+1)2^{p+1}}\left(\frac{1-g}{2}-p(a-1)\right)\xi^{\frac{g-p(a-1)-1}{2}}\,\nu^{-(p+1)}\exp(-1/2\nu)$$

$$\left[1+O\left(\frac{1}{\nu^2\xi^{a-1}};\frac{1}{\nu\xi^{a-1}}\right)\right]. \qquad (167)$$

When ν is large,

$$J(r,n) = -\frac{N|a-1|kx_1^{a-1}}{\Gamma(p+1)\,2^{p+1}}\left(\frac{1-g}{2} - p(a-1)\right)\xi^{\frac{g-p(a-1)-1}{2}}\nu^{-(p+1)}$$

$$\left[1+O\left(\frac{1}{\nu^2\xi^{a-1}};\frac{1}{\nu\xi^{a-1}};\frac{1}{\nu}\right)\right]. \qquad (168)$$

This can be expressed in terms of a mean drift velocity U toward increasing ξ

$$U = J/\phi^* .$$

Equations 165 and 168 yield:

$$U = -kLx_1^a\,\xi^a\left[\frac{1-g}{2} - p(a-1)\right]\left[1+O\left(\frac{1}{\nu^2\xi^{a-1}};\frac{1}{\nu\xi^{a-1}};\frac{1}{\nu}\right)\right] \qquad (169)$$

cm per magnetic storm. At the other extreme, when $\nu\xi^{\frac{a-1}{2}} \ll 1$, the asymptotic expressions of the Bessel function and its derivative give

$$J(r,n) = \frac{-kN(a-1)^2x_1^{a-1}}{4}\,\xi^{\frac{g+1-2a}{2}}\,\nu^{-2}\exp\left[-\frac{1}{2\nu}\left(1-\frac{1}{\xi^{\frac{a-1}{2}}}\right)^2\right]$$

$$\left[1+O\left(\nu\xi^{\frac{a-1}{2}};\nu\xi^{a-1};\xi^{\frac{a-1}{2}}\right)\right] \qquad (170)$$

The $\Psi(\xi,\nu)$ resulting from $\phi^*(x,o) = \frac{N}{L}\,\delta(x-x_1)$ may be described as a "wave," for setting $\frac{\partial\Psi}{\partial\xi} = 0$ in both equations 161 and 163 shows the maximum of $\Psi(\xi,\nu)$ to occur at a position ξ_c given by:

$$\xi_c^{a-1} = O(\frac{1}{\nu}) . \tag{171}$$

Equation 171 in conjunction with equation 163 leads to a simple expression for $\Psi(\xi,\nu)$ in the vicinity of the wave. For in equation 163, we are neglecting terms of $O(\frac{1}{\nu^2 \xi^{a-1}})$, and in the wave

$$O(\frac{1}{\nu^2 \xi^{a-1}}) = O(\frac{1}{\nu}) \tag{172}$$

which is small in the limit as ν becomes large. Thus, when $\nu >> 1$,

$$\Psi(\xi,\nu) = \frac{N|a-1|}{\kappa L^3 x_1^{b+1} \Gamma(p+1) 2^{p+1}} \xi^{\frac{g-1-2(a+b)-p(a-1)}{2}} \nu^{-(p+1)}$$

$$\exp(-\frac{1}{2\nu\xi^{a-1}})(1+O(\frac{1}{\nu})) \tag{173}$$

is a valid expression anywhere Ψ is not negligibly small. The crest of the wave, where $\frac{\partial\Psi}{\partial\xi} = 0$, has the position ξ_c, where

$$\xi_c^{a-1} = [\frac{a-1}{2(a+b)+1+p(a-1)-g}] \frac{1}{\nu} . \tag{174}$$

The total number of particles n in the wave for $\nu >> 1$ may be found by integrating the ϕ^* corresponding to equation 173 over $r = x_1 L\xi$:

$$n = \int_0^\infty \phi^* \, dr = \frac{N \nu^{-(p+1)}}{\Gamma(p+1)2^{p+1}} \Gamma\left(\frac{1-g+p(a-1)+2(a-1)}{2(a-1)}\right) (2\nu)^{\frac{1-g+p(a-1)+2(a-1)}{2(a-1)}} \tag{175}$$

If $\frac{g-1}{a-1} > 0$, equation 175 gives

$$n = \frac{N}{\Gamma(p+1)2^p} \nu^{-p} \tag{176}$$

whereas if $\frac{g-1}{a-1} < 0$, equation 175 gives

$$n = N . \tag{177}$$

In the latter case, the number of the particles in the wave does not decrease with time, but remains equal to the original number injected.

Assuming that the first adiabatic invariant is not violated, the energy E of a particle at ξ which had an initial energy E_o at $\xi = 1$ is

$$E = E_o \xi^{-\ell} \tag{178}$$

with $\ell = 3$ for nonrelativistic energies and $\ell = 3/2$ for ultrarelativistic energies. Thus, the total particle energy in the wave due to the injection of N particles of energy E_o is for large ν

$$\epsilon = \int_0^\infty E_o \xi^{-\ell} \phi^* dr = \frac{N E_o (2\nu)^{(p+1)}}{\Gamma(p+1)} \Gamma\left(\frac{1-g+p(a-1)+2\ell+2(a-1)}{2(a-1)}\right) (2\nu)^{\frac{1-g+p(a-1)+2\ell+2(a-1)}{2(a-1)}} . \tag{179}$$

When $\frac{g-1}{a-1} > 0$, equation 179 states

$$\mathcal{E} = NE_o(2\nu)^{\frac{1+\ell-g}{a-1}} \frac{\Gamma(\frac{\ell+a-1}{a-1})}{\Gamma(p+1)} , \tag{180}$$

and when $\frac{g-1}{a-1} < 0$,

$$\mathcal{E} = NE_o(2\nu)^{\frac{\ell}{a-1}} \frac{\Gamma(\frac{\ell+a-g}{a-1})}{\Gamma(\frac{a-g}{a-1})} . \tag{181}$$

The mean energy per particle is

$$\langle E \rangle = \frac{\mathcal{E}}{n} = E_o \Gamma(\frac{\ell+a-1}{a-1}) (2\nu)^{\frac{\ell}{a-1}} \tag{182}$$

when $\frac{g-1}{a-1} > 0$ and

$$\langle E \rangle = E_o(2\nu)^{\frac{\ell}{a-1}} \frac{\Gamma(\frac{\ell+a-g}{a-1})}{\Gamma(\frac{a-g}{a-1})} \tag{183}$$

when $\frac{g-1}{a-1} < 0$.

Finally, in terms of the position ξ_c of the wave, the mean energy per particle is

$$\langle E \rangle = E_o \Gamma(\frac{\ell+a-1}{a-1}) (\frac{a-1}{a+b})^{\frac{\ell}{a-1}} \xi_c^{-\ell} \tag{184}$$

when $\frac{g-1}{a-1} > 0$, and

$$\langle E \rangle = E_o \frac{\Gamma\left(\frac{\ell+a-g}{a-1}\right)}{\Gamma\left(\frac{a-g}{a-1}\right)} \left(\frac{a-1}{a+b+1-g}\right)^{\frac{\ell}{a-1}} \xi_c^{-\ell} \tag{185}$$

when $\frac{g-1}{a-1} < 0$. The number of particles in the wave in terms of the position of the crest is

$$n = \frac{N}{\Gamma(p+1)} \left(\frac{a+b}{a-1}\right)^{\frac{g-1}{a-1}} \xi_c^{g-1} \tag{186}$$

when $\frac{g-1}{a-1} > 0$, and does not depend on the position when $\frac{g-1}{a-1} < 0$.

The form of the solution, especially when $\frac{g-1}{a-1} < 0$, suggests that the particle diffusion resulting from large-scale magnetic fluctuations might be of importance in transferring electrons from the solar wind to the outer Van Allen belts of planets. If the other features of the magnetic storm are such that the first and second adiabatic invariants are not violated, the electrons both gain energy and attain flatter helices on inward diffusion. The last two features make attractive the hypothesis that this mechanism might provide the relativistic flat-helix electrons required if the decimeter radiation from Jupiter is to be synchrotron radiation. The time scales involved in the diffusion might present some problem. For instance, estimating the number n_D of storms required to cause a particle to diffuse a distance D by setting $n_D = D^2 / \langle (\Delta r)^2 \rangle$, and taking the $\langle (\Delta r)^2 \rangle$ given by equations 130 and 131, we have

$$n_D = D^2 / [\, \frac{1}{2} (\frac{15}{112})^2 r^2 (\frac{r}{L})^8 \,] \,. \qquad (187)$$

Setting $r = D$ and taking $(r/L) = 1/5$ as a typical value, this gives $n_D \approx \frac{1}{2} \times 10^8$. Parker (1960) estimates that on the order of fifteen sudden commencements occur per year on the earth, so that this would indicate that of the order of 10^7 years is required for appreciable diffusion. This is a much longer time scale than that estimated in section IIIA for scattering and loss by other mechanisms. On the other hand, it might be that magnetic activity at Jupiter is much greater than on the earth, in which case shorter diffusion times could obtain.

IV. SUMMARY

The Stokes parameter description developed in Appendix B for synchrotron radiation from a group of ultrarelativistic electrons with an arbitrary angular distribution, is summarized in Table IV, page 145 , and Table V, page 154 . The results of applying this development in section II to the radiation from a shell of relativistic electrons trapped in a dipole field are presented in graphical form in Figures 12-20 of Appendix D. As discussed in section II, the results confirm Davis' suggestion that the degree of polarization observed for the 31 cm radiation from Jupiter is obtained for synchrotron radiation from ultrarelativistic electrons in a dipole field if the electrons have relatively flat helices. As suggested by Davis, the observational result that the outer regions of the source are more strongly polarized than the central region might be explained if the equivalent of two shells of electrons are present, the outer shell comprising the electrons with flat helices and the inner shell having electrons with steeper helices. The overall polarization does not depend very strongly on the frequency or on the energy distribution of the electrons as long as the electrons radiate efficiently at the frequency of interest. For the details of the variation of the polarization and intensity and the corresponding cosine transform quantities, reference is made to the graphs of Appendix D. The results to be expected if the dipole axis is not at right angles to

the line of sight have not been studied here.

Discussion in section III of the problem of obtaining high energy, flat helix electrons in a dipole field has centered on a study of the particle drift and diffusion due to the effects of large scale magnetic fluctuations. The asymptotic approximation method of Bogolyubov and Zubarev has been used in Appendix C to show that the relativistic drift velocity expressions differ from those of nonrelativistic particles only by the presence of the relativistic mass in place of the rest mass. These drift velocity expressions have been used in the particle diffusion analysis of section III to derive the coefficients of an appropriate Fokker Planck equation by following the particle guiding center motions through a large-scale magnetic fluctuation. It has been found that this mechanism might lead to a high density of high energy, flat helix electrons; on the other hand, many fluctuations are required for appreciable diffusion to occur. Magnetic activity at Jupiter must be very great if this type of mechanism is to provide the relatively flat helix electrons required for the decimeter radiation from Jupiter to be synchrotron radiation. The effectiveness of this type of mechanism depends in part on the scattering, loss and diffusion to be expected from other causes, and these have yet to be studied.

APPENDIX A

Summary of the Published* Observations of Jupiter's Decimeter Radiation

In this appendix, the published* data on intensities are summarized in tabular form. The brightness of radio sources is conventionally given in terms of the equivalent blackbody temperature T_D ; i.e., the temperature at which a blackbody subtending the same solid angle as the source would emit the observed radio noise in the frequency interval under consideration. In Table III, the second column lists these temperatures as given by the various authors or as deduced from their data. The temperatures are derived from the Rayleigh-Jeans law assuming the source to subtend a solid angle Ω_J equal to that of the optical disk. More explicitly, if $P(f)df$ is the flux in watts per square meter received in the frequency interval df at f, then T_D in degrees Kelvin is determined by the equation

$$P\left(\frac{c}{\lambda}\right) = \frac{2kT_D}{\lambda^2}\Omega_J$$

where $k = 1.380 \times 10^{-23}$ joule per degree Kelvin is Boltzmann's constant, λ is the wavelength in meters and f is given in cycles/sec. For Jupiter, $2k\Omega_J$ varies between 5.16×10^{-31} and 1.118×10^{-30} joules

*And also the prepublication results of Morris at 31 cm.

per degree Kelvin, depending on the position of the earth in its orbit. For nonthermal sources T_D is not particularly significant, and it is sometimes more revealing to give a quantity proportional to the flux. Thus, the third column gives $T_D\lambda^{-2}$, which is proportional to the flux received at the earth and also, if multiplied by $2\pi k R_J^2 = 4.46 \times 10^{-7}$ -- where R_J is the radius of Jupiter, is equal to the watts per steradian per unit frequency radiated in the direction of the earth. Column 4 lists $(T_D - 130°)/\lambda^2$, which is proportional to the actual flux minus the flux corresponding to the infrared disk temperature of 130° obtained by Menzel, Coblentz and Lampland (1926). The remainder of the table is self-explanatory. The general nature of the remarks in columns 7 and 8 of various observers on variability point out the difficulties and uncertainties presented by noise in the observations. For completeness, no attempt has been made to avoid duplication; i.e., some of the entries refer to the same observations but are different due presumably to reinterpretation of the data.

TABLE III. OBSERVATIONS OF JUPITER'S RADIATIONS

Wavelength cm	Disk Temp. T_D °K	Flux T_D/λ^2 °K cm^{-2}	$\frac{T_D-130}{\lambda^2}$ °K cm^{-2}	Date of Observation	Angle between Jupiter's equatorial plane, and the plane of polarization of antenna (degrees)	Variability and Correlations: Variability	Correlations	Source
3.03	171±20	18.6±2.2	4.5±2.2	Aug. 22-Sept. 4, 1958		-	Giordmaine(1960)in summarizing the 3-cm. observations reports"--One can conclude that there are detectable fluctuations in the 3 cm radiation temp. of the planet, with the suggestion that changes in the apparent temp. may be correlated with changes in the appearance of the planet. No correlation was observed between the apparent temp. and the rotation of the planet, nor between apparent temp. and solar activity as measured by the 10 cm solar flux intensity. There was no detectable linear polarization."	Giordmaine, et al. (1959)
3.15	140±56	14.1±5.6	1.0±5.6	May 13 & May 31, 1956		-		Mayer, et al. (1958)
	145±26	14.6±2.6	1.5±2.6	Mar. 23-Apr. 1, 1957				
3.17	173±20	17.2±2.0	4.3±2.0	May 24-Jul. 29, 1958 Jan. 31-Feb. 7, 1959		-		Giordmaine, et al. (1959)
3.18	165±17	16.3±1.7	3.5±1.7	April, 1958		"--any variation in apparent blackbody temp. with rotation of Jupiter is less than 10%."		Alsop, et al. (1958)
3.36	189±20	16.7±1.8	5.2±1.8	Apr. 16-May 8, 1958 (except for Apr. 30-May 1)		"--evidence of an anomalously high temp. approx. 268°K, on 4/30-5/1/58."		Giordmaine, et al. (1959)
3.75	slightly greater than 200° (but may be in error by factor of 2)	140 (but may be off by factor of 2)	5	None given		-		Drake & Ewen (1958)
10.3	860-395 (estimated rel. uncertainty of ±160) ave. 580	8.1-3.7 (est. rel. uncertainty of ±1.5) ave. 5.5	6.9-2.5 ave. 4.2	5 days during period: June 10-28, 1958	67±0.5*	"--measured equivalent blackbody temp. varied from 860 to 395°K with an estimated rel. uncertainty of ±160°K;" "during one night's observation, the equivalent blackbody temp. varied from 860 to 390°K."	"--Attempts to correlate the variations in equivalent blackbody temp. with the planet rotation, while slightly suggestive, are by no means conclusive."	McClain & Sloanaker (1959)

*Sloanaker & Boland (1961)

TABLE III (cont.)

Wavelength cm	Disk Temp. T_D °K	Flux T_D/λ^2 °K cm^{-2}	$\frac{T_D-130}{\lambda^2}$ °K cm^{-2}	Date of Observation	Angle between Jupiter's equatorial plane, and the plane of polarization of antenna (degrees)	Variability and Correlations: Variability	Correlations	Source
10.2 & 10.3	640±85	6.0±0.8	4.8±0.8	June 10-Aug. 20, 1958	67±0.5*	"--measured apparent blackbody temp. ranged from 300°K to 1010°K about a mean of 64°K±85°K est. standard error--." "...present measurements give a roughly normal dist. of apparent temp. with a standard dev. of 190°K. On the basis of the est. measurement errors, the expected standard dev. is about 145°K, which is in reasonably good agreement with the observed scatter, but does not preclude the possibility of a variable component in the intensity of the radiation."	"...The measured temps. show no long-time trends over the 71 day measurement interval, but show a suggestion of a cyclical variation of about 30% correlated with a rotation rate between 40" and 2' longer than the rotation period of System II."	Sloanaker (1959)
10.2 & 10.3	315±65	3.0±0.6	1.7±0.6	Oct. 16-30, 1959	79±0.5*	"...observed change in intensity of about 2 to 1 between 1958 & 1959 is real and may be related to polarization of the radiation or to a correlation with solar activity. In addition, the 1958 measurements show some evidence of short-time variability, possibly correlated with the rotation of the planet."	"...the 1958 measurements show correlation for all rotation periods between about 1 min. and 2 1/2 min. longer than the period of System II; however, it is considered that the number of measurements is too small to decide whether this correlation is really connected with the rotation of Jupiter." "...the solar activity was 3.5 to 6 times as intense immediately preceding and during the period of the 10-cm. observations in 1958 as it was for the 1959 measurements..."	Sloanaker & Boland (1961)
21	~6200	~14	~14	May 16-June 2, 1959		"...the amount of the emission varies with time, by as much as a factor of 2 in a period of a few hours -"		Epstein (1959)

*Sloanaker & Boland (1961)

TABLE III (cont.)

Wavelength cm	Disk Temp. T_D °K	Flux T_D/λ^2 °K cm^{-2}	$\frac{T_D-130}{\lambda^2}$ °K cm^{-2}	Date of Observation	Angle between Jupiter's equatorial plane, and the plane of polarization of antenna (degrees)	Variability and Correlations: Variability	Correlations	Source
21	2496±450	5.6±1.0	5.3±1.0	May 14-June 18, 1959	67.9*	"...the measurements are highly suggestive of a cyclical variation."	"...An attempt has been made to correlate this data with System I and System II rotation. In the case of System II an elevated temp. has been noted at a longitude of 200°. This enhancement of about 30% appears to lie between 75° to 225°. While rather significant when subjected to a statistical test, the amount of data is limited, and this conclusion should be considered tentative. Correlation might actually be more pronounced with a system differing from both System I and II but sufficient data is not available at the time this is written." The remarks on the attempt to correlate these data with solar activity are essentially the same as those reported in 1960. [McClain, et al. (1960)].	McClain (1959)
21	2860±380	6.5±0.9	6.2±0.9	May 15-June 1, 1959	67.9*	"...suggestive of a cyclical change." "...average temp. in each group decreases successively with time "	"...No correlation was found with the 10-cm. solar index. In the case of solar particles, the fact that Jupiter was in opposition at the time of the measurements would lead one to expect that particles causing magnetic storms on the earth following a solar flare might reasonably be expected to arrive in the vicinity of Jupiter a few days later (first suggested by Drake). No definite correlation of this sort was found in these measurements. However, there is a slight suggestion of elevated temp. following an important 3+ flare on May 10, 1959 and the intense aurorae of May 11 and 12, 1959."	McClain, et al. (1960)
	2410±340	5.4±0.8	5.2±0.8	June 1-June 23, 1959				
	2050±430	4.6±1.0	4.3±1.0	June 23-July 31, 1959				

*Calculated from correction factors used in Field (1961).

TABLE III (cont.)

Wavelength cm	Disk Temp. T_D °K	Flux T_D/λ^2 °K cm^{-2}	$\frac{T_D-130}{\lambda^2}$ °K cm^{-2}	Date of Observation	Angle between Jupiter's equatorial plane, and the plane of polarization of antenna (degrees)	Variability and Correlations: Variability	Correlations	Source
							"...appears that there is no significant correlation between the low frequency events and the high frequency data on Jupiter. Based on the limited amount of data we have available, the 21-cm radiation from Jupiter seems to vary at a rate quite close to that of System II or System III."	
21.4	3500±1700†	7.6±3.7†	7.4±3.7†					
22	~3000	~6.2	~5.9	May, 1959	67.9*	"...An extensive set of observations at 22 cm suggests that variations of the order of 30% occur in the flux in time of the order of days."	"...There is no statistically significant correlation between the apparent variations and planetary rotation."	Drake & Hvatum (1959)
31	~5500 (80% of the values lie between 3.8×10^3 & 6.4×10^3 °K)	~5.7 (80% of the values lie between 3.9 and 6.7)	~5.6	April 15-June 17, 1959	77°	"...the apparent variations in the Jupiter values were not significantly greater than those for the other presumably non-varying weak sources."	"...we did check for a correlation with Jovian longitude, both system I & system II, and also for a correlation, either direct or delayed, with the Sacramento Peak Flare Index. In no case was there any significant correlation."	Roberts & Stanley (1959)
31	5500±1500**	5.7±1.6**	5.6±1.6**					
31	5100±1300	5.3±1.3	5.2±1.3	Mar.-May, 1960	1 1/2°	"...The possibility of intrinsic variations is not excluded."		Morris (1961)
	5175±1300	5.4±1.3	5.3±1.3	Jan.-Feb., 1961	80°			

*Calculated from correction factors used in Field (1961).
**Bolton & Roberts quoted by Field (1959).
† Drake as quoted by Field (1959).

TABLE III (cont.)

Wavelength cm	Disk Temp. T_D °K	Flux T_D/λ^2 °K cm^{-2}	$\frac{T_D}{\lambda^2}$ °K cm^{-2}	Date of Observation	Angle between Jupiter's equatorial plane, and the plane of polarization of antenna (degrees)	Variability and Correlations: Variability	Correlations	Source
68	70,000±30,000†	15±6.5†	15±6.5†					
68	~70,000	~15	~15	May 26 & May 27, 1959	24*	"High sensitivity monitoring of the planet at 440 Mc showed no statistically significant short period variations in flux during two nights of observing."		Drake & Hvatum (1959)
	~30,000 (less certain than the 70,000 meas.)	~6.5	~6.5	July 20-July 30, 1959				
68	[40,000±5000]***	[8.6±1.1]***	[8.6±1.1]***	[end of May, 1959]***				Drake (1960 as quoted by Field (1961)
	[31,000±5000]***	[6.7±1.1]***	[6.7±1.1]***	[end of July, 1959]***				
	[8500±9500]***	[1.8±2.0]***	[1.8±3.0]***	[end of Oct., 1959]***				

[ ]*** estimated from Figure 1 (and correction factors) of Field (1961).

*Calculated from correction factors used in Field (1961).

†Drake as quoted by Field (1959).

TABLE III (cont.)

Wavelength cm	Disk Temp. T_D °K	Flux T_D/λ^2 °K cm^{-2}	$\frac{T_D-130}{\lambda^2}$ °K cm^{-2}	Date of Observation	Angle between Jupiter's equatorial plane, and the plane of polarization of antenna (degrees)	Variability and Correlations: Variability	Correlations	Source
73****	<29,300	<5.5	<5.5	Sept. 16 & 17, 1959				Long & Elsmore (1960)
	< 7450[1]	<1.4[1]	<1.4[1]	Mar. 4-9, 1960				
	<10,100[2]	<1.9[2]	<1.9[2]	Mar. 15-18, 1960				
	<18,600[3]	<3.5[3]	<3.5[3]					
	<39,400[4]	<7.4[4]	<7.4[4]					
	<64,000	<12	<12	Mar. 20-23, 1961				

****These results are based on Figures 1 & 2 of Long & Elsmore (1960).

1 If source diameter < 1' when Jupiter is 4.375 A.U. from the earth
2 " " " < 2' " " " " " " " " " " (D_J=45")
3 " " " < 3' " " " " " " " " " "
4 " " " < 4' " " " " " " " " " "

APPENDIX B

Properties of Synchrotron Radiation

Synchrotron radiation, the radiation of relativistic electrons gyrating in a magnetic field, has been discussed in a variety of contexts. Fifty years ago, calculations of the spectral and angular distributions of the radiation from an electron in a circular orbit were presented by Schott (1912) as an example of radiation from an accelerated charge. In 1940, Pomeranchuk published a paper on the maximum energy which primary electrons in the cosmic radiation could have on reaching the earth's surface, the maximum being determined by loss of energy due to radiation in the earth's magnetic field. Schwinger (1949) and Arzimovich and Pomeranchuk (1945) are among those who have investigated the radiation in connection with energy loss in synchrotrons. The possibility that high speed electrons might be of importance in radiation from the sun was raised by Giovanelli (1948) and Hoyle (1949). Alfven and Herlofsen (1950) suggested that radio star emission might be due to cosmic ray electrons in the trapping field of a star. In 1950 Kiepenheuer, and in 1952 Hutchinson, discussed the possible relation of galactic radio noise to cosmic rays. Ginzburg and Shklovskii in 1953 suggested that relativistic electrons exist in space and that they give rise to the emission from nonthermal sources. And

since then, many articles [Twiss (1954, 1958), Hoyle (1954, 1957, 1960), Oort and Walraven (1956), Burbidge (1956a, 1956b, 1959), Korchak (1957), Ginzburg (1959), Tunmer (1959), Takakura (1959), Wallis (1959), Dyce and Nakada (1959), Biermann and Davis (1960)] have discussed synchrotron radiation in an astronomical context.

The interest in synchrotron radiation led Westfold (1959) to study in more detail the polarization properties. He studied the synchrotron radiation from an electron moving in a helical orbit, obtaining the polarization properties as well as the spectral and angular distribution of the radiation. His method was to straightforwardly Fourier analyze the field obtained from the Lienard-Wiechert potentials. The radiation was also calculated for a group of particles with an isotropic velocity distribution. Oster (1960, 1961) has recently studied the effects of collisions on the spectral and angular distribution of synchrotron radiation. In his 1960 paper, the spectrum is calculated by Fourier analyzing the electric field obtained from the Lienard-Wiechert potential of a single particle moving in a circular orbit. The results are generalized in his second paper to a particle moving in a helical orbit, both by direct Fourier analysis, and by Lorentz transforming the spectrum for a particle in a circular orbit. The power spectrum due to an assembly of particles having an isotropic Maxwellian distribution function is also obtained. It is found that for practical applications, collision

broadening of the spectral lines is of much less importance than the broadening due to purely relativistic effects.

More recently, synchrotron radiation has received a lively discussion in the literature in connection with power losses from proposed controlled thermonuclear reactors. This problem has been studied by Trubnikov (1958, 1961), Beard (1959, 1960), Drummond and Rosenbluth (1960, 1961a, 1961b), and Beard and Baker (1961a, 1961b). Recent related contributions have been made by Bekefi, Hirshfield and Brown (1961a, 1961b), Hirshfield, Baldwin and Brown (1961), and Hirshfield and Brown (1961). The concern here is mainly with the power loss from mildly relativistic plasmas. Calculations are based either on the spectrum of a single electron or on a group of electrons all moving in a plane or distributed isotropically.

In spite of these numerous references, an abbreviated derivation of the properties of synchrotron radiation is presented below. There are two reasons for this. First, none of the references give results for the radiation from a group of particles with an arbitrary angular distribution, and we need to consider such distributions in connection with the dipole model of Jupiter's field. Secondly, we wish to obtain a Stokes parameter description of the radiation. The derivation is divided into two parts. The first part develops the expressions for the component power spectra from a single electron moving ultrarelativistically in a helical orbit. This is done by using Feynman's "effective

transverse acceleration" to obtain the properties of the radiation from an electron in a circular orbit, and then using a Lorentz transformation to obtain the results for a helical orbit. In the second part, the Stokes parameters are developed for a group of electrons with an arbitrary angular distribution.*

1. Synchrotron Radiation from a Single Electron

(a) Radiation from an electron in a circular orbit.

Feynman (1958) has pointed out that it is physically revealing to express the radiation electric field of an accelerated charge as being simply proportional to an effective transverse acceleration $\ddot{d}$. It is an acceleration transverse to the line of sight since the fields at great distances from the charge appear to be those of plane waves. It is an effective acceleration --- rather than an instantaneous projection of the actual acceleration onto a plane transverse to the line of sight --- since allowance must be made for the fact that light has a finite velocity, and that therefore the radiation emitted in an interval τ by an accelerating charge moving toward (away from) an observer will arrive at the observer in an interval less (greater) than τ. The effective transverse acceleration is the acceleration which would be required of an electron

*The derivation in this form has appeared in Chang (1960). The method of obtaining the single electron results for helical motion by Lorentz transforming the results for circular motion has also been employed independently by Oster (1961).

moving always at right angles to the line of sight in order for it to give the same radiation as that produced by the electron in its actual orbit. It is the acceleration a naive observer would give for the electron if he viewed it by light which actually travelled with velocity c but which he regarded as traveling with infinite velocity and if he could not perceive the motion along the line of sight.

The expression for the radiation electric field $\vec{\mathcal{E}}(t')$ in terms of $\ddot{\vec{d}}(t)$ in rationalized MKS units is*:

$$\vec{\mathcal{E}}(t') = -\frac{q}{4\pi\epsilon_o}\,\frac{\ddot{\vec{d}}(t)}{Rc^2}\,, \tag{B1}$$

where $-q$ is the charge of an electron, ϵ_o is the permitivity of free space, c is the velocity of light, and R is the distance from the trajectory to the field point at which we wish to know the electric field at the time t'. The time t is related to t' by the time that it takes light to travel the distance R from the source region to the observer: $c(t'-t) = R$. The prescription for finding $\ddot{\vec{d}}(t)$ in terms of the actual motion of the electron is straightforward. Thus, define a unit vector $\vec{i}$ to be directed from the trajectory to the field point (it being assumed that the dimensions of the source region are much smaller than the distance to the observer). If $\vec{r}_1(t'')$ is the position vector of the electron in its trajectory, then $\vec{d}(t)$ - from which $\ddot{\vec{d}}(t)$ is obtained by differentiating twice with respect

---

*This expression can be shown to follow from the usual expression obtained from the Lienard-Wiechert potentials whenever the dimensions of the source region are much less than the distance to the observer. See, for instance, Chang (1960).

to t - is the (retarded) projection of $\vec{r}_1(t'')$ on the plane of sight (i.e., on any plane in the region of the source perpendicular to $\vec{i}$):

$$\vec{d}(t) = \vec{r}_1(t'') - (\vec{r}_1(t'')\cdot \vec{i})\,\vec{i}$$

$$(t-t'')c = |\vec{r}_1(t'')\cdot \vec{i}| = -\vec{r}_1(t'')\cdot \vec{i} \ . \qquad \text{(B2)}$$

We wish here to evaluate $\ddot{\vec{d}}(t)$ for an electron moving in a circular orbit. For this purpose, consider the diagram of Figure 7. The diagram depicts the circular orbit of the electron about the magnetic field as seen from different directions. In particular, the view in which the orbit appears as an ellipse represents that seen by an observer for which Ψ is the angle between the line of sight and the orbital plane. In this view, $\ddot{d}_{\parallel}$ is the value of the effective transverse acceleration component along the projection of the magnetic field onto the plane perpendicular to the line of sight --- and is shown in its positive sense; $\ddot{d}_{\perp}$ is the value of the effective transverse acceleration component along the direction in the plane perpendicular to the line of sight, perpendicular to the projection of the magnetic field --- and is shown in its positive sense. In the plan view, a is the radius of the circle, which for an electron of speed v (and energy $E = m_o c^2(1 - v^2/c^2)^{-\frac{1}{2}}$) in a magnetic field of magnitude B is

$$a = \frac{vE}{qBc^2} \ ; \qquad \text{(B3)}$$

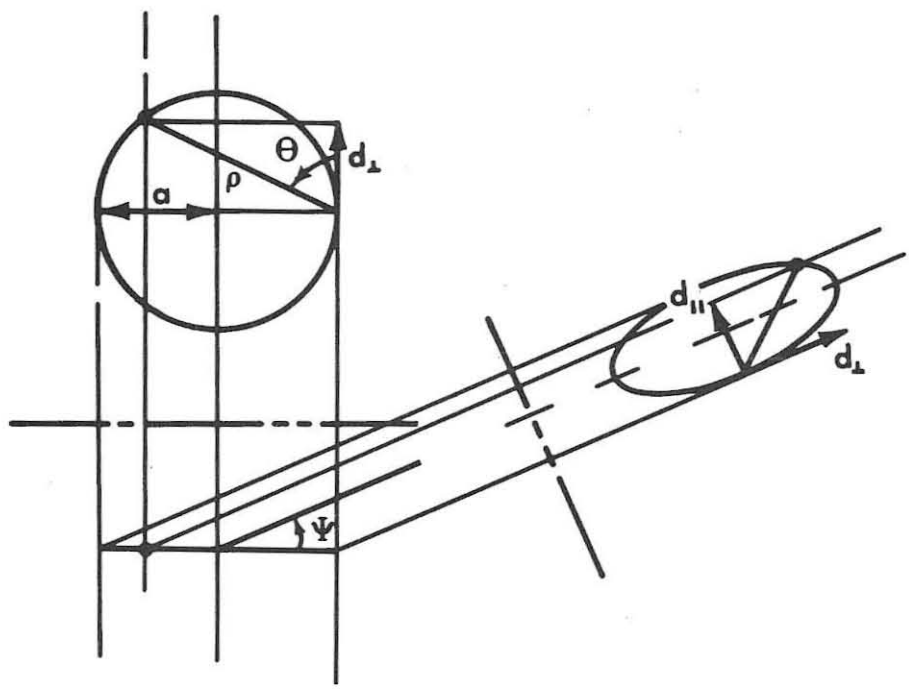

Figure 7. Coordinates used in describing an electron in a circular orbit.

ρ is the distance from the origin to the electron; and θ is the angle between ρ and the direction of $\vec{d}_\perp$.

From the geometry:

$$d_\perp = \rho \cos\theta = a \sin 2\theta \tag{B4}$$

$$d_\parallel = \rho \sin\theta \sin\Psi = 2a \sin^2\theta \sin\Psi \ . \tag{B5}$$

From the definition of the times,

$$t - t'' = \frac{\rho}{c} \sin\theta \cos\Psi = \frac{2a}{c} \sin^2\theta \cos\Psi \ . \tag{B6}$$

From the geometry and the fact that the electron has a frequency of $\omega = qBc^2/E$,

$$\frac{d\theta}{dt''} = \frac{\omega}{2} \ . \tag{B7}$$

From equations B4-B7, form

$$\ddot{\vec{d}} = \frac{d^2\vec{d}}{dt^2} = \frac{d}{dt''}\left[\left(\frac{d\vec{d}}{dt''}\right)\left(\frac{dt''}{dt}\right)\right]\frac{dt''}{dt} \tag{B8}$$

giving

$$\ddot{d}_\perp = \frac{d^2 d_\perp}{dt^2} = -\omega^2 a \frac{\left[\frac{\omega a}{c}\cos\Psi + \sin 2\theta\right]}{\left[1 + \frac{\omega a}{c}\cos\Psi \sin 2\theta\right]^3} \tag{B9}$$

and

$$\ddot{d}_{\parallel} = \frac{d^2 d_{\parallel}}{dt^2} = \frac{\omega^2 a \sin\Psi \cos 2\theta}{\left[1 + \frac{\omega a}{c} \cos\Psi \sin 2\theta\right]^3} \tag{B10}$$

Both $\ddot{d}_{\perp}$ and $\ddot{d}_{\parallel}$ have a resonance denominator. It is apparent that for $(\omega a/c) \approx 1$, the field is effectively confined to Ψ near 0. The perpendicular component $\ddot{d}_{\perp}$ will have its maximum magnitude in the plane $\Psi = 0$, whereas $\ddot{d}_{\parallel}$, being zero in the plane $\Psi = 0$, will have its maximum magnitude for some angles $\pm\Psi_{\parallel} \neq 0$ where $\Psi_{\parallel}$ approaches zero as $\omega a/c$ approaches unity.

Some feeling for the radiation can be had by examining $\ddot{d}_{\perp}$ in the plane $\Psi = 0$. From equations B5 and B9, it is easy to obtain the picture of Figure 8 --- where the "widths" shown are obtained by equating the areas under the appropriate humps to the products of the maximum values and the "widths."

From the duration of the pulse (Fig. 8),

$$\tau = \frac{1}{2}\left(mc^2/E\right)^2 (m/qB) , \tag{B11}$$

we can infer that the electron effectively radiates into a "cone of radiation" whose axis lies along the electron's direction of motion, and whose apex angle is about mc^2/E. Thus, in the interval $\Delta t = \tau$, the electron turns through an angle

$$\omega\Delta t'' = \omega(\Delta t''/\Delta t)\,\tau . \tag{B12}$$

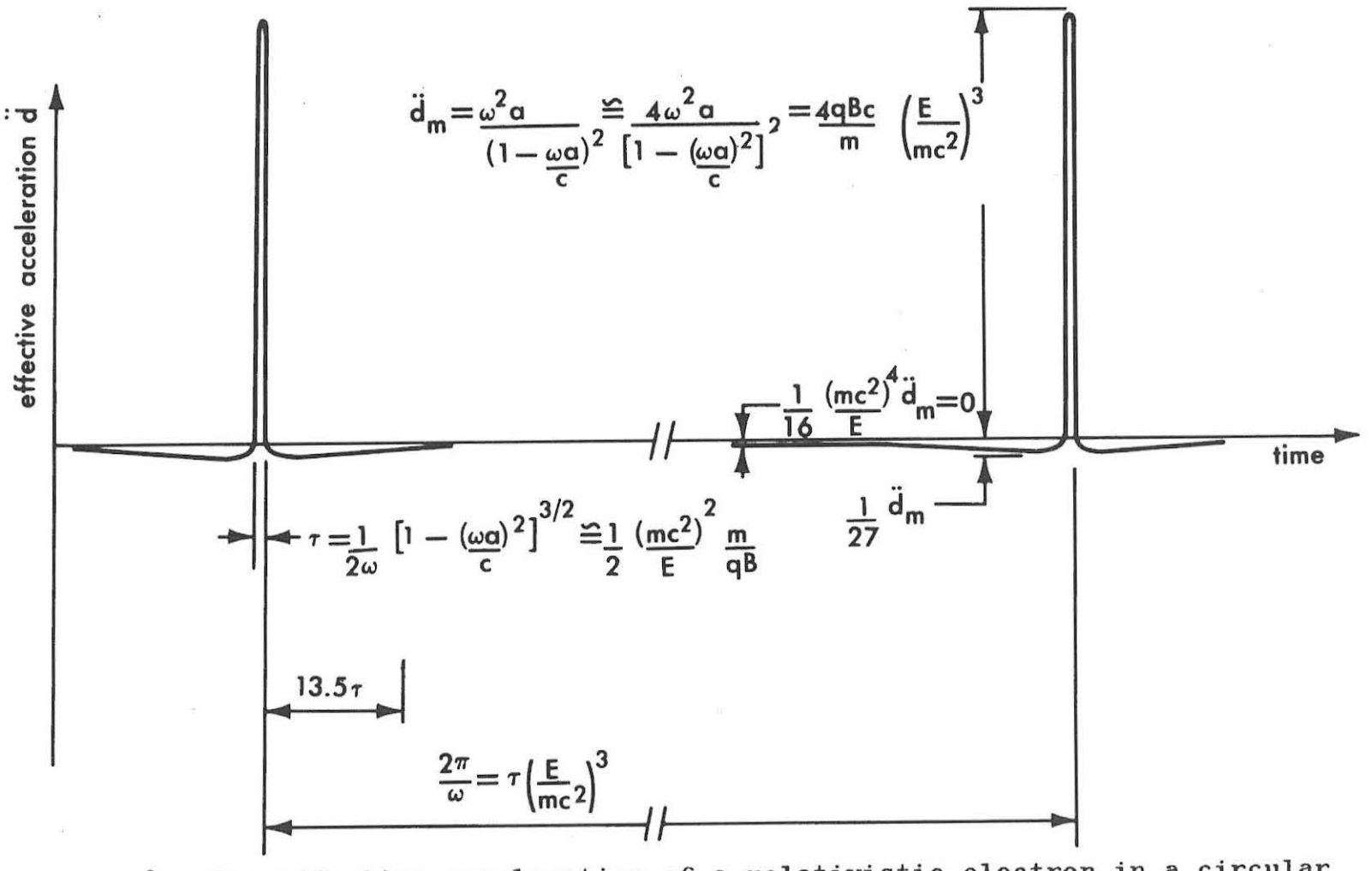

Figure 8. The effective acceleration of a relativistic electron in a circular orbit as observed in the plane of the orbit.

From equations B6 and B7, we have that at $\theta = 3\pi/4$ (the condition for the resonance denominator to give a maximum),

$$\left.\frac{dt''}{dt}\right|_{\substack{\theta = 3\pi/4 \\ \Psi = 0}} = (1 - \omega a/c)^{-1} \tag{B13}$$

which for $(\omega a/c) \approx 1$ can be written approximately as

$$\left.\frac{dt''}{dt}\right|_{\substack{\theta = 3\pi/4 \\ \Psi = 0}} = 2[1 - (\omega a/c)^2]^{-1} = 2\,(E/mc^2)^2 \tag{B14}$$

Equation B12 can then be written:

$$\omega \Delta t'' = 2\omega\,(E/mc^2)^2 \tau = mc^2/E\ , \tag{B15}$$

the second equality resulting from equation B11 and the expression for ω.

Equation B15 gives the angle that the electron turns through while contributing appreciably to the intensity at the observer. (The positive and negative areas under the curves of Figure 8 cancel, so that the contribution of the positive pulse to the intensity ($\propto \ddot{d}^2$) is much greater than that of the negative portions.) The implication is that in the plane of the orbit, the radiation is confined to angles within $\pm\, mc^2/2E$ on either side of the electron's direction of motion.

For $\theta \approx 3\pi/4$ and $\Psi \approx 0$, the resonance denominator can be written as

$$\left(1 + \frac{\omega a}{c} \cos\Psi \sin 2\theta\right)^3 \approx \left[\left(1 - \frac{v}{c}\right) + \frac{v}{2c}\left(\Psi^2 + \epsilon^2\right)\right]^3, \tag{B16}$$

where

$$\epsilon \equiv 2\theta - \frac{3\pi}{2} , \tag{B17}$$

and is the angle through which the electron turns in a time $\frac{\epsilon}{\omega}$. Thus, by noting the appearance of $\Psi^2 + \epsilon^2$ in equation B16, one can infer from equation B15 --- the equation giving the angular extent in the orbital plane only --- that in three dimensions the radiation is effectively confined to lie within a cone of apex angle

$$\eta \approx \frac{mc^2}{E} \tag{B18}$$

whose axis lies along the electron's direction of motion.

It might be well to summarize here some of the properties which have been obtained from the foregoing equations of the synchrotron radiation from a relativistic electron moving in a circular orbit. (In the following, E is the total electron energy and B is the magnetic field.)

(1) The radiation is essentially limited to within a cone of apex angle $\sim mc^2/E$ whose axis lies along the electron's direction of motion.

(2) The radiation comes to an observer in pulses of duration τ proportional to $1/BE^2$, which are separated by an interval $2\pi/\omega$, which is proportional to B/E.

(3) The maximum value of the electric field is proportional to BE^3.

From these properties, the following statements can be made:

(4) The energy per revolution received at a point which is inside the radiation cone sometime during a period of gyration is proportional to $\ddot{d}^2\tau \propto BE^4$.

(5) The power received at a point which is inside the radiation cone sometime during a period is proportional to $\omega\ddot{d}^2\tau \propto B^2E^3$.

(6) The rate at which an electron loses energy is proportional to $(\omega\ddot{d}^2\tau\ (mc^2/E) \propto B^2E^2$ (where the factor mc^2/E is proportional to the area of the strip on a sphere swept out by the radiation cone as the electron follows its circular orbit).

Furthermore, it is apparent that a spectral decomposition of the radiation will show that:

(7) each frequency component of the electric and magnetic fields is elliptically polarized, both $\ddot{d}_\parallel$ and $\ddot{d}_\perp$ being periodic with the same period, the radiation being left-handed if the angle between the direction of observation and the magnetic field is less than $\pi/2$, and right-handed if it is greater than $\pi/2$; and

(8) the radiation will contain frequencies up to at least $\frac{1}{\tau} = 2(E/mc^2)^2 qB/m$.

To obtain the spectral decomposition of the radiation, it is necessary to evaluate

$$\ddot{d}_{\perp n} = \frac{\omega}{2\pi} \int_0^{2\pi/\omega} e^{in\omega t}\, \ddot{d}_{\perp}(t)\, dt\,, \tag{B19}$$

and

$$\ddot{d}_{\parallel n} = \frac{\omega}{2\pi} \int_0^{2\pi/\omega} e^{in\omega t}\, \ddot{d}_{\parallel}(t)\, dt\,. \tag{B20}$$

By substituting the expressions of equations B6, B7, B9, and B10 in the above, $\ddot{d}_{\perp n}$ and $\ddot{d}_{\parallel n}$ can be expressed as integrals over θ,

$$\ddot{d}_{\perp n} = \frac{-\omega}{\pi} \int_0^{\pi} \exp\left[i2n\left(\theta + \frac{\omega a}{c} \sin^2\theta \cos\Psi\right)\right] \frac{\omega a\left[\frac{\omega a}{c}\cos\Psi + \sin 2\theta\right] d\theta}{\left[1 + \frac{\omega a}{c}\cos\Psi \sin 2\theta\right]^2} \tag{B21}$$

$$\ddot{d}_{\parallel n} = \frac{\omega}{\pi} \int_0^{\pi} \exp\left[i2n\left(\theta + \frac{\omega a}{c} \sin^2\theta \cos\Psi\right)\right] \frac{\omega a \sin\Psi \cos 2\theta}{\left[1 + \frac{\omega a}{c}\cos\Psi \sin 2\theta\right]^2}\, d\theta\,. \tag{B22}$$

The main contribution in each of the integrals comes near $\Psi = 0$ and $\theta = 3\pi/4$, so that for $\frac{\omega a}{c} \approx 1$, a good approximation to the integrals comes by expanding the trigonometric functions about their values at these two angles. On expanding θ and Ψ about these angles, we obtain:

$$\ddot{d}_{\perp_n} = \frac{\omega^2 a}{\pi} \exp\left[in\left(\frac{v}{c}\cos\Psi + \frac{3\pi}{2}\right)\right] \int_{-\infty}^{\infty} \frac{\exp\left[\frac{in}{2}\left\{\left(\left(\frac{mc^2}{E}\right)^2 + \Psi^2\right)\epsilon + \frac{\epsilon^3}{3}\right\}\right]\left[\left(\frac{mc^2}{E}\right)^2 + \Psi^2 - \epsilon^2\right] d\epsilon}{\left[\left(\frac{mc^2}{E}\right)^2 + \Psi^2 + \epsilon^2\right]^2} \tag{B23}$$

$$\ddot{d}_{\parallel_n} = \frac{2\omega^2 a}{\pi} \exp\left[in\left(\frac{v}{c}\cos\Psi + \frac{3\pi}{2}\right)\right] \int_{-\infty}^{\infty} \frac{\exp\left[\frac{in}{2}\left\{\left((mc^2)^2 + \Psi^2\right)\epsilon + \frac{\epsilon^3}{3}\right\}\right]\Psi\epsilon\, d\epsilon}{\left[\left(\frac{mc^2}{E}\right)^2 + \Psi^2 + \epsilon^2\right]^2} \tag{B24}$$

where

$$\epsilon = 2\theta - \frac{3\pi}{2} \tag{B25}$$

(In obtaining equations B23 and B24, we have set ($v = \omega a$)

$$1 - v/c = \frac{1}{2}\left(1 - v^2/c^2\right) \tag{B26}$$

and have employed our knowledge of the short duration of the pulse to claim that the important harmonics will be at large n, and that, therefore, by the usual stationary phase argument, the limits of integration can be changed from $\left(\frac{-3\pi}{2}, \frac{\pi}{2}\right)$ to $(-\infty, +\infty)$ without introducing appreciable error.)

The exponential appearing in equations B23 and B24 is of the form of that occurring in the Airy integral --- as given on page 190 of Watson (1944):

$$Ai(x) = \int_0^\infty \cos(t^3+xt)dt = 1/2 \int_{-\infty}^{\infty} \exp\,[i(t^3+xt)]\,dt$$

$$= \frac{\sqrt{x}}{3}\, K_{1/3}\left(\frac{2x\sqrt{x}}{3\sqrt{3}}\right) , \qquad \text{(B27)}$$

and, in fact, by integrating by parts, equations B23 and B24 can be expressed in terms of an Airy integral and its derivative, and hence in terms of modified Bessel functions (Westfold 1959). To obtain the power spectrum, one forms $\left|\ddot{d}_{\parallel_n}\right|^2$ and $\left|\ddot{d}_{\perp_n}\right|^2$.

As will be seen later, the quantities which enter the calculations of the radiation power spectrum from a group of electrons are not $\left|\ddot{d}_{\parallel_n}\right|^2$ and $\left|\ddot{d}_{\perp_n}\right|^2$, but rather $\left|\ddot{d}_{\parallel_n}\right|^2$ and $\left|\ddot{d}_{\perp_n}\right|^2$ integrated over solid angle. The integrals involved have been evaluated by Westfold (1959). The resulting expressions for the mean total power radiated in the frequency band (f, f+df) --- at high n the harmonics are so closely spaced that the radiation is essentially continuous --- are the folllowing. Let $p_f^{(1)}$ df equal the mean integrated power radiated into (f, f+df) associated with the electric vectors parallel to the projections of the magnetic field B in the planes normal to the lines of sight; and let $p_f^{(2)}$ df equal the mean integrated power radiated into (f, f+df), associated with the electric vectors perpendicular to the projections of the magnetic field B in the planes normal to the lines of sight.

Then

$$p_f^{(1)} = \frac{\sqrt{3}\,\mu e^3 cB}{4\pi m} F^{(1)}(f/f_c) \tag{B28}$$

$$p_f^{(2)} = \frac{\sqrt{3}\,\mu e^3 cB}{4\pi m} F^{(2)}(f/f_c) \tag{B29}$$

where

$$f_c = \frac{3eBE^2}{4\pi m^3 c^4} \tag{B30}$$

$$F^{(1)}(x) = \frac{x}{2}\left[\int_x^\infty K_{5/3}(\eta)d\eta - K_{2/3}(x)\right] \tag{B31}$$

$$F^{(2)}(x) = \frac{x}{2}\left[\int_x^\infty K_{5/3}(\eta)d\eta + K_{2/3}(x)\right] \tag{B32}$$

and $K_{2/3}$ and $K_{5/3}$ are modified Bessel functions. B is the magnetic field, E is the total energy of the electron, e the electronic charge, μ the permeability of free space, m the electron mass, and c the velocity of light. All are expressed in rationalized units.

By integrating the above expressions over frequency, one can obtain the expression for the total rate of energy loss. Alternatively, the total rate can be obtained directly by evaluating Poynting's vector from equation B1, and integrating over solid angle, this procedure having the advantage that the procedure is independent of any assumption regarding the magnitude of the electron velocity. The total rate of energy loss is found to be:

$$\frac{dE}{dt} = -\frac{e^4 v^2 B^2 E^2}{6\pi\epsilon_o m^4 c^7} \qquad \text{(B33)}$$

in rationalized MKS units.

(b) Radiation from an electron in a helical orbit

Having obtained the desired properties of the radiation from a relativistic electron in a circular orbit, there is more than one way of proceeding to obtain the properties for an electron in a helical orbit. The direct method would be to find the effective transverse acceleration for an electron in a helical orbit and then perform the usual Fourier analysis. This is essentially Westfold's (1959) procedure, although he does not explicitly take the effective transverse acceleration as his starting point. Alternatively, one could obtain Schwinger's (1949) result for a relativistic electron in an arbitrary orbit by noting that the short duration τ of the pulse in Figure 3 suggests that the large scale features of the orbit are not important in determining the radiation at any instant. Thus, if equations B28 and B32 are expressed in terms of the radius a of the circular orbit, the equations for an electron in an arbitrary orbit can be obtained simply by replacing a by the instantaneous radius of curvature. (The radiation that would be associated with an actual change of speed in the general case would not usually be appreciable since a relativistic particle in an accelerating field appears to experience a change in mass rather than in speed.)

In the following, the transition from the circular orbit case to the helical orbit case will be accomplished via a Lorentz transformation. The transition is based on the fact that only the relative motion of the observer and the source electron is important in determining the radiation characteristics. Thus, the two situations depicted in Figure 9 are equivalent: the same physical occurrence is simply pictured in two different frames of reference. In the reference frame Σ', the electron appears to be following a helical orbit, the velocity component along the helix axis --- i.e., along the magnetic field $\vec{B}$ --- being $v_{\parallel}'$. The reference frame Σ' is taken to be the observer's frame of reference --- i.e., in Σ', the observer is at rest. The frame Σ moves relative to Σ' with the axial velocity $\vec{v}_{\parallel}'$ of the electron. In Σ, then, the electron executes a circular orbit while the observer moves with a velocity $\vec{v}_{\parallel} = -\vec{v}_{\parallel}'$.

We shall need to keep in mind the following Lorentz transformation relations (primed and unprimed quantities referring to Σ' and Σ, respectively):

I. The electron in the circular orbit which has the energy E in Σ has the energy E' in Σ', where

$$E' = E(1 - v^2/c^2)^{-1/2} \tag{B34}$$

II. If the line of sight in Σ makes an angle Ψ with the plane perpendicular to the magnetic field, then in Σ' the angle is

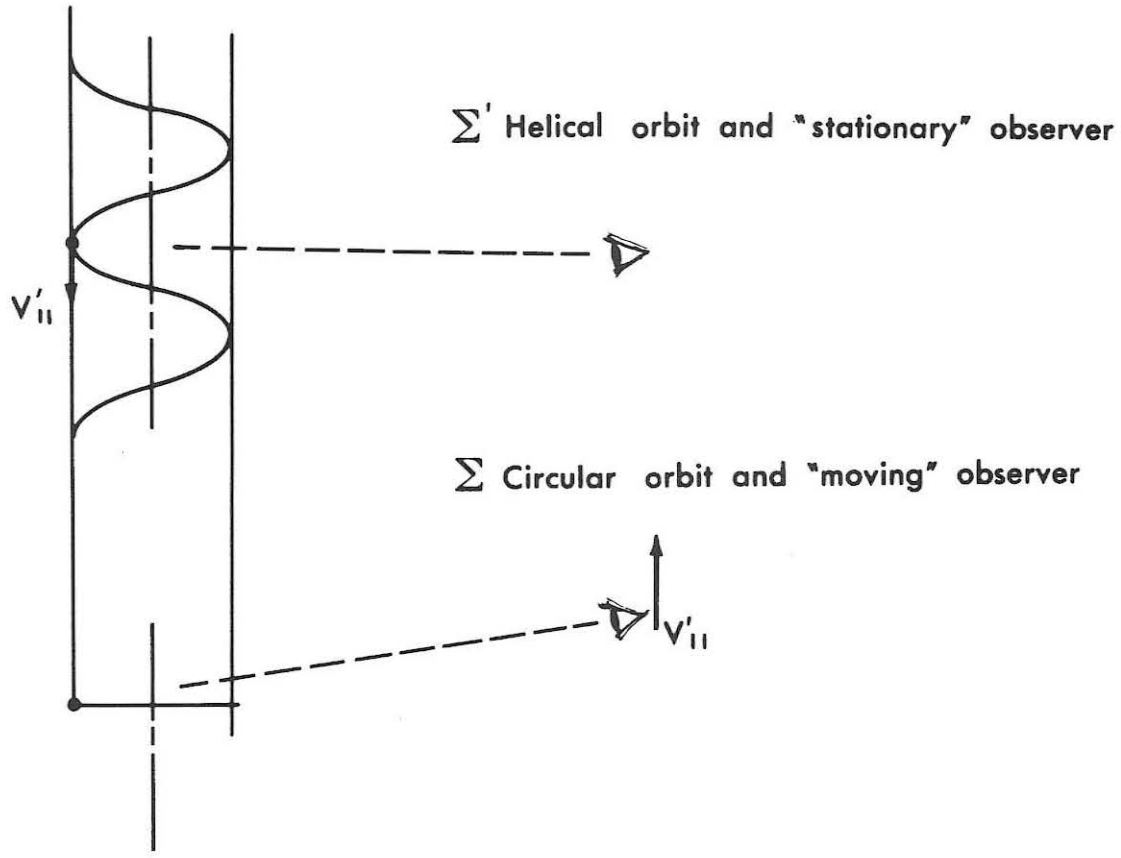

Figure 9. Electron motion in a uniform magnetic field as seen in the two reference frames $\sum$ and $\sum'$.

$$\Psi' = \sin^{-1}\left[\frac{\sin\Psi \pm (v_{\parallel}/c)}{1 \pm (v_{\parallel}/c)\sin\Psi}\right] \tag{B35}$$

the + sign being used if $\vec{v}_{\parallel}'$ is in the same direction as $\vec{B}$ and the - sign if in the opposite.

III. A differential solid angle $d\Omega$ at the angle Ψ in Σ transforms into the differential solid angle $d\Omega'$ at the angle Ψ' in Σ', where

$$d\Omega' = \frac{1 - v_{\parallel}^2/c^2}{\left[1 \pm (v_{\parallel}/c)\sin\Psi\right]^2}\, d\Omega, \tag{B36}$$

the same rule holding for the sign.

IV. The time interval τ in Σ, associated with the reception of a signal by an observer, is measured in the observer's frame Σ' to be of duration τ', where

$$\tau' = \tau\,[1 - (v_{\parallel}/c)^2]^{+1/2} \tag{B37}$$

and so a signal of frequency f in Σ will be a signal of frequency f' in Σ', where

$$f' = f[1 - (v_{\parallel}/c)^2]^{-1/2}\ . \tag{B38}$$

V. The transformation laws for the electromagnetic fields $\vec{\mathcal{E}}$ and $\vec{\mathcal{B}}$ are:

$$\mathcal{B}'_{par} = \mathcal{B}_{par} \qquad \mathcal{E}'_{par} = \mathcal{E}_{par}$$

$$\vec{\mathcal{B}}'_{perp} = [1-(v_{\parallel}/c^2]^{-1/2}[\vec{\mathcal{B}}-(\vec{v}_{\parallel} \times \vec{\mathcal{E}})/c^2]_{perp} \tag{B39}$$

$$\vec{\mathcal{E}}'_{perp} = [1-(v_{\parallel}/c)^2]^{-1/2}(\vec{\mathcal{E}}+ \vec{v}_{\parallel} \times \vec{\mathcal{B}})_{perp}$$

where the subscript "par" indicates components parallel to the field $\vec{B}$ and "perp" indicates components perpendicular to $\vec{B}$.

VI. Power is an invariant under Lorentz transformations.

Relations II and VI enable us to make a statement, independent of any assumption regarding the magnitude of the electron energy, concerning the ratio of the two power components associated with the radiation electric vectors parallel and perpendicular to the projection of the magnetic field onto the plane normal to the line of sight, namely, that:

VII. for an electron of energy E' following a helical orbit, the ratio of the two power components of frequency f' radiated at an angle Ψ' is the same as the ratio of the powers radiated by an electron of energy E in a circular orbit at the frequency f and at the angle Ψ, where E, f, and Ψ are given by relations I, II, and IV.

That this is so follows immediately from expressing $\mathcal{E}'_{\parallel}/\mathcal{E}'_{\perp}$ in terms of $\mathcal{E}_{\parallel} / \mathcal{E}_{\perp}$ where the subscripts refer to components parallel and perpendicular to the line of sight. Thus, we have from V,

$$\mathcal{E}_{\parallel} \cos\Psi = \mathcal{E}'_{\parallel} \cos\Psi' \quad , \tag{B40}$$

which, using II, leads to

$$\mathcal{E}'_{\parallel} = \frac{1\mp(v_{\parallel}/c)\sin\Psi}{[1-(v_{\parallel}/c)^2]^{1/2}}\,\mathcal{E}_{\parallel} \tag{B41}$$

Using V, and the fact that

$$\vec{\mathcal{B}} = \vec{i} \times \vec{\mathcal{E}}/c \quad , \tag{B42}$$

we find

$$\mathcal{E}'_{\perp} = \frac{1\mp(v_{\parallel}/c)\sin\Psi}{[1-(v_{\parallel}/c)^2]^{1/2}}\,\mathcal{E}_{\perp} \tag{B43}$$

Finally, then, from the equation

$$\frac{\mathcal{E}'_{\parallel}}{\mathcal{E}'_{\perp}} = \frac{\mathcal{E}_{\parallel}}{\mathcal{E}_{\perp}} \quad , \tag{B44}$$

we see that the ratio of the associated primed and unprimed Poynting vectors are equal.

Applying the information of relation VI to the power emitted into the corresponding differential solid angles $d\Omega'$ and $d\Omega$, one can then make the statement that

VIII. for an electron of energy E' following a helical orbit, the ratio of the integrated power components at a frequency f' --- where integration refers to integration over all solid angle --- is the same as that at frequency f for an electron of energy E in a circular orbit, where f and E are given by IV and II.

From relations I-VIII and the results for the circular orbit, we can now state the properties of synchrotron radiation from an electron in a helical orbit. We note first that for a relativistic electron,

$$\sin \alpha \cong (1 - v_{\parallel}^2/c^2)^{1/2} \qquad \cos \alpha \cong v_{\parallel}/c \,, \tag{B45}$$

where α is the helix angle, i.e., the angle between $\vec{B}$ and $\vec{v}'$. The results will be stated in terms of α, the energy E of the electron, the speed v of the electron, and the magnetic field B, where now the primes are dropped from the expressions. (The brackets [ ] contain the relations and equations involved in obtaining the expressions.)

(1) The radiation is essentially limited to within a cone of apex angle

$$\eta = mc^2/E \tag{B46}$$

whose axis lies along the electron's direction of motion. Thus, whereas in the circular orbit the radiation was emitted

essentially only about directions at right angles to the magnetic field, now the radiation will be essentially restricted to directions making an angle α with the magnetic field. [(B18, B34, B36].

(2) The radiation comes to an observer in pulses of duration

$$\tau = \frac{1}{2}\left(\frac{mc^2}{E}\right)^2 \frac{m}{eB\sin\alpha} \tag{B47}$$

which are separated by an interval

$$\frac{2\pi}{\omega} = \frac{E}{qB\sin\alpha\, c^2} \tag{B48}$$

[B11, B34, B37, B39].

(3) The maximum value of the electric field is proportional to $B \sin\alpha\, E^3$ [B34, B39, and the fact that the distance from the source to an observer in the radiation cone is greater by a factor $1/\sin\alpha$ on going from $\sum$ to $\sum'$].

(4) The energy per revolution received at a point which is inside the radiation cone sometime during a period of gyration is proportional to $B \sin\alpha\, E^4$ [B47, B49].

(5) The power received at a point which is inside the radiation cone sometime during a period is proportional to $B^2 \sin^2\alpha\, E^3$ [B47, B48, B39].

(6) The total rate of energy loss is [B33, B34, VI]

$$\frac{dE}{dt} = -\frac{e^4 v^2 B^2 E^2 \sin^2 \alpha}{6\pi\epsilon_o m^4 c^7} \tag{B49}$$

(7) Each frequency component of the electric and magnetic fields is elliptically polarized (both $\ddot{d}_{\parallel}$ and $\ddot{d}_{\perp}$ being periodic with the same period), the radiation being left-handed if the angle between the magnetic field and the direction of observation is less than the helix angle α and right-handed if it is larger.

(8) Let $p_f^{(1)}$ df equal the power radiated into all directions in (f, f+df) associated with the electric vectors parallel to the projections of the magnetic field B in the planes normal to the lines of sight; and let $p_f^{(2)}$ df equal the power radiated into all directions in (f, f+df) associated with the electric vectors perpendicular to the projections of the magnetic field B in the planes normal to the lines of sight.

Then [B28-B32, B38, B39, VIII],

$$P_f^{(1)} = \frac{\sqrt{3}\mu e^3 cB\sin\alpha}{4\pi m} F^{(1)}(f/f_c) \tag{B50}$$

$$P_f^{(2)} = \frac{\sqrt{3}\mu e^3 cB\sin\alpha}{4\pi m} F^{(2)}(f/f_c) \tag{B51}$$

where

$$f_c = \frac{3eB \sin \alpha E^2}{4\pi m^3 c^4} \tag{B52}$$

$$F^{(1)}(x) = \frac{x}{2} \left[\int_x^\infty K_{5/3}(\eta) d\eta - K_{2/3}(x) \right] \tag{B53}$$

$$F^{(2)}(x) = \frac{x}{2} \left[\int_x^\infty K_{5/3}(\eta) d\eta + K_{2/3}(x) \right] \tag{B54}$$

and $K_{2/3}$ and $K_{5/3}$ are modified Bessel functions. E is the total energy of the electron, e the electronic charge, μ the permeability of free space, m the electron mass and c the velocity of light. These results are expressed in rationalized MKS units. Equations B50-B54 agree with the results of Westfold (1960).

2. Radiation from a Group of Electrons

In this section, the properties of the radiation from a group of electrons are derived from those for a single electron. The power spectrum is derived first. Following this, a complete description of the radiation is obtained through a calculation of the Stokes parameters.

The effects of any intervening or ambient plasma are neglected. The frequency of the radiation is taken to be much greater than the plasma and gyro frequencies: the index of refraction is considered to be unity. Faraday rotation is neglected, which amounts to a requirement

on the relation of the frequency to the number of electrons and the strengths and orientations of the fields between the source and observer. (From Yeh and Gonzalez (1960), we obtain an approximate expression for the rotation of the plane of polarization,

$$\zeta = \frac{K}{f^2} \int NMds \, , \tag{B55}$$

where

$$M = B \cos\phi \tag{B56}$$

and where ζ is the rotation of the plane of polarization in radians, $K = 2.972 \times 10^{-2}$ (MKS rationalized units), f is the frequency in c/s, N is the electron density in electrons/m^2, B is the magnetic field strength in amp/m, ϕ is the angle between the ray and the field, and ds is the differential distance along the ray.) Collective plasma effects, such as bunching, are neglected; this is valid when the average energy of the random motion of the particles is much greater than average coulomb interaction energies. Absorption and stimulated emission are ignored. (Twiss (1958) has stated that for net stimulated emission to be significant, it is necessary that

$$E_c(f) \cong kT_f \, , \tag{B57}$$

where $E_c(f)$ is the critical energy at frequency f --- i.e., the energy which an electron must have for f to equal the critical frequency f_c of equation B52, k is Boltzmann's constant, and T_f is the effective blackbody temperature of the radiation at frequency f.)

(a) Derivation of the power spectrum

The properties of the radiation from a group of electrons are obtained from those from a single electron by superposition. For electrons whose motions are uncorrelated, the radiation is incoherent: the total power spectrum $\mathcal{P}(f)$ is obtained by simply adding the power spectrum $P_j(f)$ of the individual electrons, i.e.

$$\mathcal{P}(f) = \sum_j P_j(f) . \tag{B58}$$

For a group of uncorrelated relativistic electrons emitting synchrotron radiation, this addition is a simple matter, made so mainly by the fact that a relativistic electron effectively radiates only into a small cone of apex angle mc^2/E about its direction of motion.

Thus, suppose one wishes to calculate power spectrum of the radiation in a direction denoted by the unit vector $\vec{i}$, from the uncorrelated electrons in a differential volume dV at the position $\vec{r}$. Let the magnetic field have the value $\vec{B}(\vec{r})$. Suppose that the number density distribution function of the electrons is given by $\rho(\vec{r}, E, \alpha)$, i.e., let $\rho(\vec{r}, E, \alpha)\, dV dE d\alpha$ equal the number of electrons in the volume dV at $\vec{r}$ with energies in the range dE at E and helix angles in the range $d\alpha$ at α. Furthermore, let $P_{\vec{i}}(\vec{B}, E, \alpha; f)\, df d\alpha$ denote the power emitted in the frequency range df at f into the differential solid angle $d\Omega$ whose axis lies along the unit vector $\vec{i}$, by an electron of total energy E whose velocity lies along the unit vector $\vec{s}$. With the angle between $\vec{s}$ and $\vec{B}$

being α, then $[\rho(\vec{r}, E, \alpha)/2\pi \sin\alpha]\,dV\,dE\,d\omega$ gives the number of electrons in the interval $dV\,dE$ with $\vec{s}$ in the differential solid angle $d\omega$. The total power radiated into $d\Omega\,df$ by the electrons in dV with energies in the interval dE at E is

$$\mathscr{P}'_{\vec{i}}(\vec{r}; f)\,df\,d\Omega\,dV\,dE = \left[\int_{\omega} \frac{\rho(\vec{r}, E, \alpha)}{2\pi \sin\alpha} P_{\vec{i}}(\vec{B}, E, \vec{s}; f)\,d\omega\right] df\,d\Omega\,dV\,dE\ . \tag{B59}$$

Since $P_{\vec{i}}(\vec{B}, E, \vec{s}; f)$ for a relativistic electron is practically zero unless $\vec{s}$ lies within a very small solid angle about $\vec{i}$, equation B59 may be written

$$\mathscr{P}'_{\vec{i}}(\vec{r}; f) \approx \frac{\rho(\vec{r}, E, \alpha^*)}{2\pi \sin\alpha^*} \int_{\omega} P_{\vec{i}}(\vec{B}, E, \vec{s}; f)\,d\omega\ , \tag{B60}$$

where α^* is the angle between $\vec{i}$ and $\vec{B}$. In the integral of equation B60, $\vec{s}$ is what varies and $\vec{i}$ and $\vec{B}$ are fixed. But if $\vec{\epsilon}$ is a small vector perpendicular to $\vec{s}$,

$$P_{\vec{i}+\vec{\epsilon}}(\vec{B}, E, \vec{s} + \vec{\epsilon}; f) \approx P_{\vec{i}}(\vec{B}, E, \vec{s}; f)\ . \tag{B61}$$

If in equation B61 we set $\vec{s} + \vec{\epsilon} = \vec{i}$ and substitute the resulting expression into the integral of equation B60, we find

$$\int_{\omega} P_{\vec{i}}(\vec{B}, E, \vec{s}; f)\,d\omega = \int_{\omega} P_{\vec{i}+\vec{\epsilon}}(\vec{B}, E, \vec{i}; f)\,d\omega = P(\vec{B}, E, \vec{i}; f), \tag{B62}$$

where $P_{\vec{i}+\vec{\epsilon}}(\vec{B}, E, \vec{i}; f)\, df d\Omega$ is the power emitted in the frequency interval df into the solid angle $d\Omega$ whose axis lies along $\vec{i} + \vec{\epsilon}$ by an electron of energy E whose velocity vector lies along the unit vector $\vec{i}$. Since the dependence of the radiation power spectrum of an electron on its direction of motion occurs only through the angle α between its velocity and $\vec{B}$, we may now write for the total power per steradian emitted in the frequency interval df at f in the direction $\vec{i}$ by the electrons in dV,

$$\mathcal{P}_{\vec{i}}(\vec{r}; f)\, dV df = \frac{1}{2\pi \sin\alpha^*} \int_{E_{min}}^{E_{max}} \rho(\vec{r}, E, \alpha^*) P(\vec{B}(\vec{r}), E, \alpha^*; f) dE dV df \qquad \text{(B63)}$$

where α^* is the angle between $\vec{i}$ and $\vec{B}$.

(b) Stokes parameters for synchrotron radiation from electrons with an arbitrary angular distribution

To completely specify the nature of radiation, four real quantities must be specified in each differential frequency interval, the four quantities relating to the intensity, the degree of polarization, the plane of polarization, and the ellipticity of the radiation (Born and Wolf (1959)). G. G. Stokes in 1852 pointed out that it would be convenient for the four quantities to have the same physical dimensions,

and introduced four such parameters in his investigation of partially polarized light. The Stokes parameter description will be employed here in specifying the nature of synchrotron radiation from a group of electrons.

Chandrasekhar's (1960) terminology will be used. Thus, select two mutually orthogonal directions $\vec{i}_\ell$, $\vec{i}_r$ at right angles to the direction of propagation; $\vec{i}_r$, $\vec{i}_\ell$ and the direction of propagation forming a right-handed coordinate system. For a beam resulting from a mixture of several independent streams of elliptically polarized light, the Stokes parameters are

$$I = \sum I^{(n)} \tag{B64}$$

$$Q = \sum Q^{(n)} = \sum I^{(n)} \cos 2\beta_n \cos 2\chi_n \tag{B65}$$

$$U = \sum U^{(n)} = \sum I^{(n)} \cos 2\beta_n \sin 2\chi_n \tag{B66}$$

$$V' = \sum V^{(n)} = \sum I^{(n)} \sin 2\beta_n \tag{B67}$$

where $I^{(n)}$, $\chi^{(n)}$, and $\beta^{(n)}$ define the average intensity, the plane of polarization, and the ellipticity of the component streams, the latter two through the following relations: (a) The principal axes of the ellipse traced by the end point of the electric vector are in directions making angles χ and $\chi + \pi/2$ to the direction $\vec{i}$, and (b) $\tan \beta^{(n)}$ is the ratio of the axis in the $\chi + \pi/2$ direction to that in the χ direction of the ellipse traced by the end point of the electric vector (the numerical value of β lying between 0 and $\frac{\pi}{2}$, and the sign being positive or negative according as the polarization is right handed or left handed).

These are to be evaluated as functions of the frequency f.

An experimental procedure for determining the properties of the radiation consists of introducing a known amount of retardation in the phase of vibrations in one direction relative to the phase of vibrations at right angles to it, and then measuring the intensities in various directions in the transverse plane. Thus, suppose the component in the $\vec{i}_r$ direction is retarded by a phase ϵ from that in the $\vec{i}_l$ direction; in terms of the Stokes parameters, the intensity received in a direction making an angle ψ with respect to $\vec{i}_l$ is (Born and Wolf (1959))

$$I(\psi, \epsilon) = 1/2 [I + Q \cos 2\psi + (U \cos\epsilon - V \sin\epsilon) \sin 2\psi] . \quad \text{(B68)}$$

One finds, then, that

$$I = I(0°, 0) + I(90°, 0) \quad \text{(B69)}$$

$$Q = I(0°, 0) - I(90°, 0) \quad \text{(B70)}$$

$$U = I(45°, 0) - I(135°, 0) \quad \text{(B71)}$$

$$V' = I(45°, \tfrac{\pi}{2}) - I(135°, \tfrac{\pi}{2}) \quad \text{(B72)}$$

The parameter I is the total intensity. Q is the amount by which the intensity transmitted by a polarizer which accepts linear polarization in the $\vec{i}_l$ direction is greater than that transmitted by a polarizer which accepts linear polarization in the $\vec{i}_r$ direction. U has the same interpretation with respect to the directions $\chi = 45°$ and 135°. V' is the amount by which the intensity of the radiation transmitted by a device

which accepts right-handed circular polarization is larger than that transmitted by a device which accepts left-handed circular polarization.

The calculation of the Stokes parameters for the synchrotron radiation from relativistic electrons in dV is straightforward. Denoting the parameters at the frequency f for the radiation in the direction $\vec{l}$ and at a distance R from the differential volume $dV(\vec{r})$ by $I_{\vec{l},R}(\vec{r},f)dV$, $Q_{\vec{l},R}(\vec{r},f)dV$, $U_{\vec{l},R}(\vec{r},f)dV$ and $V'_{\vec{l},R}(\vec{r},f)dV$, we have immediately that

$$I_{\vec{l},R}(\vec{r},f)dV = \frac{\mathcal{S}_f(\vec{r};f)dV}{R^2} = \frac{1}{R^2 2\pi \sin\alpha^*} \int_{E_{min}}^{E_{max}} \rho(\vec{r},E,\alpha^*)P(\alpha^*,E,f)dEdV \tag{B73}$$

Furthermore, it is apparent that

$$V'_{\vec{l},R}(\vec{r},f)dV = 0 \tag{B74}$$

since for every right-handed ($\beta_n>0$) contribution, there will be an equal left-handed ($\beta_n<0$) one (a result of the small range of helix angles α contributing, and the fact that if the line of sight makes a smaller angle α^* with the magnetic field than α, the radiation is left-handed, whereas if the line of sight makes a larger angle α^* with the magnetic field than α, the radiation is right-handed).

The parameters $Q_{\vec{l},R}(\vec{r},f)dV$ and $U_{\vec{l},R}(\vec{r},f)dV$ are easily evaluated by recalling that in the direction $\vec{l}$ the principal axes of the

radiation ellipse from an electron in a magnetic field $\vec{B}$ are in the directions

$$\frac{(\vec{i} \times \vec{B}) \times \vec{i}}{|\vec{B}| \sin \alpha^*} \quad \text{and} \quad \frac{\vec{B} \times \vec{i}}{|\vec{B}| \sin \alpha^*} \; . \tag{B75}$$

This means that to a good approximation the angles χ_n appearing in the definitions of Q and U in equations B65 and B66 can be regarded as equal for all electrons in the differential volume dV. Thus,

$$Q_{\vec{i},R}(\vec{r},f)dV \approx \frac{\cos 2\chi}{R^2} \int_{E_{min}}^{E_{max}} \int_0^{\pi} P_{\vec{i}}(\vec{B}(\vec{r}),E,\alpha;f)\cos 2\beta \, \rho(\vec{r},E,\alpha)d\alpha dE dV \tag{B76}$$

$$U_{\vec{i},R}(\vec{r},f)dV \approx \frac{\sin 2\chi}{R^2} \int_{E_{min}}^{E_{max}} \int_0^{\pi} P_{\vec{i}}(\vec{B}(\vec{r}),E,\alpha;f)\cos 2\beta \, \rho(\vec{r},E,\alpha)d\alpha dE dV \tag{B77}$$

Take

$$\left|\cos\chi\right| = \left| \frac{\vec{i}_\ell \cdot (\vec{i}\times\vec{B}) \times \vec{i}}{|\vec{B}|\sin\alpha^*} \right| \; , \quad \sin\chi = +(1-\cos^2\chi)^{1/2} \; , \tag{B78}$$

the sign of $\cos\chi$ to be positive if either $(\vec{i}\times\vec{B})\times\vec{i}$ or $\vec{i}\times(\vec{i}\times\vec{B})$ lies between $\vec{i}_\ell$ and $\vec{i}_r$, and negative otherwise.

Then, since

$$\cos 2\beta = \cos^2\beta - \sin^2\beta \; , \tag{B79}$$

it is seen that

$$P_{\vec{i}}(\vec{B}(\vec{r}), E, a; f) \cos 2\beta \cdot$$

$$P_{\vec{i}}^{(1)}(\vec{B}(\vec{r}), E, a; f) - P_{\vec{i}}^{(2)}(\vec{B}(\vec{r}), E, a; f) \qquad \text{(B80)}$$

where $P_{\vec{i}}^{(1)}$ and $P_{\vec{i}}^{(2)}$, respectively, are the portions of $P_{\vec{i}}$ associated with the electric vectors parallel and perpendicular to the projection of $\vec{B}$ in the plane normal to $\vec{i}$.

By exactly the same arguments as were used with $P_{\vec{i}}$ to obtain equation B63 from equation B59, the following approximations may be employed:

$$\int_0^{\pi} P_{\vec{i}}^{(1)}(\vec{B}(\vec{r}), E, a; f)\, \rho(\vec{r}, E, a)\, da = \qquad \text{(B81)}$$

$$\frac{\rho(\vec{r}, E, a^*)}{2\pi \sin a^*}\, P^{(1)}(\vec{B}(\vec{r}), E, a^*; f)$$

$$\int_0^{\pi} P_{\vec{i}}^{(2)}(\vec{B}(\vec{r}), E, a; f)\, \rho(\vec{r}, E, a)\, da = \qquad \text{(B82)}$$

$$\frac{\rho(\vec{r}, E, a)}{2\pi \sin a^*}\, P^{(2)}(\vec{B}(\vec{r}), E, a^*; f)$$

where $P^{(1)}$ and $P^{(2)}$ are the integrated functions for a single electron defined by equations B50 and B57. Equations B76 and B82 yield:

$$Q_{\hat{l},R}(\vec{r},f)dV \cong \frac{\cos 2\chi}{R^2 2\pi \sin a^*}$$

$$\int_{E_{min}}^{E_{max}} \rho(\vec{r},E,a^*)\,[P^{(1)}(\vec{B}(\vec{r}),E,a^*;f) \qquad \text{(B83)}$$

$$-P^{(2)}(\vec{B}(\vec{r}),E,a^*;f)]\,dE dV$$

and

$$U_{\hat{l},R}(\vec{r},f)dV \cong \frac{\sin 2\chi}{R^2 2\pi \sin a^*}$$

$$\int_{E_{min}}^{E_{max}} \rho(\vec{r},E,a^*)\,[P^{(1)}(\vec{B}(\vec{r}),E,a^*;f) \qquad \text{(B84)}$$

$$-P^{(2)}(\vec{B}(\vec{r}),E,a^*;f)]\,dE dV$$

Equations B73, B74, B83, and B84 give the Stokes parameters for the synchrotron radiation from the electrons in dV. The functions $P^{(1)}$ and $P^{(2)}$ are given by equations B50 and B51, and

$$P = P^{(1)} + P^{(2)} \qquad \text{(B85)}$$

For a given magnetic field configuration, if the density distribution function ρ is known, we have here a complete description of the properties of the synchrotron radiation. The results are summarized in Table IV and Figures 10 and 11. In Table IV, the cumbersome subscripts and arguments, $R, \vec{B}(\vec{r}), \hat{l}$, have been omitted, and the combinations of

TABLE IV. STOKES PARAMETERS FOR SYNCHROTRON RADIATION

This table lists the Stokes parameters of the synchrotron radiation in the frequency range df at f from a distribution of electrons $\rho(E, \alpha^*)$ in the differential volume dV. The observer is taken to be a distance R from the source; B is the magnetic field intensity at the source; $\rho(E,\alpha^*)dVdEd\alpha$ is the number of electrons in the volume dV with energies in the range dE at E and helix angles in the range $d\alpha$ at α^* - where an electron's helix angle α is the angle between the magnetic field and the electron's velocity; α^* is the angle between the magnetic field and a vector $\vec{i}$ directed toward the observer. The angle χ is the angle measured clockwise by the observer from the (arbitrary) coplanar vector $\vec{i}_\ell$ involved in the definition of the Stokes parameters to the projection of the magnetic field onto a plane at right angles to the line of sight, (i.e., QdV is the portion of the intensity IdV with electric vector along the direction $\vec{i}_\ell$ minus the portion of IdV with electric vector along the direction $\vec{i}_r = \vec{i}_\ell \times \vec{i}$). The functions $F(x) = x\int_x^\infty K_{5/3}(\eta)d\eta$ and $F_p(x) = xK_{2/3}(x)$ are plotted in Figure 10 .

$$I(f)dVdf = \frac{CBdVdf}{R^2}\int \rho(E,\alpha^*)F(f/f_c^*)dE$$

$$Q(f)dVdf = \frac{-CB\cos 2\chi\, dVdf}{R^2}\int \rho(E,\alpha^*)F_p(f/f_c^*)dE$$

$$U(f)dVdf = \frac{-CB\sin 2\chi\, dVdf}{R^2}\int \rho(E,\alpha^*)F_p(f/f_c^*)dE$$

$$V'(f)dVdf = 0$$

where

$$f_c^* = LB\sin\alpha^* E^2$$

and

$$C = 3.73 \times 10^{-23} \text{ erg sec}^{-1} \text{ gauss}^{-1}$$

$$L = 1.608 \times 10^{13} \text{ c/s gauss}^{-1} \text{ Bev}^{-2}$$

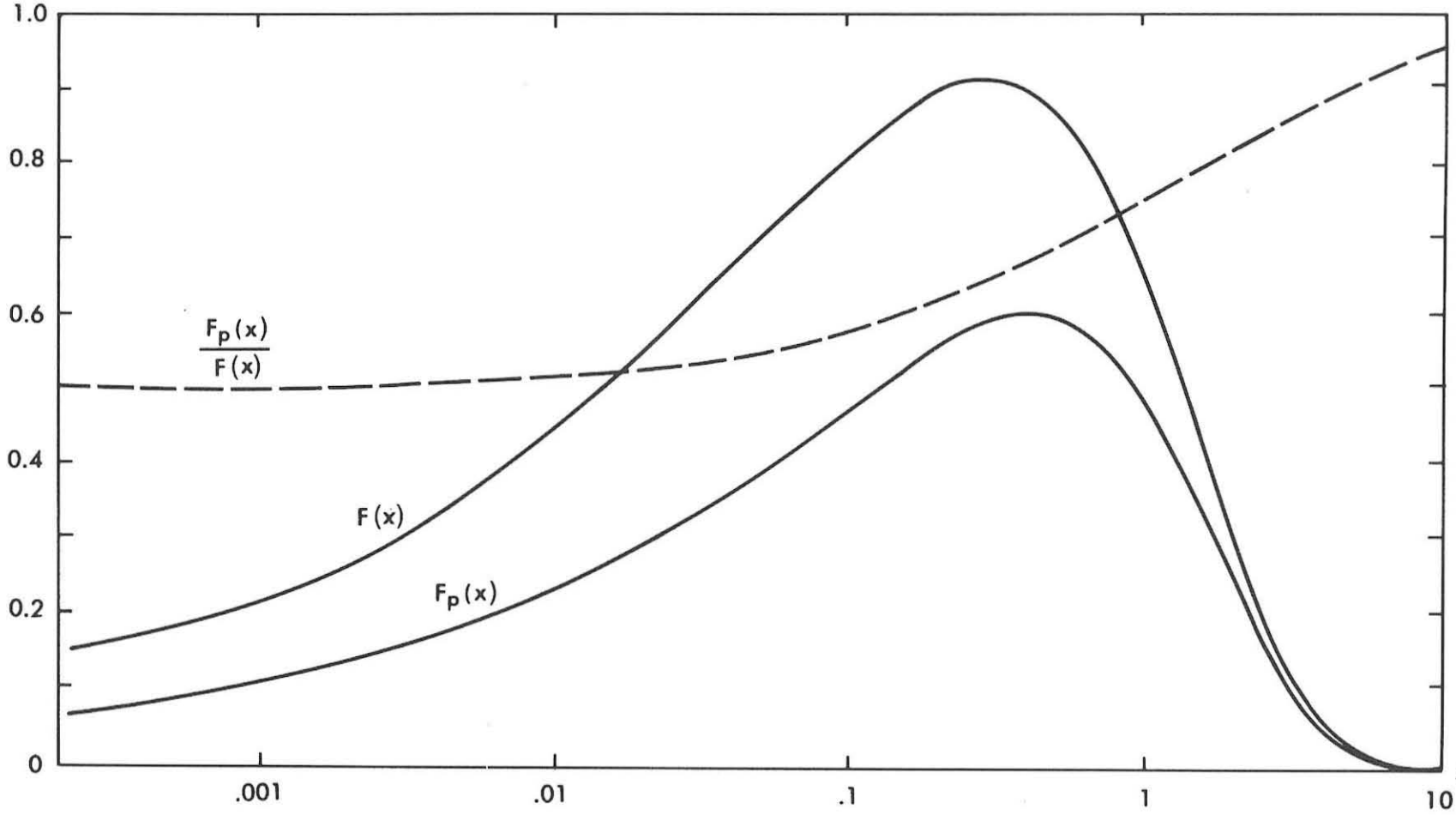

Figure 10. The functions F(x) and $F_p(x)$ and the polarization ratio $\frac{F_p(x)}{F(x)}$ [after Westfold (1959).]

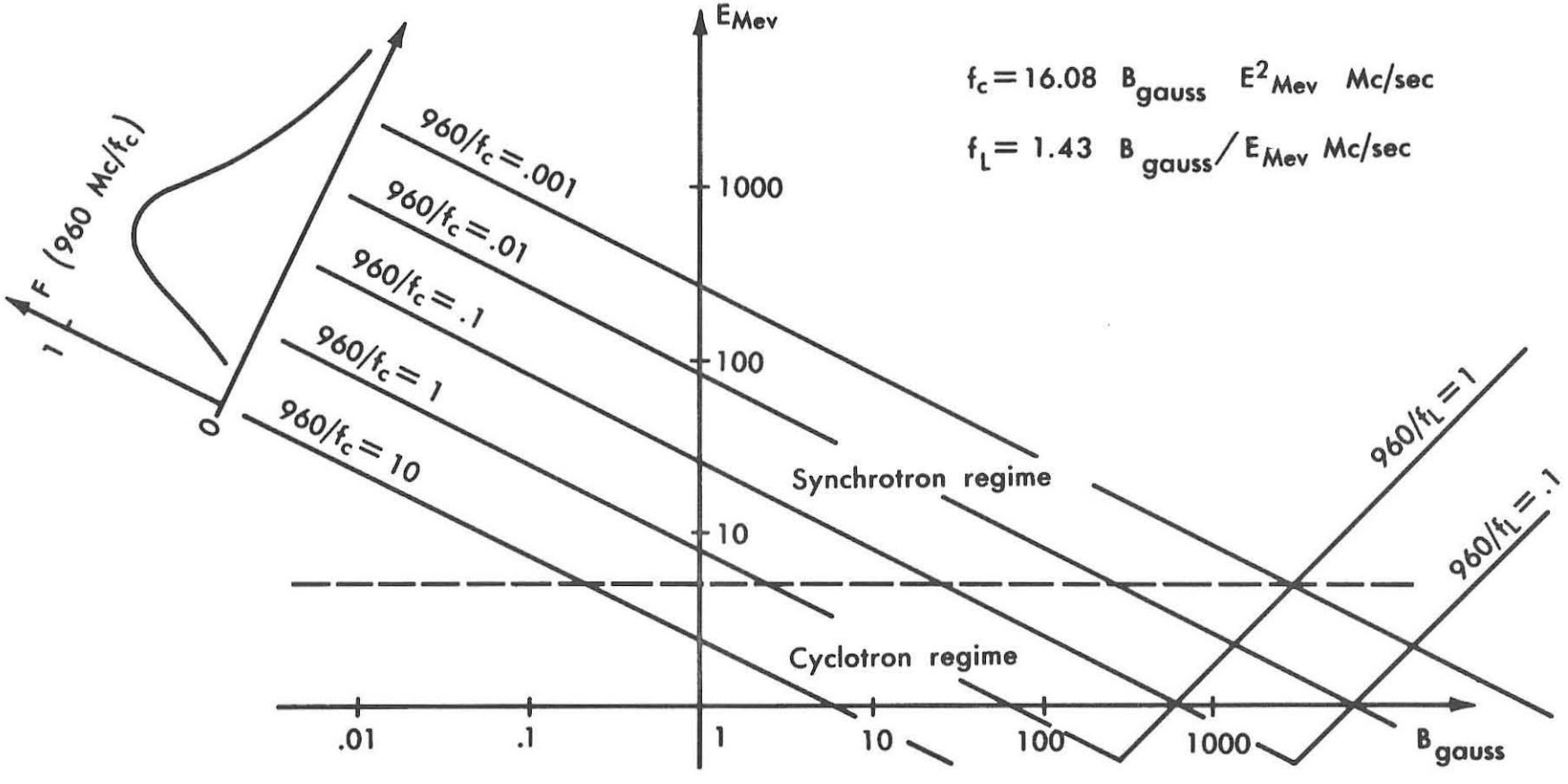

Figure 11. f/f_c and f/f_L contours on the "electron energy E vs. magnetic field B" plane.

constants have been evaluated. In Figure 10 (plotted from figures given by Westfold (1959)), the functions F, F_p and F_p/F are presented.

The range of energies and magnetic fields which can be of importance in giving rise to synchrotron radiation of given frequency is shown in Figure 11. In this figure, some f/f_c contours are plotted for electrons on the energy - magnetic field plane. An electron of energy E in a magnetic field B will radiate most efficiently at the frequency f for which

$$\frac{f}{f_c} = \frac{f}{LB \sin \alpha E^2} = 0.3 .$$

In the upper left hand corner of the diagram, the function $F(\frac{960 \text{ Mc}}{f_c})$ is plotted. The function would be simply shifted, shape unchanged, perpendicular to the f/f_c contours for different frequencies. Some f/f_c contours are also shown, where

$$f_L = \frac{2\pi \ eBc^2}{E} \qquad \text{(B86)}$$

is the Larmor frequency of an electron of energy E in a magnetic field B. Points lying along these contours are of importance in defining the radiation in the "cyclotron radiation" region of the diagram. The latter is the region of relatively low electron energies. The dotted line at E = 5 Mev might (somewhat arbitrarily) be taken as the dividing line between cyclotron and synchrotron regions.

The region on the diagram for efficient synchrotron radiation for wavelengths up to 68 cm is identified as being above the curve $\frac{f}{f_c} = \frac{2000}{f_c}$ and to the left of the curve $B \cong 1$ gauss. The smaller the magnetic field, the higher the electron energies required; thus, at $B = 1$ gauss, the minimum energy effective for synchrotron radiation is on the order of 5 Mev, whereas at $B = 1/100$ gauss, the minimum effective energy is about 20 Mev.

(c) An example: power law distribution function

To illustrate the type of behavior to be expected, consider the radiation from a group of electrons with a power law distribution in energy and an arbitrary angular distribution:

$$\rho(\vec{r}, E, \alpha) = \begin{cases} n(\vec{r}, \alpha) E^{-(\gamma+1)} & E_{min} < E < E_{max} \\ 0 & \text{otherwise} \end{cases} \qquad \text{(B87)}$$

Then, using the results of the previous section, it is found directly that (again dropping $\vec{r}$ from the arguments):

$$I(f)dV = \frac{CL^{\gamma/2}}{2R^2 f^{\gamma/2}} B^{(\gamma+2)/2} n(\alpha^*)(\sin\alpha^*)^{\gamma/2} dV \int_{x_{min}}^{x_{max}} x^{(\gamma-2)/2} F(x)dx \qquad \text{(B88)}$$

$$Q(f)dV = \frac{-CL^{\gamma/2}}{2R^2 f^{\gamma/2}} B^{(\gamma+2)/2} n(\alpha^*)(\sin\alpha^*)^{\gamma/2} \cos 2\chi\, dV \int_{x_{min}}^{x_{max}} x^{(\gamma-2)/2} F_p(x)dx \qquad \text{(B89)}$$

$$U(f)dV = \frac{-CL^{\gamma/2}}{2R^2 f^{\gamma/2}} B^{(\gamma+2)/2} n(\alpha^*)(\sin\alpha^*)^{\gamma/2} \sin 2\chi dV \int_{x_{min}}^{x_{max}} x^{(\gamma-2)/2} F_p(x)dx \tag{B90}$$

$$V'(f)dV = 0 \tag{B91}$$

where

$$x = \frac{f}{f_c^*} = \frac{f}{LB \sin\alpha^* E^2} \tag{B92}$$

and

$$x_{min} = \frac{f}{LB \sin\alpha^* E^2_{max}} \quad , \quad x_{max} = \frac{f}{LB \sin\alpha^* E^2_{min}} . \tag{B93}$$

The integrals have been discussed by Westfold (1959)* who uses the identity

$$\int_0^\infty \xi^{s-1} \int_\xi^\infty K_{\nu-1}(\eta)d\eta d\xi = \frac{\nu+s}{s} \int_x^\infty \xi^{s-1} K_\nu(\xi)d\xi - \frac{x^s}{s}\left[\int_x^\infty K_{\nu+1}(\xi)d\xi - K_\nu(x)\right] \tag{B94}$$

to write*:

$$\int_{x_{min}}^{x_{max}} x^{(\gamma-2)/2} F_p(x)dx = \mathcal{G}_p(x_{min}) - \mathcal{G}_p(x_{max}) \tag{B95}$$

and the corresponding equation without the subscript "p", with

---

*The $\mathcal{G}$ and $\mathcal{G}_p$ functions here are obtained by replacing γ in Westfold's G and G_p functions by $\gamma+1$.

$$\mathcal{G}(x) = \frac{\gamma + \frac{10}{3}}{\gamma + 2}\, \mathcal{G}_p(x) - \frac{2x^{\gamma/2}}{\gamma + 2}\, [F(x) - F_p(x)] \qquad \text{(B96)}$$

$$\mathcal{G}_p(x) = \int_x^\infty \xi^{\gamma/2} K_{2/3}(\xi)\, d\xi . \qquad \text{(B97)}$$

The variation of the Stokes parameters with frequency depends on the variation of the functions $\mathcal{G}(x)$ and $\mathcal{G}_p(x)$ with frequency. Consider four cases in which $\mathcal{G}(x)$ and $\mathcal{G}_p(x)$ are expressible in terms of easily calculable functions. The first case occurs when $x_{min} \to 0$ and $x_{max} \to \infty$: for then,

$$\mathcal{G}(x_{max}) = \mathcal{G}_p(x_{max}) = \mathcal{G}(\infty) = \mathcal{G}_p(\infty) = 0 , \qquad \text{(B98)}$$

and the values at the lower limit are found from the formula

$$\int_0^\infty x^{s-1} K_\nu(x)dx = 2^{s-2}\, \Gamma\left(\tfrac{1}{2}s - \tfrac{1}{2}\nu\right) \Gamma\left(\tfrac{1}{2}s + \tfrac{1}{2}\nu\right) \quad \Re s > |\Re \nu| \qquad \text{(B99)}$$

to be

$$\mathcal{G}_p(o) = 2^{(\gamma-2)/2}\, \Gamma\left(\frac{3\gamma+2}{12}\right) \Gamma\left(\frac{3\gamma+10}{12}\right) \qquad \gamma > -\frac{2}{3} \qquad \text{(B100)}$$

$$\mathcal{G}(o) = \left(\frac{\gamma + \frac{10}{3}}{\gamma + 2}\right) \mathcal{G}_p(o) = 2^{(\gamma-2)/2} \left(\frac{\gamma + \frac{10}{3}}{\gamma + 2}\right) \Gamma\left(\frac{3\gamma+2}{12}\right) \Gamma\left(\frac{3\gamma+10}{12}\right) \quad \gamma > -\frac{2}{3} . \qquad \text{(B101)}$$

(Biermann and Davis (1960) point out that practically, the condition

$x_{min} \to 0$ and $x_{max} \to \infty$ may be replaced by $x_{min} \leq 0.01$ and $x_{max} > 4.$)

The second case occurs when $x_{max} \lesssim 0.01$. Series expansion of the modified Bessel functions gives

$$F(x) \approx 2.15\, x^{1/3} \tag{B102}$$

(at $x = 0.01$, this gives a value for $F(x)$ 4% higher than the rigorous formula) and

$$F_p(x) \approx 1.075\, x^{1/3} \; ; \tag{B103}$$

the corresponding expressions for $\mathcal{G}(x)$ and $\mathcal{G}_p(x)$ are

$$\mathcal{G}(x) = \frac{\gamma + \frac{10}{3}}{\gamma + 2}\, \mathcal{G}_p(o) - \frac{12.9}{3\gamma + 2}\, x^{(3\gamma+2)/6} \tag{B104}$$

and

$$\mathcal{G}_p(x) = \mathcal{G}_p(o) - \frac{6.45}{3\gamma + 2}\, x^{(3\gamma+2)/6} \quad . \tag{B105}$$

The third case obtains when $x_{min} \gtrsim 10$. The asymptotic forms of the functions $F(x)$, $F_p(x)$, $\mathcal{G}(x)$ and $\mathcal{G}_p(x)$ are:

$$F(x) = \left(\frac{\pi}{2}\right)^{1/2} e^{-x}\, x^{1/2} \left(1 + \frac{55}{72x} + \cdots\right) \tag{B106}$$

$$F_p(x) = \left(\frac{\pi}{2}\right)^{1/2} e^{-x}\, x^{1/2} \left(1 + \frac{7}{72x} + \cdots\right) \tag{B107}$$

$$\mathcal{G}(x) \approx \mathcal{G}_p(x) \approx \left(\frac{\pi}{2}\right)^{1/2} x^{(\gamma-1)/2}\, e^{-x} \, , \tag{B108}$$

where the forms for $\mathcal{G}(x)$ and $\mathcal{G}_p(x)$ are obtained from the asymptotic form of the incomplete gamma function given by Erdelyi, et al. (1954)

$$\int_0^x \xi^{(\gamma-1)/2} e^{-\xi} d\xi = \Gamma\left(\frac{\gamma-1}{2}\right) - \left(\frac{\pi}{2}\right)^{1/2} x^{(\gamma-1)/2} e^{-x} + O\left(\frac{1}{x}\right). \quad \text{(B109)}$$

Westfold has pointed out that a fourth case occurs when $\gamma = \frac{2}{3}$. In this case, use of the formula

$$\int_x^\infty \xi^{1-\nu} K_\nu(\xi) d\xi = x^{1-\nu} K_{\nu-1}(x) \qquad \Re\nu < 1 \quad \text{(B110)}$$

gives

$$\mathcal{G}_p(x) = x^{1/3} K_{1/3}(x) \qquad \left(\gamma = \frac{2}{3}\right) \quad \text{(B111)}$$

$$\mathcal{G}(x) = \frac{3}{2} x^{1/3} K_{1/3}(x) - \frac{3}{4} x^{1/3} \left[F(x) - F_p(x)\right], \quad \left(\gamma = \frac{2}{3}\right) \quad \text{(B112)}$$

Westfold gives tables of $\mathcal{G}$ and $\mathcal{G}_p$ for this case.

The Stokes parameters for the power law distribution function are summarized in Table V, along with the degree of polarization $p = \frac{Q dV}{I dV}$. The simplified forms which obtain for the four special cases are also indicated. It is interesting to note that in the first three special cases, the degree of polarization is independent of the frequency.

TABLE V. STOKES PARAMETERS AND THE DEGREE OF POLARIZATION FOR SYNCHROTRON RADIATION FROM THE POWER LAW DISTRIBUTION:

$$\rho(\vec{r}, E, \alpha) = \begin{cases} n(\vec{r}, \alpha) E^{-(\gamma+1)} & E_{min} < E < E_{max} \\ 0 & \text{otherwise} \end{cases}$$

In the table, $x_{min} = \dfrac{f}{LB \sin\alpha^* E_{max}^2}$ and $x_{max} = \dfrac{f}{LB \sin\alpha^* E_{min}^2}$.

See Table IV for an explanation of the remaining symbols. Again the $\vec{r}$ is suppressed in the arguments.

Arbitrary γ, x_{min} and x_{max}.

$$I(f)dV = \frac{CL^{\gamma/2}}{2R^2 f^{\gamma/2}} B^{(\gamma+2)/2} n(\alpha^*)(\sin\alpha^*)^{\gamma/2} dV [\mathcal{G}(x_{min}) - \mathcal{G}(x_{max})]$$

$$Q(f)dV = -\cos 2\chi \frac{\mathcal{G}_p(x_{min}) - \mathcal{G}_p(x_{max})}{\mathcal{G}(x_{min}) - \mathcal{G}(x_{max})} I(f)dV$$

$$U(f)dV = \tan 2\chi \; Q(f)dV$$

$$V'(f)dV = 0$$

$$p = -\cos 2\chi \frac{\mathcal{G}_p(x_{min}) - \mathcal{G}_p(x_{max})}{\mathcal{G}(x_{min}) - \mathcal{G}(x_{max})}$$

where

$$\mathcal{G}(x) = \frac{\gamma + \frac{10}{3}}{\gamma + 2} \mathcal{G}_p(x) - \frac{2x^{\gamma/2}}{\gamma + 2} [F(x) - F_p(x)]$$

$$\mathcal{G}_p(x) = \int_x^\infty \xi^{\gamma/2} K_{2/3}(\xi) d\xi$$

TABLE V. (cont.)

Special case: $x_{min} \to 0$, $x_{max} \to \infty$

$$I(f)dV = \left[\frac{CL^{\gamma/2}}{R^2}\, 2^{(\gamma-4)/2}\, \frac{\gamma+10/3}{\gamma+2}\, \Gamma\left(\frac{3\gamma+2}{12}\right)\Gamma\left(\frac{3\gamma+10}{12}\right) B^{(\gamma+2)/2} (\sin\alpha^*)^{\gamma/2}\, n(\alpha^*)dV\right] \frac{1}{f^{\gamma/2}}$$

$$Q(f)dV = -\frac{\gamma+2}{\gamma+10/3} \cos 2\chi\, I(f)dV$$

$$U(f)dV = \tan 2\chi\, Q(f)dV$$

$$V'(f)dV = 0$$

$$p = -\frac{\gamma+2}{\gamma+10/3} \cos 2\chi$$

Special case: $x_{max} \lesssim 0.01$

$$I(f)dV \cong \frac{6.45\, CB^{2/3} n(\alpha^*)dV}{R^2 L^{1/3} (\sin\alpha^*)^{1/3}} \left[\frac{1}{E_{min}^{(3\gamma+2)/3}} - \frac{1}{E_{max}^{(3\gamma+2)/3}}\right] f^{1/3}$$

$$Q(f)dV \cong \frac{-\cos 2\chi}{2}\, I(f)dV$$

$$U(f)dV \cong \frac{-\sin 2\chi}{2}\, I(f)dV$$

$$V'(f)dV = 0$$

$$p \cong \frac{-\cos 2\chi}{2}$$

Special case: $x_{min} \gtrsim 10$

$$I(f)dV \cong \frac{\pi^{1/2} CL^{1/2} B^{3/2}}{2^{3/2} R^2} n(\alpha^*)(\sin\alpha^*)^{1/2} dV \left[\frac{\exp\left(-\frac{f}{LB \sin\alpha^* E_{max}^2}\right)}{f^{1/2} E_{max}^{\gamma-1}} - \frac{\exp\left(-\frac{f}{LB \sin\alpha^* E_{min}^2}\right)}{f^{1/2} E_{min}^{\gamma-1}}\right]$$

TABLE V. (cont.)

$Q(f)dV \cong - \cos 2\chi\, I(f)dV$

$U(f)dV \cong - \sin 2\chi\, I(f)dV$

$V'(f)dV = 0$

$$p = -1 \cos 2\chi$$

Special case: $\gamma = 2/3$

$$I(f)dV = \frac{CL^{1/3}}{2R^2 f^{1/3}} B^{4/3} n(a^*)(\sin a^*)^{1/3} dV[\, G^W(x_{min}) - G^W(x_{max})\,]$$

$$Q(f)dV = -\cos 2\chi \, \frac{G_p^W(x_{min}) - G_p^W(x_{max})}{G^W(x_{min}) - G^W(x_{max})} \, I(f)dV$$

$U(f)dV = \tan 2\chi \; Q(f)dV$

$V'(f)dV = 0$

$$p = -\cos 2\chi \, \frac{G_p^W(x_{min}) - G_p^W(x_{max})}{G^W(x_{min}) - G^W(x_{max})}$$

where

$$G_p^W(x) = x^{1/3} K_{1/3}(x)$$

$$G^W(x) = \frac{3}{2} x^{1/3} K_{1/3} - \frac{3}{4} x^{1/3} [\, F(x) - F_p(x)\,] \; .$$

($G_p^W(x)$ and $G^W(x)$ are tabulated in Westfold (1959).)

APPENDIX C

A Derivation of Relativistic Drift Velocities by the Asymptotic Approximation Method of Bogolyubov and Zubarev

In this appendix, the asymptotic approximation method developed by Bogolyubov and Zubarev (1955) for the treatment of systems with rotating phases will be used to provide a systematic derivation of drift velocities for relativistic charged particles. Bogolyubov and Zubarev have themselves applied this method to the derivation of drift velocities for nonrelativistic particles in time-independent fields. Their treatment has been extended by Fried (1960) to the case of nonrelativistic particles in time-dependent fields. The purpose of this section is to remove the restriction of Fried's work to nonrelativistic particles, and so to obtain drift velocity expressions which are valid for relativistic particles in time-dependent fields.

The asymptotic approximation method of Bogolyubov and Zubarev is a formal method of solving a system of differential equations having the general structure

$$\frac{dx}{dt} = X(x, \theta, t)$$

$$\frac{d\theta}{dt} = \lambda\omega(x, t) + A(x, \theta, t) , \qquad \text{(C1)}$$

where x and X are vectors in a space of any number of dimensions, θ is the rotating phase, $X(x, \theta, t)$ and $A(x, \theta, t)$ are periodic functions of θ with period 2π, and λ is a large parameter. Their form of solution has the advantage that it is separated into a systematic part and a "shivering." More explicitly, Bogolyubov and Zubarev show how to perform a transformation of the form

$$x = \bar{x} + \frac{\xi_1(\bar{x}, \bar{\theta})}{\lambda} + O\left(\frac{1}{\lambda^2}\right)$$

$$\theta = \bar{\theta} + \frac{u_1(\bar{x}, \bar{\theta})}{\lambda} + O\left(\frac{1}{\lambda^2}\right) \qquad \text{(C2)}$$

such that in the transformed equations of motion,

$$\frac{d\bar{x}}{dt} = X_o(\bar{x}, t) + \frac{1}{\lambda} X_1(\bar{x}, t) + O\left(\frac{1}{\lambda^2}\right)$$

$$\frac{d\bar{\theta}}{dt} = \lambda \omega(\bar{x}, t) + \psi_o(\bar{x}, t) + \frac{1}{\lambda} \psi_1(\bar{x}, t) + O\left(\frac{1}{\lambda^2}\right), \qquad \text{(C3)}$$

the angular variable $\bar{\theta}$ does not appear, and such that

$$\langle \xi_1(\bar{x}, \bar{\theta}) \rangle = \langle u_1(\bar{x}, \bar{\theta}) \rangle = 0, \qquad \text{(C4)}$$

(where the brackets indicate an average with respect to θ). The $\bar{x}$ and $\bar{\theta}$ represent the averaged behavior of x and θ, whereas ξ_1 and u_1 represent the "shivering," i.e., the oscillations about this average. The method begins by substituting equations C3 and C4 in equation C1:

keeping terms up to $O(\frac{1}{\lambda^2})$ and equating terms of the same order in λ, this leads to a system of four equations for the six functions ξ_1, u_1, X_o, X_1, ψ_o and ψ_1. Equations C4 bring the total number of equations up to six.

If the functions $X(x,\theta,t)$ and $A(x,\theta,t)$ are expressed in Fourier series in θ so that equation C1 takes on the form

$$\frac{dx}{dt} = X(o) + \sum_1^\infty [F_n \cos n\theta + G_n \sin n\theta]$$

$$\frac{d\theta}{dt} = \lambda\omega + A(o) + \sum_1^\infty [f_n \cos n\theta + g_n \sin n\theta] , \tag{C5}$$

then this method leads to the solutions

$$x = \bar{x} + \frac{1}{\omega\lambda} \sum_1^\infty \frac{1}{n} (F_n \sin n\theta - G_n \cos n\theta) + O(\frac{1}{\lambda^2})$$

$$\theta = \bar{\theta} + \frac{1}{\omega\lambda} \sum_1^\infty \{\frac{1}{n}(f_n \sin n\theta - g_n \cos n\theta) - \frac{1}{\omega n^2}(F_n \cos n\theta + G_n \sin n\theta)\cdot \frac{\partial\omega}{\partial x}\}$$

$$+ O(\frac{1}{\lambda^2}) , \tag{C6}$$

and to the transformed equations of motion,

$$\frac{d\bar{x}}{dt} = X(o) + \frac{1}{2\omega\lambda} \sum_1^\infty \Big[\frac{1}{\omega n}(F_n G_n - G_n F_n)\cdot\frac{\partial\omega}{\partial x} - (f_n F_n + g_n G_n) + \frac{1}{n}$$

$$(F_n \cdot \frac{\partial G_n}{dx} - G_n \cdot \frac{\partial G_n}{\partial x})\Big] + O(\frac{1}{\lambda^2}) \tag{C7}$$

$$\frac{d\bar{\theta}}{dt} = \lambda\omega + A(o) + \frac{1}{2\omega\lambda} \sum_1^\infty \Big[\frac{1}{2\omega n^2}(F_n F_n + G_n G_n)\cdot\frac{\partial^2\omega}{\partial x \partial x} + \frac{1}{n}(F_n \cdot \frac{\partial g_n}{\partial x} - G_n \cdot \frac{\partial f_n}{\partial x})$$

$$+ \frac{1}{n\omega}(f_n G_n - g_n F_n)\cdot\frac{\partial\omega}{\partial x} - f_n^2 - g_n^2 + O(\frac{1}{\lambda^2})\Big] .$$

(A dot has been used to indicate inner products in x-space. All quantities on the right hand side are evaluated at $\bar{x}$.)

To apply this result to the case of a relativistic particle in a magnetic field, we shall start with the equations

$$\frac{d(m\vec{v})}{dt} = \vec{F} + \frac{e\vec{v}}{c} \times \vec{B} \quad \text{and}$$
$$\frac{d(mc^2)}{dt} = \vec{F} \cdot \vec{v} \tag{C8}$$

(where m is the (relativistic) mass, e is the particle charge, $\vec{v}$ is the particle velocity, c is the speed of light, $\vec{B}$ is the magnetic field and $\vec{F}$ represents the sum of electrical and gravitational forces.) Since our interest is in drift velocities, we shall combine these equations to give

$$\frac{d\vec{v}}{dt} = \vec{F} + \vec{v} \times \lambda \vec{\omega} - \frac{(\vec{F} \cdot \vec{v})\vec{v}}{c^2} \tag{C9}$$

where we have also introduced the angular velocity

$$\lambda \vec{\omega} = \frac{e\vec{B}}{mc} \quad . \tag{C10}$$

To put equation C9 into the form of equation C5, the rotating phase must be explicitly exhibited. For this purpose, introduce a coordinate system with one axis parallel to the local magnetic field. Define three orthonormal vectors, $\vec{i}_1$, $\vec{i}_2$ and $\vec{i}_3$ such that the three taken in this order define a right handed coordinate system, and such that the third lies along the magnetic field,

$$\vec{i}_3 = \frac{\vec{B}}{B} \quad . \tag{C11}$$

In this coordinate system, we write

$$\vec{v} = w \cos\theta\, \vec{i}_1 - w \sin\theta\, \vec{i}_2 + u\, \vec{i}_3 \, . \tag{C12}$$

It is also convenient to introduce the unit vectors

$$\vec{\sigma} = \vec{i}_1 \cos\theta - \vec{i}_2 \sin\theta \tag{C13}$$

and

$$\vec{\tau} = \vec{i}_3 \times \vec{\sigma} \quad . \tag{C14}$$

For then,

$$\vec{v} = u\vec{i}_3 + w\vec{\sigma} \, , \tag{C15}$$

and equation C9 becomes:

$$\begin{aligned} \dot{u}\vec{i}_3 + \dot{w}\vec{\sigma} + u\dot{\vec{i}}_3 + w(\dot{\vec{i}}_1\cos\theta - \dot{\vec{i}}_2\sin\theta) - w\dot{\theta}\vec{\tau} = \\ \vec{F} - w\lambda\omega\vec{\tau} - \left[\frac{(\vec{F}\cdot\vec{i}_3)u^2}{c^2} + \frac{(\vec{F}\cdot\vec{\sigma})}{c^2}\, wu\right]\vec{i}_3 \\ - \left[\frac{(\vec{F}\cdot\vec{i}_3)}{c^2}\, uw + \left(\frac{\vec{F}\cdot\vec{\sigma}}{c^2}\right) w^2\right]\vec{\sigma} \quad , \end{aligned} \tag{C16}$$

where the dot over a quantity has been used to indicate the transport derivative, i.e.,

$$\dot{a} \equiv \frac{\partial a}{\partial t} + \vec{v}\cdot\nabla a \quad . \tag{C17}$$

Taking the scalar product of equation C16 with $\vec{i}_3$, $\vec{\sigma}$ and $\vec{\tau}$, and using the relation

$$\vec{i}_3 \cdot (\dot{\vec{i}}_1 \cos\theta - \dot{\vec{i}}_2 \sin\theta) = -\vec{\sigma} \cdot \dot{\vec{i}}_3 \quad , \tag{C18}$$

the following equations are obtained for $\dot{u}$, $\dot{w}$ and $\dot{\theta}$:

$$\begin{aligned}
\dot{u} &= \vec{F} \cdot \vec{i}_3 - w\vec{\sigma} \cdot \vec{i}_3 - (\vec{F} \cdot \vec{i}_3) \frac{u^2}{c^2} - (\vec{F} - \vec{\sigma}) \frac{wu}{c^2} \\
\dot{w} &= \vec{F} \cdot \vec{\sigma} - u\vec{\sigma} \cdot \dot{\vec{i}}_3 - \left(\frac{\vec{F} \cdot \vec{i}_3}{c}\right) uw - (\vec{F} \cdot \vec{\sigma}) \frac{w^2}{c^2} \\
\dot{\theta} &= \lambda w - \frac{\vec{F} \cdot \vec{\tau}}{w} + \vec{\tau} \cdot (\dot{\vec{i}}_1 \cos\theta - \dot{\vec{i}}_2 \sin\theta) + \frac{u}{w} \vec{\tau} \cdot \dot{\vec{i}}_3 \quad ,
\end{aligned} \tag{C19}$$

The quantities $\vec{\tau}$, $\dot{\vec{i}}_1$, $\dot{\vec{i}}_2$ and $\dot{\vec{i}}_3$ appearing in the foregoing expressions all contain the rotating phase θ. To put equation C19 into a form where the asymptotic expansion formalism may be easily applied, the explicit dependence of quantities on θ should be displayed. Thus, following Fried, we write

$$\begin{aligned}
-\vec{\sigma} \cdot \dot{\vec{i}}_3 &= -\vec{\sigma} \cdot \frac{\delta \vec{i}_3}{\delta t} - \vec{\sigma} \cdot (u\vec{i}_3 + w\vec{\sigma}) \cdot \nabla \vec{i}_3 \\
&= (\sin\theta \vec{i}_2 - \cos\theta \vec{i}_1) \cdot \frac{\delta \vec{i}_3}{\delta t} - \frac{w}{2} \nabla \cdot \vec{i}_3 - \frac{w \cos 2\theta}{2} (\vec{i}_1\vec{i}_1 - \vec{i}_2\vec{i}_2) : \nabla \vec{i}_3 \\
&\quad + \frac{w \sin 2\theta}{2} (\vec{i}_1\vec{i}_2 + \vec{i}_2\vec{i}_1) : \nabla \vec{i}_3 \quad ,
\end{aligned} \tag{C20}$$

$$\begin{aligned}
\vec{\tau} \cdot \dot{\vec{i}}_3 &= -\frac{d\vec{\sigma}}{d\theta} \cdot \dot{\vec{i}}_3 = (\cos\theta \vec{i}_2 + \sin\theta \vec{i}_1) \cdot \frac{\delta \vec{i}_3}{\delta t} \\
&\quad + [w \sin 2\theta (\vec{i}_1\vec{i}_1 - \vec{i}_2\vec{i}_2) + w \cos 2\theta (\vec{i}_1\vec{i}_2 + \vec{i}_2\vec{i}_1)] : \nabla \vec{i}_3
\end{aligned} \tag{C21}$$

and

$$\vec{\tau} \cdot (\dot{\vec{i}}_1 \cos\theta - \dot{\vec{i}}_2 \sin\theta) = \frac{1}{2} (\dot{\vec{i}}_1 \cdot \vec{i}_2 - \dot{\vec{i}}_2 \cdot \vec{i}_1) = -\vec{i}_1 \cdot \frac{\delta \vec{i}_2}{\delta t} - w\vec{i}_1 \cdot [(\vec{i}_1 \cos\theta - \vec{i}_2 \sin\theta) \cdot \nabla \vec{i}_2] \tag{C22}$$

where

$$\frac{\delta}{\delta t} \equiv \frac{\partial}{\partial t} + u\vec{i}_3 \cdot \nabla . \tag{C23}$$

If we now identify the vector consisting of the displacement $\vec{r}$ and the velocity components u and w as the vector x of the formalism,

$$x = \begin{pmatrix} \vec{r} \\ u \\ w \end{pmatrix} \tag{C24}$$

the comparison of equations C12, C19-C23 with equation C5 for $\frac{dx}{dt}$ gives the following results:

$$X(o) = \begin{pmatrix} u\vec{i}_3 \\ \vec{F}\cdot\vec{i}_3\left[1-\frac{u^2}{c^2}\right] + \frac{w^2}{2}\nabla\cdot\vec{i}_3 \\ -\frac{uw}{2}\nabla\cdot\vec{i}_3 - (\vec{F}\cdot\vec{i}_3)\frac{uw}{c^2} \end{pmatrix}$$

$$F_1 = \begin{pmatrix} w\vec{i}_1 \\ w\vec{i}_1\cdot\frac{\delta\vec{i}_3}{\delta t} - (\vec{F}\cdot\vec{i}_1)\frac{wu}{c^2} \\ \vec{F}\cdot\vec{i}_1 - (\vec{F}\cdot\vec{i}_2)\frac{w^2}{c^2} \end{pmatrix} \qquad F_2 = \begin{pmatrix} \vec{o} \\ w^2 \\ -uw \end{pmatrix} \frac{(\vec{i}_1\vec{i}_1 - \vec{i}_2\vec{i}_2):\nabla\vec{i}_3}{2}$$

$$G_1 = \begin{pmatrix} -w\vec{i}_2 \\ -w\vec{i}_2\cdot\frac{\delta\vec{i}_3}{\delta t} + (\vec{F}\cdot\vec{i}_2)\frac{wu}{c^2} \\ -\vec{F}\cdot\vec{i}_2 + (\vec{F}\cdot\vec{i}_2)\frac{w^2}{c^2} \end{pmatrix} \qquad G_2 = \begin{pmatrix} \vec{o} \\ -w^2 \\ uw \end{pmatrix} \frac{(\vec{i}_1\vec{i}_2 + \vec{i}_2\vec{i}_1):\nabla\vec{i}_3}{2}$$

$$f_1 = \frac{-\vec{F}\cdot\vec{i}_2}{w} - w\vec{i}_1\cdot(\nabla\vec{i}_2)\cdot\vec{i}_1 \qquad g_1 = \frac{-\vec{F}\cdot\vec{i}_1}{w} + w\vec{i}_2\cdot(\nabla\vec{i}_2)\cdot\vec{i}_1$$

$$f_2 = u(\vec{i}_1\vec{i}_2 + \vec{i}_2\vec{i}_1):\nabla\vec{i}_3 \qquad g_2 = u(\vec{i}_1\vec{i}_1 - \vec{i}_2\vec{i}_2):\nabla\vec{i}_3 \tag{C25}$$

with all other F_n, G_n, f_n and g_n equal to zero. In these expressions, the variable $\vec{\mathfrak{F}}$ is given by:

$$\vec{\mathfrak{F}} = \vec{F} - u \frac{\delta \vec{i}_3}{\delta t} \tag{C26}$$

The expressions for $X(o)$, F_1 and G_1 differ from those for the non-relativistic case, although the remaining quantities are the same. To obtain the relativistic drift velocities, we need only apply the results of equation C7 to the $\frac{d\vec{r}}{dt}$ components of $\frac{d\bar{x}}{dt}$. With the $(F_2G_2-G_2F_2)\cdot\frac{d(\lambda\omega)}{dx}$, $F_2f_2 + g_2G_2$ and $F_2\cdot\frac{\partial G_2}{\partial x} - G_2\cdot\frac{\partial F_2}{\partial x}$ terms giving zero contribution, we find

$$\frac{d\vec{r}}{dt} = u\vec{i}_3 + \frac{1}{2\Omega}\left[\bar{w}^2\{\vec{i}_2\vec{i}_1\cdot\frac{\nabla\Omega}{\Omega} - \vec{i}_1\vec{i}_2\cdot\frac{\nabla\Omega}{\Omega}\} + \bar{w}^2\{\vec{i}_1\vec{i}_1\cdot(\nabla\vec{i}_2)\cdot\vec{i}_1 + \vec{i}_2\vec{i}_2\cdot(\nabla\vec{i}_2)\cdot\vec{i}_1\}\right.$$

$$\left. + \vec{i}_1(\vec{\mathfrak{F}}\cdot\vec{i}_2) - \vec{i}_2(\vec{\mathfrak{F}}\cdot\vec{i}_1) - \bar{w}^2\{\vec{i}_1\cdot\nabla\vec{i}_2 - \vec{i}_2\cdot\nabla\vec{i}_1\} - (\vec{\mathfrak{F}}\cdot\vec{i}_1)\vec{i}_2 - (\vec{\mathfrak{F}}\cdot\vec{i}_2)\vec{i}_1\right]$$

$$+ \frac{1}{2\Omega}\left[\{(\vec{F}\cdot\vec{i}_1)\vec{i}_2 - (\vec{F}\cdot\vec{i}_2)\vec{i}_1\}\frac{\bar{w}^2}{c^2} + \frac{\partial\Omega}{\partial u}\{\frac{\bar{w}^2}{\Omega}(\vec{i}_1\cdot\frac{\delta\vec{i}_3}{\delta t}\vec{i}_2 - \vec{i}_2\cdot\frac{\delta\vec{i}_3}{\delta t}\vec{i}_1) + \frac{\bar{w}^2\bar{u}}{\Omega c^2}\right.$$

$$\left.(\vec{F}\cdot\vec{i}_2\vec{i}_1 - \vec{F}\cdot\vec{i}_1\vec{i}_2)\} + \frac{\partial\Omega}{\partial w}\{\frac{\bar{w}}{\Omega}(\vec{\mathfrak{F}}\cdot\vec{i}_1\vec{i}_2 - \vec{\mathfrak{F}}\cdot\vec{i}_2\vec{i}_1) + \frac{\bar{w}^3}{\Omega c^2}(\vec{F}\cdot\vec{i}_2\vec{i}_1 - \vec{F}\cdot\vec{i}_1\vec{i}_2)\}\right]$$

$$+ O\left(\frac{1}{\lambda^2}\right) \tag{C27}$$

The portion in the second square brackets is absent in the non-relativistic case. Substituting

$$\frac{\partial \lambda\omega}{\partial u} = -\frac{\bar{u}\lambda\omega}{c^2-\bar{v}^2} \quad \text{and} \quad \frac{\partial \lambda\omega}{\partial \omega} = -\frac{\bar{w}\lambda\omega}{c^2-\bar{v}^2} \tag{C28}$$

in this equation, and rearranging terms, equation C27 becomes

$$\frac{d\vec{r}}{dt} = \bar{u}\vec{i}_3 + \frac{1}{2\Omega}\left\{\bar{w}^2(\vec{i}_2\vec{i}_1 - \vec{i}_1\vec{i}_2)\cdot\frac{\nabla\Omega}{\Omega} - (\vec{i}_2\vec{i}_1 - \vec{i}_1\vec{i}_2)\cdot\vec{\dot{v}} + (\vec{i}_1\vec{i}_2 - \vec{i}_2\vec{i}_1)\cdot\vec{f}\right.$$

$$\left. + \bar{w}^2\left[(\vec{i}_1\vec{i}_1 + \vec{i}_2\vec{i}_2)\cdot(\nabla\vec{i}_2)\cdot\vec{i}_1 - \vec{i}_1\cdot\nabla\vec{i}_2 + \vec{i}_2\cdot\nabla\vec{i}_1\right]\right\} . \tag{C29}$$

This is exactly the same as the expression obtained in the non-relativistic treatment (Fried's equation 47) except that here the relativistic mass $m = \dfrac{m_o}{\left[1-\dfrac{v^2}{c^2}\right]^{\frac{1}{2}}}$ must be used in evaluating $\lambda\omega$. This is the result one would expect from the familiar kinematic-type derivations of drift velocities.

The expression may be reduced to a more familiar form by using the identities listed by Fried in his equations 48 and 49:

$$\vec{i}_3 \times \vec{F} = \vec{i}_3 \times (\vec{i}_1\vec{i}_1\cdot\vec{F} + \vec{i}_2\vec{i}_2\cdot\vec{F}) = (\vec{i}_2\vec{i}_1 - \vec{i}_1\vec{i}_2)\cdot\vec{F} \tag{F48}$$

and

$$\vec{i}_3\vec{i}_3\cdot\nabla\times\vec{i}_3 = \vec{i}_3\vec{i}_3\cdot(\vec{i}_2\cdot\nabla\vec{i}_1 - \vec{i}_1\cdot\nabla\vec{i}_2) = \vec{i}_2\cdot\nabla\vec{i}_1 - \vec{i}_1\cdot\nabla\vec{i}_2 + \vec{i}_1(\vec{i}_1\vec{i}_1):\nabla\vec{i}_2$$

$$-\vec{i}_2(\vec{i}_2\vec{i}_2):\nabla\vec{i}_1 = \vec{i}_2\cdot\nabla\vec{i}_1 - \vec{i}_1\cdot\nabla\vec{i}_2 + (\vec{i}_1\vec{i}_1 + \vec{i}_2\vec{i}_2)\cdot(\nabla\vec{i}_2)\cdot\vec{i}_1 . \tag{F49}$$

One obtains finally

$$\frac{d\vec{r}}{dt} = \left[\bar{u}\vec{i}_3 + \frac{\vec{i}_3}{\lambda\omega} \times \left\{\frac{\bar{w}^2}{2\lambda\omega} \nabla\lambda\omega - \vec{F} + \bar{u}\left[\frac{\partial \vec{i}_3}{\partial t} + \bar{u}\vec{i}_3 \cdot \nabla \vec{i}_3\right]\right\}\right] \left(1+O\left(\frac{1}{\lambda}\right)\right). \quad (C30)$$

The first term $\bar{u}\vec{i}_3$ represents motion along the field line. The second term is the $\vec{B} \times \nabla B$ drift:

$$\vec{V}_B = \frac{mcw^2}{2eB^3} (\vec{B} \times \nabla B) . \quad (C31)$$

The third term is the $\vec{F} \times \vec{B}$ drift; e.g., if $\vec{F} = \frac{e\vec{E}}{m}$, then this describes the drift due to crossed electric and magnetic fields:

$$\vec{V}_E = c\frac{\vec{E} \times \vec{B}}{B^2} . \quad (C32)$$

The last term is an $\vec{F} \times \vec{B}$ type drift, with the centripetal force*

$-m\bar{u}\left[\frac{\partial \vec{i}_3}{\partial t} + \bar{u}\vec{i}_3 \cdot \nabla\vec{i}_3\right]$ playing the role of $\vec{F}$. The relativistic drift velocities are obtained from those for the nonrelativistic case simply by replacing the rest mass m_o by the relativistic mass $m = m_o\left(1 - \frac{v^2}{c^2}\right)^{-1/2}$ wherever it appears.

---

*(That this is a centripetal force is made clear by noting that $\frac{\partial \vec{i}_3}{\partial t} + \bar{u}\vec{i}_3 \cdot \nabla\vec{i}_3$, being the rate at which the velocity $\bar{u}\vec{i}_3$ is changing direction, may be written as the cross product of $\vec{i}_3$ with some angular velocity $\vec{\Omega}'$, i.e.

$$\vec{\Omega}' \times \vec{i}_3 = \frac{\partial \vec{i}_3}{\partial t} + \bar{u}\vec{i}_3 \cdot \nabla\vec{i}_3 .$$

The assertion follows immediately, since the centripetal acceleration associated with a velocity $\bar{u}\vec{i}_3$ undergoing a rotation $\vec{\Omega}'$ is $\vec{\Omega}' \times \bar{u}\vec{i}_3$.

APPENDIX D

Numerical Results for Synchrotron Radiation from Ultrarelativistic Electrons in a Dipole Field

In this appendix, the numerical calculations described in Table II, page 32 , and in the related discussion on pages 29-40 are summarized in graphical form. The calculations were done on an IBM 7090 computer at the Plasma Physics Laboratory of the Boeing Scientific Research Laboratories: the problem was programmed for the computer by George Pettigrew and James May of the Applied Mathematics Section of the Boeing Airplane Company.

The symbols and cases mentioned in the following are explained in Table II and in the related discussion. The first three figures, Figures 12-14, apply to case (i) in which the radiation originates from a group of monoenergetic electrons. Figures 15-17 apply to case (ii) in which the radiation is due to a group of electrons with a power law energy spectrum. The final three figures, Figures 18-20, apply to case (iii) in which the radiation comes from a group of electrons with a power law spectrum with cutoffs. Figure 12 displays for case (i) the first and second Stokes parameters and the percentage polarization: more specifically, Figure 12 consists of histograms of I/A_I, Q/A_I and

$p = Q/I$ vs. $\ell/r_E = \sin^3\theta \cos\phi$. In Figure 13 are plotted for case (i) the normalized cosine transforms $\mathcal{I}_\ell = \int_0^\infty (I/A_I) \cos k\ell \, d\ell$ and $Q_\ell = \int_0^\infty (Q/A_I) \cos k\ell \, d\ell$ and the degree of polarization $p_\ell = Q_\ell/\mathcal{I}_\ell$. Figure 14 presents for case (i) the transform results with respect to the polar direction; i.e., in Figure 14 are plotted the normalized cosine transforms $\mathcal{I}_y = \int_0^\infty (I/A_I) \cos ky \, dy$ and $Q_y = \int_0^\infty (Q/A_I) \cos ky \, dy$, and the degree of polarization $p_y = Q_y/\mathcal{I}_y$, where $y = r\cos\theta = r_E \sin^2\theta \cos\theta$. Figures 15-17 and Figures 18-20 are the analogous plots for cases (ii) and (iii), respectively.*

*Due to the limit on the accuracy obtained with the numerical computation, the ratios p_ℓ and p_y are not shown for those values of k where the corresponding parameter transforms are very close to zero.

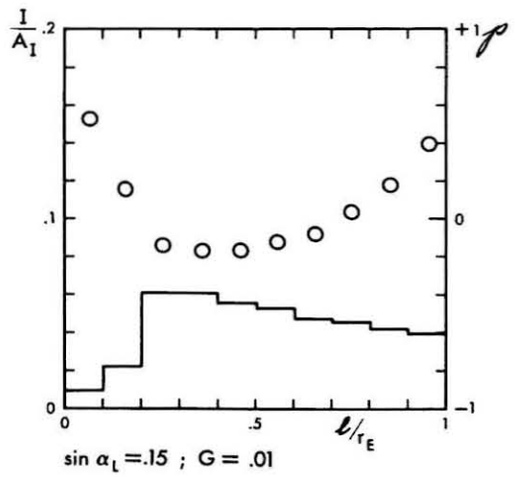

sin α_L = .15 ; G = .01

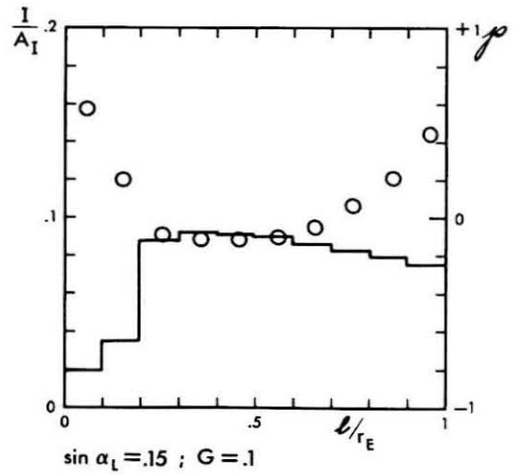

sin α_L = .15 ; G = .1

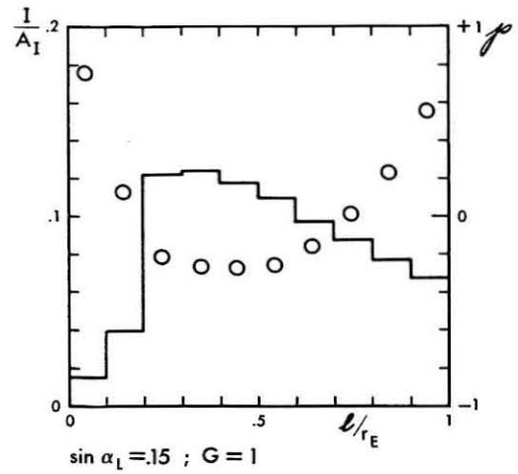

sin α_L = .15 ; G = 1

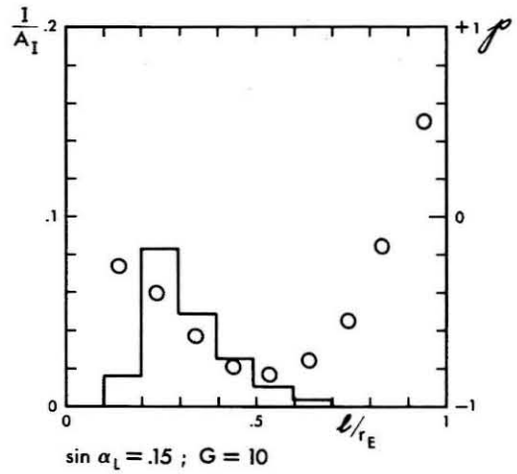

sin α_L = .15 ; G = 10

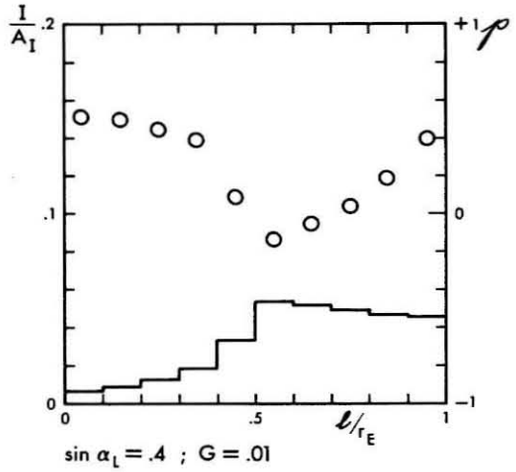

sin α_L = .4 ; G = .01

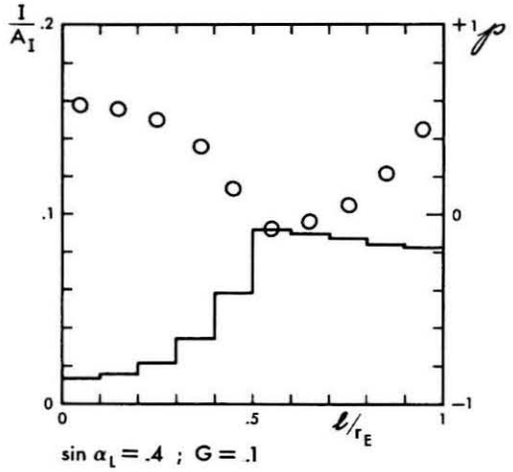

sin α_L = .4 ; G = .1

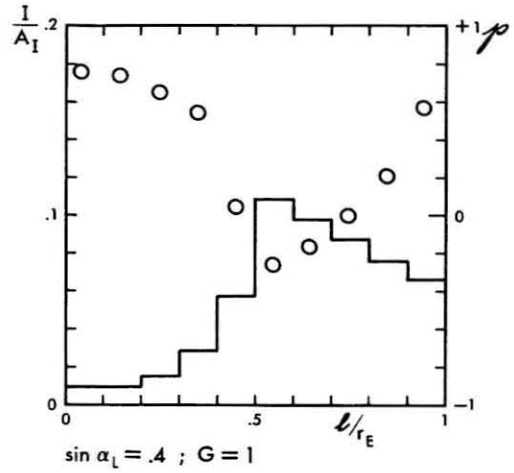

sin α_L = .4 ; G = 1

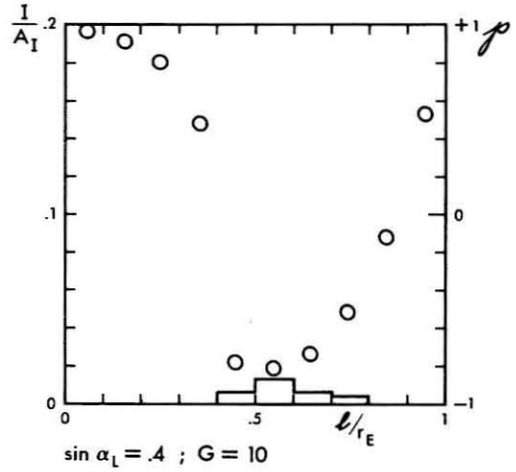

sin α_L = .4 ; G = 10

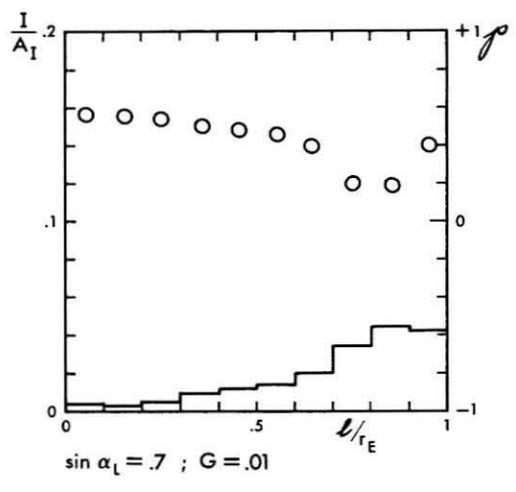

sin α_L = .7 ; G = .01

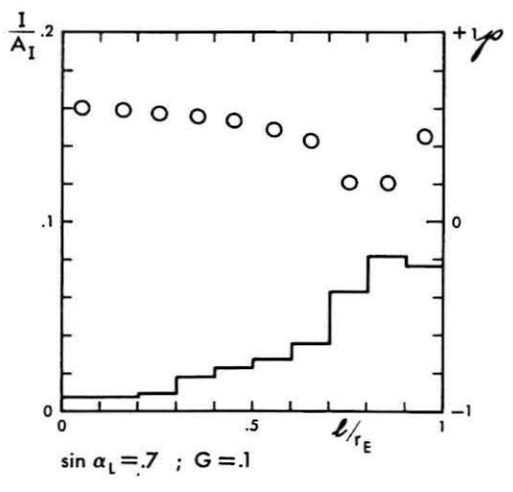

sin α_L = .7 ; G = .1

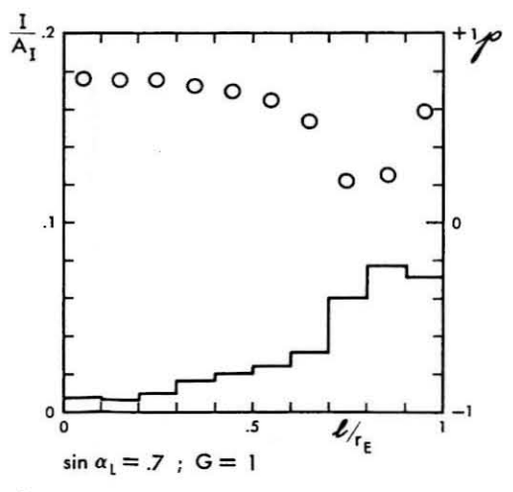

sin α_L = .7 ; G = 1

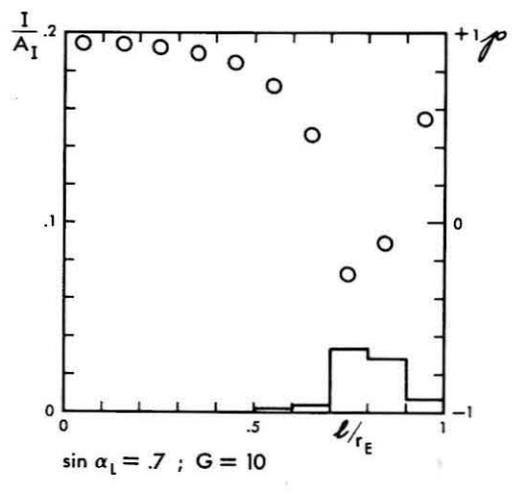

sin α_L = .7 ; G = 10

FIGURE 12 CASE (iii) INTENSITY AND THE DEGREE OF POLARIZATION: $\frac{I}{A_I}$ (SHOWN BY THE HISTOGRAMS) AND $p = \frac{Q}{I}$ (INDICATED BY THE CIRCLES) VS. ℓ/r_E

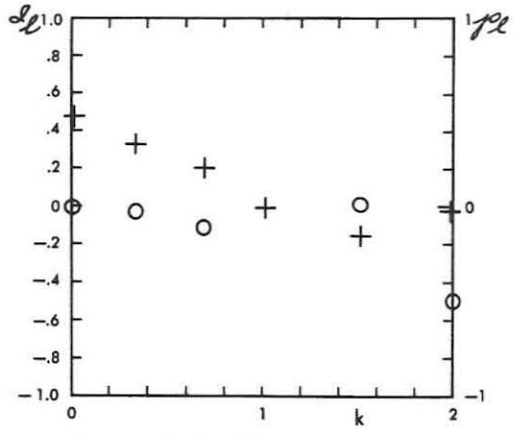

sin α_L = .15 ; G = .01

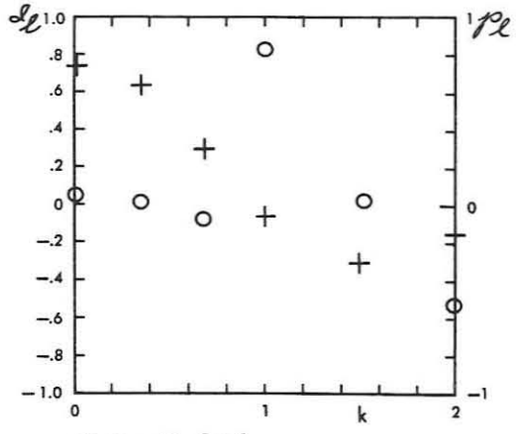

sin α_L = .15 ; G = .1

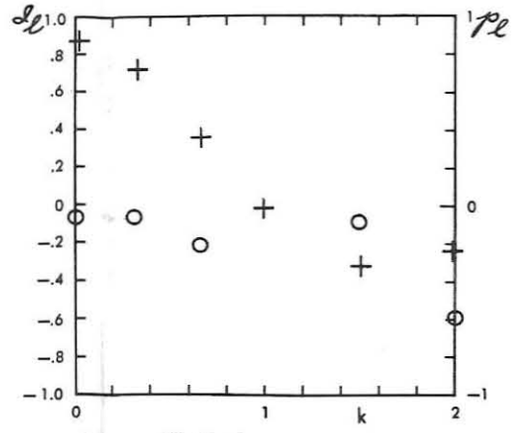

sin α_L = .15 ; G = 1

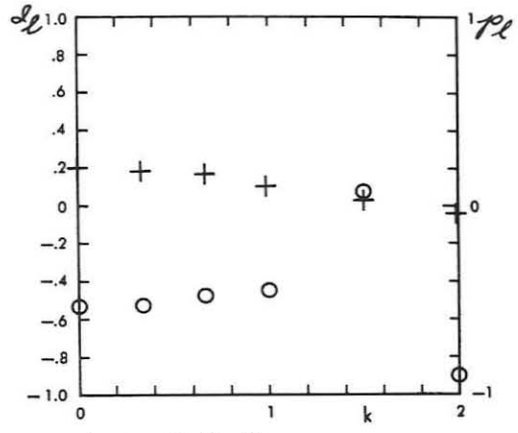

sin α_L = .15 ; G = 10

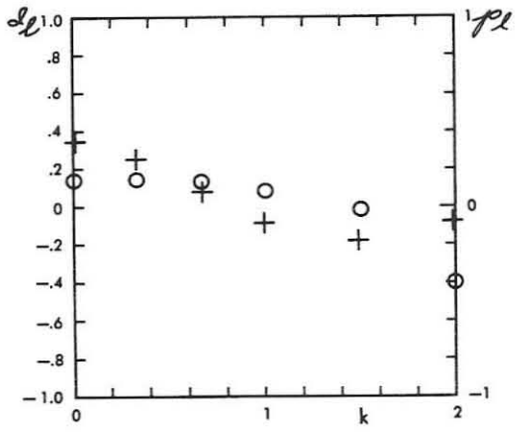

sin α_L = .4 ; G = .01

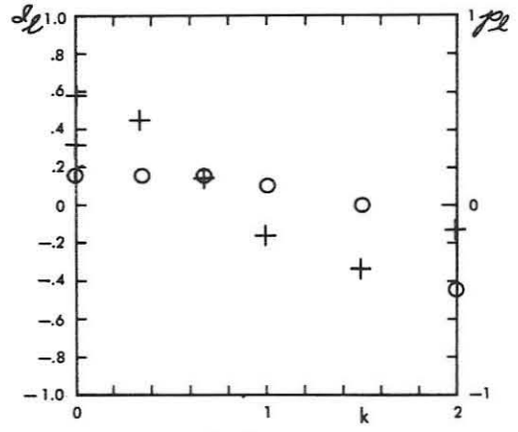

sin α_L = .4 ; G = .1

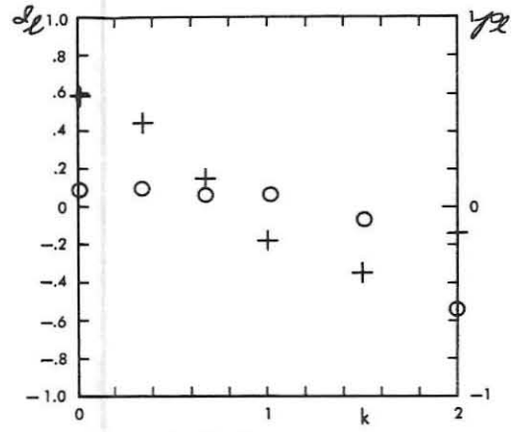

sin α_L = .4 ; G = 1

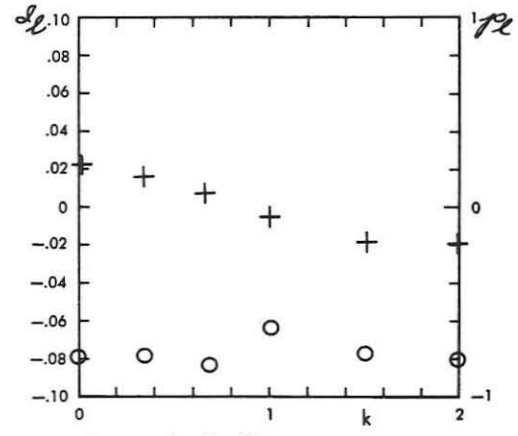

sin α_L = .4 ; G = 10

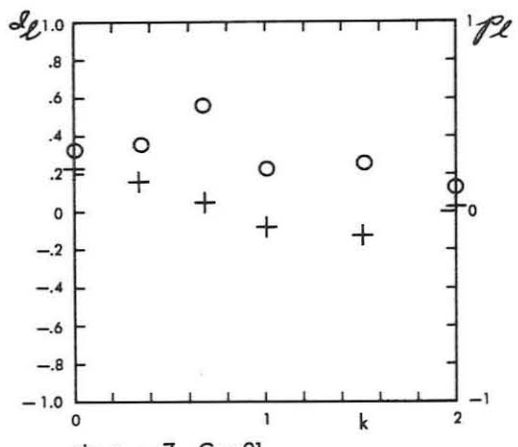

sin α_L = .7 ; G = .01

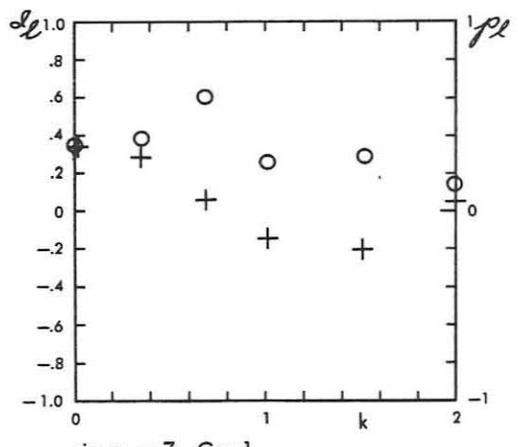

sin α_L = .7 ; G = .1

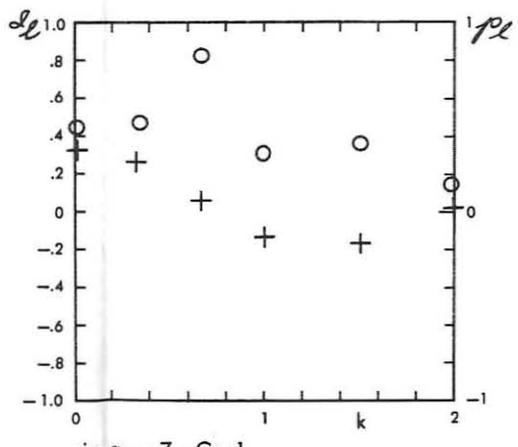

sin α_L = .7 ; G = 1

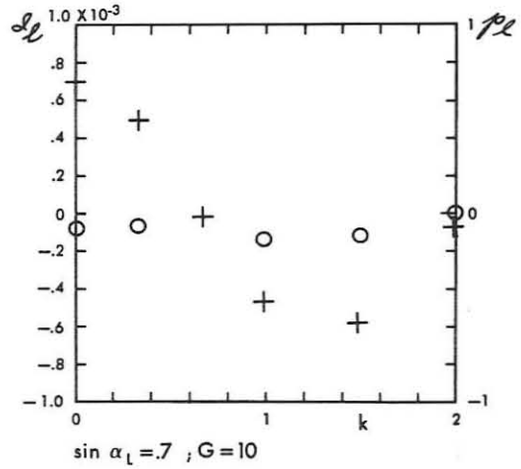

sin α_L = .7 ; G = 10

FIGURE 13 CASE (i) EQUATORIAL COSINE TRANSFORM OF THE INTENSITY AND THE DEGREE OF POLARIZATION: $\mathcal{I}_\ell$ (INDICATED BY +) AND $\mathcal{P}_\ell = \frac{\mathcal{Q}_\ell}{\mathcal{I}_\ell}$ (INDICATED BY O) VS. k

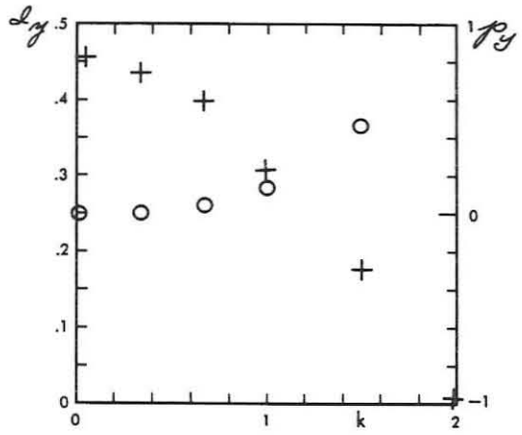

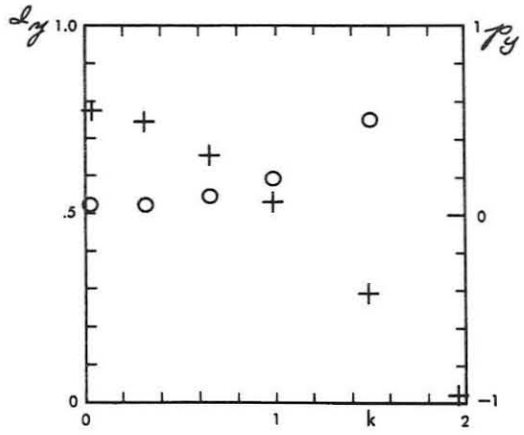

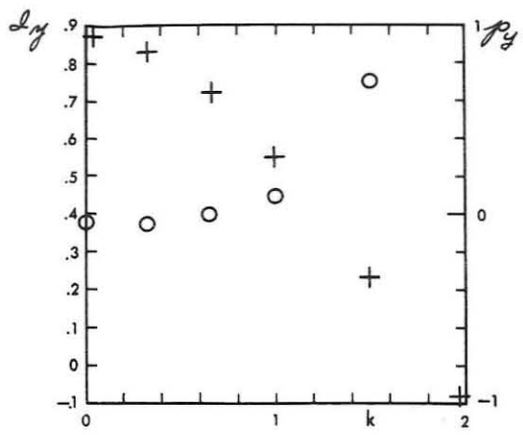

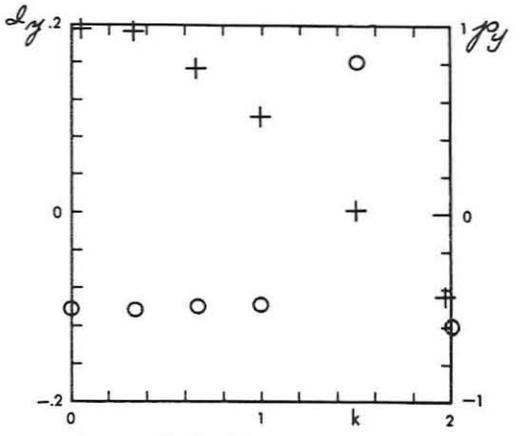

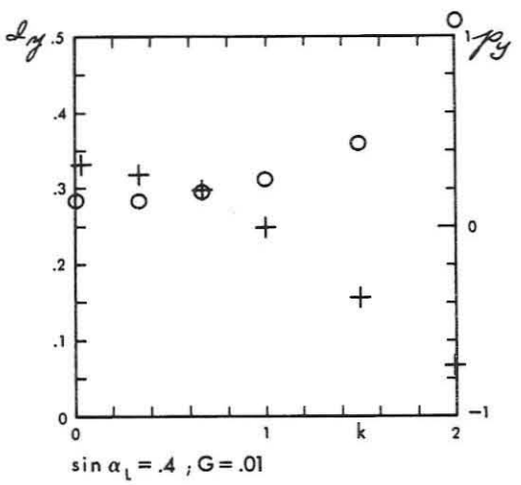

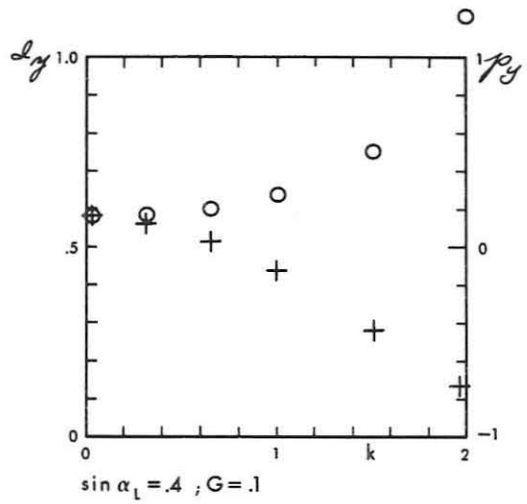

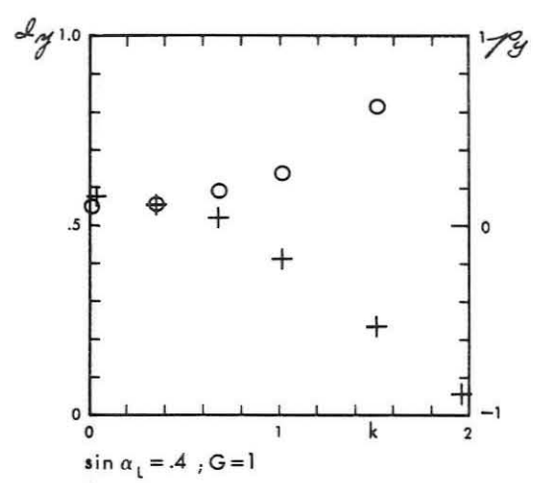

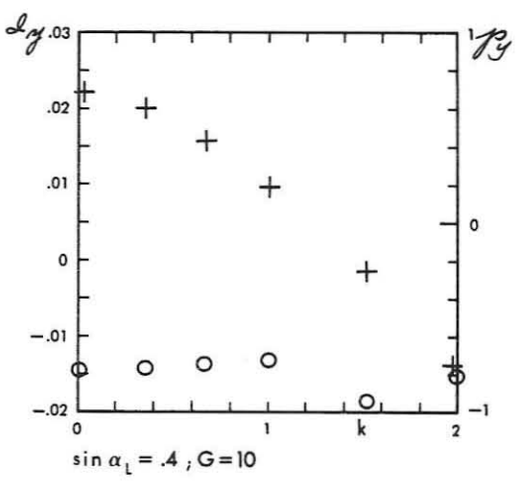

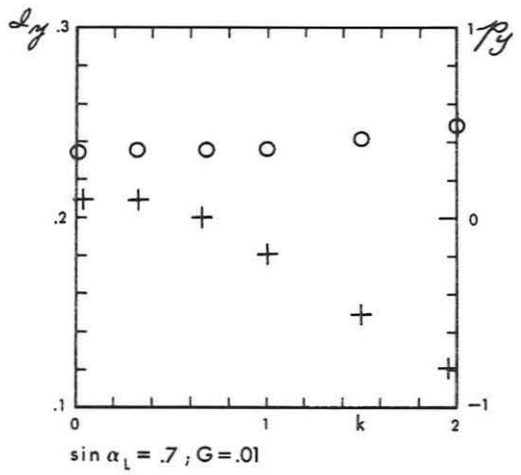

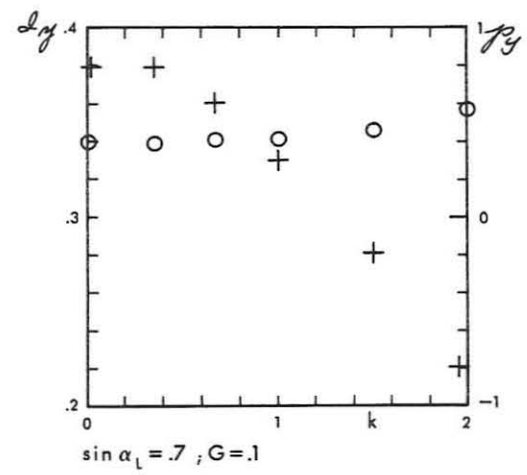

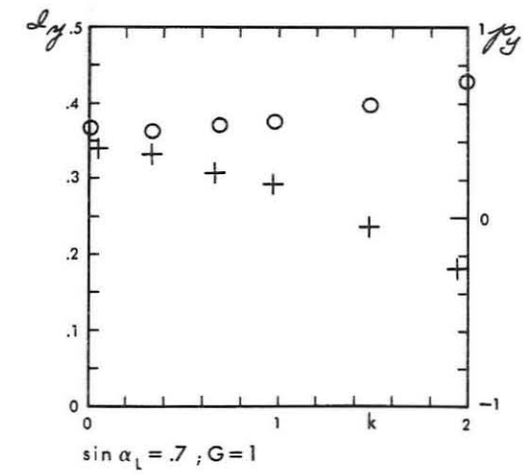

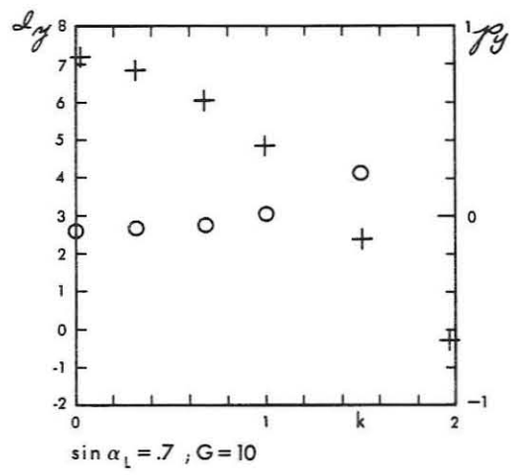

FIGURE 14. CASE (i) POLAR COSINE TRANSFORMS OF THE INTENSITY AND THE DEGREE OF POLARIZATION: $\mathcal{I}_y$ (INDICATED BY +) AND $\mathcal{P}_y = \frac{\mathcal{Q}_y}{\mathcal{I}_y}$ (INDICATED BY O) VS. k

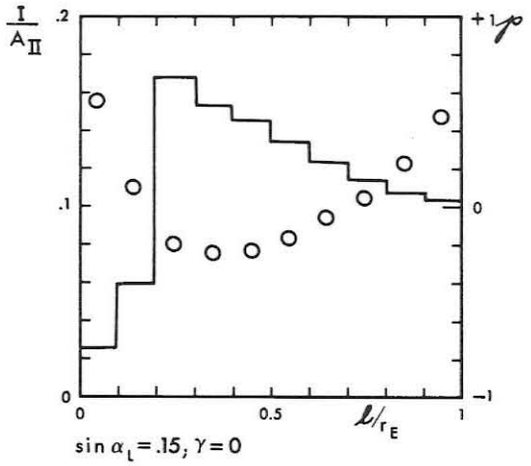

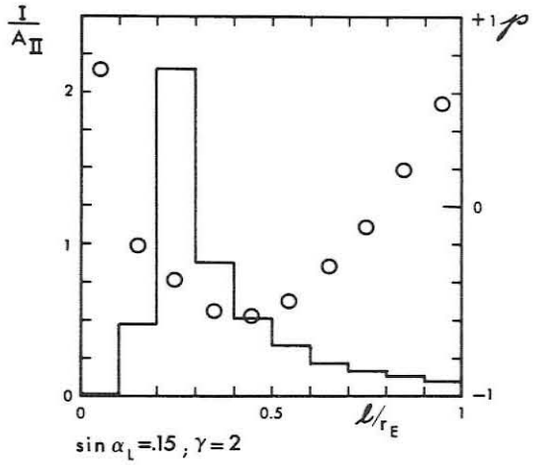

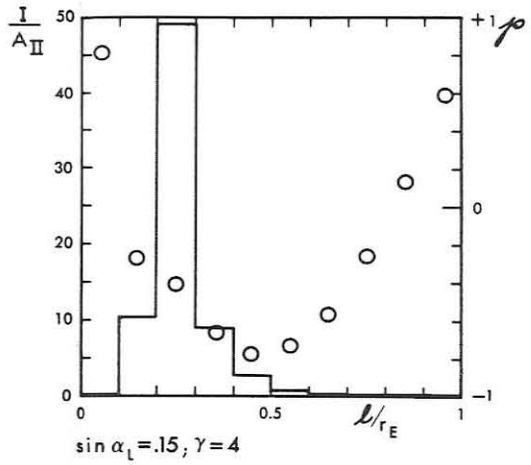

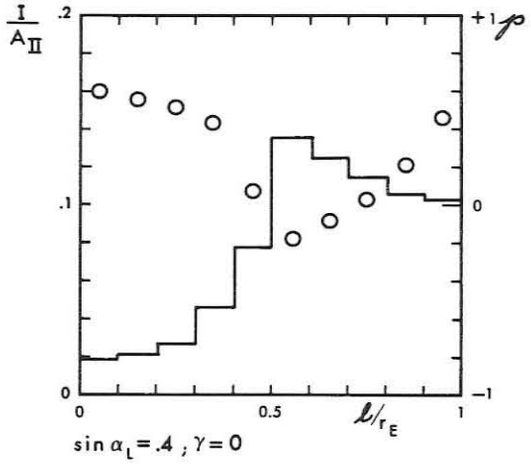

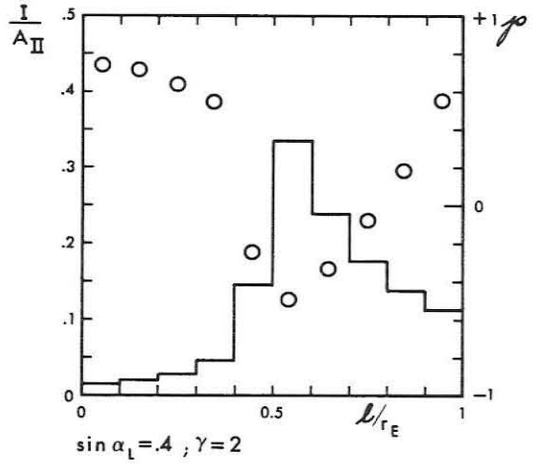

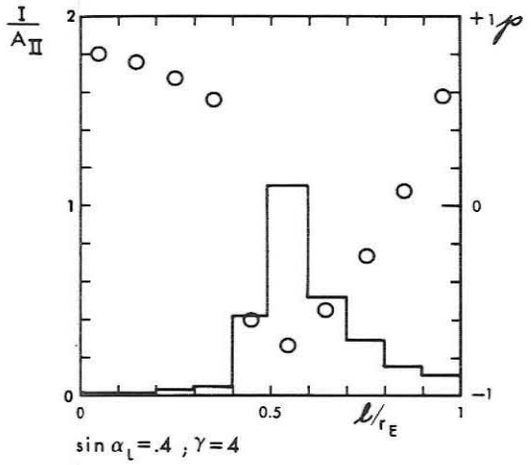

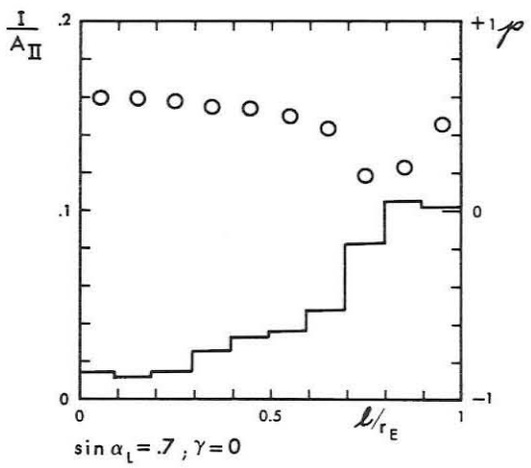

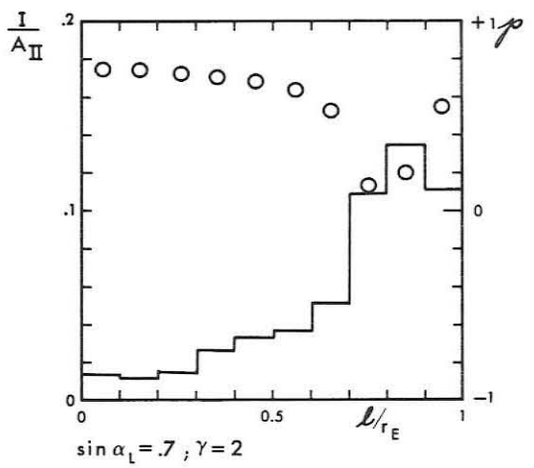

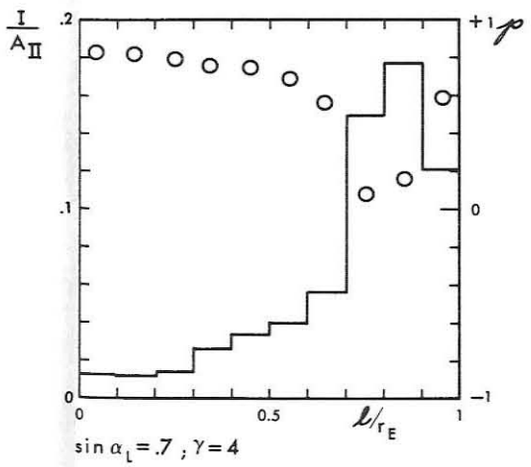

FIGURE 15. CASE (ii) INTENSITY AND THE DEGREE OF POLARIZATION: $\frac{I}{A_{II}}$(SHOWN BY THE HISTOGRAMS) AND $p=\frac{Q}{I}$ (INDICATED BY THE CIRCLES) VS. ℓ/r_E

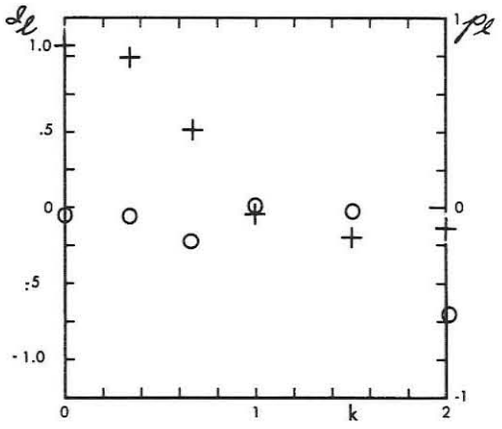

$\sin\alpha_L = .15$; $\gamma = 0$

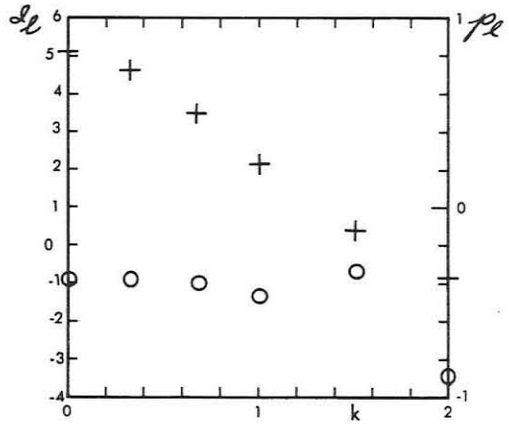

$\sin\alpha_L = .15$; $\gamma = 2$

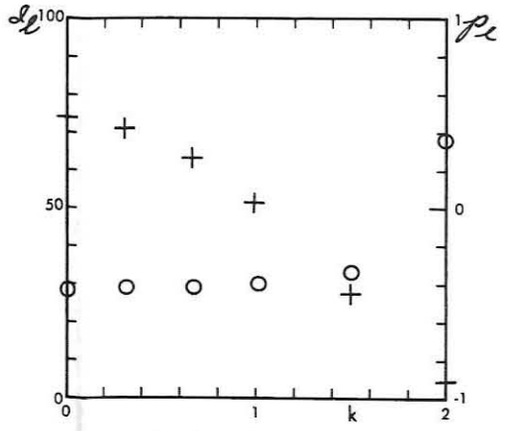

$\sin\alpha_L = .15$; $\gamma = 4$

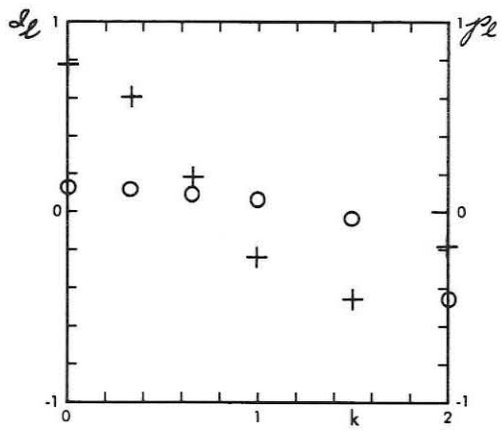

$\sin\alpha_L = .4$; $\gamma = 0$

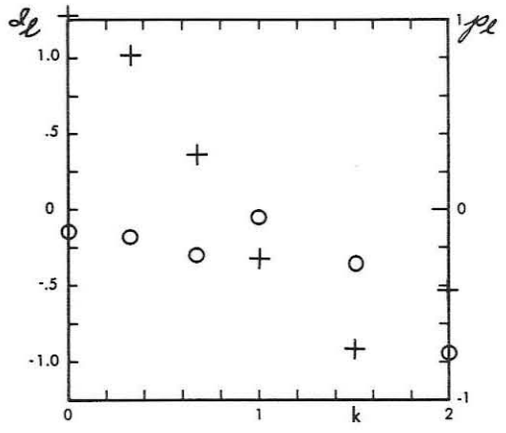

$\sin\alpha_L = .4$; $\gamma = 2$

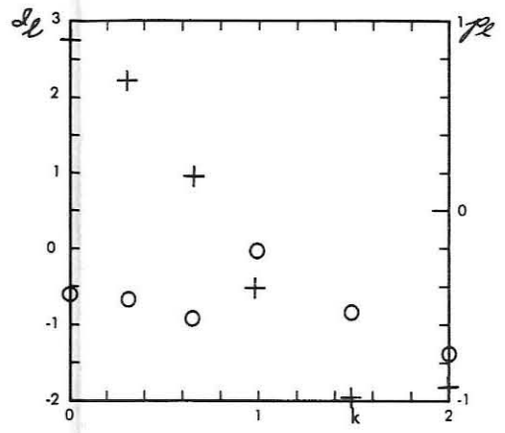

$\sin\alpha_L = .4$; $\gamma = 4$

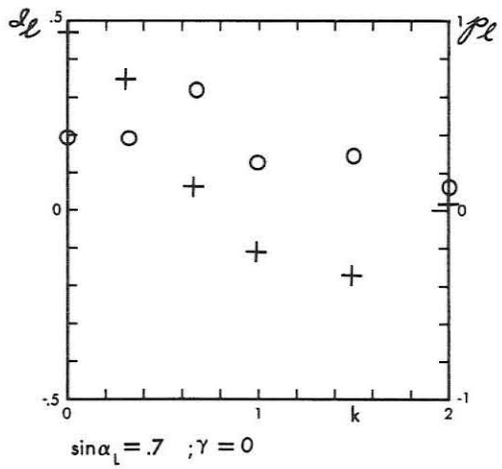

$\sin\alpha_L = .7$; $\gamma = 0$

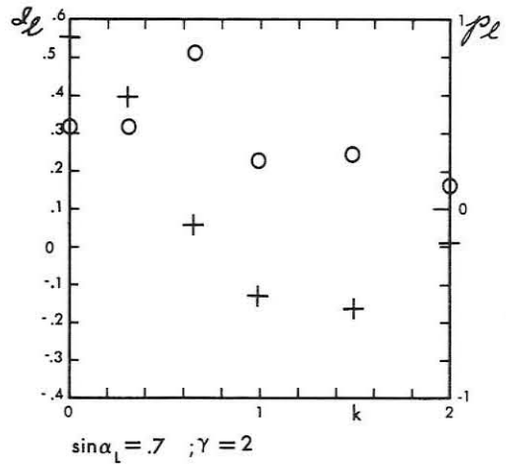

$\sin\alpha_L = .7$; $\gamma = 2$

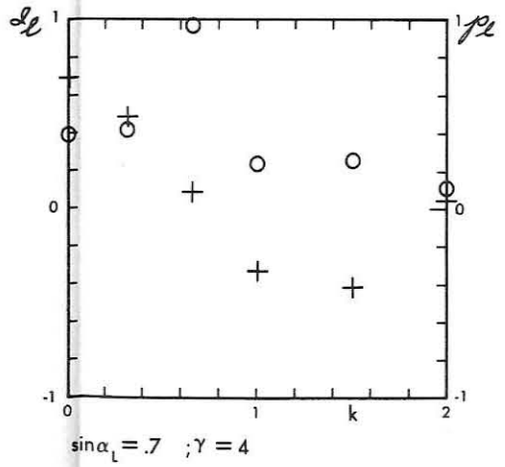

$\sin\alpha_L = .7$; $\gamma = 4$

FIGURE 16 CASE (ii) EQUATORIAL COSINE TRANSFORM OF THE INTENSITY AND THE DEGREE OF POLARIZATION: $\mathscr{I}_\ell$ (INDICATED BY +) AND $\mathscr{P}_\ell = \frac{\mathscr{Q}_\ell}{\mathscr{I}_\ell}$ (INDICATED BY 0) VS. k

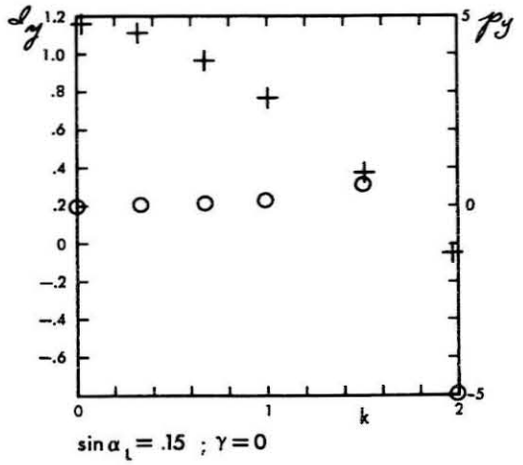

$\sin\alpha_L = .15$; $\gamma = 0$

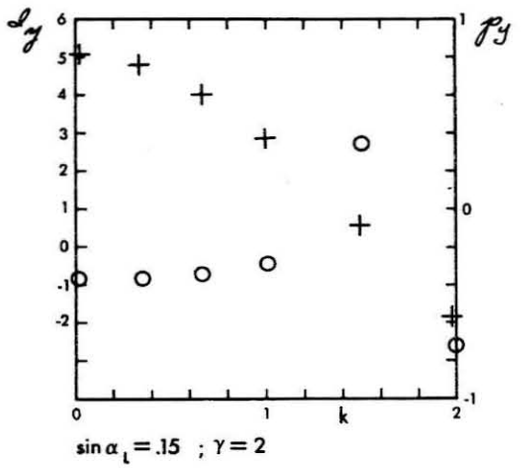

$\sin\alpha_L = .15$; $\gamma = 2$

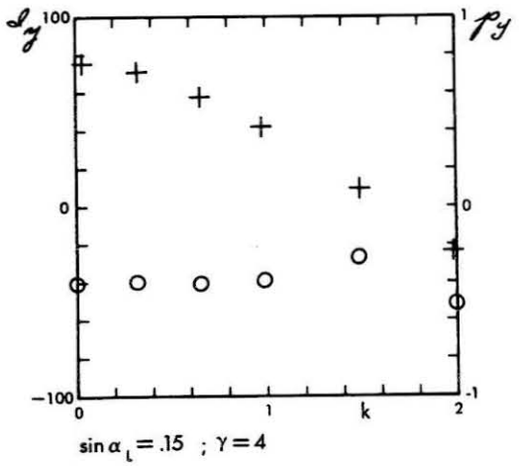

$\sin\alpha_L = .15$; $\gamma = 4$

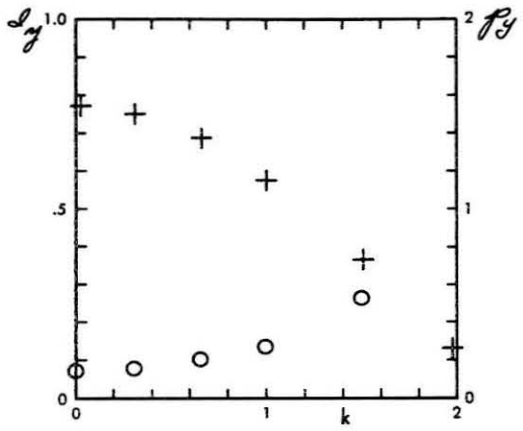

$\sin\alpha_L = .4$; $\gamma = 0$

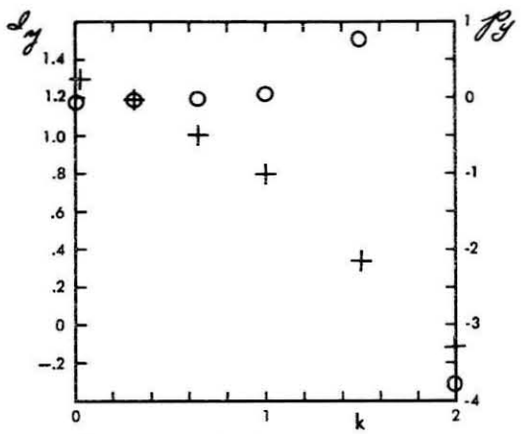

$\sin\alpha_L = .4$; $\gamma = 2$

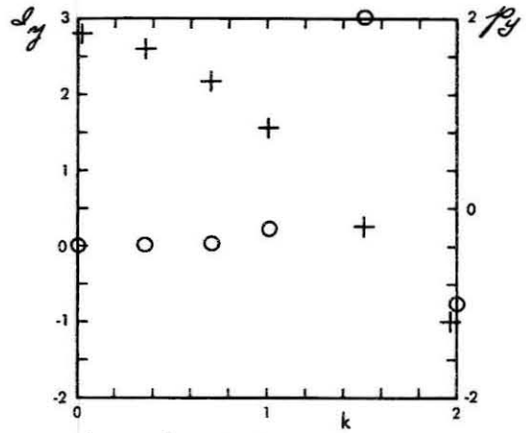

$\sin\alpha_L = .4$; $\gamma = 4$

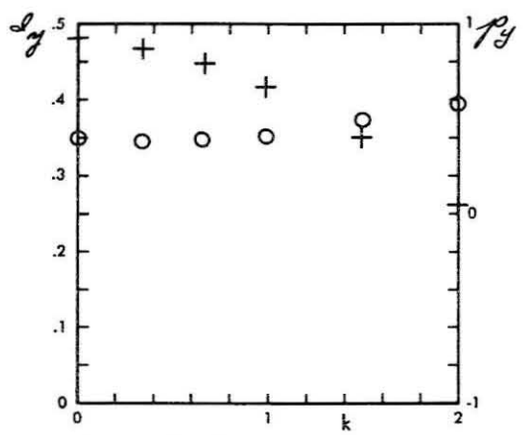

$\sin\alpha_L = .7$; $\gamma = 0$

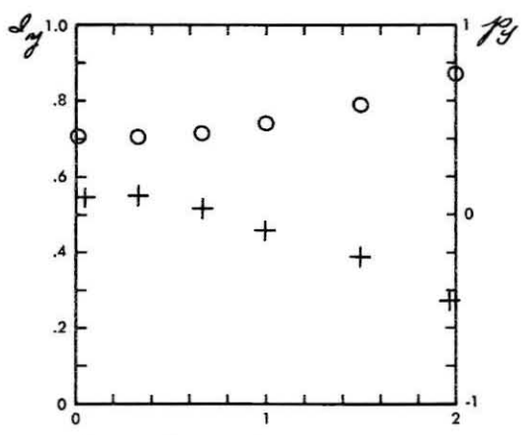

$\sin\alpha_L = .7$; $\gamma = 2$

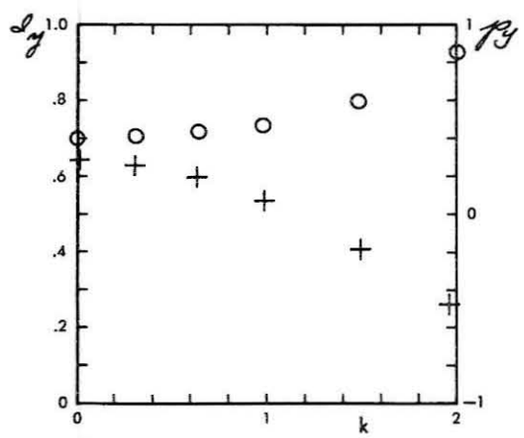

$\sin\alpha_L = .7$; $\gamma = 4$

FIGURE 17. CASE (ii) POLAR COSINE TRANSFORMS OF THE INTENSITY AND THE DEGREE OF POLARIZATION: $\mathcal{I}_y$ (INDICATED BY +) AND $\mathcal{M}_y = \frac{\mathcal{Q}_y}{\mathcal{I}_y}$ (INDICATED BY O) VS. k

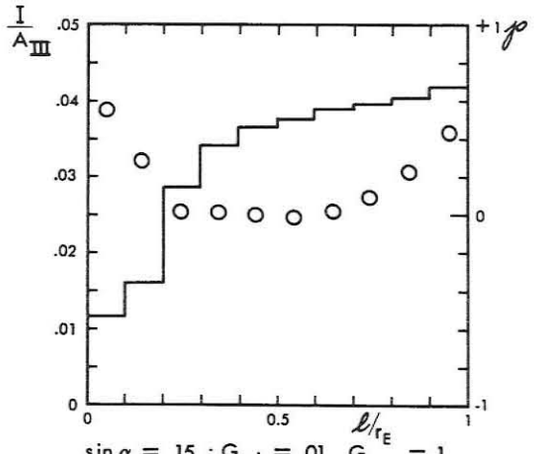

sin α_L= .15 ; G_{min}= .01 , G_{max}= .1

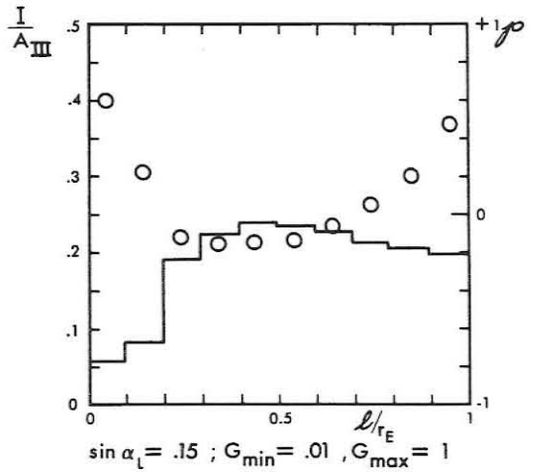

sin α_L= .15 ; G_{min}= .01 , G_{max}= 1

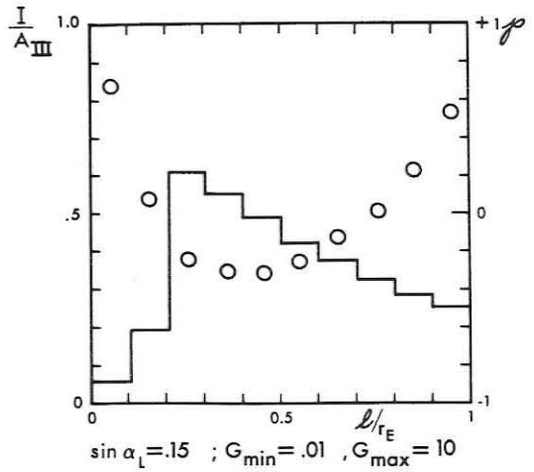

sin α_L=.15 ; G_{min}= .01 , G_{max}= 10

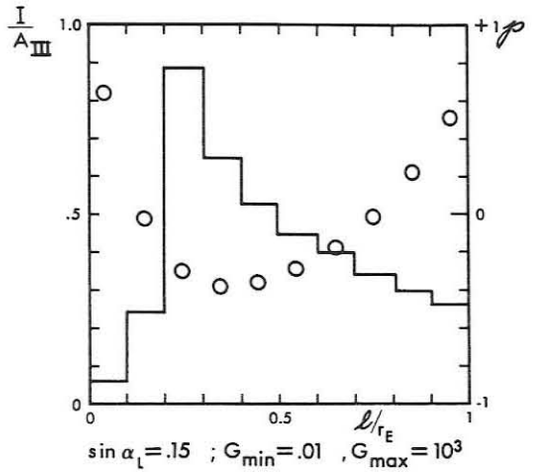

sin α_L=.15 ; G_{min}=.01 , G_{max}= 10^3

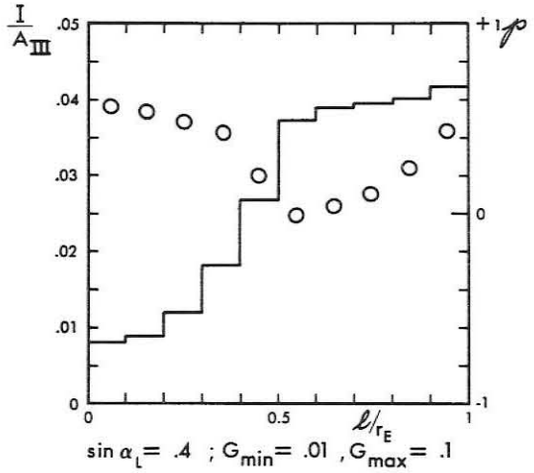

sin α_L= .4 ; G_{min}= .01 , G_{max}= .1

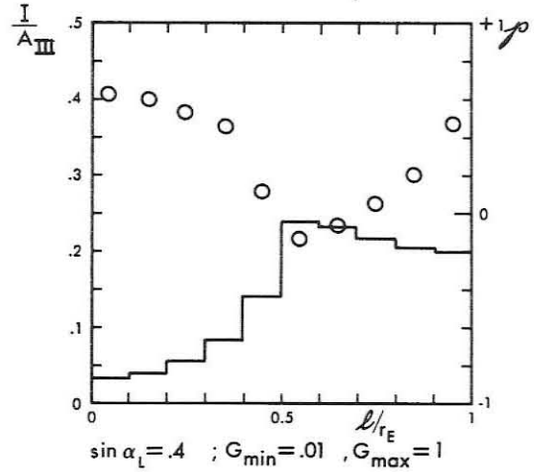

sin α_L=.4 ; G_{min}=.01 , G_{max}=1

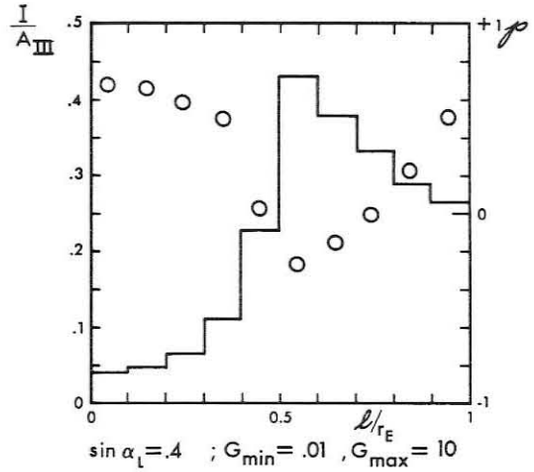

sin α_L=.4 ; G_{min}= .01 , G_{max}= 10

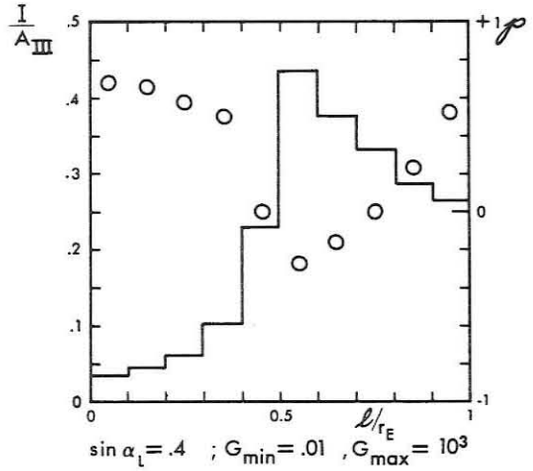

sin α_L=.4 ; G_{min}= .01 , G_{max}= 10^3

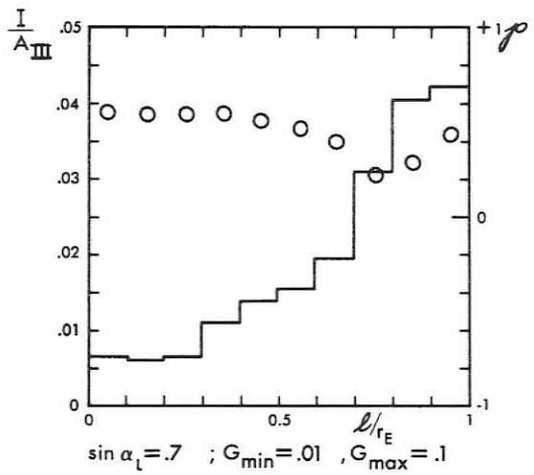

sin α_L=.7 ; G_{min}=.01 , G_{max}=.1

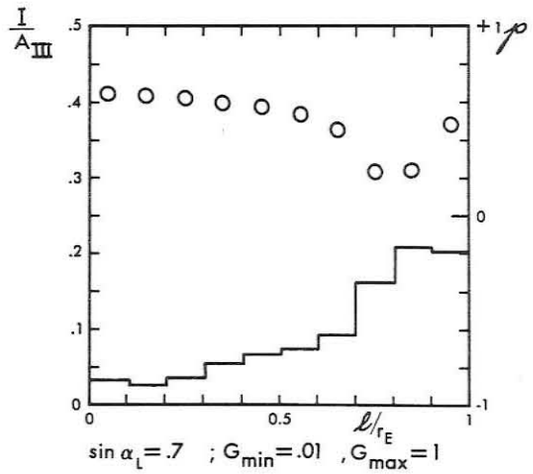

sin α_L=.7 ; G_{min}=.01 , G_{max}=1

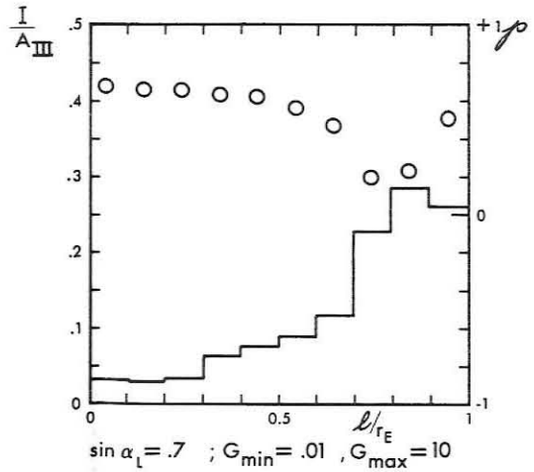

sin α_L=.7 ; G_{min}= .01 , G_{max}=10

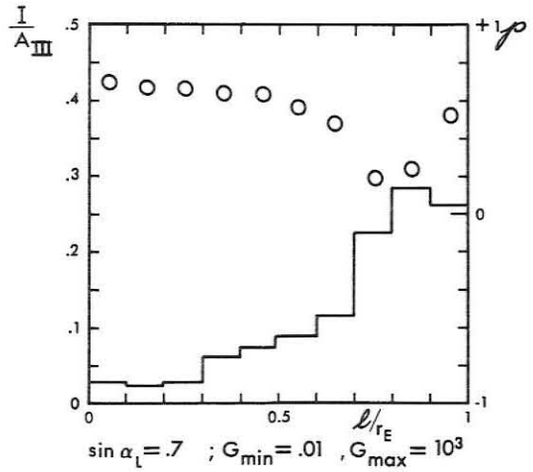

sin α_L=.7 ; G_{min}= .01 , G_{max}= 10^3

FIGURE 18 CASE (iii) INTENSITY AND THE DEGREE OF POLARIZATION: $\frac{I}{A_{III}}$ (SHOWN BY THE HISTOGRAMS) AND $p = \frac{Q}{I}$ (INDICATED BY THE CIRCLES) VS. ℓ/r_E

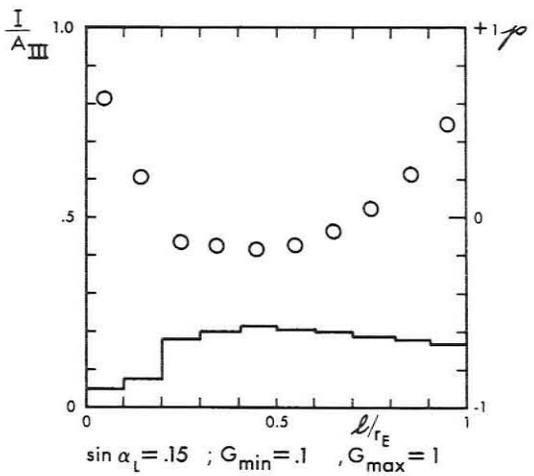

sin α_L = .15 ; G_{min} = .1 , G_{max} = 1

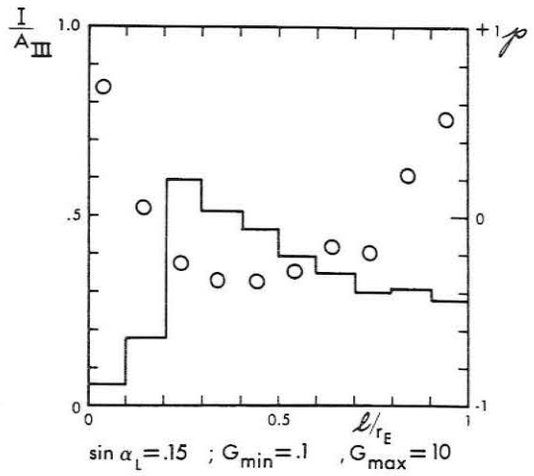

sin α_L = .15 ; G_{min} = .1 , G_{max} = 10

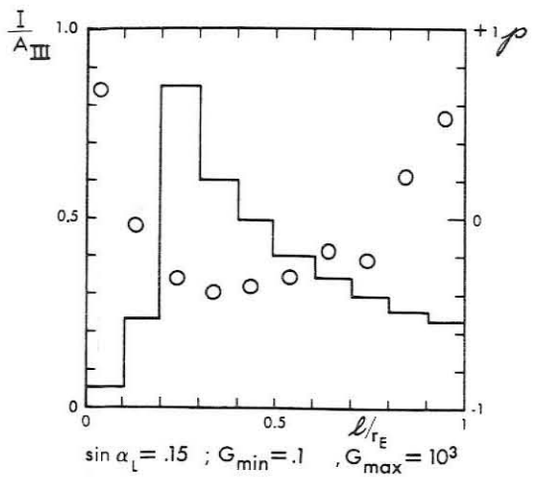

sin α_L = .15 ; G_{min} = .1 , G_{max} = 10^3

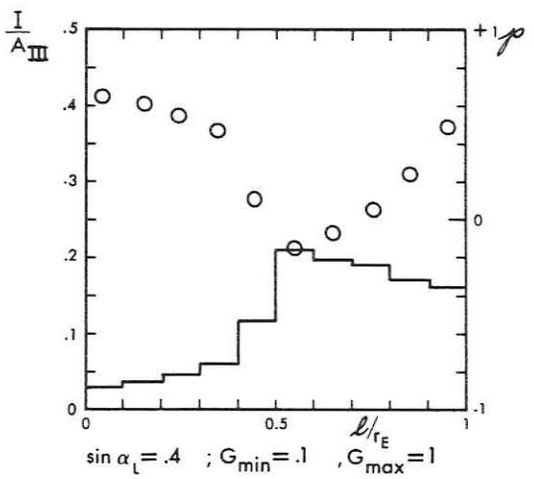

sin α_L = .4 ; G_{min} = .1 , G_{max} = 1

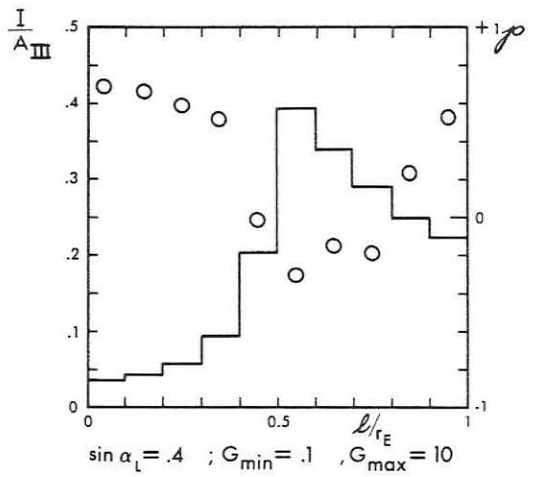

sin α_L = .4 ; G_{min} = .1 , G_{max} = 10

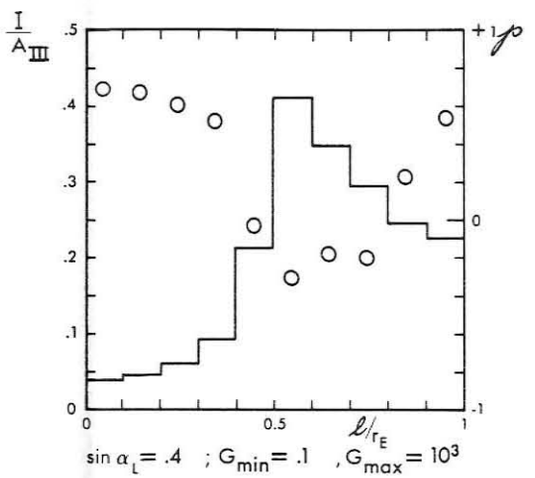

sin α_L = .4 ; G_{min} = .1 , G_{max} = 10^3

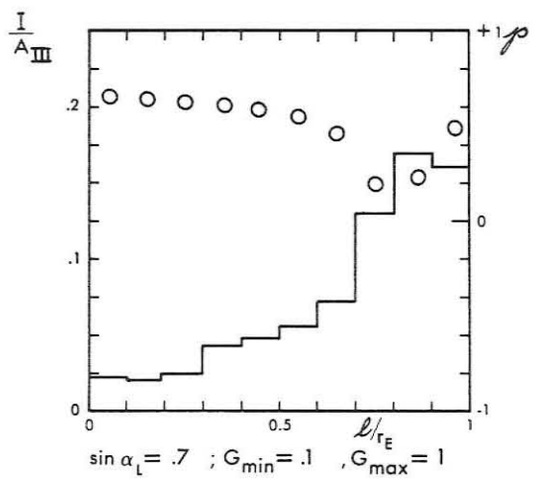

sin α_L = .7 ; G_{min} = .1 , G_{max} = 1

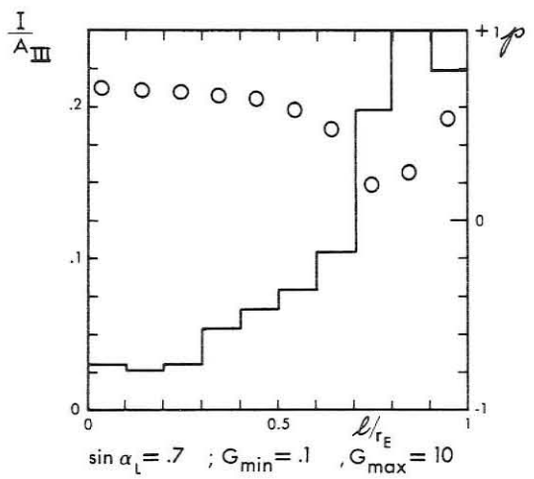

sin α_L = .7 ; G_{min} = .1 , G_{max} = 10

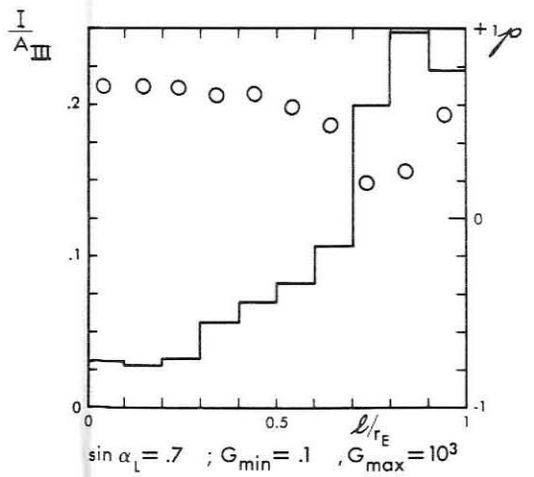

sin α_L = .7 ; G_{min} = .1 , G_{max} = 10^3

FIGURE 18 CASE (iii) INTENSITY AND THE DEGREE OF POLARIZATION: $\frac{I}{A_{III}}$ (SHOWN BY THE HISTOGRAMS) AND $\rho = \frac{Q}{I}$ (INDICATED BY THE CIRCLES) VS. ℓ/r_E
(CONT.)

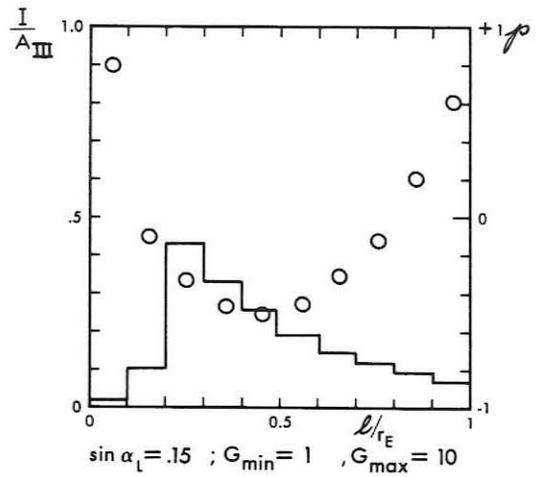

sin α_L = .15 ; G_{min} = 1 , G_{max} = 10

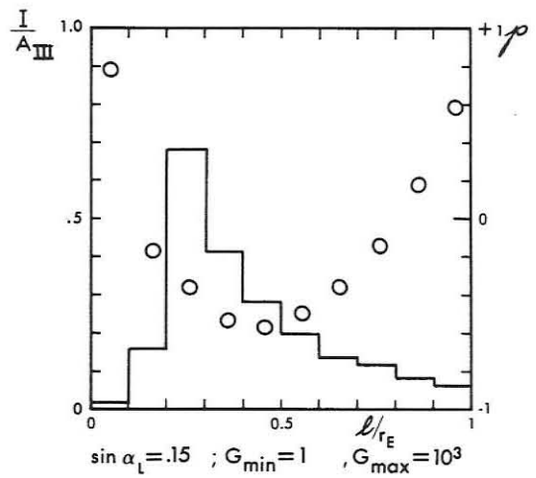

sin α_L = .15 ; G_{min} = 1 , G_{max} = 10^3

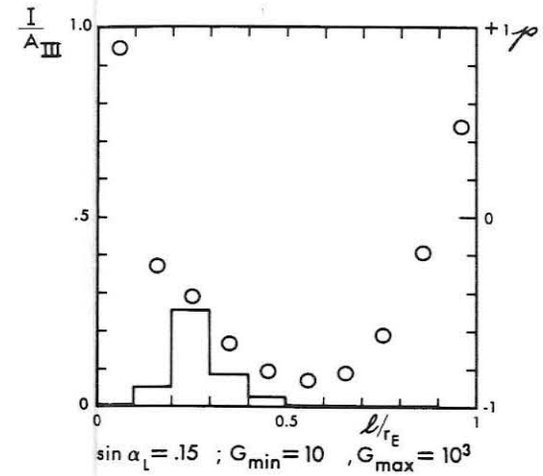

sin α_L = .15 ; G_{min} = 10 , G_{max} = 10^3

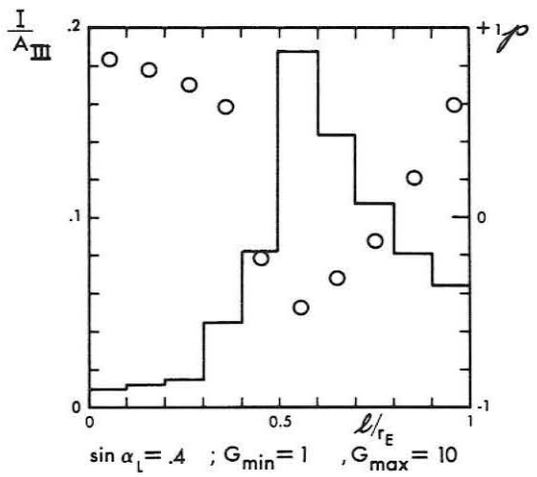

sin α_L = .4 ; G_{min} = 1 , G_{max} = 10

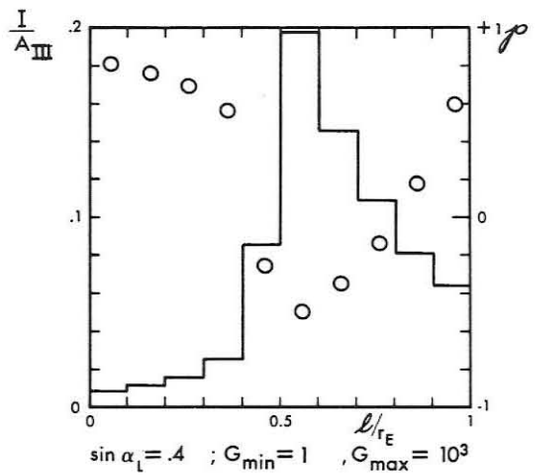

sin α_L = .4 ; G_{min} = 1 , G_{max} = 10^3

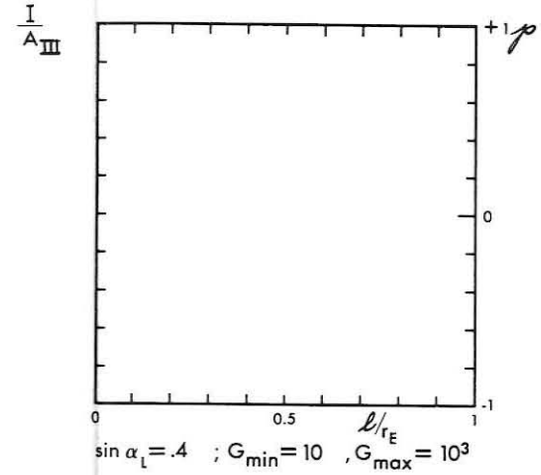

sin α_L = .4 ; G_{min} = 10 , G_{max} = 10^3

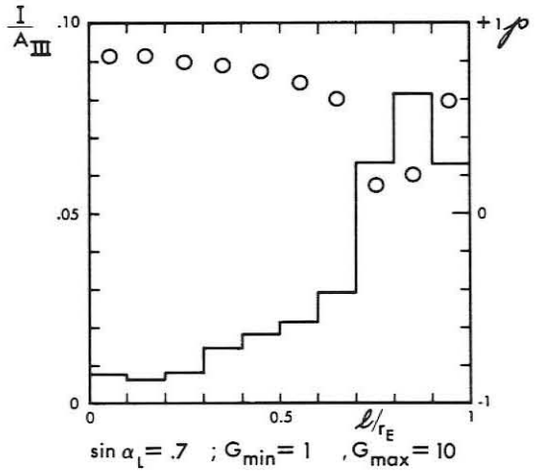

sin α_L = .7 ; G_{min} = 1 , G_{max} = 10

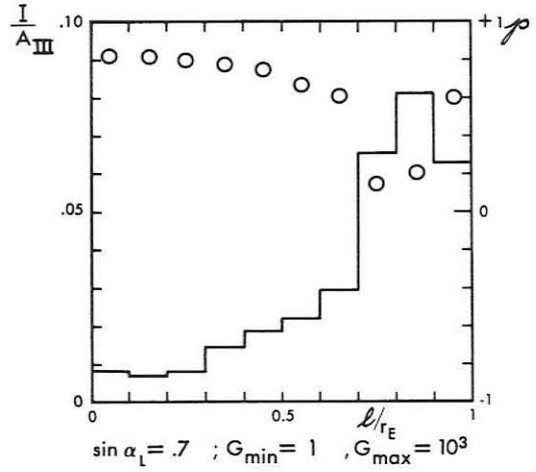

sin α_L = .7 ; G_{min} = 1 , G_{max} = 10^3

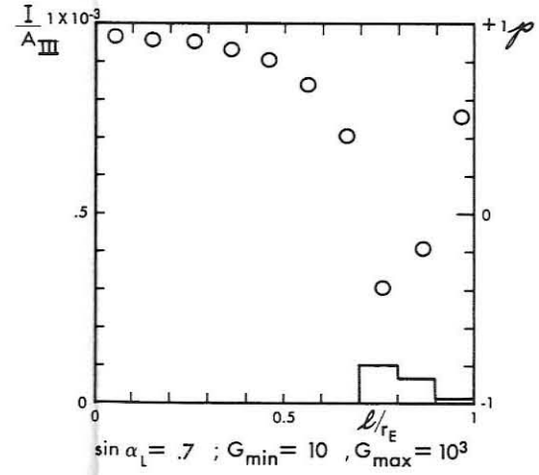

sin α_L = .7 ; G_{min} = 10 , G_{max} = 10^3

FIGURE 18 (CONT.) CASE (iii) INTENSITY AND THE DEGREE OF POLARIZATION $\frac{I}{A_{III}}$ (SHOWN BY THE HISTOGRAMS) AND $p = \frac{Q}{I}$ (INDICATED BY THE CIRCLES) VS. ℓ/r_E

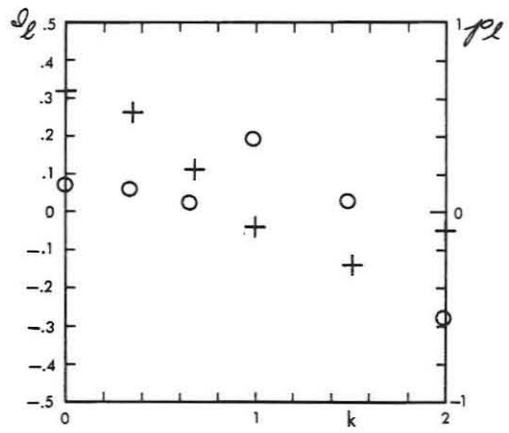

$\sin\alpha_L = .15$; $G_{min} = .01$, $G_{max} = .1$

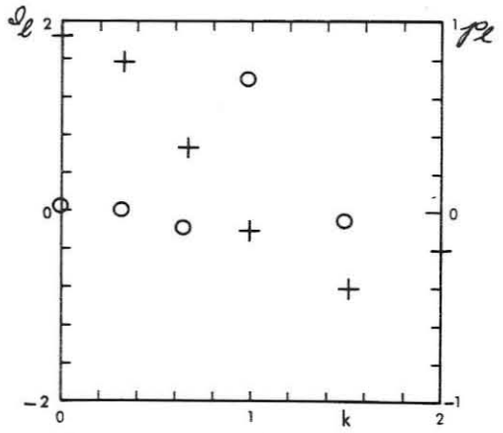

$\sin\alpha_L = .15$; $G_{min} = .01$, $G_{max} = 1$

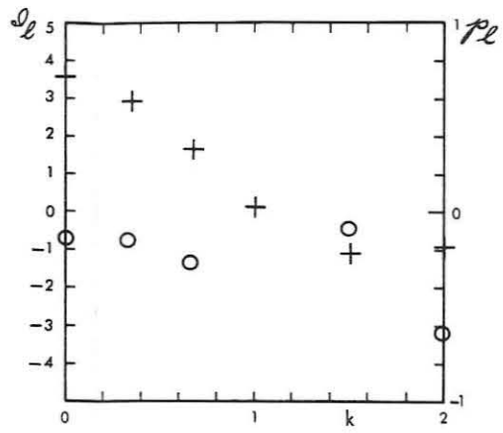

$\sin\alpha_L = .15$; $G_{min} = .01$, $G_{max} = 10$

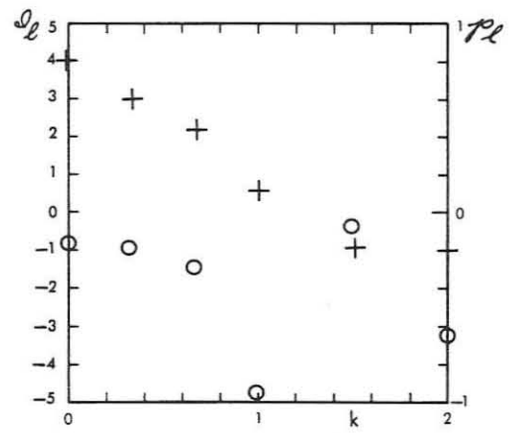

$\sin\alpha_L = .15$; $G_{min} = .01$, $G_{max} = 10^3$

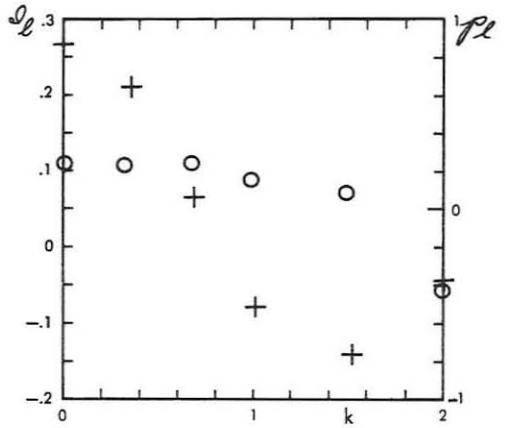

$\sin\alpha_L = .4$; $G_{min} = .01$, $G_{max} = .1$

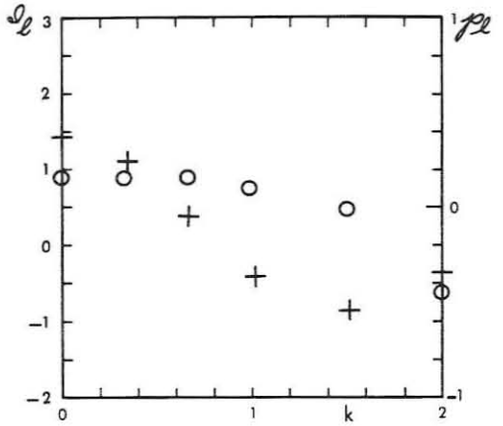

$\sin\alpha_L = .4$; $G_{min} = .01$, $G_{max} = 1$

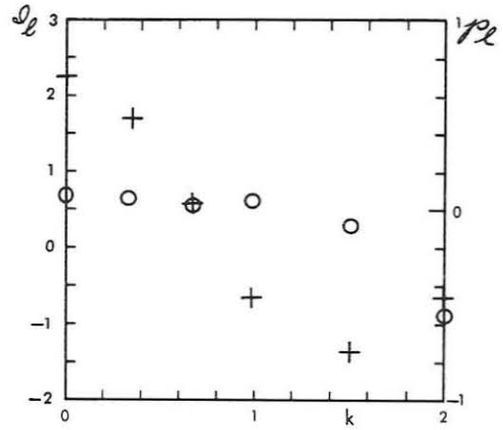

$\sin\alpha_L = .4$; $G_{min} = .01$, $G_{max} = 10$

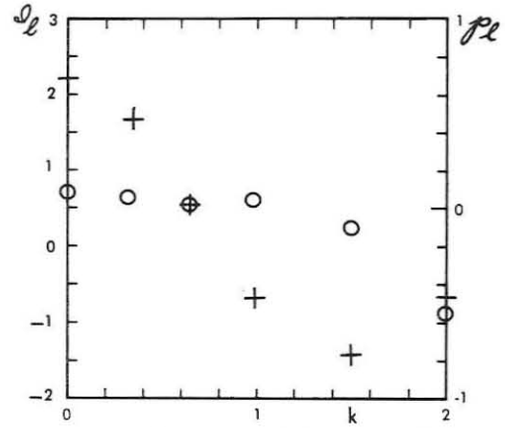

$\sin\alpha_L = .4$; $G_{min} = .01$, $G_{max} = 10^3$

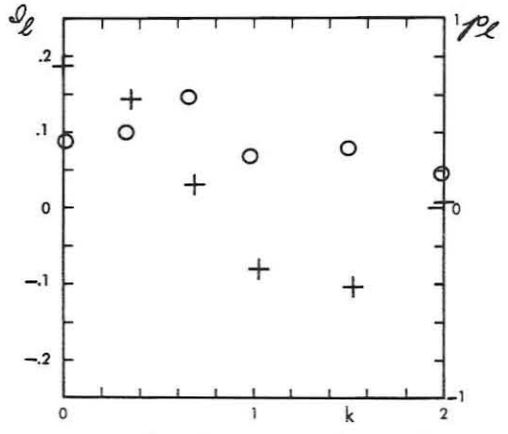

$\sin\alpha_L = .7$; $G_{min} = .01$, $G_{max} = .1$

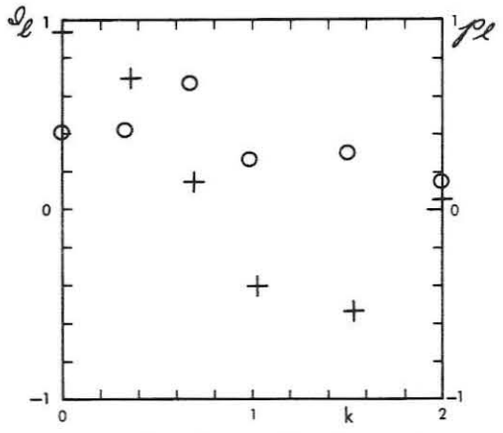

$\sin\alpha_L = .7$; $G_{min} = .01$, $G_{max} = 1$

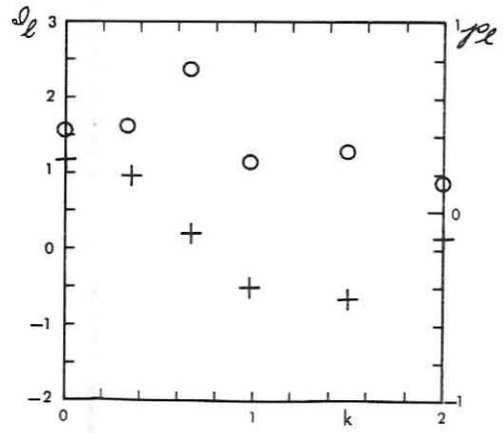

$\sin\alpha_L = .7$; $G_{min} = .01$, $G_{max} = 10$

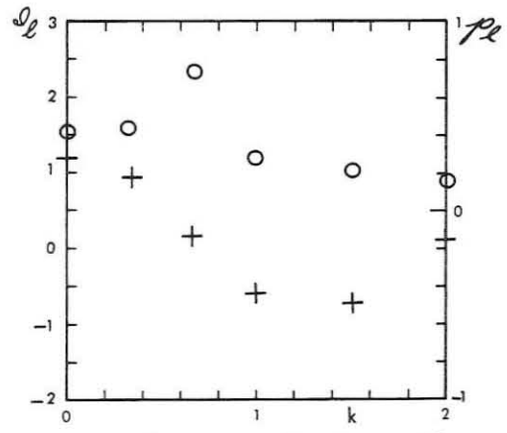

$\sin\alpha_L = .7$; $G_{min} = .01$, $G_{max} = 10^3$

FIGURE 19 CASE (iii) EQUATORIAL COSINE TRANSFORM OF THE INTENSITY AND THE DEGREE OF POLARIZATION: $\mathcal{I}_\ell$ (INDICATED BY +) AND $p_\ell = \frac{Q_\ell}{\mathcal{I}_\ell}$ (INDICATED BY O) VS. k

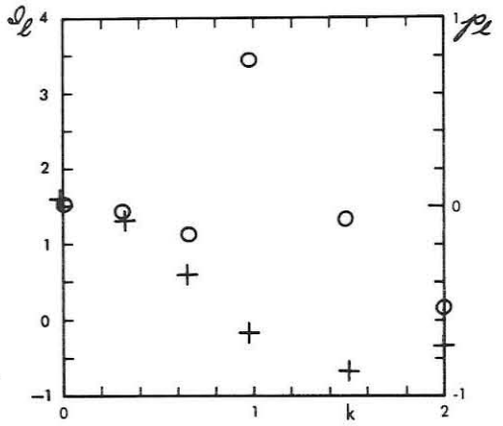

$\sin\alpha_L = .15$; $G_{min} = .1$, $G_{max} = 1$

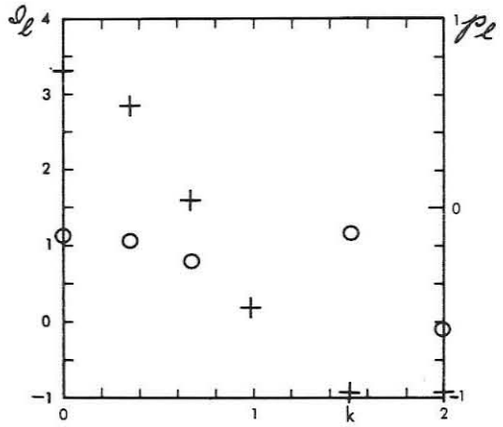

$\sin\alpha_L = .15$; $G_{min} = .1$, $G_{max} = 10$

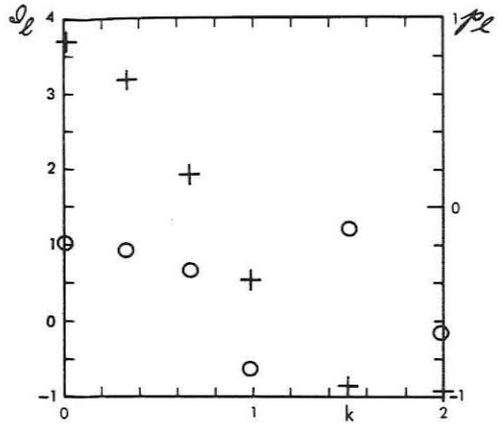

$\sin\alpha_L = .15$; $G_{min} = .1$, $G_{max} = 10^3$

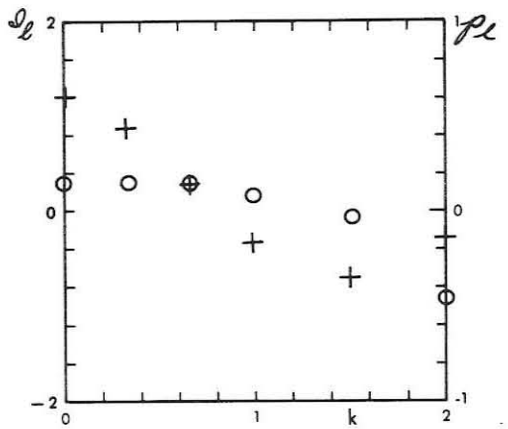

$\sin\alpha_L = .4$; $G_{min} = .1$, $G_{max} = 1$

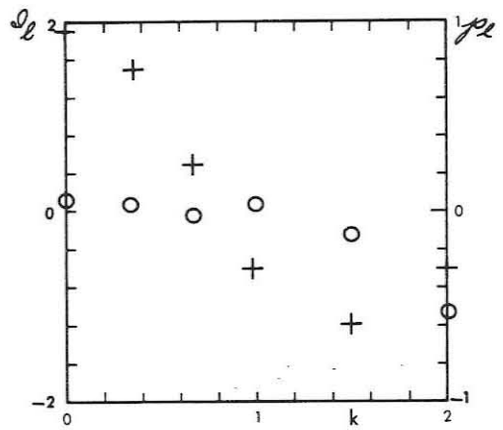

$\sin\alpha_L = .4$; $G_{min} = .1$, $G_{max} = 10$

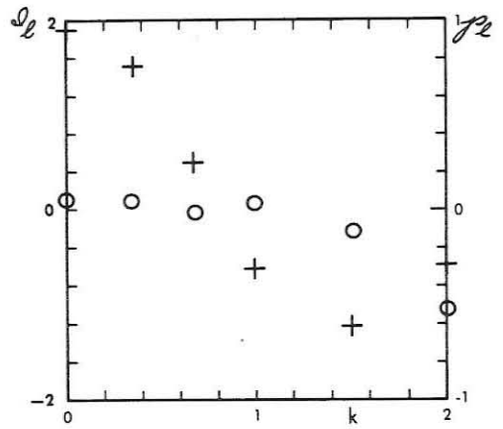

$\sin\alpha_L = .4$; $G_{min} = .1$, $G_{max} = 10^3$

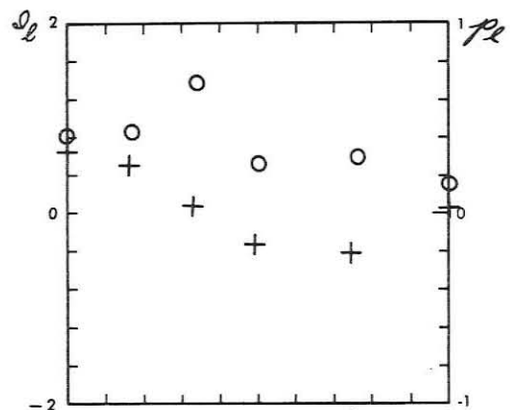

$\sin\alpha_L = .7$; $G_{min} = .1$, $G_{max} = 1$

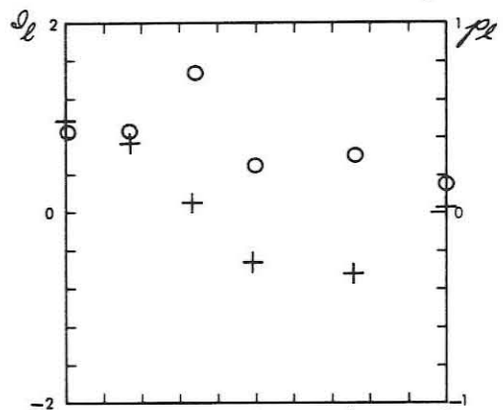

$\sin\alpha_L = .7$; $G_{min} = .1$, $G_{max} = 10$

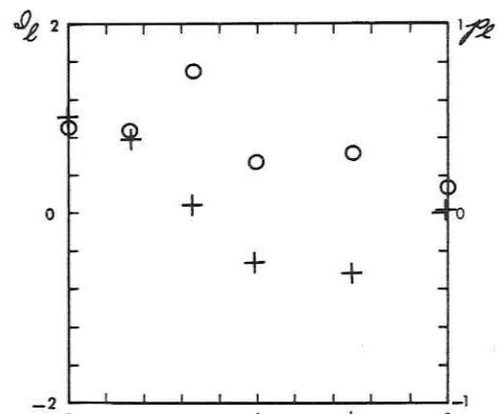

$\sin\alpha_L = .7$; $G_{min} = .1$, $G_{max} = 10^3$

FIGURE 19 CASE (iii) EQUATORIAL TRANSFORM OF THE INTENSITY AND THE DEGREE OF POLARIZATION: (CONT.)

$\mathcal{I}_\ell$ (INDICATED BY +) AND $\mathcal{P}_\ell = \frac{\mathcal{Q}_\ell}{\mathcal{I}_\ell}$ (INDICATED BY O) VS. k

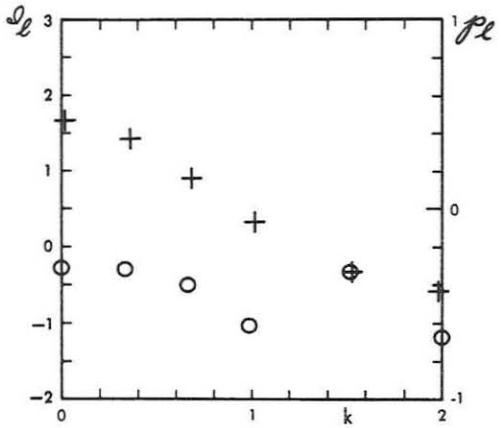

$\sin\alpha_L = .15$; $G_{min} = 1$, $G_{max} = 10$

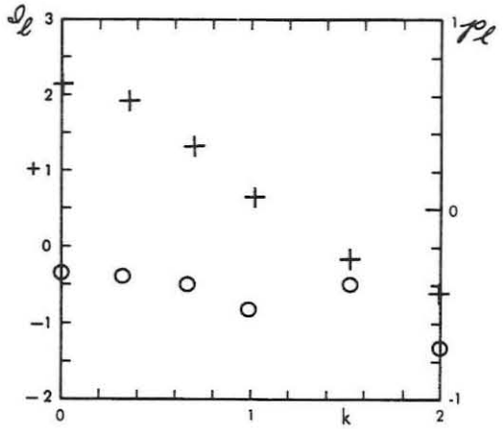

$\sin\alpha_L = .15$; $G_{min} = 1$, $G_{max} = 10^3$

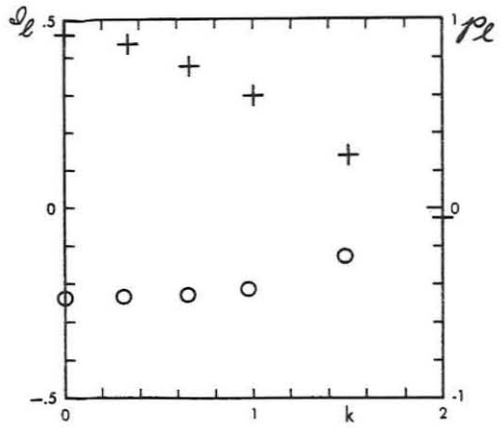

$\sin\alpha_L = .15$; $G_{min} = 10$, $G_{max} = 10^3$

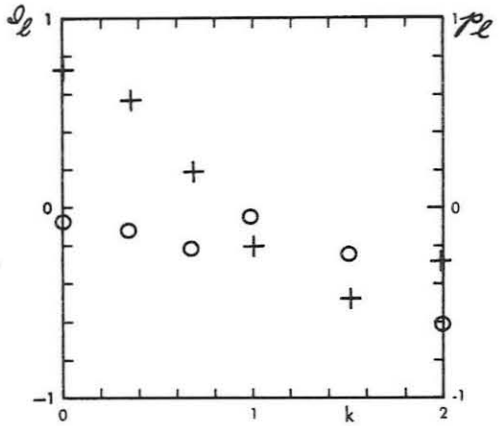

$\sin\alpha_L = .4$; $G_{min} = 1$, $G_{max} = 10$

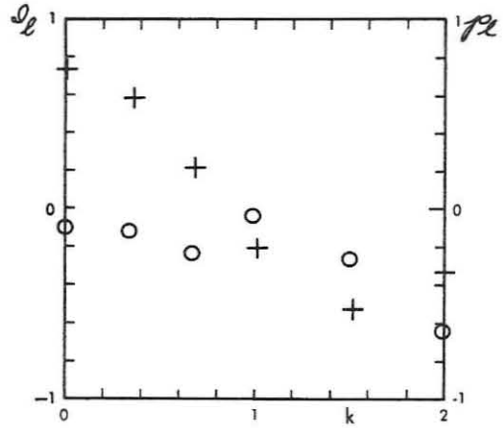

$\sin\alpha_L = .4$; $G_{min} = 1$, $G_{max} = 10^3$

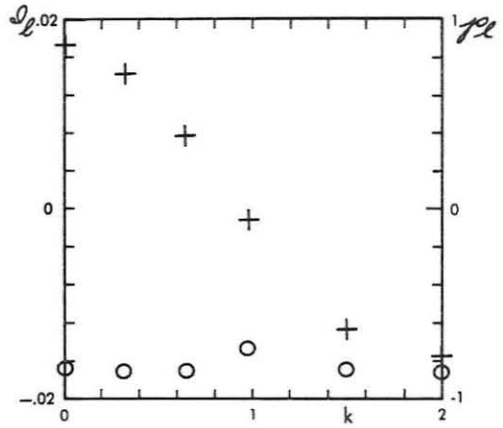

$\sin\alpha_L = .4$; $G_{min} = 10$, $G_{max} = 10^3$

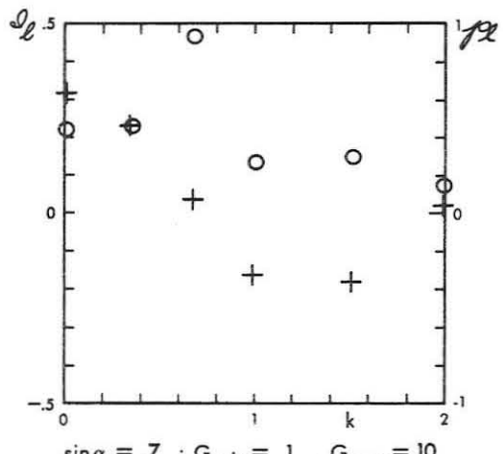

$\sin\alpha_L = .7$; $G_{min} = 1$, $G_{max} = 10$

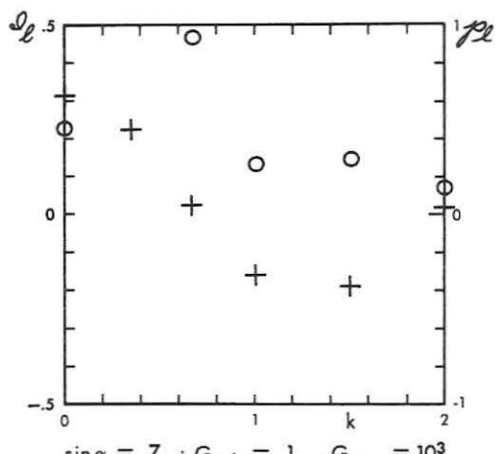

$\sin\alpha_L = .7$; $G_{min} = 1$, $G_{max} = 10^3$

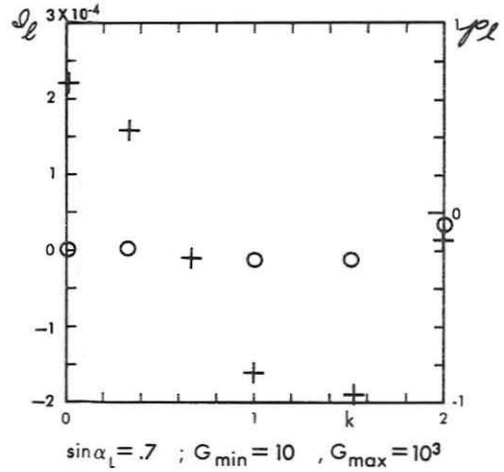

$\sin\alpha_L = .7$; $G_{min} = 10$, $G_{max} = 10^3$

FIGURE 19 CASE (iii) EQUATORIAL COSINE TRANSFORM OF THE INTENSITY AND THE DEGREE OF POLARIZATION: $\mathscr{I}_\ell$ (INDICATED BY +) AND $\mathscr{P}_\ell = \frac{\mathscr{Q}_\ell}{\mathscr{I}_\ell}$ (INDICATED BY O) VS. k (CONT.)

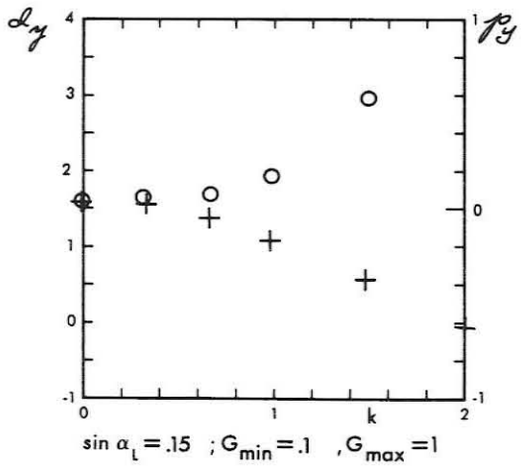

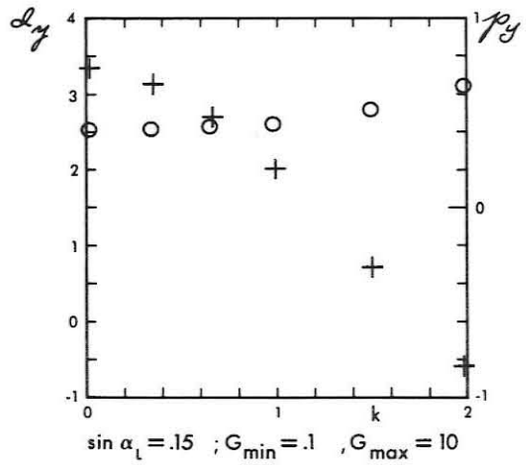

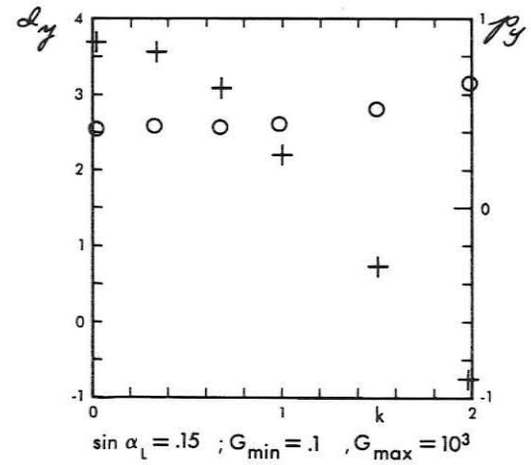

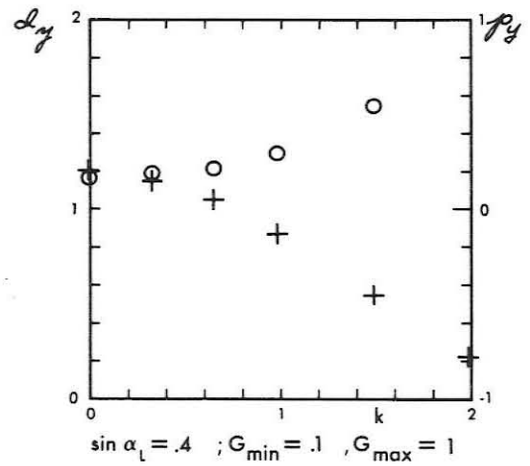

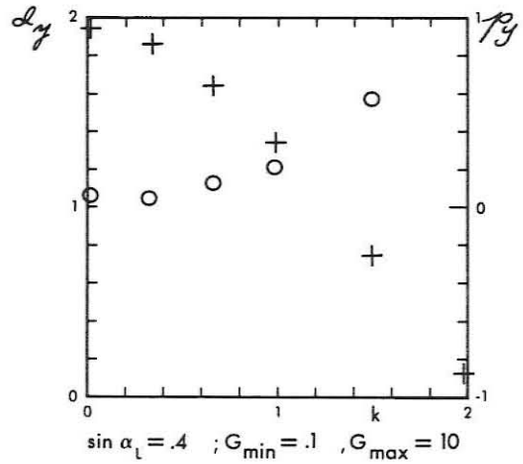

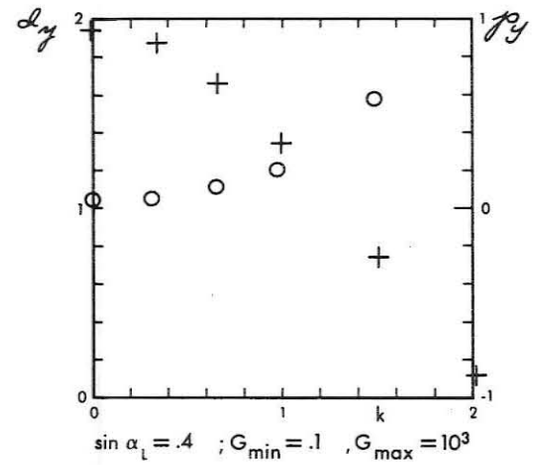

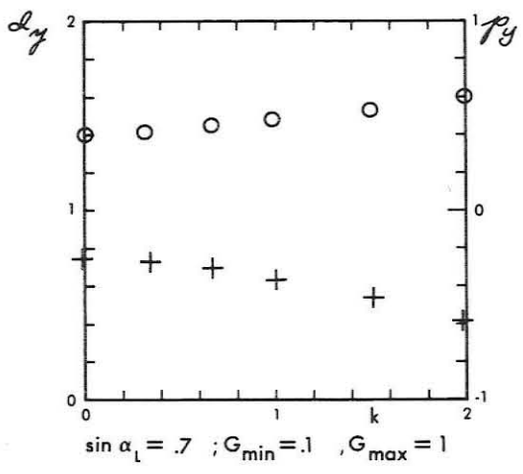

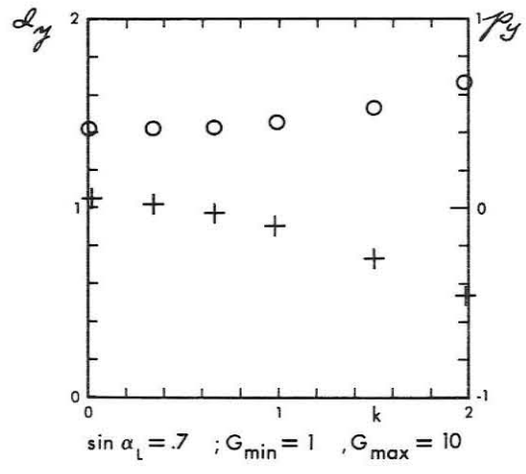

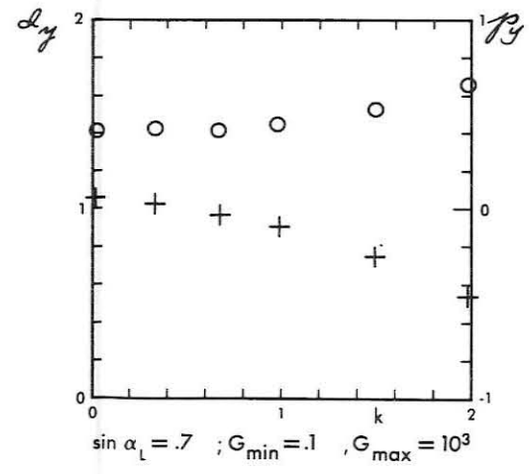

FIGURE 20. CASE (iii) (CONT.) POLAR COSINE TRANSFORMS OF THE INTENSITY AND THE DEGREE OF POLARIZATION: $\mathcal{I}_y$ (INDICATED BY +) AND $\mathcal{P}_y = \frac{\mathcal{Q}_y}{\mathcal{I}_y}$ (INDICATED BY O) VS. k

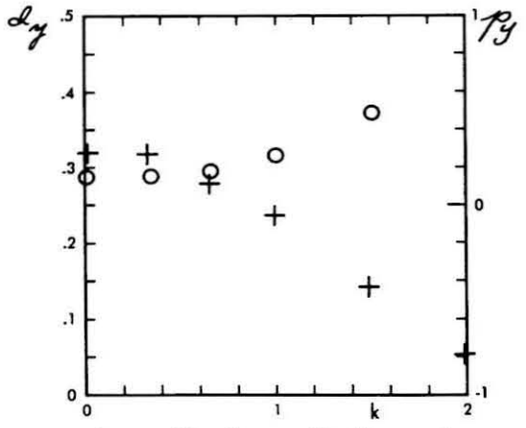

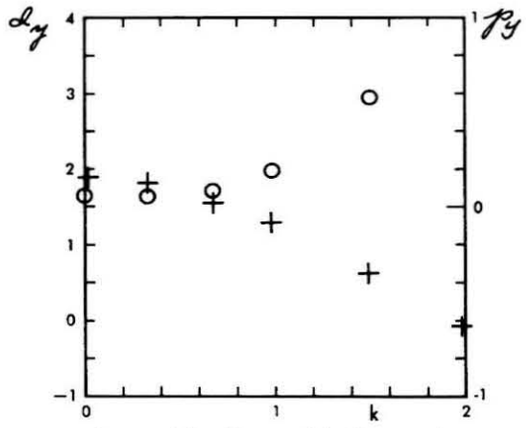

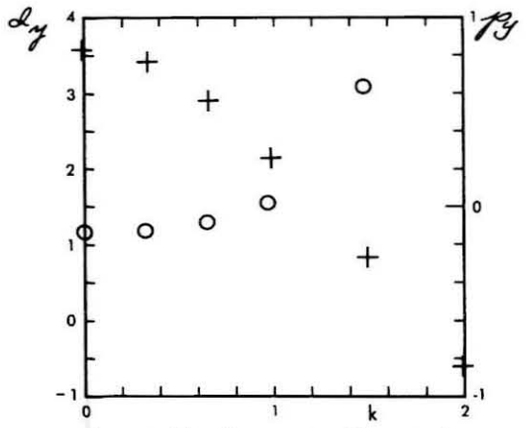

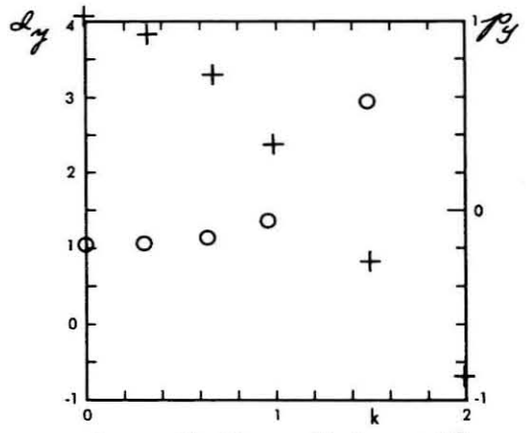

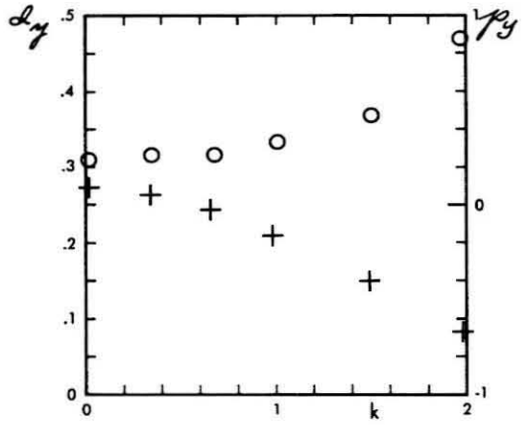

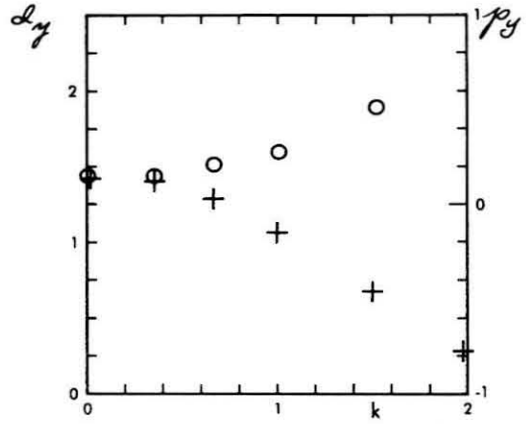

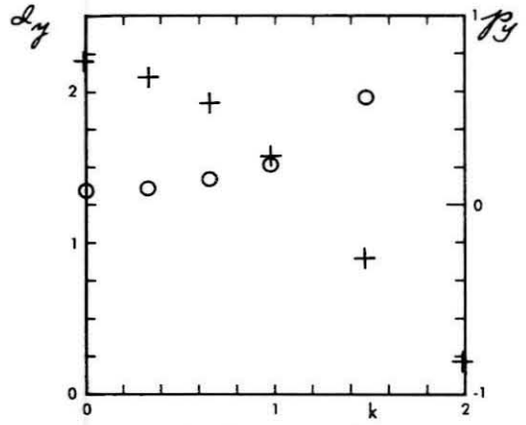

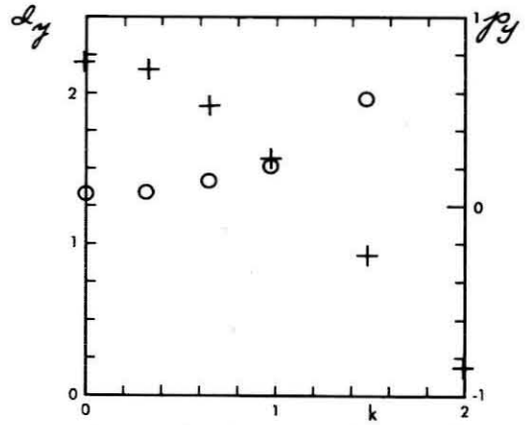

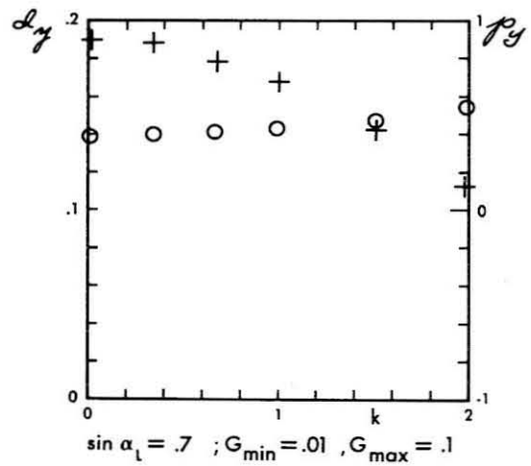

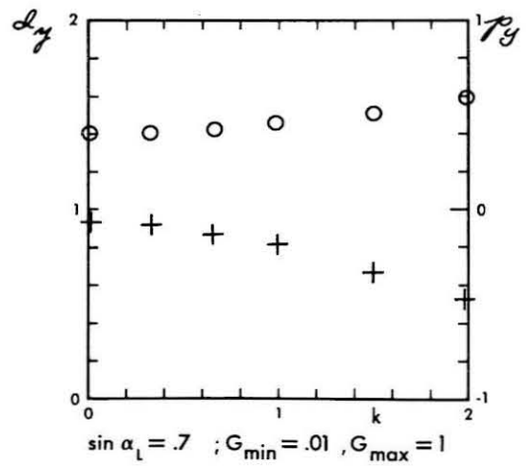

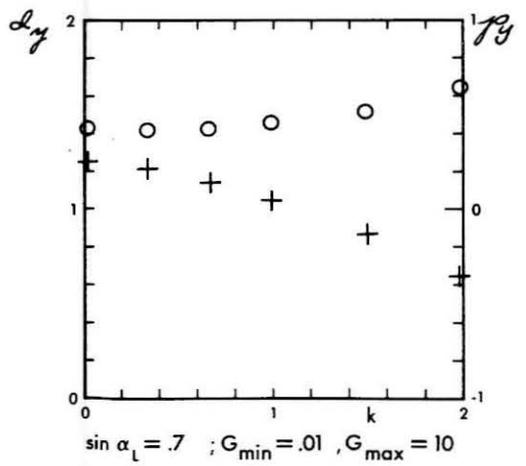

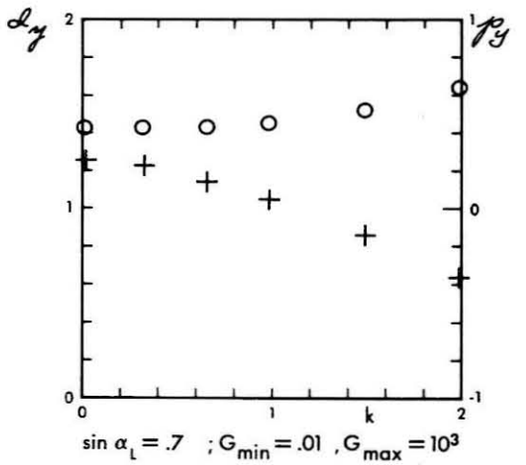

M_1

FIGURE 20. CASE (iii) POLAR COSINE TRANSFORM OF THE INTENSITY AND THE DEGREE OF POLARIZATION: d_y (INDICATED BY +) AND $p_y = \frac{Q_y}{I_y}$ (INDICATED BY O) VS. k

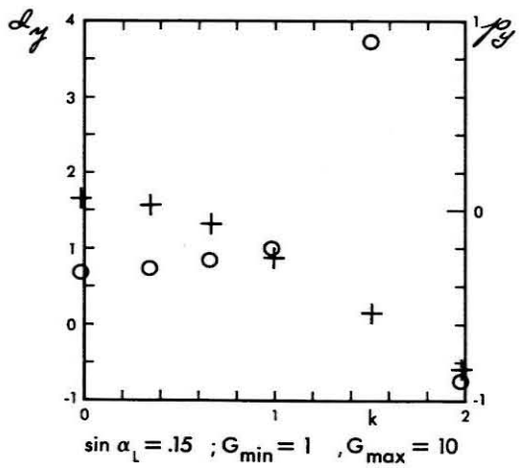

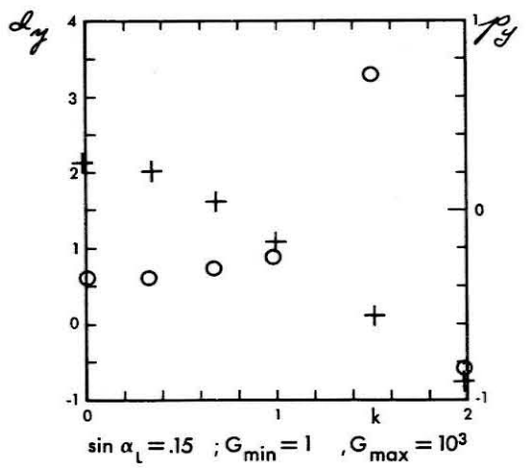

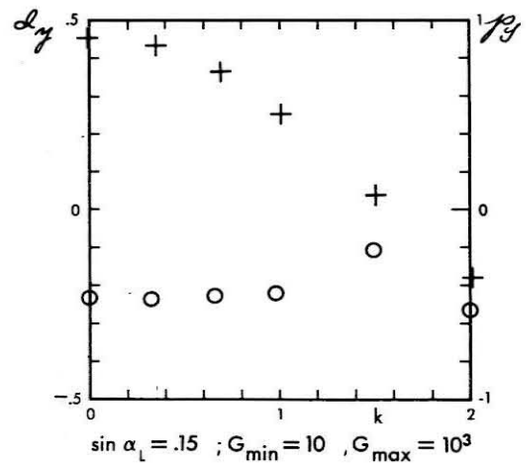

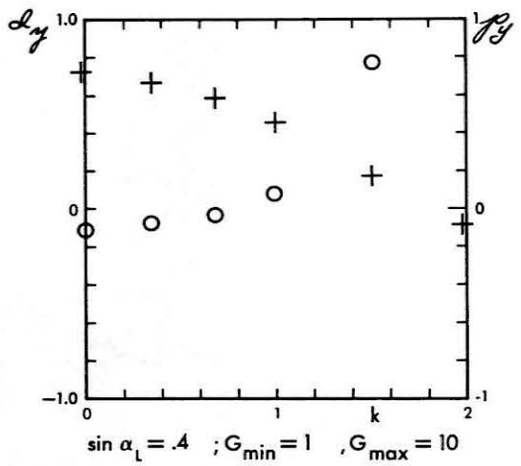

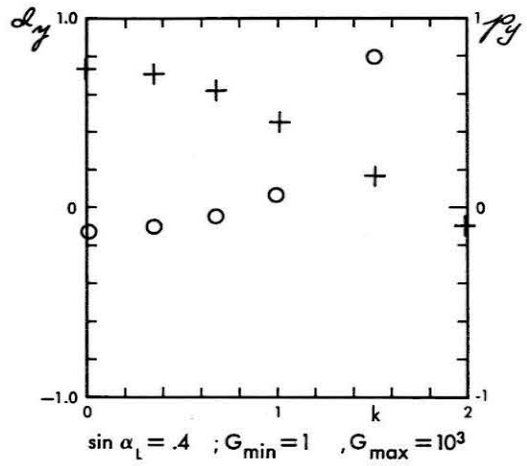

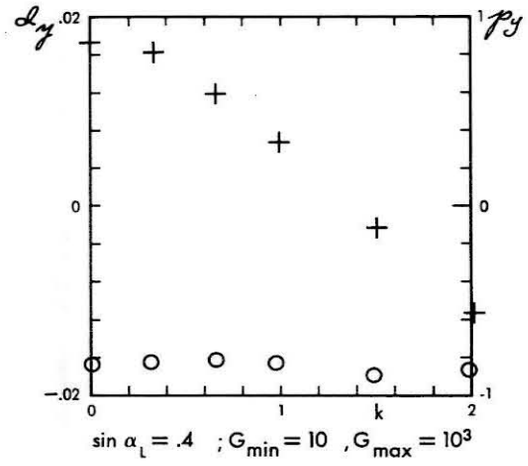

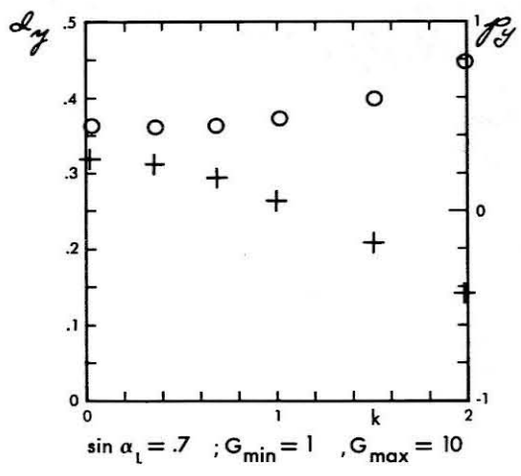

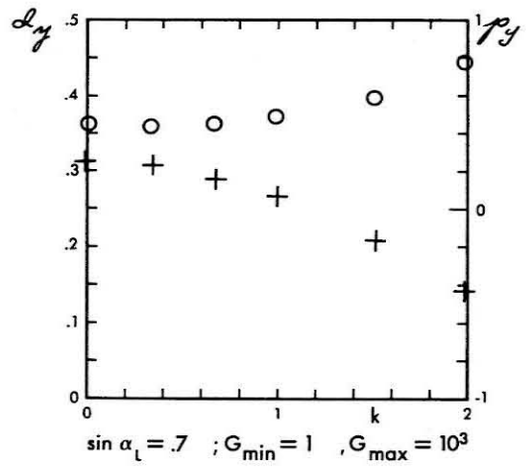

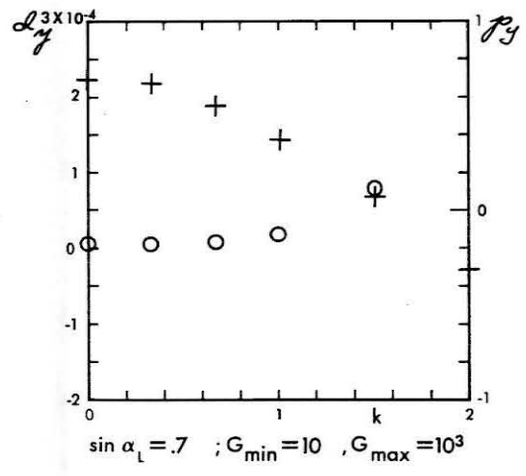

FIGURE 20 CASE (iii) (CONT.) POLAR COSINE TRANSFORM OF THE INTENSITY AND THE DEGREE OF POLARIZATION: $\mathcal{L}_y$ (INDICATED BY +) AND $\mathcal{P}_y = \frac{Q_y}{\mathcal{L}_y}$ (INDICATED BY O) VS. k

REFERENCES

Alfven, H., and N. Herlofsen, Cosmic radiation and radio stars, Phys. Rev. 78, 616, 1950.

Alsop, L. E., J. A. Giordmaine, C. H. Mayer and C. H. Townes, Paris Symposium on Radio Astronomy, I.A.U. Symposium No. 9, ed. R. N. Bracewell, Stanford Univ. Press, 69-74, 1959.

Arzimovich, L., and I. Pomeranchuk, The radiation of fast electrons in the magnetic field, J. Phys. USSR 9, 267-276, 1945.

Beard, David B., Cyclotron radiation from magnetically confined plasmas, Phys. Fluids 2, 379-389, 1959; Microwave emission from high temperature plasmas, Phys. Rev. Letters 2, 81-82, 1959.

Beard, David B., Relativistic calculation for cyclotron radiation from hot plasmas, Phys. Fluids 3, 324, 1960.

Beard, David B., and John C. Baker, Comment on the angular dependence of plasma synchrotron emission, Phys. Fluids 4, 278, 1961a.

Beard, David B., and John C. Baker, Synchrotron radiation from mirror machine geometries, Phys. Fluids 4, 611-618, 1961b.

Bekefi, G., J. L. Hirshfield, and S. C. Brown, Cyclotron emission from plasmas with non-maxwellian distributions, Bull. Am. Phys. Soc. Ser. II, 6, 205, 1961; Phys. Rev. 122, 1037-1042, 1961a.

Bekefi, G., J. L. Hirshfield and S. C. Brown, Kirchoff's radiation law for plasmas with non-maxwellian distributions, Phys. Fluids 4, 176-178, 1961b.

Biermann, L., and Leverett Davis, Jr., Considerations bearing on the structure of the galaxy, Zeitschrift fur Astrophysik, 61, 19-31, 1960.

Bogolyubov, N. N., and D. N. Zubarev, An asymptotic approximation method for a system with rotating phases and its application to the motion of a charged particle in a magnetic field, Ukranian Math. Journal, VII 5, 1955. (Translation available as Physical Research Laboratory Report, January, 1960, Space Technology Laboratories, Inc., L.A., Calif.)

Born, M., and E. Wolf, Principles of Optics, Pergamon Press, New York, 550-552, 1959.

Brown, R. Hanbury, and A. C. B. Lovell, The Exploration of Space by Radio, Chapman and Hall, Ltd., London, 1957.

Burbidge, G. R., Galactic radio emission and the energy released in nuclear collisions of primary cosmic ray protons, Phys. Rev. 103, 264-265, 1956a.

Burbidge, G. R., On synchrotron radiation from Messier 87, Astrophys. J. 124, 418-429, 1956b.

Burbidge, G. R., The theoretical explanation of radio emission, Paris Symposium on Radio Astronomy, I.A.U. Symposium No. 9, ed. R. N. Bracewell, Stanford Univ. Press, 541-551, 1959.

Carr, T. D., Radio frequency emission from the planet Jupiter, Astronom. J. 64, 39-41, 1959.

Carr, T. D., A. G. Smith, R. Pepple, O. H. Barrow, 18-megacycle observations of Jupiter in 1957, Astrophys. J. 127, 274-283, 1958.

Chandrasekhar, S., Stochastic problems in physics and astronomy, Revs. Modern Phys. 15, 31, 1943.

Chandrasekhar, S., Radiative Transfer, New York, Dover Publications, 1960.

Chang, David B., Synchrotron radiation from the planet Jupiter, (Boeing document D1-82-0060), 1960.

Chapman, S., and V.C.A. Ferarro, A new theory of magnetic storms, Terrestrial Magnetism and Atmospheric Elec. 36, 77, 171, 1931.

Christophilos, N. C., The Argus experiment, J. Geophys. Research 64, 869-876, 1959.

Davis, Jr., Leverett, An examination of the Fermi mechanism, N. 2 del Supplemento al Vol. 8, Serie X, del Nuovo Cimento, 444-456, 1958.

Davis, Jr., Leverett, and David B. J. Chang, Synchrotron radiation as the source of Jupiter's polarized decimeter radiation, J. Geophys. Research 66, No. 4, 1961a.

Davis, Jr., Leverett, and David B. Chang, On the effect of geomagnetic fluctuations on trapped particles, (submitted to J. Geophys. Research), 1961b.

Dessler, A. J., (private communication), 1961.

Dragt, A. J., Effect of hydromagnetic waves on the lifetime of Van Allen radiation protons, J. Geophys. Research, (Lockheed memo, Jan. 24, 1961).

Drake, F. D., Radio emission by Jupiter at 68 cm wavelength, Paper presented at XIII General Assembly of URSI, London, 1960, (results presented in graphical form by Field, 1961).

Drake, F. D., Radio emission from the planets, Physics Today 14, 30-34, 1961.

Drake, F. D., and H. I. Ewen, Proc. I.R.E. 46, 53-60, 1958.

Drake, F. D., and H. Hvatum, Non-thermal microwave radiation from Jupiter, Astronom. J. 64, 329-330, 1959.

Drummond, W. E., and M. N. Rosenbluth, Cyclotron radiation from a hot plasma, Phys. Fluids 3, 45-51, 1960.

Drummond, W. E., and M. N. Rosenbluth, Comments on synchrotron radiation, Phys. Fluids 4, 277-278, 1961a.

Drummond, W. E., and M. N. Rosenbluth, Synchrotron radiation from a plasma cylinder, Bull. Am. Phys. Soc. Ser. II 6, 205, 1961b.

Dyce, R. B., and M. P. Nakada, On the possibility of detecting synchrotron radiation from electrons in the Van Allen belts, J. Geophys. Research 64, 1163-1168, 1959.

Epstein, E. E., Anomalous continuum radiation from Jupiter, Nature 184, 52, 1959.

Erdelyi, A., W. Magnus, F. Oberhettinger and F. G. Tricomi, Tables of Integral Transforms, Vol. I, McGraw-Hill Book Co., Inc., New York, 284, 1954.

Feenberg, E., and H. Primakoff, Interaction of cosmic-ray primaries with sunlight and starlight, Phys. Rev. 73, 449-469, 1948.

Feynman, R. P., related by M. Sands, Caltech, 1958. See also Wheeler, J.A., and R. P. Feynman, Rev. Mod. Phys. 17, 157-181, 1945.

Field, G. B., The source of radiation from Jupiter at decimeter wavelengths, J. Geophys. Research 64, 1169-1777, 1959.

Field, G. B., The source of radiation from Jupiter at decimeter wavelengths, 2. cyclotron radiation by trapped electrons, J. Geophys. Research 65, 1661-1671, 1960.

Field, G. B., The source of radiation from Jupiter at decimeter wavelengths, 3. time dependence of cyclotron radiation, J. Geophys. Research 66, 1395-1405, 1961.

Franklin, K. L., and B. F. Burke, Radio observations of the planet Jupiter, J. Geophys. Research 63, 807-824, 1958.

Fried, Burton D., Physics of the Plasma State, Chapter 1 of lecture notes, Physical Research Laboratory Report, Space Technology Laboratories, Inc., Los Angeles, California, 1960.

Ginzburg, V. L., Usp. Fiz. Nauk 51, 343, 1953.

Ginzburg, V. L., The origin of cosmic radiation, Prog. in Elem. Particles and Cosmic Ray Physics IV, North Holland Publ. Co., Amsterdam, 339-420, 1959.

Gisrdmaine, J. A., Centimeter wavelength radio astronomy including observations using the maser, Proc. Nat. Acad. Sci. 46, 267-276, 1960.

Giordmaine, J. A., L. E. Alsop, C. H. Townes and C. H. Mayer, Observations of Jupiter and Mars at 3 cm wavelength, Astronom. J. 64, 332-333, 1959.

Giovanelli, R. G., Emission of enhanced microwave solar radiation, Nature 161, 133-134, 1948.

Hamlin, D. A., R. Karplus, R. C. Vik and K. M. Watson, Mirror and azimuthal drift frequencies for geomagnetically trapped particles, J. Geophys. Research 66, 1-4, 1961.

Heitler, W., Quantum Theory of Radiation, 3rd ed., Oxford at the Clarendon Press, 247, 1954.

Helliwell, R. A., and T. F. Bell, A new mechanism for accelerating electrons in the outer ionosphere, J. Geophys. Research 65, 1839-1842, 1960.

Hirshfield, Jay L., D. E. Baldwin, and Sanborn C. Brown, Cyclotron radiation from a hot plasma, Phys. Fluids 4, 198-203, 1961.

Hirshfield, Jay L., and Sanborn C. Brown, Incoherent microwave radiation from a plasma in a magnetic field, Phys. Rev. 122, 719-725, 1961.

Hooper, J. E., and M. Scharff, The Cosmic Radiation, London: Menthuen & Co., Ltd., 42-48, 1958.

Hoyle, F., Some Recent Researches in Solar Physics, p. 117, 1949.

Hoyle, F., A mechanism for radio noise generation, J. Geophys. Research 59, 180-182, 1954.

Hoyle, F., Concluding lecture, Paris Symposium on Radio Astronomy, I.A.U. Symposium No. 9, ed. R. N. Bracewell, Stanford Univ. Press, 598-601, 1959.

Hoyle, F., Radio-source problems, Monthly Not. Roy. Astron. Soc. 120, No. 4, 338-39, 1960.

Hutchinson, G. W., On the possible relation of galactic radio noise in cosmic rays, Phil. Mag. 43, 847-852, 1952.

Jahnke, E., and F. Emde, Tables of Functions, 4th ed., Dover Publications, New York, 146, 1945.

Kellogg, Paul J., Electrons of the Van Allen radiation, J. Geophys. Research 65, 2705-2714, 1960.

Kellogg, Paul J., Stimulated emission of synchrotron radiation from Jupiter, Bull. Am. Phys. Soc. Ser. II, 6, 264, 1961.

Kiepenheuer, J. O., Cosmic rays as the source of general galactic radio emission, Phys. Rev. 79, 738-739, 1950.

Korchak, A. A., Electromagnetic radiation by cosmic ray particles in the galaxy, Soviet Astronomy, A. J. 1, 360-365, 1957.

Long, R., and B. Elsmore, Radio emission from Jupiter at 408 mc/s, The Observatory 80, 112-114, 1960.

Mayer, C. H., T. P. McCullough and R. W. Sloanaker, Observations of Mars and Jupiter at a wavelength of 3.15 cm, Astrophys. J. 127, 11-16, 1958.

McClain, E. F., A test for non-thermal radiation from Jupiter at a wavelength of 21 cm., Astronom. J. 64, 339-340, 1959.

McClain, E. F., J. H. Nichols and J. A. Waak, An investigation of possible variations in the centimeter wave emission from Jupiter, paper presented to the XIIIth General Assembly, URSI, London, Sept. 5-15, 1960.

McClain, E. F., and R. M. Sloanaker, Preliminary observations at 10 cm. wavelength using the NRL 84 foot radio telescope, 1959 Paris Symposium on Radio Astronomy (IAU Symp., No. 9, and U.R.S.I. Symp., No. 1, 1958, Stanford, Calif.: Stanford University Press), 61-68, 1959.

Menzel, D. H., W. W. Coblentz and C. O. Lampland, Planetary temperatures derived from water-cell transmissions, Astrophys. J 63, 177-187, 1926.

Morris, David, (private communication), May 29, 1961.

Northrup, T. G., and E. Teller, Stability of the adiabatic motion of charged particles in the earth's magnetic field, Univ. Calif., Lawrence Radiation Lab., Livermore, UCRL-5615, 1959.

Oort, J. H., and Th. Walraven, Polarization and composition of the crab nebula, B.A.N. XIII, 285-308, 1956.

Oster, L., Effects of collisions on the cyclotron radiation from relativistic particles, Phys. Rev. 119, 1444-1456, 1960.

Oster, L., Cyclotron radiation from relativistic particles with an arbitrary velocity distribution, Phys. Rev. 121, 961-967, 1961.

Parker, E. N., Dynamics of the interplanetary gas and magnetic fields, Ap. J. 128, 664-675, 1958.

Parker, E. N., Geomagnetic fluctuations and the form of the outer zone of the Van Allen radiation belt, J. Geophys. Research 65, 3117-3130, 1960.

Parker, E. N., Effect of hydromagnetic waves in a dipole field on the longitudinal invariant, J. Geophys. Research 66, 693-708, 1961.

Pomeranchuk, I., On the maximum energy which the primary electrons of cosmic rays can have on the earth's surface due to radiation in the earth's magnetic field, Journ. of Phys. USSR 2, 65-69, 1940.

Radhakrishnan, V., and J. A. Roberts, Polarization and angular extent of the 960-mc/sec. radiation from Jupiter, Phys. Rev. Letters 4, 493-494, 1960.

Roberts, J. A., and G. J. Stanley, Radio emission from Jupiter at a wavelength of 31 centimeters, Pub. A.S.P. 71, 485-496, 1959.

Schott, G. A., Electromagnetic Radiation, Cambridge University Press, Cambridge, 109-110, 1912.

Schwinger, J., On the classical radiation of accelerated electrons, Phys. Rev. 75, 1912-1925, 1949.

Shklovskii, I. S., A. Zh. 30, 15, 1953.

Sloanaker, R. M., Apparent temperature of Jupiter at a wavelength of 10 cm., Astronom. J. 64, 346, 1959.

Sloanaker, Russell M., and John W. Boland, Observations of Jupiter at a wavelength of 10 cm., Astrophys. J. 133, 649-656, 1961.

Spitzer, Lyman, Physics of Fully Ionized Gases, New York, Interscience Publishers, 1956.

Stokes, G. G., Trans. Cambr. Phil. Soc., p. 339, 1852; reprinted in his Mathematical and Physical Papers, Vol. III, Cambridge University Press, p. 233, 1901.

Takakura, B. A., Synchrotron radiation and solar radio outbursts at microwave frequencies, IAU-URSI Paris Symposium on Radio Astronomy, ed. Bracewell, Stanford, 562-570, 1959.

Trubnikov, B. A., Magnetic emission of high temperature plasma, AEC-tr-4073 (translation of a thesis submitted to the Institute of Atomic Energy, Moscow Institute of Engineering and Physics, Academy of Sciences, S.S.S.R., 1958) United States Atomic Energy Commission, Technical Information Service, 1960.

Trubnikov, B. A., On the angular distribution of cyclotron radiation from a hot plasma, Phys. Fluids 4, 195-198, 1961.

Twiss, R. Q., On the nature of the discrete radio sources, Phil. Mag., 45, 249-258, 1954.

Twiss, R. Q., Radiation transfer and the possibility of negative absorption in radio astronomy, Australian J. Phys. 11, 564-579, 1958.

Tunmer, Harriet, The relation of cosmic radio emission to the electronic component of cosmic rays, Monthly Notices 119, 184-193, 1959.

Vernov, S. N. A. Ye. Chudakov, R. V. Vakulov and Y. I. Logachev, Astronautics 4, No. 7, 23, 1959.

Wallis, G., The determination of the energy distribution of relativistic electrons by the frequency distribution of their "synchrotron radiation," Paris Symposium on Radio Astronomy, I.A.U. Symposium No. 9, ed. R. N. Bracewell, Stanford Univ. Press, 595-597, 1959.

Welch, Jasper A., Jr., and William A. Whitaker, Theory of Geomagnetically trapped electrons from an artificial source, J. Geophys. Research 64, 909-922, 1959.

Wentworth, R. C., W. M. MacDonald, and S. F. Singer, Lifetimes of trapped radiation belt particles determined by Coulomb scattering, Phys. Fluids 2, 499-509, 1959.

Wentzel, Donat G., Hydromagnetic waves and the trapped radiation, Part I. Breakdown of the adiabatic invariance, J. Geophys. Research 66, 359-362, 1961a.

Wentzel, Donat G., Hydromagnetic waves and the trapped radiation, Part 2. Displacements of the mirror points, J. Geophys. Research 66, 363-369, 1961b.

Westfold, K. C., The polarization of synchrotron radiation, Astrophys. J. 130, 241-258, 1959.

Yeh, K. C., and V. H. Gonzalez, Note on the geometry of the earth's magnetic field useful to Faraday effect experiments, J. Geophys. Research 65, 3209-3214, 1960.